UNIVERSITÀ DEGLI STUDI DI PAVIA

DOTTORATO IN SCIENZE CHIMICHE E FARMACEUTICHE E INNOVAZIONE INDUSTRIALE
(XXXVI Ciclo)
Coordinatore: Chiar.mo Prof. Giorgio Colombo

ATOM-ECONOMIC APPROACHES TO CARBO- AND HETEROPOLYCYCLIC PRODUCTS

Tesi di Dottorato di
Andraž Oštrek

AA 2023/2024

Tutor
Chiar.mo Prof. Giuseppe Zanoni

Kdo zna snov preobraziti v eliksir življenja,
kot mag napoj zvariti, ki prežene vražje bolečine,
z naravo skrbno se igrati z drobcem potrpljenja,
da obrodi ti strupe, barve, drage kamne in kovine?
(A. Oštrek)

To my family for all the help, support, and everything that might be beyond words.

To my friends all around the globe for enriching my life.

To my colleagues for expanding my professional horizons.

Atom-economic approaches to carbo- and heteropolycyclic products

Summary: Nature can rapidly build molecular complexity from linear polyenes with enzymatic cascade cyclizations and derivatization of intermediates. These products are having wide range of biological activities, therefore, highly stereoselective methods for their synthesis are desired, considering also their further structural diversification.

The first part of this thesis is focused on iridium nitrenoid initiated cyclization cascades of olefinic dioxazolones containing aryl, heteroaryl or alkyne termini. Dioxazolone motif serves as a precursor of acyl nitrenoid intermediates that are formed *in situ* in presence of iridium catalysts. Reactions are achieved at moderately elevated or room temperature with fluorinated alcohols as solvents. Ring-fused *δ*-lactam products are formed in highly stereoselective fashion and their further diversification is easily achieved with several chemical transformations.

The second part of the thesis focuses on electrochemical generation of stabilized carbocations that serve as cyclization initiators of polyene substrates with aryl or allylsilane termini. Different cation pool techniques show low to moderate cyclization product yields. With extensively optimized cation flow conditions, in the means of flash carbocation generation and further short cyclization reaction times, several substrates successfully give carbopolycyclic products in moderate to good yields.

Approcci per la sintesi di composti carbo- ed eteropoliciclici

Sommario: La natura è in grado di creare policicli a partire da polieni lineari mediante ciclizzazioni catalizzate da enzimi. Questi prodotti hanno una vasta gamma di attività biologiche, pertanto è necessario trovare metodi stereoselettivi per la loro sintesi.

La prima parte di questa tesi si concentra su ciclizzazioni biomimetiche catalizzate da iridio-nitrenoidi. Come precursori di questi ultimi vengono utilizzati diossazoloni, i quali reagendo con complessi a base di iridio formano quelli che saranno gli iniziatori della reazione a cascata. Grazie a questa ciclizzazione si possono ottenere *δ*-lattami in modo altamente stereoselettivo.

La seconda parte della tesi si concentra sulla generazione elettrochimica di carbocationi stabilizzati che fungono da innesco per la ciclizzazione di substrati polienici con terminazioni ariliche o allylsilaniche. Diverse tecniche di accumulo di cationi mostrano rese di ciclizzazione variabili. Ottimizzando le condizioni di flusso, mediante la generazione istantanea di carbocationi e brevi tempi di reazione di ciclizzazione, sono stati ottenuti con successo prodotti carbo-policiclici con rese moderate o buone.

Table of contents

Abbreviations

9-BBN	9-borabicyclo[3.3.1]nonane
Ac	acetyl
Acac	acetylacetone
Ar	aryl
AIBN	azobisisobutyronitrile
BDSB	bromodiethylsulfonium bromopentachloroantimonate
BINAP	2,2′-bis(diphenylphosphino)-1,1′-binaphthyl
BINOL	1,1′-b-2-naphthol
$[BMIm]^+$	1-butyl-3-methylimidazolium
BOX	bis(oxazoline)
BSTFA	*N*,*O*-bis(trimethylsilyl)trifluoroacetamide
Bz	benzoyl
CCDC	Cambridge Crystallographic Data Centre
CDI	1,1'-carbonyldiimidazole
CDSC	chlorodiethylsulfonium hexachloroantimonate
COD	cycloocta-1,5-diene
Cp*	pentamethylcyclopentadienyl
d.r.	diasteromeric ratio
DBDMH	1,3-dibromo-5,5-dimethylhydantoin
DCDMH	1,3-dichloro-5,5-dimethylhydantoin
DC	direct current
DCC	*N*,*N*′-dicyclohexylcarbodiimide
DCE	1,2-dichloroethane
DDQ	2,3-dichloro-5,6-dicyano-1,4-benzoquinone
DFT	density functional theory
DIBAL-H	diisobutylaluminium hydride
DMF	dimethylformamide
DMSO	dimethyl sulfoxide
dppf	1,1′-bis(diphenylphosphino)ferrocene
dppp	1,3-bis(diphenylphosphino)propane
ee	enantiomeric excess
e.r.	enantiomeric ratio
HFIP	1,1,1,3,3,3-hexafluoropropan-2-ol (*also* hexafluoroisopropanol)
HOMO	highest occupied molecular orbital
HRMS	high-resolution mass spectrometry
IR	infrared spectroscopy
KHMDS	potassium bis(trimethylsilyl)amide (*also* potassium hexamethyldisilazide)

LBA	Lewis acid-assisted activation of Brønsted acids
LDA	lithium diisopropylamide
LUMO	lowest unoccupied molecular orbital
*m*CPBA	meta-chloroperoxybenzoic acid
Ms	methanesulfonyl (*also* mesyl)
MTBE	methyl *tert*-butyl ether
$NaBAr^F_4$	sodium tetrakis[3,5-bis(trifluoromethyl)phenyl]borate
NaHMDS	sodium bis(trimethylsilyl)amide (*also* sodium hexamethyldisilazide)
NBS	*N*-bromosuccinimide
NCS	*N*-chlorosuccinimide
NFTB	1,1,1,3,3,3-hexafluoro-2-trifluoromethyl-2-propanol (*also* nonafluoro-*tert*-butanol)
NIS	*N*-iodosuccinimide
NMR	nuclear magnetic resonance
NOESY	nuclear Overhauser effect spectroscopy
PCC	pyridinium chlorochromate
PIDA	(diacetoxyiodo)benzene (*also* phenyliodine(III) diacetate)
Piv	pivaloyl (2,2-dimethylpropanoyl)
PMB	para-methoxybenzyl
PMP	*para*-methoxyphenyl
py or pyr	pyridine
RT	room temperature
SC-XRD	single crystal XRD
SE	squalene epoxidase
SHC	squalene-hopene cyclase
SOMO	singly occupied molecular orbital
TBAF	tetra-*n*-butylammonium fluoride
TBCO	2,4,4,6-tetrabromo-2,5-cyclohexadienone
TBS	*tert*-butyldimethylsilyl
TEMPO	(2,2,6,6-tetramethylpiperidin-1-yl)oxyl
Tf	trifluoromethanesulfonyl (*also* triflyl)
TFA	trifluoroacetic acid (NaTFA – sodium trifluoroacetate)
THF	tetrahydrofuran
TIPS	triisopropylsilyl
TLC	thin-layer chromatography
TMPAP	trimethylphenylammonium perbromide
TMS	trimethylsilyl
Ts	toluenesulfonyl (*also* tosyl)
XRD	X-ray diffraction

Chapter 1: Polyene cyclizations

1.1. General introduction: Polyene cyclizations – from biosynthesis to total synthesis

Nature can precisely build molecular complexity with enzymatic transformations resulting in numerous complex products. Among them, natural products are classified as secondary metabolites, which are not directly involved in organism's survival [1]. Due to possessing a variety of biological activities – e.g., being cytotoxic, antiviral or antibacterial – they are often sources of new pharmaceutical drugs [2]; and, therefore, their synthesis and possible diversification is highly desired [3]. Organic synthetic strategies en route to synthesis of such molecules might greatly differ from biological enzymatic reactions, and face more challenges in efficiency, chemical selectivity, and stereoselectivity. Research in this area gives opportunity to explore basic chemical concepts and create new chemical methodologies.

Synthetic efforts over the years have greatly approached to the concept of mimicking biological transformations with the research in the field of biomimetic polyene cyclizations. A remarkable example of nature's polycyclization, facilitated by squalene-hopene cyclase, showcases how linear polyolefinic hydrocarbon substrate squalene, which is not bearing any other functional group, undergoes a complex transformation. This enzyme-catalyzed cyclization reaction, forming hopene, proceeds in one synthetic step and forms a pentacyclic product with five new C–C bonds resulting in nine new contiguous stereocenters (Scheme 1.1) [4]. Enzymatic reaction is executed with extreme precision and forms corresponding product as sole isomer, despite all theoretically possible products that could arise from different chemo-, regio-, and stereoselectivity. Biogenetic isoprene rule, based on Wallach's [5] and Ruzicka's [6] work, postulated isoprene as the building block of linear aliphatic precursors (such as geraniol, farnesol, geranylgeraniol and squalene) that can be further cyclized and functionalized to yield cyclic terpenes – a wide field of natural products.

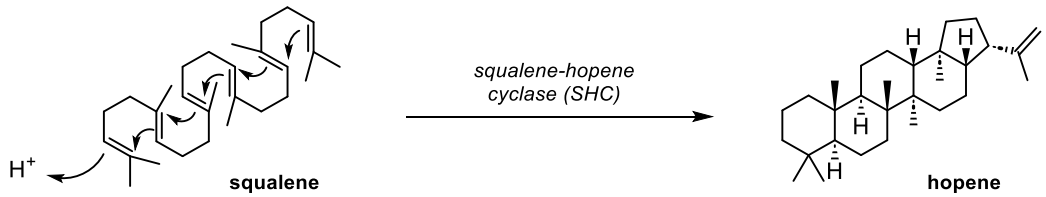

***Scheme 1.1**: Cyclization of squalene to hopene by the enzyme squalene-hopene cyclase (SHC).*

In a wide range of microorganisms and higher eukaryotes several enzymes can in one step stereoselectively cyclize and skeletally rearrange either squalene or its epoxidized analogue 2,3-oxidosqualene, forming different polycyclic triterpenoids such as hopene, diplopterol, tetrahymanol, lanosterol, cycloartenol, and β-amyrin (Figure 1.1). Further, these triterpenes are identified as the precursors of all hopanoids and steroids, which include cholesterol, glucocorticoids, estrogens, androgens, and progesterones. [7]

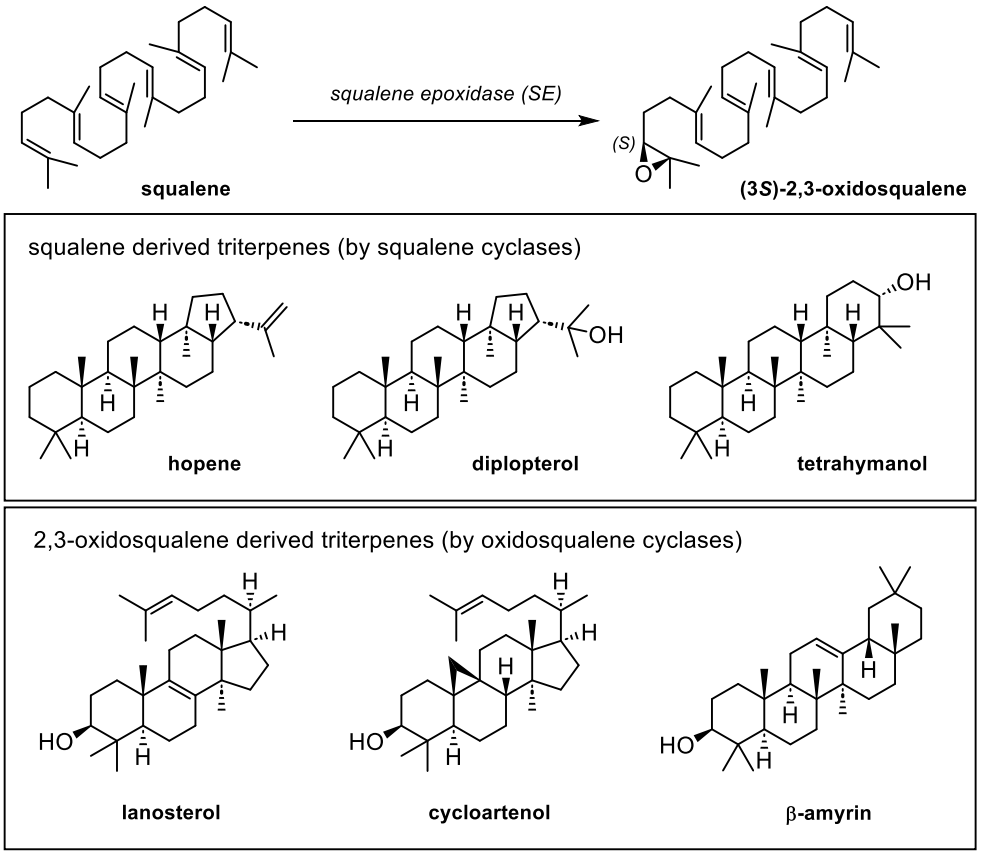

***Figure 1.1**: Enzymatic oxidation of squalene to 2,3-oxidosqualene and natural products derived from both of them.*

Historically, the link between squalene and cholesterol was not obvious but has gradually become evident. In 1950s, a fraction of scientists believed that fatty acids (including arachidonic acid) might be more viable precursors to sterols in contrast to other polyenes known at the time [7]. A hypothesis by Robinson in 1934 [8] introduced squalene as precursor to cholesterol, despite the considerations of significant structural reorganization reactions – namely, methyl shifts and demethylations – needed during the proposed biosynthetic process. Isotopic labeling experiments by Bloch and Rittenberg in 1945 [9] showed evidence supporting the hypothesis of the squalene as cholesterol precursor; and lanosterol's structure elucidation in 1952 [10] offered a connecting link between these two compounds [11] (Scheme 1.2) and elucidated the connection between squalene and many tetra- and pentacyclic triterpenes.

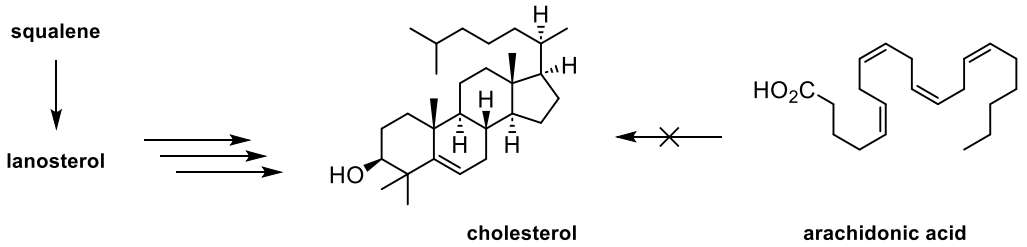

***Scheme 1.2**: Lanosterol structure elucidation offered a plausible explanation of squalene being cholesterol precursor and not arachidonic acid.*

In 1950s an important breakthrough had been made by Stork and Eschenmoser who have independently made advances in π-cation cyclization reactions. Their studies on the stereochemical outcomes have become recognized as Stork-Eschenmoser hypothesis (Scheme 1.3) [12,13,14]. The stereospecific *anti* addition mechanism of proton and donor olefin is effective in cyclization of 1,5-dienes and this principle can be extended to further addition of formal carbenium ion in longer polyenes. Experimental results of carefully selected substrates – to minimize possible steric influences to the stereocontrol – suggested that cyclization proceeds either in a concerted way through a tight transition state involving charge delocalization and chair like conformation of newly forming rings or, minimally, a nonclassical cyclic carbonium ion is being formed. Cyclization of *E*- or *Z*-olefins in formic acid and further deformylation yielded *trans* and *cis* cyclized products, respectively, as single diastereoisomers in each case. Findings were well reflected in biosynthesis of triterpenes where diene conformation is reflected in cyclization diastereoselection. Additionally, some stereochemical discrepancies observed in these natural products were rationalized with the importance of squalene's precyclization fold, which influences the cyclization outcome through a possible combination of chair- and boat-like conformations in transition state [7].

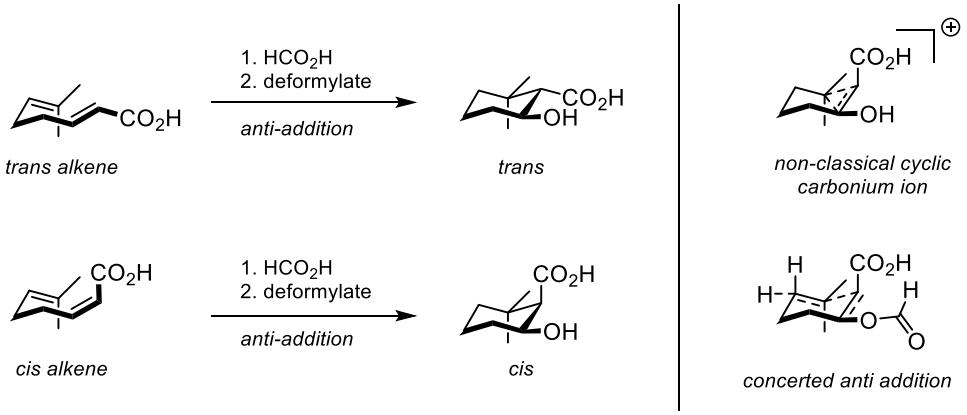

***Scheme 1.3**: The basis of Stork-Eschenmoser hypothesis. Cyclization was suggested to proceed either via concerted anti addition or non-classical cyclic carbonium ion.*

1.2. Initiators of polyene cyclizations

Cationic polyene cyclizations, also known as cation π-cyclizations, are initiated by electrophilic initiators, and newly formed formal carbocation has a central role in cyclization propagation. Electrophiles can vary from simple proton [7], carbon- [15], sulfur- [16] or selenium-based [17] cationic species to electrophilic halogen species [18] and π-acids (such as Hg, Pt, Au, Ir) [19]. To gain a greater control over cyclization process, substrates can have a functionalized initiation site. Inspired by Nature's strategy, cyclizations can, for example, begin at the epoxide moiety in the presence of Lewis acids. Such biomimetic polyene cyclizations are a powerful synthetic tool in synthesis of complex frameworks with several stereocenters. In order to achieve a high control over stereoselectivity, great efforts are made to design enantioselective approaches.

1.3. Towards enantioselective proton-initiated polyene cyclizations

Historically, one of the first and main strategies of polyene cyclizations was based on proton initiation achieved by strong acids. Nevertheless, the concept of enantioselective approaches remained elusive until 1999 [20], when Yamamoto reported his principle of Lewis acid-assisted activation of Brønsted acids (LBA). In this adduct, Lewis acid increases Brønsted acid's reactivity through coordination. First experimental examples included complexes of $SnCl_4$ and BINOL derivatives applied to cyclization of polyenes with phenolic terminating groups (Scheme 1.4). Authors proposed that good levels of absolute stereocontrol were achieved because the developing positive charge at protonation step was electronically stabilized by an n-π* interaction between oxygen lone pair and the LUMO of the olefin. Despite relatively moderate enantioselectivities, it was an important contribution for further enantioselective transformations.

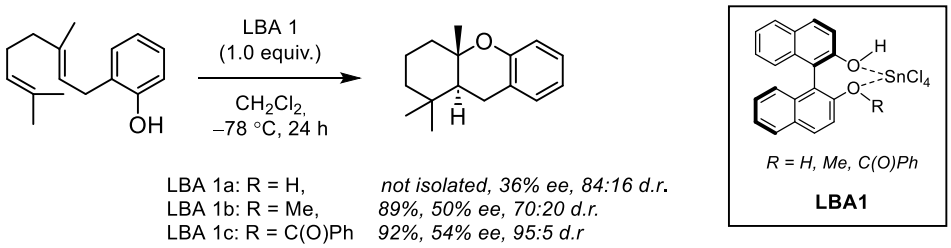

***Scheme 1.4**: Yamamoto's first examples of enantioselective LBA catalysis.*

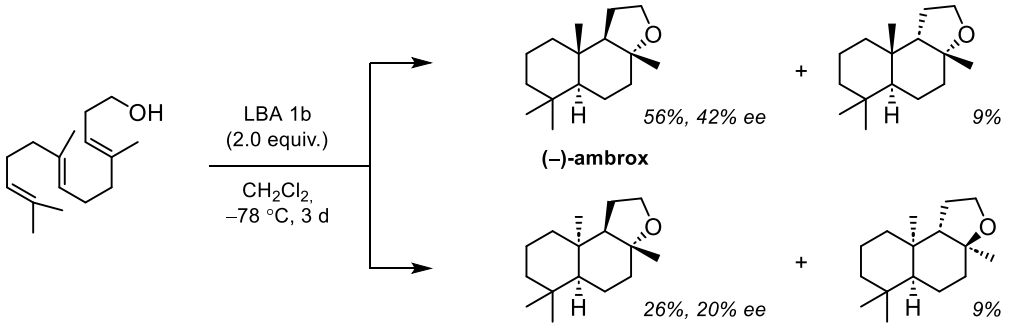

***Scheme 1.5**: LBA approach in synthesis of (−)-ambrox.*

First application of LBA approach in total synthesis of natural products was seen in synthesis of (–)-ambrox, starting from homofarnesyl alcohol (Scheme 1.5). In the second-generation approach [21], Yamamoto reported a pyrogallol based Brønsted acid scaffold which offered stronger chelation to Lewis acid and restricted the O–H bond in the chiral pocket. Exposure of the polyene substrate to the new LBA scafold resulted in a mixture of mono- and fully cyclized products, and only further exposure to acidic conditions resulted in complete cyclization with overal 90% yield and 85% ee (Scheme 1.6).

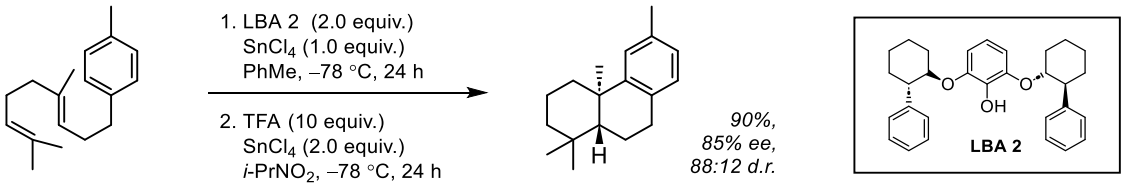

***Scheme 1.6**: Yamamoto's second generation enantioselective LBA catalysis.*

Corey's group has taken inspiration from Yamamoto and introduced a more electron deficient dichloro-BINOL-derived scafold together with more sterically demanding Lewis acid $SbCl_5$ [22]. They promoted polycyclization of several polyenes with high enantioselectivities (Figure 1.2).

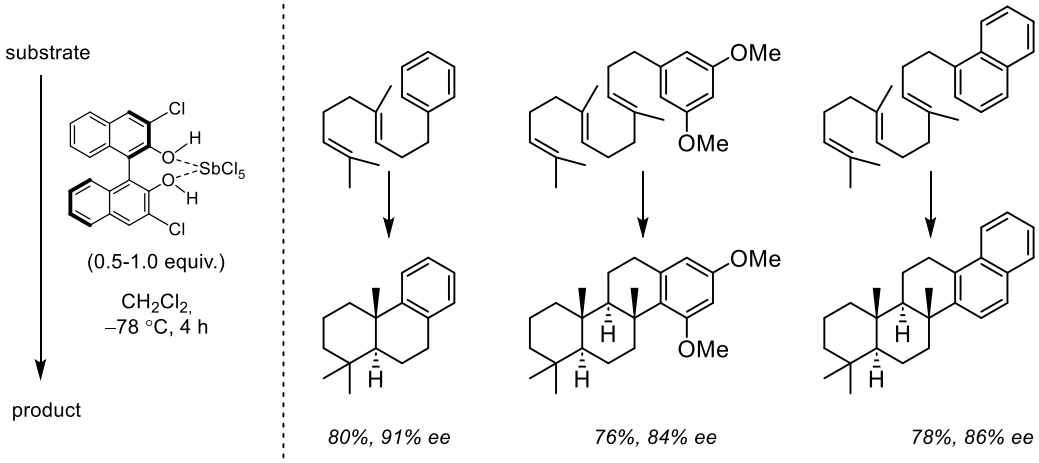

***Figure 1.2**: Corey's LBA enantioselective cyclization approach of polyenes.*

1.4. Transition metal catalyzed polyene cyclizations

Transition metals play an important role in polyene cyclizations, and they often offer a very good platform for enantioselective transformations. Gagné group made extensive studies on Pt(II) catalyzed polyene cyclizations, observing selective activation of terminal olefins in initial experiments [23]. With stoichiometric amounts of platinum-triphospine complexes, stable platinum-alkyl species were generated (Figure 1.3, A). Addition of hydride abstractor (methyl trityl ether) and a change of the ligand were necessary to achieve catalyst turnover and to finish the diastereoselective cyclization terminated by phenolic group. By employing (*S*)-xylyl-phanephos ligand, asymmetric transformations were achieved [24], where good enantioselectivites were observed also within the scope of terminal aliphatic alcohols (Figure 1.3, B). Additionally, alkene terminating group was well tolerated in reactions using (*R*)-BINAP ligand [25]. When Pt(II)/PyBOX complex was used, protodemetalation event occurred in the process of cyclization, which formed saturated products in good to excellent yields, and enantioselectivities in a range of 25–38% ee (Figure 1.4) [26].

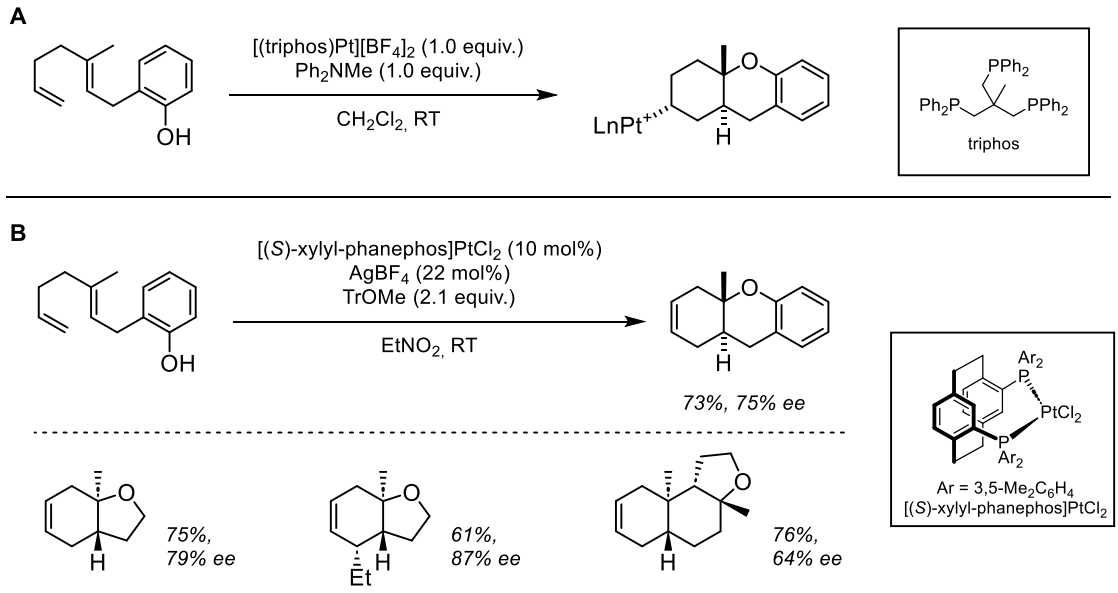

***Figure 1.3**: A) Polyene cyclization with stoichiometric amount of Pt(II)-complex and formation of stable platinum-alkyl species. B) Catalytic Pt(II)-initiated enantioselective polyene cyclization of phenols and terminal alcohols.*

Gold(I) was able to promote enyne substrates towards the cyclization reactions with alkynes as initiation sites. Even though computational studies have shown that olefins exhibit stronger σ-donation to Au^+ species compared to acetylenes, experimental results showed that kinetic control leads to preferential attack of nucleophiles to metal-bound alkynes, resulting in selective activation of the alkyne site in substrates containing both triple and double bonds. Toste group

applied this observation from their previous work on asymmetric gold(I) catalysis and promoted cyclizations of enyne substrates with various aryl, phenolic and sulfonamide terminating groups (Figure 1.5) [27].

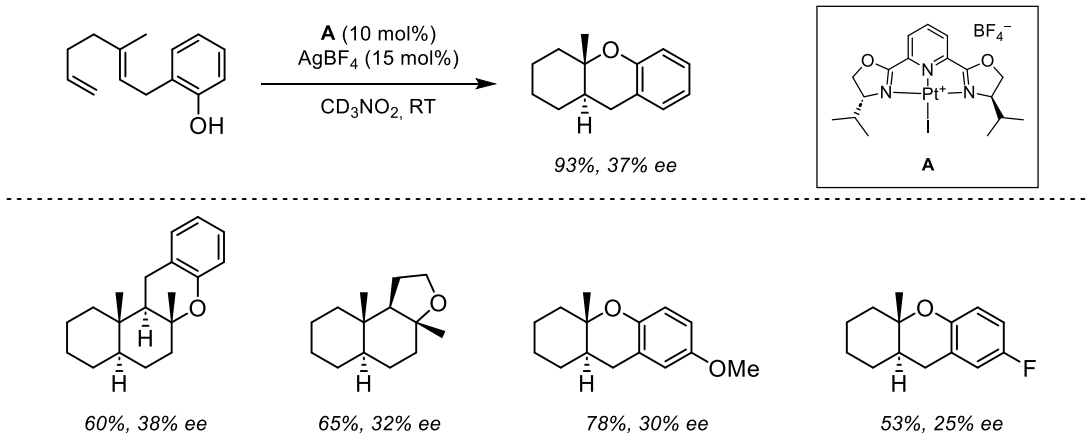

***Figure 1.4**: Polyene cyclizations employing Pt(II)/PyBOX catalyst.*

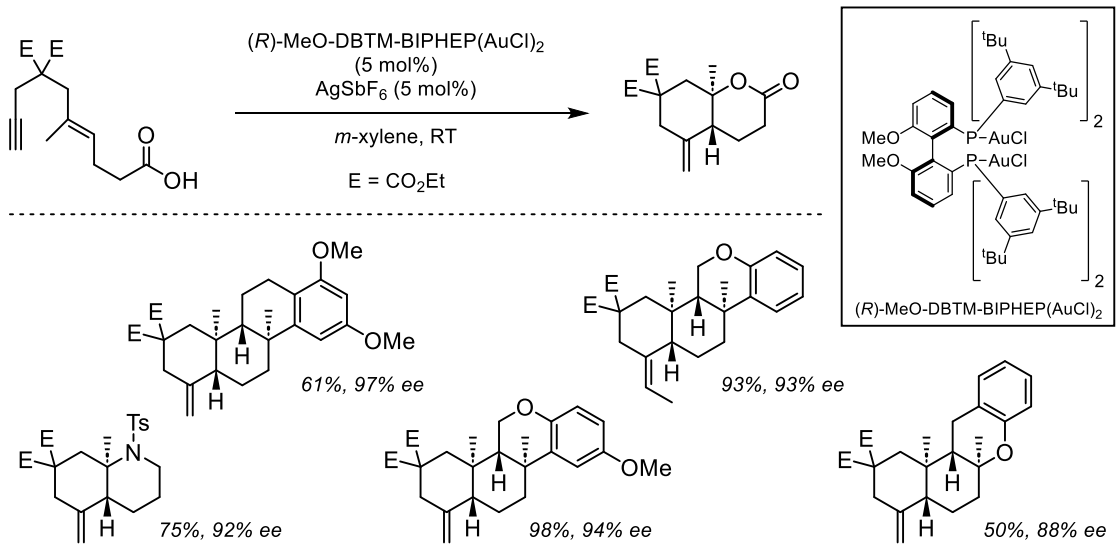

***Figure 1.5**: Gold(I) promoted cyclization of eneynes.*

In 2012, Carreira reported that branched allylic alcohols served as good substrates in polyene cyclizations with iridium(I) complexes [28]. Catalysts were bearing olefinic and phosphoramidite ligands and cyclization occurred in the presence of Lewis acidic promoter $Zn(OTf)_2$ via an iridium π-allyl species. Several (hetero)polycyclic products were prepared with this approach which resulted in excellent enantioselectivities (> 99% ee) and good to excellent yields (> 69%) (Figure 1.6). Some longer polyenes had shown difficulties in completion of cyclization cascade, which resulted in a mixture of desired products and partially cyclized products (Figure 1.7).

Addition of strong acids, such as TFA, to these products yielded the desired polycycles through protonation and cyclization propagation. Iridium catalysis approach was applied to total synthesis of (+)-asperolide C (Scheme 1.7) [29], which is a labdane-type terpenoid and displays a variety of biological activities. Synthesis was achieved starting from a linear precursor bearing trimethylsilyl group as internal terminus that allowed site selective termination in polycyclization event. Formed bicyclic product was in additional steps transformed to the natural product (+)-asperolide C.

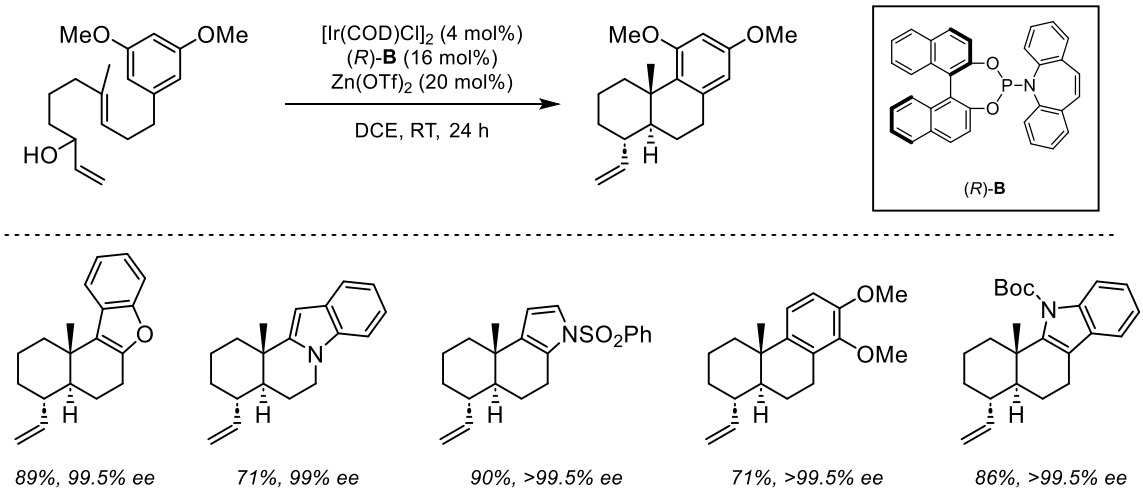

***Figure 1.6**: Ir(I) promoted enantioselective polyene cyclization.*

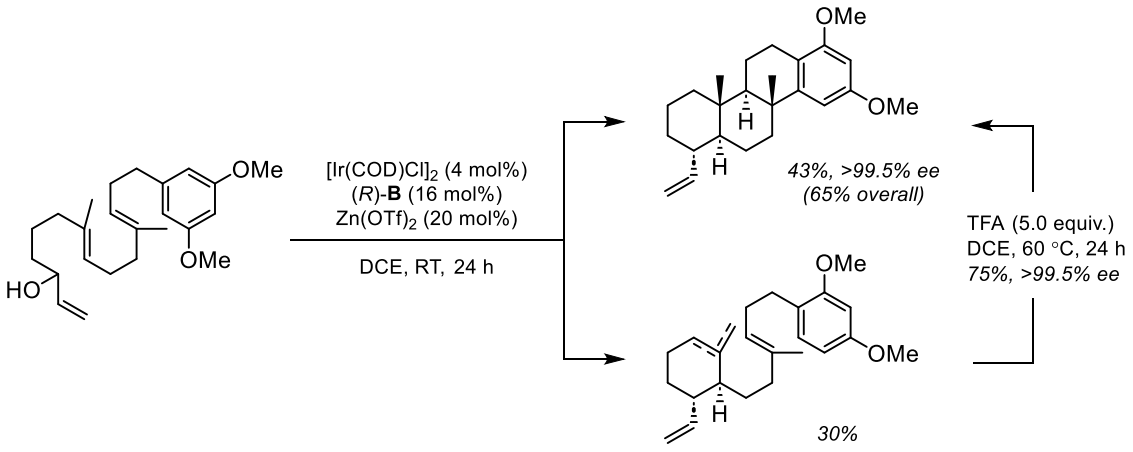

***Figure 1.7**: Ir(I) catalyzed cyclization of higher polyene and full cyclization of partially cyclized product under acidic conditions.*

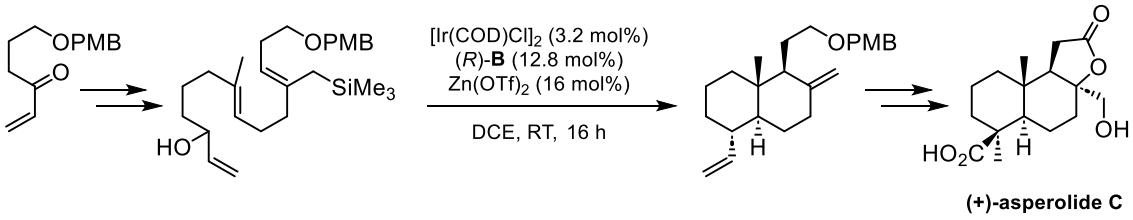

***Scheme 1.7**: Carreira polycyclization en route to asperolide C synthesis.*

1.5. Halonium induced polyene cyclizations

Early reports on halonium induced polyene cyclizations from 1966 by Van Tamelen showed that methyl farnesate, unlike most of the other terpene derivatives, exposed to NBS in water/THF solvent mixture gave small amounts of mono- or polycyclized products (Scheme 1.8, A) [30]. Similarly, a decade later, Nasipuri observed that *m*-anisyl polyene derivative under these conditions resulted in a small amount of tricyclic product (Scheme 1.8, B) [31]. While bromocyclization pathway was not favored with standard reagents, reaction could be promoted by additives (such as silver salts) [32], or by designing new reagents.

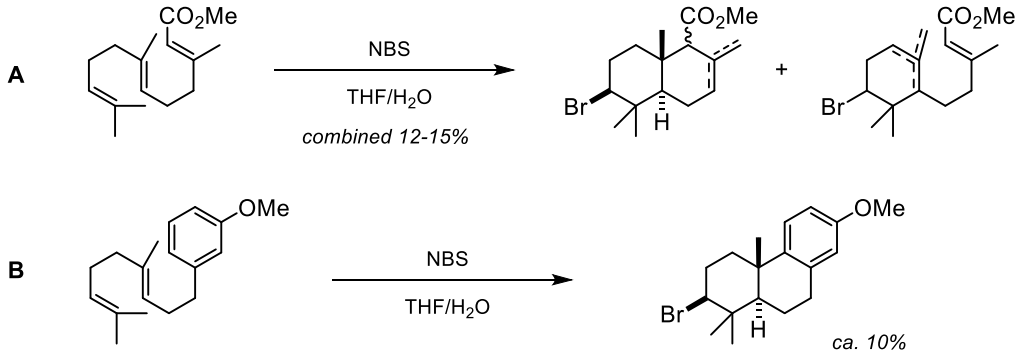

***Scheme 1.8**: NBS promoted cyclization of A) methyl farnesate; B) m-anisyl polyene.*

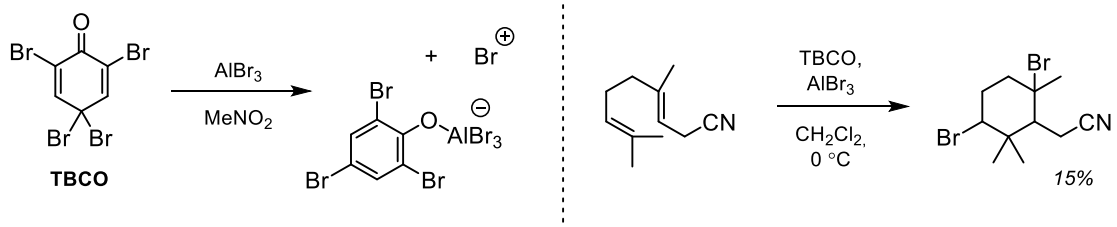

***Figure 1.8**: Activation with $AlBr_3$ and polyene cyclization using TBCO.*

2,4,4,6-Tetrabromo-2,5-cyclohexadienone (TBCO) was proposed by Kato to be a source of electrophilic bromonium ion after activation with $AlBr_3$. Formed aluminate would be a rather poor nucleophile, which would minimize the interference with the cyclization pathway (Figure 1.8) [33]. Another highly activated bromonium source with a weak counter anion was designed by Snyder in 2009 [34] – reaction of Br_2 with $SbCl_5$ and Et_2S resulted in BDSB (bromodiethylsulfonium bromopentachloroantimonate), which is still one of important reagents for polyene bromocyclization (Figure 1.9) [35]. Aletrnatively, phosphines were used as nucleophilic promoters that enabled NBS – and its iodo-analogue NIS – to be effective in halonium-promoted cyclizations [36]. Comparison of reagents BDSB, TBCO, NBS/Ph_3P and Br_2/$AgBF_4$ in halonium-cyclization reactions on selected substrates is shown in Table 1.1 [34].

***Table 1.1**: Comparison of different reagents as halonium sources in polyene cyclization reactions of selected substrates.*

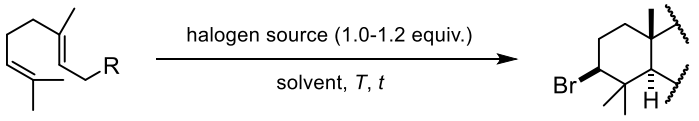

substrate	product		**BDSB** CH_3NO_2 (5 min)	**$Br_2/AgBF_4$** CH_3NO_2 (5 min)	**TBCO** CH_3CN (15-60 min)	**NBS/Ph_3P** CH_2Cl_2 (6-24 h)
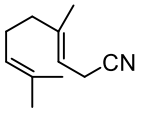	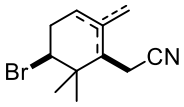		73% (25 °C)	8% (25 °C)	< 5% (25 °C)	< 5% (–40 °C)
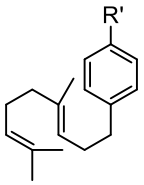	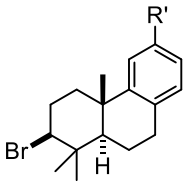	R' = H	75% (–25 °C)	9% (–25 °C)	27% (–25 °C)	13% (–78 or 40°C)
		R' = OMe	76% (–25 °C)	11% (–25 °C)	27% (–25 °C)	20% (–78 or 40°C)
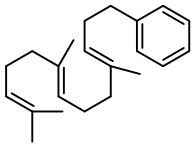	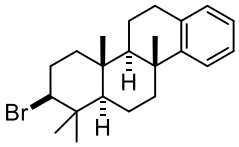		58% (–25 °C)	< 5% (–25 °C)	14% (–25 °C)	< 5% (–78 or 40°C)

Snyder has extended halonium sources to iodo- and chloro-variants [37]. Iodo-variant IDSI existed as chlorine bridged dimer, while chlorine analogue CDSC (chlorodiethylsulfonium hexachloroantimonate) was structurally analogous to BDSB and was operational in a more limited scope of polyene substrates than IDSI (Figure 1.9). However, as reported, they achieved a first chloronium-induced polyene cyclization. Another iodonium source, bis(pyridine)iodonium tetrafluoroborate ($I(pyr)_2BF_4$, Figure 1.9), was developed by Barluenga, achieving good results in various cyclizations [38].

In the field of halonium induced cyclizations many other reagents (Figure 1.9) have been developed and used [18], even such as perbromides (TMPAP) [39] and stable bromiranium species of biadamantylidene [40]. Some promoters based on phospite-urea motif, phosphoramidite or thiophosphoramidite were used in combination with NBS, NCS or halohydantoins (DBDMH and DCDMH) and successfully promoted cyclizations and even served as chiral inductors for asymmetric transformations [41-45].

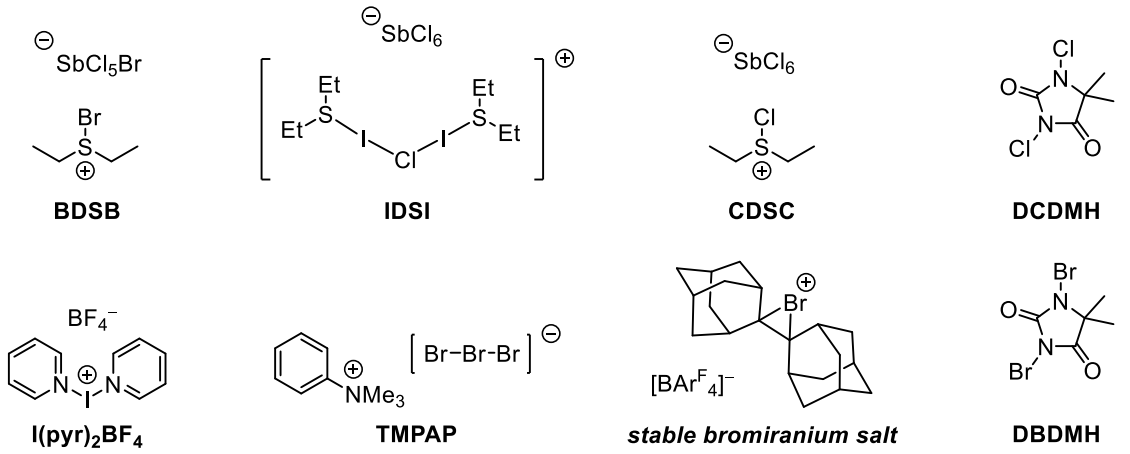

***Figure 1.9**: Selected halonium-source reagents.*

1.6. Intramolecular cyclizations with carbon based electrophiles

Formation of new C–C bonds in polyene cyclizations is usually associated with their intermolecular formation during the cyclization cascade. In the initiation step, formation of the formal carbocation can be achieved by the intramolecular attack of electrophilic species on olefinic bond or with activation of more elaborated initiators already installed in the molecule (such as epoxide, acetal, *N*-acetal, allylic alcohol, 1,3-dicarbonyl). Despite a variety of different initiating strategies available, there is a scarce amount of intermolecular carbon-based electrophiles as cyclization initiators. Advances in this field were done by Loh in 2007, when optically pure acetals were introduced as precursors of carbon-based electrophiles. Their activation by $SnCl_4$ formed non-cyclic oxocarbenium ions that promoted cyclization cascade and delivered tricyclic products (Figure 1.10) [15, 46, 47]. By analogy, mixed-*N*-acetals (example shown in Scheme 1.9) were also successful cyclization promotors in presence of $TiCl_4$ [47].

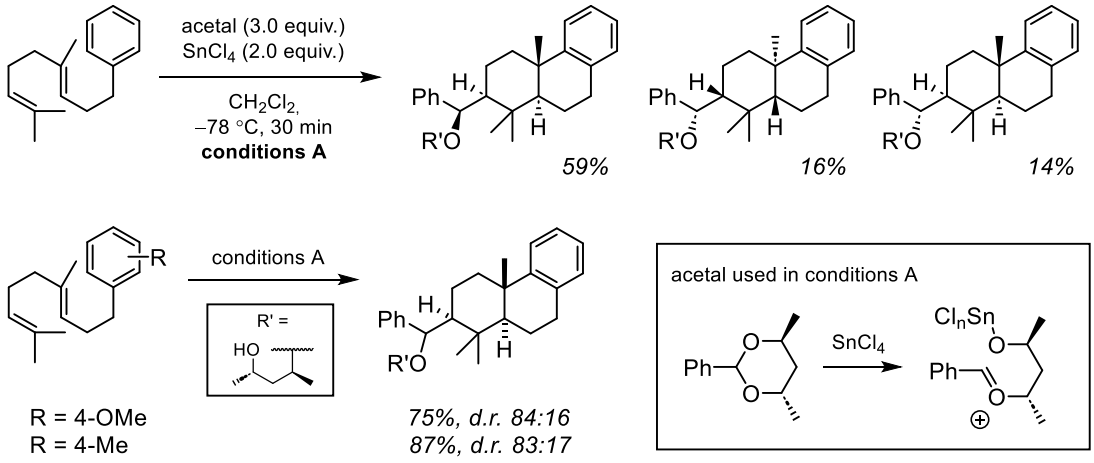

***Figure 1.10**: Intermolecular acetal-promoted polyene cyclization.*

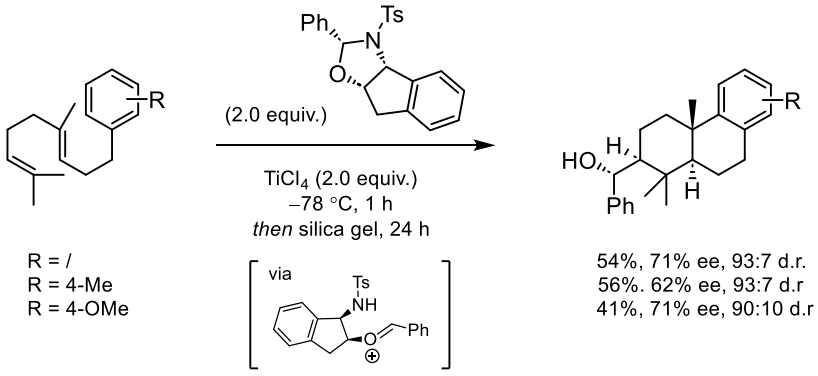

***Scheme 1.9**: Mixed N-acetal-promoted intermolecular polyene cyclization.*

With acetal-promoted polyene strategy, total synthesis of antiochic acid was achieved as shown in Scheme 1.10 [46]. Silyl protected allylic alcohol with olefin motif and bromophenyl terminus underwent the acetal promoted polycyclization in the presence of $SnCl_4$. Further sequence of swern oxidation to aldehyde, ether cleavage under basic conditions, acetylation, and silyl protecting group removal afforded primary alcohol. Additional Swern and Pinnick oxidations yielded corresponding carboxylic acid which underwent esterification in the presence of DCC and methanol, and acetyl group was hydrolyzed in methanolic K_2CO_3. Pendant alkyl group possessing secondary alcohol and phenyl ring was removed in a sequence of bromination, elimination, olefin ozonolysis and reduction. 2-Propenyl group was installed by Suzuki coupling and finally carboxylic group of antiochic acid was revealed by LiOH mediated hydrolysis.

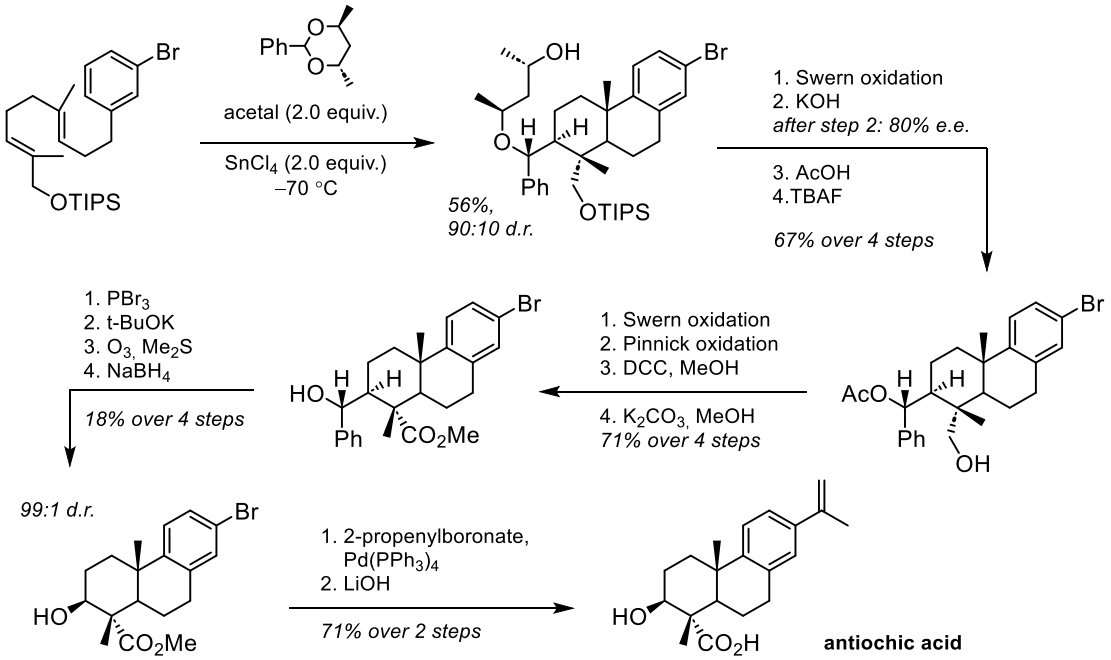

***Scheme 1.10**: Total synthesis of antiochic acid with acetal promoted polyene cyclization as a key step.*

Donohoe's more recent report shows that primary and secondary readily available benzylic and allylic alcohols are a source of new carbon electrophiles [48]. Ionization of these alcohols with Ti(O*i*Pr)$_4$ forms carbocations which are able to participate in highly atom-economic polyene cyclizations showing high stereocontrol and forming water as a by-poduct. Additionally, several solvents (*i*-PrOH, MeOH, DMF, MeCN, DCE, toluene) were screened in combination with Ti(O*i*Pr)$_4$ additive, however, no productive cyclization was observed. Perfluorinated alcohol, HFIP, was therefore the only solvent of choice. Different Lewis acids (Zn(OAc)$_2$, Zn(OTf)$_2$, AlCl$_3$) or Brønsted acids did not give improvements in terms of yields compared to Ti(O*i*Pr)$_4$ in HFIP. With this contribution Donohoe and coworkers vastly expanded the scope of carbon-based intermolecular cyclization promotors – selected examples are shown in Figure 1.11. Methodology was also applied to formal synthesis of ±-18-norestradiol and offered a method for synthesis of its analogues.

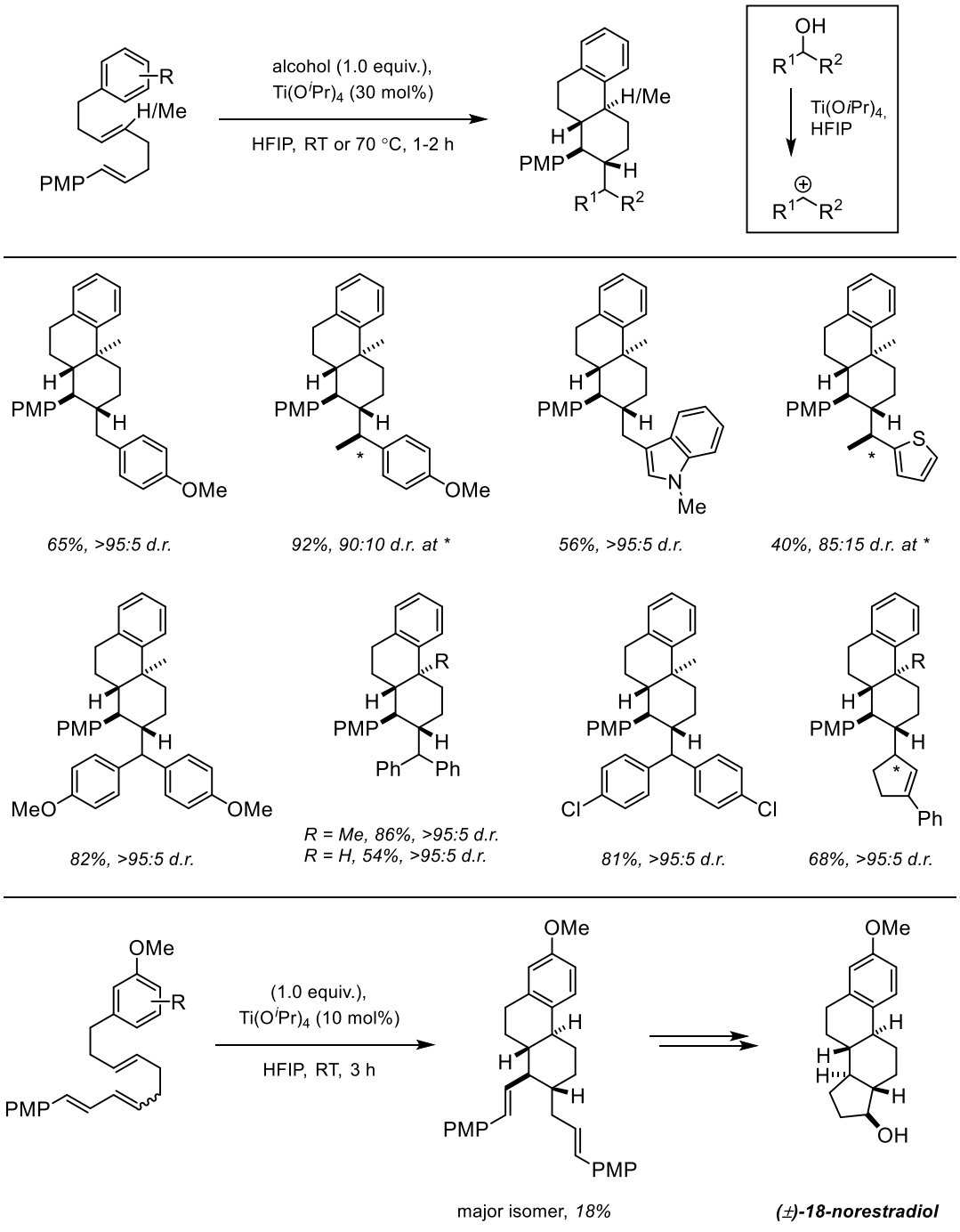

***Figure 1.11**: Ti(O^{i}Pr)$_4$ promoted ionization of benzylic and allylic alcohols as source of electrophilic carbon-based initiators for polyene cyclizations and using this strategy in total synthesis of 18-norestradiol.*

1.7. Organocatalytic polyene cyclizations

Aromatic amino acid residues in active sites of cyclase enzymes play an important role in cation-π stabilizing interactions during polycyclization event [49]. To mimic this concept, Jacobsen developed a thiourea-based organocatalyst bearing a diverse set of aromatic cores attached to a pyrrolidine unit [50]. Eyring analysis revealed that the size of aromatic system directly correlates with observed enantioselectivity, suggesting that cation-π interactions are operational between the substrate and catalyst. On this basis, 2-pyren-4-ylpyrrolidine unit was selected as the most suitable building part of thiourea-based organocatlyst. Cyclization of substrates with electron-rich terminating groups proceeded in good yields with high enantioselectivities (Figure 1.12).

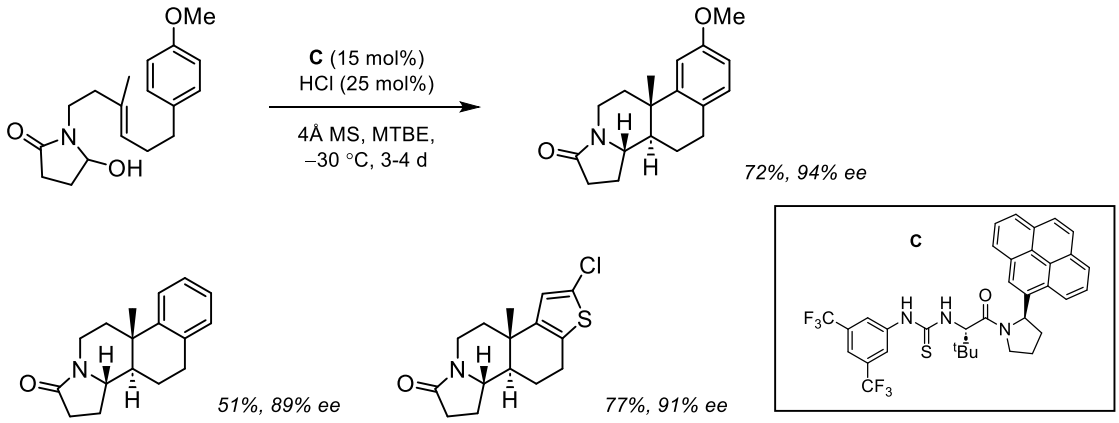

***Figure 1.12**: Thiourea-based organocatalyst for enantioselective polyene cyclization.*

Another important milestone was set by MacMillan with development of enantioselective organo-SOMO catalyzed polyene cyclization [51]. Mechanistically this transformation belongs to radical cyclizations, a broad class of transformations, which appeared in 1960s [52], but has not been discussed in this chapter as it goes beyond the scope of cationic-π cyclizations. MacMillan's approach in 2010 offered a first method for enantioselective radical polyene cyclizations (Figure 1.13). Chiral imidazolidinones have been used as catalysts for enamine oxidation, using $Cu(OTf)_2$ as an oxidant. Dienyl and trienyl aldehydes were used in a substrate scope and delivered steroidal type products in modest to good yields and high enantioselectivities. Both electron-rich and electron-poor terminating groups were tolerated, however, to maintain electrophilic character of the propagating radicals, cyano groups had to be installed to the alkene motifs. Remarkably, higher-order polycyclic products with up to five new carbon rings could be achieved.

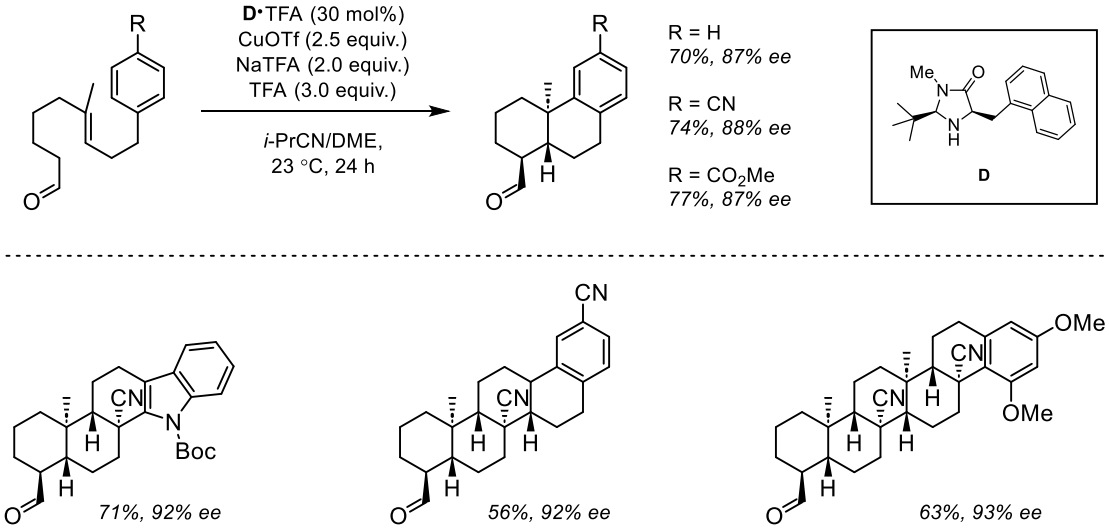

***Figure 1.13**: Organo-SOMO catalyzed enantioselective polyene cyclization.*

1.8. Selected examples of polyene cyclizations in total synthesis

Method of polyene cyclizations is applied to a synthesis of a wide variety of natural products belonging to different natural product classes. As mentioned in introduction, biomimetic total synthesis strategies can take inspiration from Nature and employ epoxides as initiation groups to deliver natural products with steroidal frameworks. Among Corey's reported total syntheses, two examples of squalene-derived natural products used the mentioned strategy, resulting in synthesis of dammarenediol II and scalarenedial.

Dammarenediol II is a plant natural product that arises from cyclization of (*S*)-2,3-oxidosqualene. Corey has reported a biosynthetic-like synthesis starting from farnesyl acetate (Scheme 1.11) [53]. Enol silyl ether moiety was introduced with function to direct the carbon ring formation during cyclization and ensure the formation of a six-membered C-ring. Farnesol derived epoxide was achieved by regioselective, enantioselective Sharpless dihydroxylation. Acyl silane, formed with silyl imine homologation, was further olefinated by addition of vinyl lithium species, Brook rearrangement and alkylation sequence. Methyl aluminium dichloride promoted tricyclization, and subsequent desilylation with HF and further thioacetal hydrolysis delivered corresponding ketone. Free hydroxy group was protected as carbamate and aldol condenzation in presence of TsOH resulted in enone product. Stereoselective enone reduction and carbamate deprotection with final Grignard reagent addition completed the Dammarenediol II syntesis.

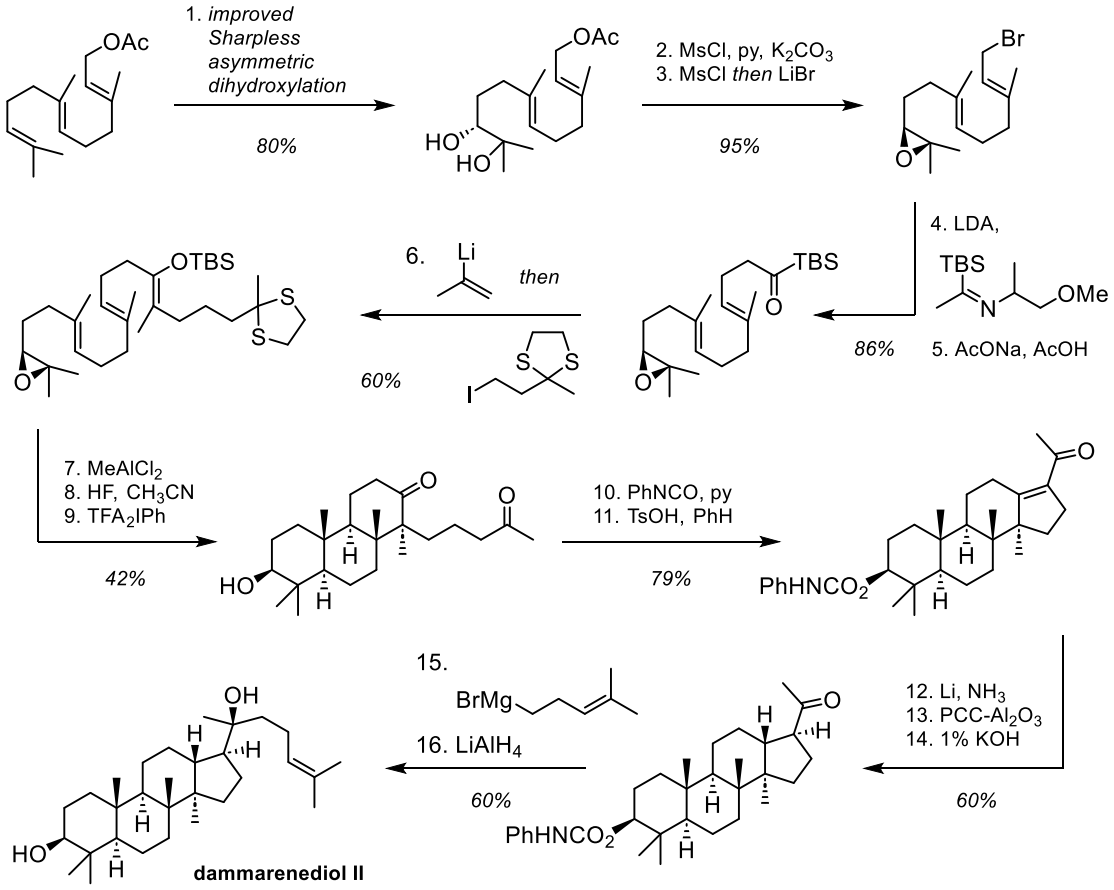

***Scheme 1.11**: Corey's total synthesis of dammarenediol II.*

As the C ring formation posed some difficulties, in contrast to Corey's enol silane approach, Johnson incorporated fluorine in linear precursor to control the regioselection in his biomimetic synthesis of Damarenendiol II as shown in Scheme 1.12 [54].

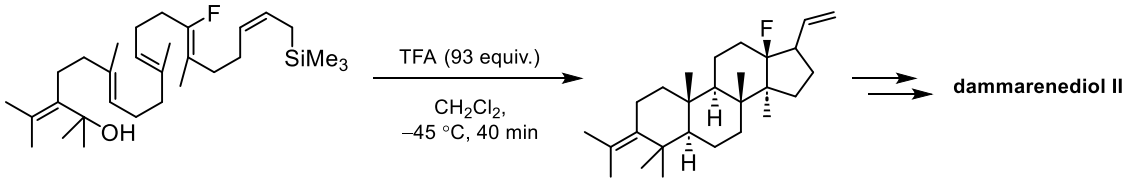

***Scheme 1.12**: Johnson's cyclization of fluorine-containing substrate as a key step in total synthesis of damarenediol II.*

In total synthesis of squalene-derived scalarenedial (Scheme 1.13) [55], Corey used similar strategy of acyl silane preparation as seen in his total synthesis of dammarenediol II, this time starting from geranylgeranyl acetate. Sequence of addition, Brook rearrangement and elimination transformed acyl silane to key epoxytetraene. Cyclization again proceeded with addition of Lewis acidic $MeAlCl_2$, and treatment with HF allowed to cleave silyl ether partially formed by silicon transfer. Methanolic KOH equilibrated the epimers in the α-position to the keto group to converge to equatorial isomer. Barton-McCombie deoxygenation of A ring was followed with triflate formation and oxidative desilylation. Paladium mediated carbonylation delivered *γ*-lactone which was reduced to diol and then oxidized to dialdehyde to finish the total synthesis of scalarenedial.

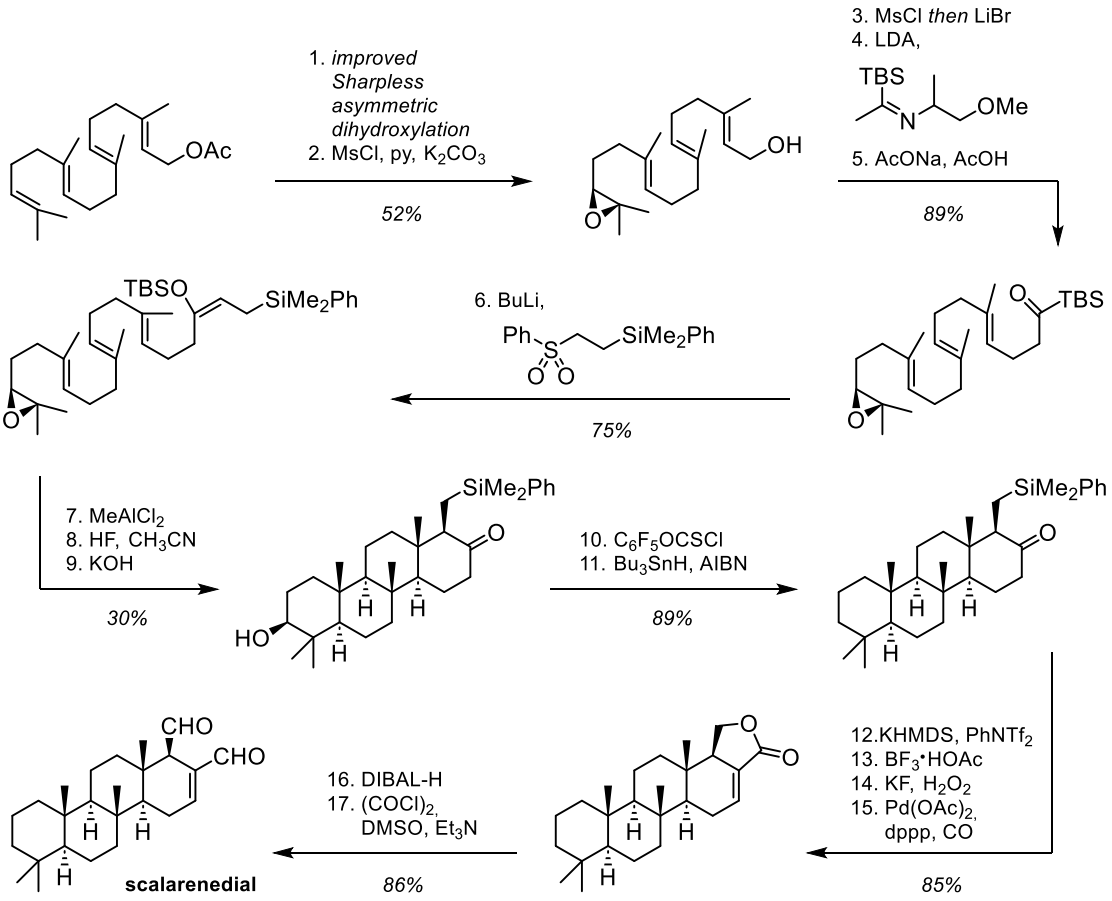

***Scheme 1.13**: Corey's total synthesis of scalarenedial.*

1.9. References

1 D. H. Williams, M. J. Stone; P. R. Hauck, S. K. Rahman: Why Are Secondary Metabolites (Natural Products) Biosynthesized? *J. Nat. Prod.* **1989**, *52*, 1189–1208. DOI: 10.1021/np50066a001

2 D. J. Newman, G. M. Cragg: Natural Products as Sources of New Drugs from 1981 to 2014. *J. Nat. Prod.* **2016**, *79*, 3, 629–661. DOI: 10.1021/acs.jnatprod.5b01055

3 K. E. Kim, A. N. Kim, C. J. McCormick, B. M. Stoltz: Late-Stage Diversification: A Motivating Force in Organic Synthesis. *J. Am. Chem. Soc.* **2021**, *143*, 41, 16890–16901. DOI: 10.1021/jacs.1c08920

4 K. U. Wendt, G. E. Schulz, E. J. Corey, D. R. Liu: Enzyme Mechanisms for Polycyclic Triterpene Formation. *Angew. Chem. Int. Ed.* **2000**, 39, 2812–2833. DOI: 10.1002/1521-3773(20000818)39:16%3C2812::AID-ANIE2812%3E3.0.CO;2-%23

5 M. Christmann: Otto Wallach: Founder of Terpene Chemistry and Nobel Laureate 1910. *Angew. Chem. Int. Ed.* **2010**, *49*, 9580–9586. DOI: 10.1002/anie.201003155

6 L. Ruzicka: The isoprene rule and the biogenesis of terpenic compounds. *Experientia* **1953**, *9*, 357–367. DOI: 10.1007/BF02167631

7 R. A. Yoder, J. N. Johnston: A Case Study in Biomimetic Total Synthesis: Polyolefin Carbocyclizations to Terpenes and Steroids. *Chem. Rev.* **2005**, *105*, 12, 4730–4756. DOI: 10.1021/cr040623l

8 R. Robinson, *Chem. Ind. (London)* **1934**, *53*, 1062. DOI: 10.1002/jctb.5000535004

9 K. Bloch, D. Rittenberg: An estimation of acetic acid formation in the rat. *J. Biol. Chem*. **1945**, *159*, 45. DOI: 10.1016/S0021-9258(19)51300-X

10 W. Voser, M. V. Mijović, H. Heusser, O. Jeger, L. Ruzicka: Über Steroide und Sexualhormone. 186. Mitteilung. Über die Konstitution des Lanostadienols (Lanosterins) und seine Zugehörigkeit zu den Steroiden. *Helv. Chim. Acta* **1952**, *35*, 2414–2430. DOI: 10.1002/hlca.19520350730

11 K. Bloch: The Biological Synthesis of Cholesterol. *Vitamins & Hormones* **1957**, *15*, 119–150. DOI: 10.1016/S0083-6729(08)60509-9

12 G. Gamboni, H. Schinz, A. Eschenmoser: Über den sterischen Verlauf der säurekatalysierten Cyclisation in der Terpenreihe. Cyclisation der cis-7-Methyl-octadien-(2,6)-säure-(1). *Helv. Chim. Acta* **1954**, *37*, 964–971. DOI: 10.1002/hlca.19540370404

13 G. Stork, A. W. Burgstahler: The Stereochemistry of Polyene Cyclization. *J. Am. Chem. Soc.* **1955**, *77*, 19, 5068–5077. DOI: 10.1021/ja01624a038

14 A. Eschenmoser, L. Ruzicka, O. Jeger, D. Arigoni: Zur Kenntnis der Triterpene. 190. Mitteilung. Eine stereochemische Interpretation der biogenetischen Isoprenregel bei den Triterpenen. *Helv. Chim. Acta* **1955**, *38*, 1890−1904. DOI: 10.1002/hlca.19550380728

15 Y.-J. Zhao, S.-S. Chng, T.-P. Loh: Lewis Acid-Promoted Intermolecular Acetal-Initiated Cationic Polyene Cyclizations. *J. Am. Chem. Soc.* **2007**, *129*, 3, 492–493. DOI: 10.1021/ja067660+

16 Z. Tao, K. A. Robb, K. Zhao, S. E. Denmark: Enantioselective, Lewis Base-Catalyzed Sulfenocyclization of Polyenes. *J. Am. Chem. Soc*. **2018**, *140*, 10, 3569–3573. DOI: 10.1021/jacs.8b01660

17 J. T. Moore, C. Soldi, J. C. Fettinger, J. T. Shaw: Catalytic alkene cyclization reactions for the stereoselective synthesis of complex "terpenoid-like" heterocycles. *Chem. Sci.* **2013**, *4*, 292–296. DOI: 10.1039/C2SC21405A

18 A. C. A. D'Hollander, L. Peilleron, T. D. Grayfer, K. Cariou: Halonium-Induced Polyene Cyclizations. *Synthesis* **2019**, 51, 1753–1769. DOI: 10.1055/s-0037-1612254

19 C. N. Ungarean, E. H. Southgate, D. Sarlah: Enantioselective polyene cyclizations. *Org. Biomol. Chem.* **2016**, *14*, 5454–5467. DOI: 10.1039/C6OB00375C

20 K. Ishihara, S. Nakamura, H. Yamamoto: The First Enantioselective Biomimetic Cyclization of Polyprenoids. *J. Am. Chem. Soc.* **1999**, *121*, 20, 4906–4907. DOI: 10.1021/ja984064+

21 K. Kumazawa, K. Ishihara, H. Yamamoto: Tin(IV) Chloride-Chiral Pyrogallol Derivatives as New Lewis Acid-Assisted Chiral Brønsted Acids for Enantioselective Polyene Cyclization. *Org. Lett.* **2004**, *6*, 15, 2551–2554. DOI: 10.1021/ol049126h

22 K. Surendra, E. J. Corey: Highly Enantioselective Proton-Initiated Polycyclization of Polyenes. *J. Am. Chem. Soc.* **2012**, *134*, 29, 11992–11994. DOI: 10.1021/ja305851h

23 R. J. Felix, C. Munro-Leighton, M. R. Gagné: Electrophilic Pt(II) Complexes: Precision Instruments for the Initiation of Transformations Mediated by the Cation–Olefin Reaction. *Acc. Chem. Res.* **2014**, *47*, 8, 2319–2331. DOI: 10.1021/ar500047j

24 C. A. Mullen, A. N. Campbell, M. R. Gagné: Asymmetric Oxidative Cation/Olefin Cyclization of Polyenes: Evidence for Reversible Cascade Cyclization. *Angew. Chem., Int. Ed.* **2008**, *47*, 6011–6014. DOI: 10.1002/anie.200801423

25 J. G. Sokol, N. A. Cochrane, J. J. Becker, M. R. Gagné: Catalytic platinum-initiated cation-olefin reactions with alkene terminating groups. *Chem. Commun*. **2013**, *49*, 5046–5048. DOI: 10.1039/C3CC41699B

26 H. Nguyen, M. R. Gagné: Enantioselective Cascade Cyclization/Protodemetalation of Polyenes with N_3Pt^{2+} Catalysts. *ACS Catal.* **2014**, *4*, 3, 855–859. DOI: 10.1021/cs401190c

27 S. G. Sethofer, T. Mayer, F. D. Toste: Gold(I)-Catalyzed Enantioselective Polycyclization Reactions. *J. Am. Chem. Soc.* **2010**, *132*, 24, 8276–8277. DOI: 10.1021/ja103544p

28 M. A. Schafroth, D. Sarlah, S. Krautwald, E. M. Carreira: Iridium-Catalyzed Enantioselective Polyene Cyclization. *J. Am. Chem. Soc.* **2012**, *134*, 50, 20276–20278. DOI: 10.1021/ja310386m

29 O. F. Jeker, A. G. Kravina, E. M. Carreira: Total Synthesis of (+)-Asperolide C by Iridium-Catalyzed Enantioselective Polyene Cyclization. *Angew. Chem., Int. Ed.* **2013**, *52*, 12166–12169. DOI: 10.1002/anie.201307187

30 E. E. van Tamelen, E. J. Hessler: The direct brominative cyclization of methyl farnesate. Chem. Commun. **1966**, 411–413. DOI: 10.1039/C19660000411

31 D. Nasipuri, S. R. Ray Chaudhuri: Cyclisation reactions. Part III. Cyclisation of trans-2,3-epoxy-9-*m*-methoxyphenyl-2,6-dimethylnon-6-ene. *J. Chem. Soc., Perkin Trans. 1* **1975**, 262–265. DOI: 10.1039/P19750000262

32 L. E. Wolinsky, D. J. Faulkner: Biomimetic approach to the synthesis of Laurencia metabolites. Synthesis of 10-bromo-α-chamigrene. *J. Org. Chem.* **1976**, *41*, 4, 597–600. DOI: 10.1021/jo00866a003

33 T. Kato, I. Ichinose, S. Kumazawa, Y. Kitahara: Cyclization of polyenes: XII. Direct brominative ring closure of polyenes. Bioorg. Chem. 1975, 4, 188–193. DOI: 10.1016/0045-2068(75)90007-3

34 S. A. Snyder, D. S. Treitler: $Et_2SBr{\cdot}SbCl_5Br$: An Effective Reagent for Direct Bromonium-Induced Polyene Cyclizations. *Angew. Chem., Int. Ed.* **2009**, *48*, 7899–7903. DOI: 10.1002/anie.200903834

35 S. A. Snyder, D. S. Treitler: Synthesis of $Et_2SBr{\bullet}SbCl_5Br$ and its use in biomimetic brominative polyene cyclizations. *Org. Synth*. **2011**, *88*, 54–69. DOI: 10.15227/orgsyn.088.0054

36 A. Sakakura, A. Ukai, K. Ishihara: Enantioselective halocyclization of polyprenoids induced by nucleophilic phosphoramidites. *Nature* **2007**, *445*, 900–903. DOI: 10.1038/nature05553

37 S. A. Snyder, D. S. Treitler, A. P. Brucks: Simple Reagents for Direct Halonium-Induced Polyene Cyclizations. *J. Am. Chem. Soc.* **2010**, *132*, 40, 14303–14314. DOI: 10.1021/ja106813s

38 J. Barluenga, J. M. González, P. J. Campos, G. Asensio: Iodine-Induced Stereoselective Carbocyclizations: A New Method for the Synthesis of Cyclohexane and Cyclohexene Derivatives. *Angew. Chem., Int. Ed. Engl.* **1988**, *27*, 1546–1547. DOI: 10.1002/anie.198815461

39 I. G. Collado, J. G. Madero, G. M. Massanet, F. R. Luis: Partial synthesis of sesquiterpene lactones: a route to 7,11-ene-13-hydroxyeudesmanolides. *J. Org. Chem.* **1991**, *56*, 11, 3587–3591. DOI: 10.1021/jo00011a025

40 C. Ascheberg, J. Bock, F. Buß, C. Mück-Lichtenfeld, C. G. Daniliuc, K. Bergander, F. Dielmann, U. Hennecke: Stable Bromiranium Ions with Weakly-Coordinating Counterions as Efficient Electrophilic Brominating Agents. *Chem. - Eur. J.* **2017**, *23*, 11578–11586. DOI: 10.1002/chem.201701643

41 Y. Sawamura, H. Nakatsuji, A. Sakakura, K Ishihara: "Phosphite–urea" cooperative high-turnover catalysts for the highly selective bromocyclization of homogeranylarenes. *Chem. Sci.* **2013**, *4*, 4181–4186. DOI: 10.1039/C3SC51432C

42 Y. Sawamura, H. Nakatsuji, M. Akakura, A. Sakakura, K. Ishihara: Selective Bromocyclization of 2-Geranylphenols Promoted by Phosphite–Urea Cooperative Catalysts. *Chirality* **2014**, *26*, 356–360. DOI: 10.1002/chir.22297

43 C. Recsei, C. S. P. McErlean: Accessing Brominated Natural Product Motifs Using Phosphoramidite Catalysis. *Aust. J. Chem.* **2015**, *68*, 555–565. DOI: 10.1071/CH14539

44 Y. Sawamura, Y. Ogura, H. Nakatsuji, A. Sakakura, K. Ishihara: Enantioselective bromocyclization of 2-geranylphenols induced by chiral phosphite–urea bifunctional catalysts. *Chem. Commun.* **2016**, *52*, 6068–6071, DOI: 10.1039/C6CC00229C

45 R. C. Samanta, H. Yamamoto: Catalytic Asymmetric Bromocyclization of Polyenes. *J. Am. Chem. Soc.* **2017**, *139*, 4, 1460–1463. DOI: 10.1021/jacs.6b13193

46 Y.-J. Zhao, T.-P. Loh: Asymmetric Total Synthesis of Antiochic Acid. *Org. Lett.* **2008**, *10*, 11, 2143–2145. DOI: 10.1021/ol800499p

47 Y.-J. Zhao, T.-P. Loh: Bioinspired Polyene Cyclization Promoted by Intermolecular Chiral Acetal-$SnCl_4$ or Chiral N-Acetal-$TiCl_4$: Investigation of the Mechanism and Identification of the Key Intermediates. *J. Am. Chem. Soc.* **2008**, *130*, 30, 10024–10029. DOI: 10.1021/ja802896n

48 D. Aynetdinova, R. Jacques, K. E. Christensen, T. J. Donohoe: Alcohols as Efficient Intermolecular Initiators for a Highly Stereoselective Polyene Cyclisation Cascade. *Chem. Eur. J.* **2023**, *29*, e202203732. DOI: 10.1002/chem.202203732

49 J. C. Ma, D. A. Dougherty: The Cation−π Interaction. *Chem. Rev.* **1997**, *97*, 5, 1303–1324. DOI: 10.1021/cr9603744

50 R. R. Knowles, S. Lin, E. N. Jacobsen: Enantioselective Thiourea-Catalyzed Cationic Polycyclizations. *J. Am. Chem. Soc.* **2010**, *132*, 14, 5030–5032. DOI: 10.1021/ja101256v

51 S. Rendler, D. W. C. MacMillan: Enantioselective Polyene Cyclization via Organo-SOMO Catalysis. *J. Am. Chem. Soc.* **2010**, *132*, 14, 5027–5029. DOI: 10.1021/ja100185p

52 R. Breslow, E. Barrett, E. Mohaosi: Free radical additions to squalene *Tetrahedron Lett.* **1962**, *3*, 1207–1211. DOI: 10.1016/S0040-4039(00)70586-7

53 E. J. Corey, S. Lin: A Short Enantioselective Total Synthesis of Dammarenediol II. *J. Am. Chem. Soc.* **1996**, *118*, 36, 8765–8766. DOI: 10.1021/ja9620806

54 W. S. Johnson, W. R. Bartlett, B. A. Czeskis, A. Gautier, C. H. Lee, R. Lemoine, E. J. Leopold, G. R. Luedtke, K. J. Bancroft: The Fluorine Atom as a Cation-Stabilizing Auxiliary in Biomimetic Polyene Cyclizations: Total Synthesis of dl-Dammarenediol. *J. Org. Chem.* **1999**, *64*, 26, 9587–9595. DOI: 10.1021/jo991196s

55 E. J. Corey, G. Luo, L. S. Lin: A Simple Enantioselective Synthesis of the Biologically Active Tetracyclic Marine Sesterterpene Scalarenedial. *J. Am. Chem. Soc.* **1997**, *119*, 41, 9927–9928. DOI: 10.1021/ja972690l

Chapter 2: Electroorganic chemistry and electrochemical generation of reactive species

2.1. General introduction to organic electrochemistry (electro-organic chemistry)

In 1800s Volta's invention of Volta pile, a first documented example of an electric battery [1], offered a more stable source of direct electrical current and allowed the field of electricity to flourish with further discoveries. One of the fields that had emerged was electrochemistry, where transfers of electrons in reactions of oxidations or reductions are triggered by applied electrical potential. Early electroorganic transformations span from Kolbe's electrolysis (1847) of carboxylic acids forming alkyl radicals (Scheme 2.1) [2–4]; to Tafel rearrangement (1907) in synthesis of some hydrocarbons, starting from esters [5]. 20th century has broadened the field of electrochemical transformations in organic chemistry [6,7]. With further development, organic electrosynthesis proved to be important in an industrial setting, with examples such as Simons fluorination process [8] and the Monsanto adiponitrile process [9]. Nonetheless, electrochemistry found its application in total synthesis relatively early with Corey's synthesis of triterpenes (pentacyclosqualene and onoceradiene) [10].

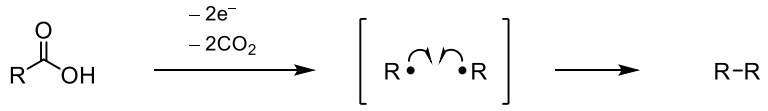

Scheme 2.1*: Kolbe reaction – formation of alkyl radicals from carboxylic acids.*

The simplest electrochemical setup, that has emerged at first, consists of two electrodes in the same reaction chamber (undivided electrochemical cell, Figure 2.1, left). It is a union of two half-reactions, one is happening at the working electrode and the other on the counter electrode. Some intermediates might, upon their generation, undergo undesired oxidation or reduction on the counter electrode. To avoid that side reactivity, chambers can be separated and connected by semipermeable membrane, porous disk, or a salt bridge (divided electrochemical cell, Figure 2.1, right). Another strategy used for cathodic reductions is employment of sacrificial anode that is made of easily oxidizable material. In an undivided setting, such anode is having lower oxidation potential and is being oxidized and dissolved before the newly formed reduced species from the cathode could react in undesired way. [7]

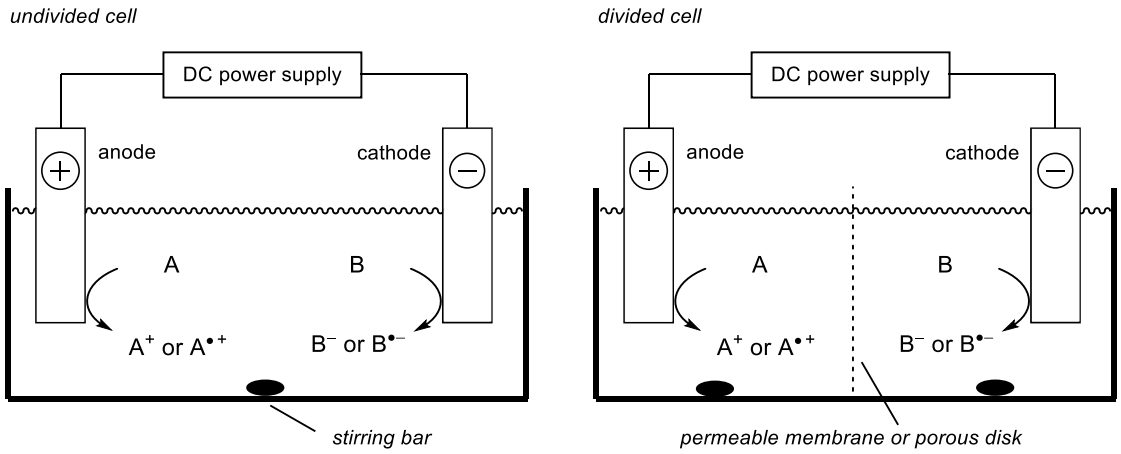

***Figure 2.1**: Undivided and divided electrochemical cell.*

Electrochemical reactions have several inherent parameters which are not present in other types of reactions. Electrical current can be applied as a constant value in galvanostatic conditions and the value of the potential is increasing over time and with the reaction progression. This setting is relatively easy to execute and usually offers full conversion, however, over-oxidation or over-reduction can be problematic. With the invention of potentiostat, reactions could be performed at constant potential [11], with a possibility to use a reference (third) electrode to exactly monitor the potential at the working electrode. This opened a field of voltammetry, and offered new techniques, such as polarography, and even further cyclic voltammetry technique where potential and current are correlated. Selective transformations of functional groups are possible by applying a constant potential, however, with the progression of the reaction the current might drop significantly, leading to partial conversion. [7,12]

Field of organic electrochemistry was developing fast in 20th century and continues its development in 21st century. One of the most studied transformations is Shono oxidation, developed in 1975, which enables functionalization of amines, amides, or carbamates at the α-position to the nitrogen atom [13,14]. The electroorganic field offered a variety of new transformations. Electrogeneration of acid [15] and base [16] offered an alternative to usual acid- and base-mediated reactions; early asymmetric transformations were addressed by the invention of the chiral electrode [17]. A new concept of electroauxiliaries – functional groups that lower electrochemical potentials of substrates – gave an alternative aspect on controlling the regio- and chemoselectivity in electrochemical transformations [18]. Indirect or mediated electrolysis has further expanded possibilities of transformations with electrochemical formation and regeneration of redox agents [19,20]. Nonetheless, paired electrolysis proved that the full advantage of the reactions at both electrodes can be taken even at the industrial scale [21].

2.2. Generation of highly reactive intermediates – cation pool and cation flow methods

Organic electrochemistry offers a straightforward, and therefore very powerful, method for redox transformations by one- or two-electron oxidations or reductions where electrons can be considered as reagents. Formed intermediates are often highly reactive and might be short-lived. Considering this fact, the reaction partner might not be compatible with the conditions electrochemical generation and therefore cannot be present in the reaction mixture at the time of electrolysis. To overcome some of the challenges with reactivity, Yoshida designed and presented an electro-organic technique where reactive intermediate is generated in absence of reaction partner and accumulated in solution – named "cation pool" (Figure 2.2) [22]. This method is focused on generation of cationic species by anodic oxidation and, due to the nature of short-lived intermediates, their accumulation is usually achieved at very low temperature in low concentration. Throughout the years, this method has found various versions and enabled generation of carbon- and heteroatom-centered cations [23]. Electrochemical generation of species has an advantage of being irreversible. In contrast, classical chemical approach of generation, for example, carbenium ions, is usually reversible as the carbon-heteroatom bond cleavage is promoted by acid.

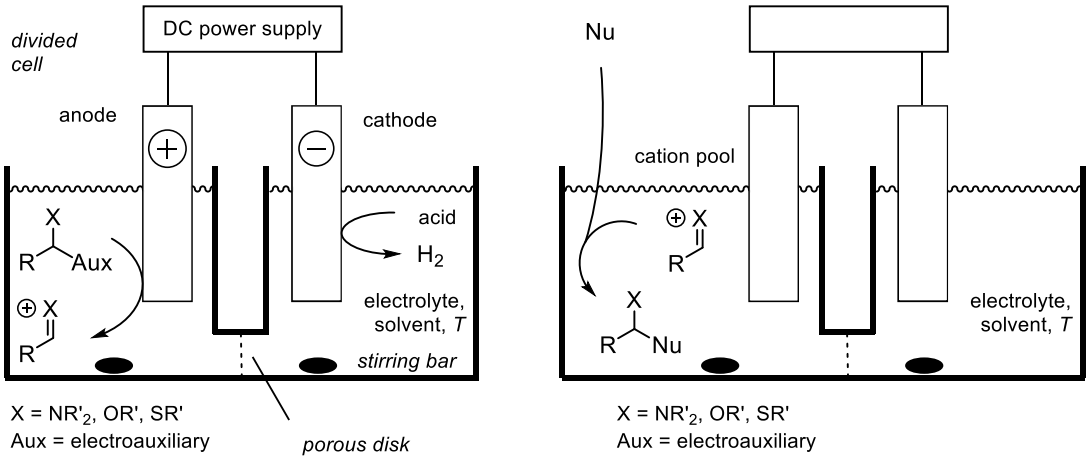

***Figure 2.2**: General example of cation pool generation and accumulation of reactive species (left) with further nucleophile addition (right).*

Especially on a larger scale, electrochemical setup can be improved by introducing the flow technique with microreactors [24]. Such setup (example shown in Scheme 2.2) has a short distance between electrodes and solves conductivity issues of many organic solvents, while high surface-to-volume ratio helps with the efficiency of the reactions happening at the electrode

surface. Due to continuous generation of reactive species, control over mixing with other reaction partners is improved, and reaction times can be extremely short, which enables very fast reactions with potentially highly unstable intermediates.

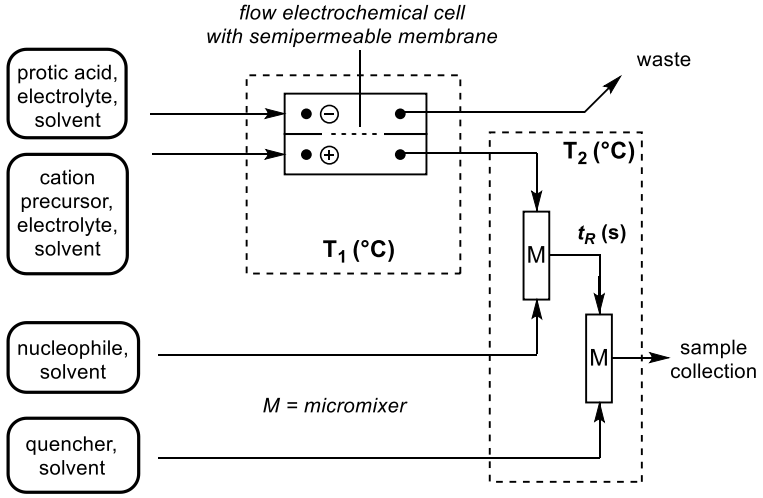

***Scheme 2.2**: Schematic presentation of a cation flow system where electrogenerated cationic species is reacted with nucleophile and reaction is later quenched in flow.*

2.3. Electroauxiliaries

Selectivity in electro-oxidation of substrates is not always easy to achieve, if not impossible, in presence of reaction partner with similar oxidation potential. To decrease oxidation potential and to have better control over oxidation selectivity, functional groups called electroauxiliaries can be introduced into substrates. They increase the energy level of the highest occupied molecular orbital (HOMO) and make the molecule more prone to oxidation, a process which happens with transfer of electron from HOMO orbital to anode. Silyl and arylthio groups are often used as electroauxiliaries at the α-position of the heteroatom (O or N), however, their principle of action is different (Figure 2.3) [18].

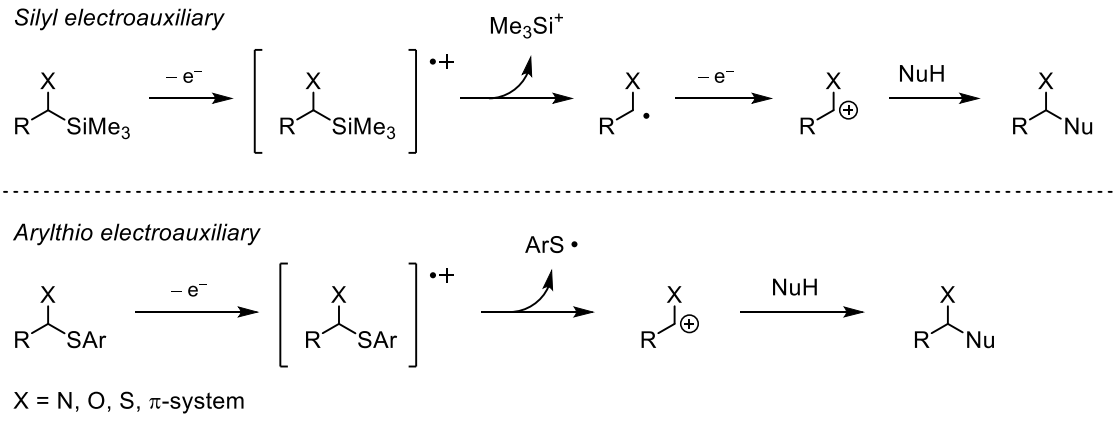

***Figure 2.3**: Principle of action of silyl and arylthio electroauxiliaries.*

Silyl group works on the principle of orbital interaction. If a high-energy filled σ-orbital of C–Si bond is in the same plane as a nonbonding *p*-orbital of the heteroatom (N, O, S), then the energy of this *p*-orbital (which is often HOMO orbital of the heteroatom substrate) will increase through σ-*n* interaction. After one-electron oxidation, formed radical cation decomposes to silyl cation and carbon-centered radical that further transforms to carbocation with one-electron oxidation. [18]

Arylthio electroauxiliary works on a different principle. In comparison with the energy of the other heteroatom (nitrogen or oxygen), energy of the sulfur *p*-orbital is usually much higher, making it the HOMO of the molecule. After the first one-electron oxidation, C–S bond of the formed radical cation is broken and gives sulfur-centered radical and carbocation. Oxidation potential of the ArS electroauxiliary can be easily tuned by changing the substituent on the aryl group – electron donating group will further decrease the oxidation potential. [18]

2.4. Cationic species formed with cation pool or cation flow method

2.4.1. Iminium cations

Nitrogen-substituted carbenium ions are greatly stabilized by nonbonding *p*-orbital of nitrogen and they are closer to the iminium resonance structure. Nitrogen atoms that are bearing electron withdrawing groups are destabilizing corresponding cations, which makes them difficult to manipulate with conventional methods. Therefore, they are good candidates for cation pool method.

Generation of iminium cations was introduced in the first examples of cation pool method and early examples showed generation of *N*-acyliminium ions from the corresponding carbamate (Scheme 2.3) [22]. Low temperature electrolysis (at −72 °C) of (methoxycarbonyl)pyrrolidine in dichloromethane with Bu_4NClO_4 as electrolyte successfully yielded only the corresponding *N*-acylaminium ion, of which structure was confirmed and characterized by NMR and IR spectroscopies. Further addition of allyltrimethyl silane as nucleophile gave the corresponding allylated product. In general, nucleophiles such as cyanide ion, allyl silanes, silyl enol ethers, ketene silyl acetals, Grignard reagents and organozinc compounds proved to be compatible with *N*-acyl iminium cation pools. In further experiments, even combinatorial parallel synthesis was executed where cation pool was generated and then divided to react with several nucleophiles [22].

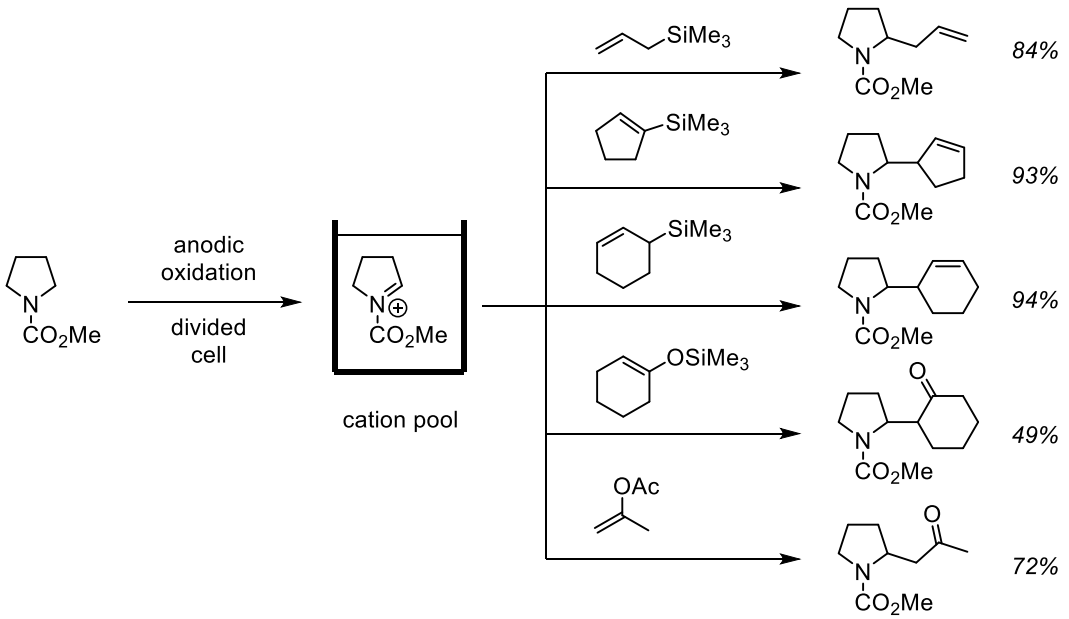

***Scheme 2.3**: First example of iminium cation pool and reactions with nucleophiles.*

Higher temperature (0 °C) electrolysis and accumulation of *N*-acyliminium ions was remarkably achieved in an undivided cell with nitromethane as solvent and $LiClO_4$ as supporting electrolyte (Figure 2.4) [25]. It is presumed that higher stability of cation was enabled by special electrolyte/solvent pair. Further trapping with allyltrimethyl silane proved to be successful and even some azanucleoside derivatives had been synthesized by this method.

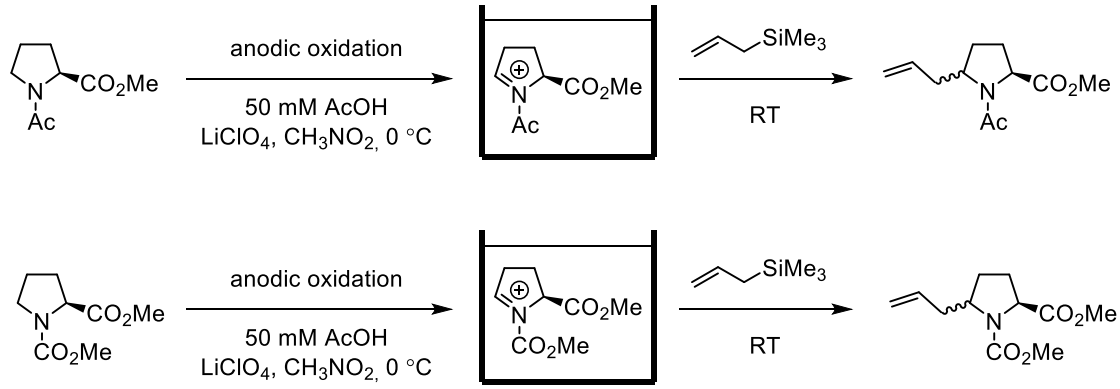

***Figure 2.4**: Iminium cation pool generated at higher temperature.*

Controlled electrolysis of *N*-phenyl amines was reported in ionic liquid and resulting *N*-phenyl iminium cations were reacted with nucleophiles (nitromethane) in presence of triethyl amine (Scheme 2.4) [26].

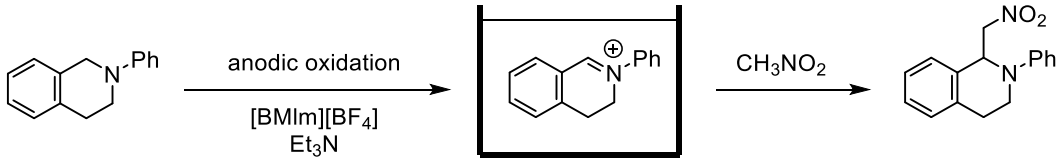

***Scheme 2.4**: Cation pool generated from N-phenyl amine.*

N-acylamines with silyl electroauxiliaries at the α-position relative to nitrogen showed that cation is regioselectively formed at the site of electroauxiliary (Scheme 2.5). If two electroauxiliary groups are present at the same carbon, stepwise double functionalization with different nucleophiles is possible [27]. If these newly introduced groups contain olefinic group, their ring-closing metathesis leads to formation of spirocyclic product.

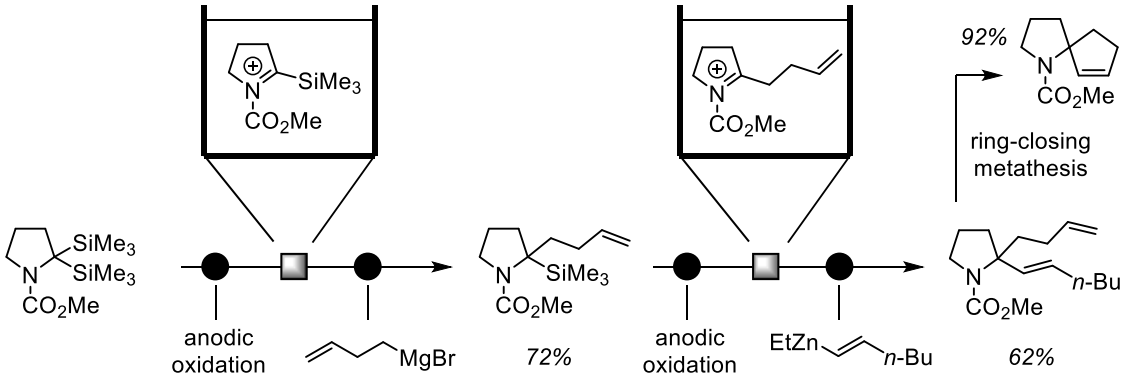

***Scheme 2.5**: Regioselective cation formation due to installed electroauxiliary group and stepwise double functionalization of the substrate.*

Reaction of *N*-acyliminium cations with olefins can lead to various products. One example yields carbohydroxylation of alkenes in diastereoselective fashion (Scheme 2.6) [28]. Some of the cations can take part in multi-component couplings with olefins as shown in Scheme 2.7. Initially, *N*-acyl iminium cation reacts with *N*-acylenamine resulting in accumulation of a new cationic species. Addition of another carbon-based nucleophile (allyl trimethyl silane) results in double functionalization of the starting olefin [29]. Flow approach can greatly improve reaction outcomes of short-lived intermediates. *N*-acyliminiums can participate in cationic polymerization reactions, and molecular weight distribution of such polymers can be well controlled with flow approach, considering fast micromixing, short residence time and rapid termination. With appropriate olefinic substrates, reaction can be controlled in such a way that *N*-acyliminium cations undergo [4+2] cycloaddition, however, styrenyl substrates usually form significant amounts of polymeric side products (Scheme 2.8) [30].

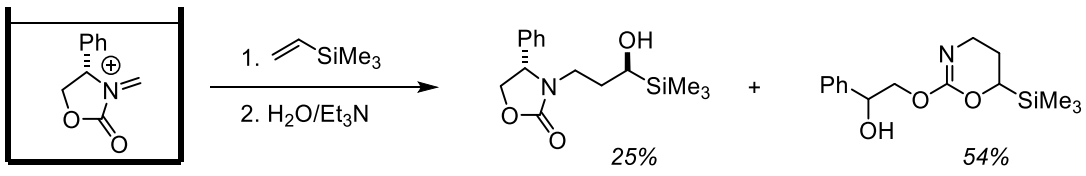

***Scheme 2.6**: Carbohydroxylation of olefin with N-acylimine cation pool.*

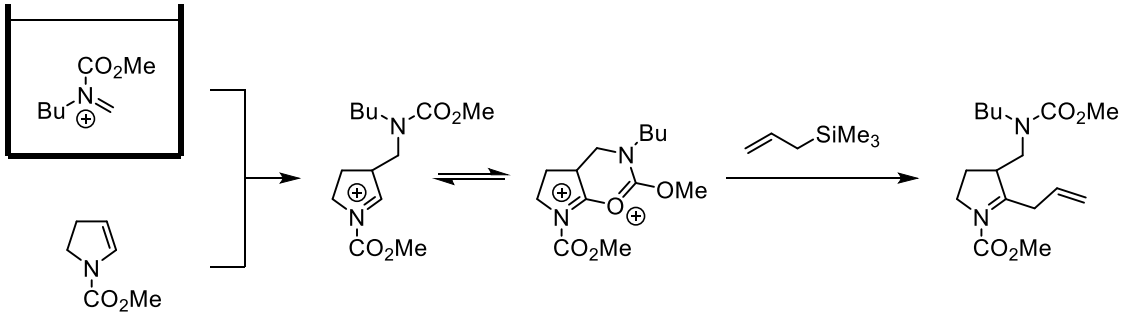

***Scheme 2.7**: Double functionalization of the olefin using cation pool technique.*

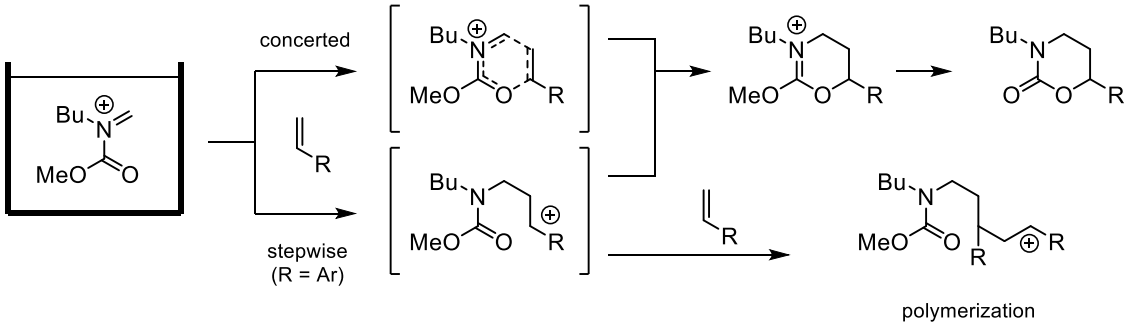

***Scheme 2.8**: Reaction of N-acyliminium cation pool with olefins in [4+2] cycloadditions and polymerizations.*

Electron rich aromatic compounds can react with *N*-acyliminiums in a Friedel-Crafts type of reactions yielding mono- or polyfunctionalized products (Scheme 2.9). Benefits of flow approach with micromixing and short residence time show a better control over monofunctionalization, compared to batch approach [31].

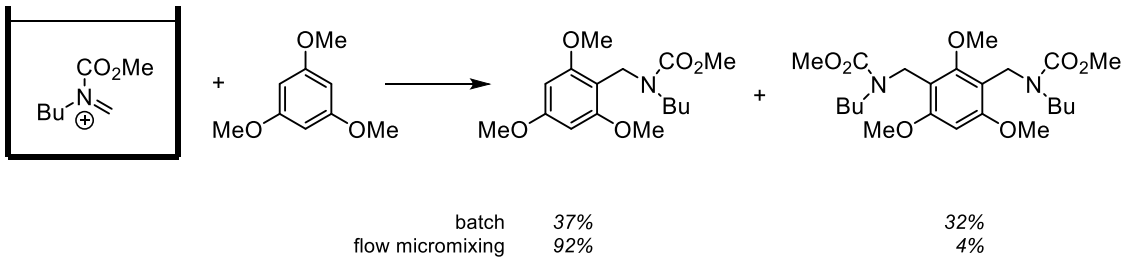

***Scheme 2.9**: Friedel–Crafts reactivity of N-acyliminiums with electron rich aromatic substrates and comparison of batch reaction with flow approach.*

2.4.2. Oxocarbenium and gylcosyl cations

Some of the reactivity and approaches to generation of oxocarbenium cations are more closely presented in the introduction to Chapter 4. Briefly, oxocarbenium cations (or more specifically alkoxycarbenium cations if oxygen atom is bearing an alkyl chain) can be generated in direct cation pool or flow setting with direct anodic oxidation of α-silyl ethers or arylthioacetals (Scheme 2.10). Their generation can also be achieved by indirect approach in cation pool or flow setting where disulfides are undergoing anodic oxidation forming sulfonium ions, which react with thioacetals to form the corresponding oxocarbenium cations.

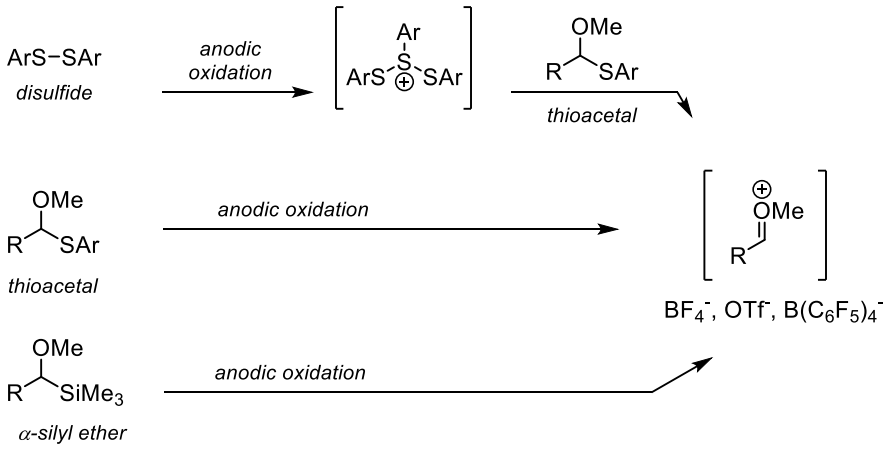

***Scheme 2.10**: Strategies for generation of alkoxycarbenium cations.*

Glycosyl cations are a special kind of oxocarbenium cations, and they proved to be much less stable than typical oxocarbenium cations. Formation of glycosyl cations in the presence of BF_4^- counter anions has yielded corresponding gylcosyl fluorides. Trapping of glycosyl ions with methanol as nucleophile was successful when other supporting electrolytes were used (Bu_4NClO_4, Bu_4NOTf, Bu_4NSbF_6) (Scheme 2.11) [32]. Accumulation of the cation in the presence of OTf^- counteranion showed that glycosyl triflate is the accumulated species and has more covalent rather than ionic character. This pool can react with carbohydrate glycosyl acceptors to form disaccharides (Scheme 2.12) [33]. Iterative glycosylation can be achieved when glycosyl acceptor is another thioglycoside species with free hydroxy group [34].

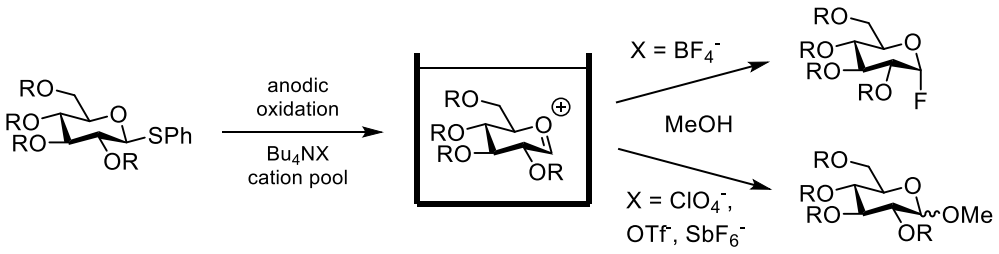

***Scheme 2.11**: Generation of glycosyl cation pool and reaction with methanol in the presence of various counter anions.*

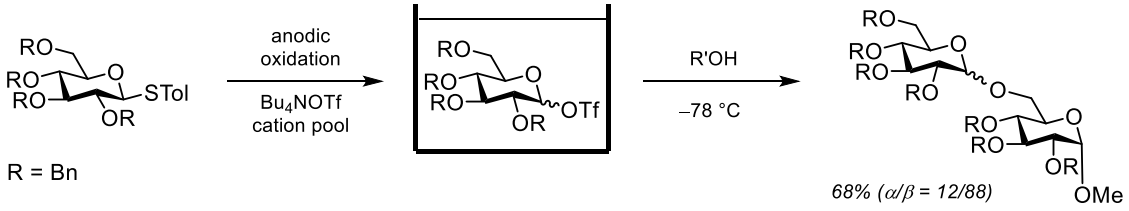

***Scheme 2.12**: Glycosyl cation pool in presence of OTf^- counter anion and formation of disaccharide.*

Indirect glycosyl cation generation was achieved in flow with $B(C_6F_5)_4^-$ as counter anion and further methanol trapping gave the corresponding methoxylated product. [45]

2.4.3. Sulfur cations

Organosulfur cations can be divided in two subgroups, sulfonium ions with structure R_3S^+ and sulfenium ions with structure RS^+. The latter of them, as well as episulfonium ions, are highly unstable and difficult to accumulate in solution. In contrast, many sulfonium ions are stable enough to be suitable for cation pool or flow method [23].

Anodic oxidation of diphenylsulfide was shown to self-dimerize and further nucleophilic attack of other aromatic compounds was not observed (Scheme 2.13) [35]. In the case of anodic oxidation of a mixture of di(*p*-methoxy)sulfide and anisole, the corresponding cationic coupling product was obtained, which could be precipitated as salt (Scheme 2.14) [36].

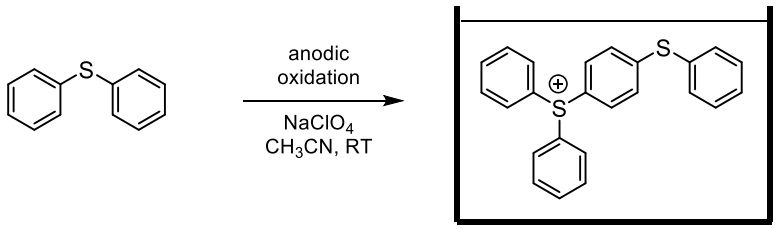

***Scheme 2.13**: Self dimerization of diphenylsulfide in the attempt of generation of cation pool.*

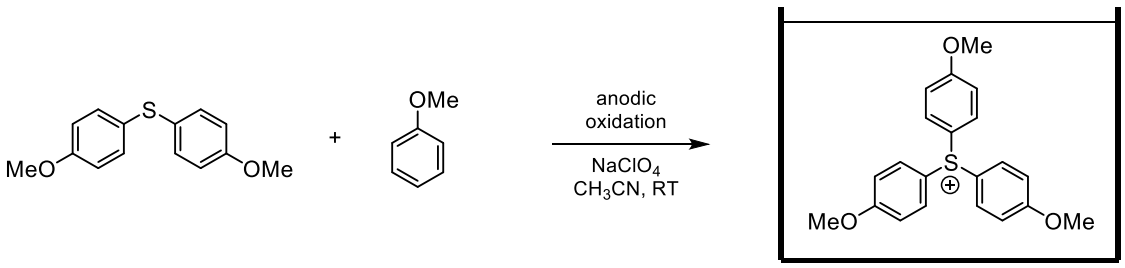

***Scheme 2.14**: Anodic oxidation of diaryl sulfide in presence of anisole.*

The instability of RS^+ species does not allow their generation as isolated species in the solution, however, anodic oxidation of disulfides leads to the formation of their stabilized cationic form – $ArS(ArSSAr)^+$ [37]. Spectroscopic methods (^1H NMR and Raman spectroscopy) and mass spectrometry have supported this hypothesis. The increase of the mentioned stabilized cationic species is observed until the theoretical 2/3 F/mol of electricity is consumed. Further increase of electricity equivalent applied decreases the amount of corresponding cation.

Reactions of $ArS(ArSSAr)^+$ with alkenes interestingly depend on the nature of the quenching reagent (Scheme 2.15) [38]. When hard nucleophiles (water, methanol) are used in the quenching step, addition of ArS group and nucleophile is observed in trans fashion. Quenching with soft nucleophiles (such as triethylamine) leads to trans addition of two ArS groups. Addition across triple bond is also possible in similar fashion with Et_3N as quenching reagent.

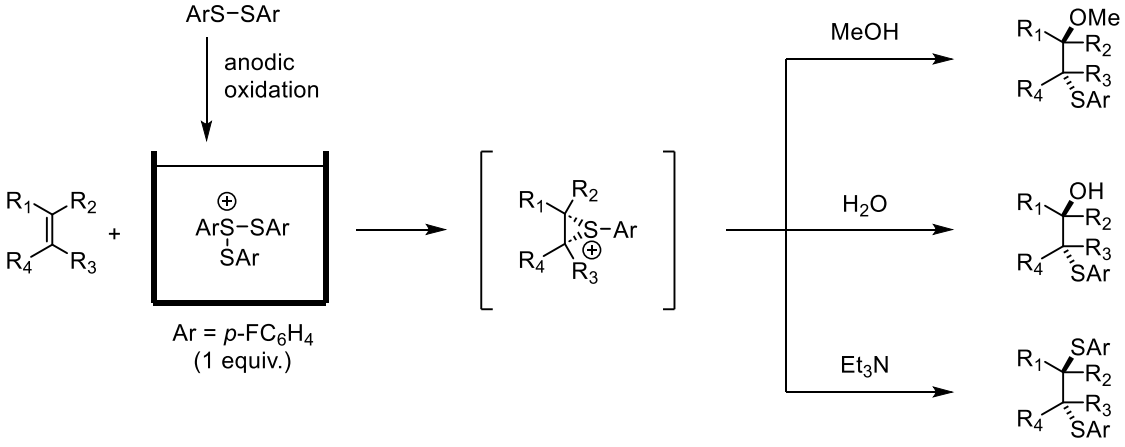

***Scheme 2.15**: Reactions of $(ArSSAr)ArS^+$ cation with olefins and different quenching reagents.*

When reactions of alkenes and alkynes were done at higher temperatures (0 °C) and in absence of quenching reagent, incorporation of fluoride ion was observed from the supporting electrolyte with BF_4^- counter anion (Scheme 2.16) [39]. This offers an alternative method of fluorine incorporation in organic compounds.

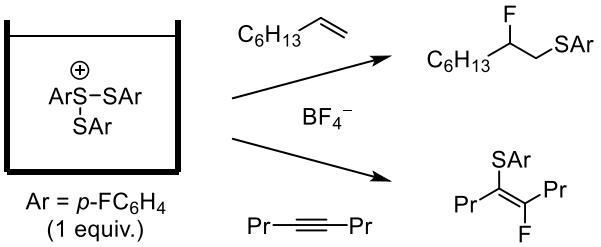

***Scheme 2.16**: Reaction of (ArSSAr)ArS⁺ with alkenes and alkynes in the presence of BF_4^- resulting in fluorine incorporation.*

Cation chain mechanism with catalytic amounts of ArS(ArSSAr)$^+$ was proposed after observations of catalytic processes in presence of stoichiometric disulfides or thioacetals, which can promote cyclizations of 1,6-dienes [40] and thioacetals that contain olefin moiety (Scheme 2.17) [41].

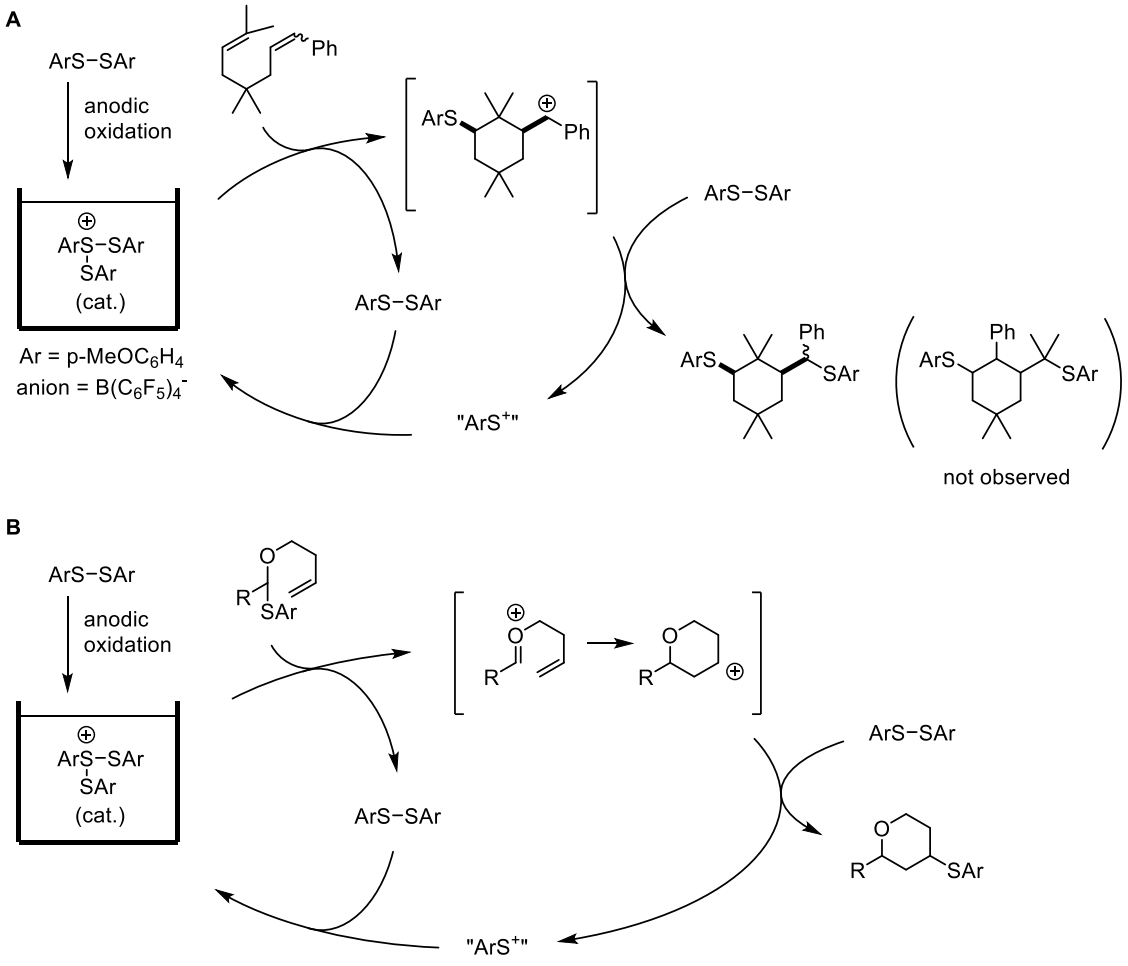

***Scheme 2.17**: Cation chain mechanism with catalytic amounts of (ArSSAr)ArS⁺ in reactions with A) 1,6-dienes; B) olefin-moiety-containing thioacetals.*

2.4.4. Silyl, nitrogen and phosphorous cations

Cation pool technique enables formation of several other heteroatom-centered cation intermediates. Generation of very unstable silyl cations (R_3Si^+) is only possible when stabilization can be achieved intramolecularly, an example is oxidation of disilane with pyridyl moiety in solution with $B(C_6F_5)_4^-$ counteranion (Scheme 2.18) [42]. BF_4^- counteranion in the case of silyl cations results in incorporation of fluoride ion with formation of Si–F bond.

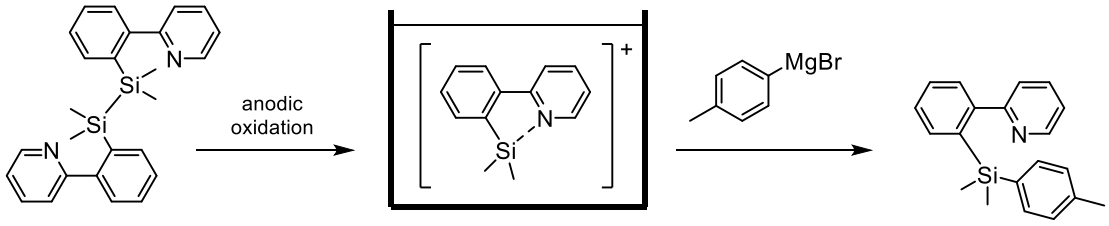

***Scheme 2.18**: Cation pool generation of internally stabilized silyl cations and reaction with Grignard reagent.*

N-arylpyridinium cations can be accumulated by anodic oxidation of corresponding arenes in the presence of pyridines. These salts (Zincke salts) can form aminopyridines after being treated with appropriate nucleophiles. With this method, in one example [43], amino group is introduced to the phenyl ring in the presence of iodo substituent. The latter halogen substituent is often not compatible with aromatic substrate oxidation and further reduction of nitro to amino group.

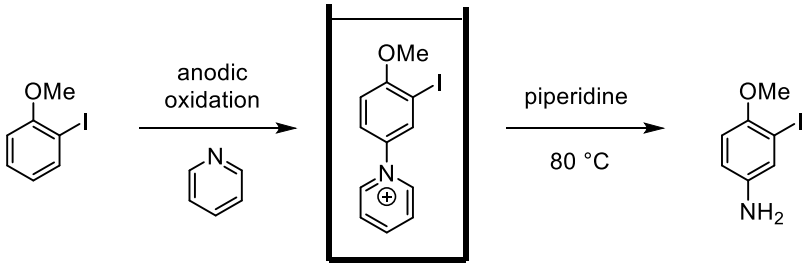

***Scheme 2.19**: Anodic oxidation of arenes in the presence of pyridines and final product of formal amination.*

Various phosphonium cations can also be prepared by anodic oxidations of triphenylphospine in the presence of silyl enol ethers, enol phosphates or enol acetates (Scheme 2.20) [44].

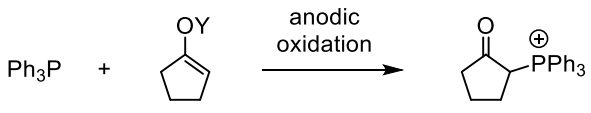

Y = $SiMe_3$, $P(O)(OEt)_2$, COMe

***Scheme 2.20**: Formation of phosphonium cations by anodic oxidation.*

2.5. References

1 A. G. A. Volta. *Nat. Philos. Chem. Arts* **1800**, *4*, 179−187.

2 H. Kolbe. *J. Prakt. Chem.* **1847**, *41*, 138.

3 H. Kolbe: Zersetzung der Valeriansäure durch den elektrischen Strom. [Decomposition of valeric acid by an electric current]. *Liebigs Ann. Chem.* **1848**, *64*, 3, 339–341. DOI: 10.1002/jlac.18480640346

4 H. Kolbe: Untersuchungen über die Elektrolyse organischer Verbindungen. [Investigations of the electrolysis of organic compounds] *Liebigs Ann. Chem.* **1849**, *69*, 3, 257–294. DOI: 10.1002/jlac.18490690302

5 J. Tafel, H. Hahl: Vollständige Reduktion Des Benzylacetessigesters. *Ber. Dtsch. Chem. Ges.* **1907**, *40*, 3312−3318. DOI: 10.1002/cber.190704003102

6 L. Henning: A Century of Organic Electrochemistry. *J. Electrochem. Soc.* **2002**, 149, S21. DOI: 10.1149/1.1462037

7 M. Yan, Y. Kawamata, P. S. Baran: Synthetic Organic Electrochemical Methods Since 2000: On the Verge of a Renaissance. *Chem. Rev.* **2017**, *117*, 21, 13230–13319. DOI: 10.1021/acs.chemrev.7b00397

8 J. H. Simons: Production of Fluorocarbons I. the Generalized Procedure and Its Use with Nitrogen Compounds. *J. Electrochem. Soc.* **1949**, *95*, 47−52. DOI: 10.1149/1.2776733

9 D. E. Danly: Development and Commercialization of the Monsanto Electrochemical Adiponitrile Process. *J. Electrochem. Soc.* **1984**, *131*, 435C. DOI: 10.1149/1.2115324

10 E. J. Corey, R. R. Sauers: The Synthesis of Pentacyclosqualene (8,8′-Cycloönocerene) and the α- and β-Onoceradienes. *J. Am. Chem. Soc.* **1959**, *81*, 7, 1739–1743. DOI: 10.1021/ja01516a054

11 A. Hickling: Studies in electrode polarisation. Part IV.—The automatic control of the potential of a working electrode. *Trans. Faraday Soc.* **1942**, *38*, 27−33. DOI: 10.1039/TF9423800027

12 C. Kingston, M. D. Palkowitz, Y. Takahira, J. C. Vantourout, B. K. Peters, Y. Kawamata, P. S. Baran: A Survival Guide for the “Electro-curious”. *Acc. Chem. Res.* **2020**, *53*, 1, 72–83. DOI: 10.1021/acs.accounts.9b00539

13 T. Shono, H. Hamaguchi, Y. Matsumura: Electroorganic chemistry. XX. Anodic oxidation of carbamates. *J. Am. Chem. Soc.* **1975**, *97*, 15, 4264–4268. DOI: 10.1021/ja00848a020

14 T. Shono: Electroorganic chemistry in organic synthesis. *Tetrahedron* **1984**, *40*, 5, 811–850. DOI: 10.1016/S0040-4020(01)91472-3

15 K. Uneyama, A. Isimura, K. Fujii, S. Torii: Electrogenerated Acid as a Powerful Catalyst for Transformation of Epoxides to Ketones and Acetonides. *Tetrahedron Lett.* **1983**, *24*, 2857−2860. DOI: 10.1016/S0040-4039(00)88043-0

16 P. E. Iversen, H. Lund: Electrolytic Generation of Strong Bases I. Wittig Reaction. *Tetrahedron Lett.* **1969**, *10*, 40, 3523−3524. DOI: 10.1016/S0040-4039(01)88438-0

17 B. F. Watkins, J. R: Behling, E. Kariv, L. L. Miller: Chiral Electrode. *J. Am. Chem. Soc.* **1975**, *97*, 12, 3549−3550. DOI: 10.1021/ja00845a061

18 J. Yoshida. Electroauxiliary. In *Encyclopedia of Applied Electrochemistry*; G. Kreysa, K. Ota, R. F: Savinell, Eds.; Springer: New York, 2014; 386−392

19 E. Steckhan: Indirect Electroorganic Syntheses—A Modern Chapter of Organic Electrochemistry [New Synthetic Methods (59)]. *Angew. Chem. Int. Ed. Engl.* **1986**, *25*, 683−701. DOI: 10.1002/anie.198606831

20 E. Steckhan: Organic Syntheses with Electrochemically Regenerable Redox Systems. In: E. Steckhan, (eds) Electrochemistry I. Topics in Current Chemistry, vol 142. Springer, Berlin, Heidelberg. DOI: 10.1007/3-540-17871-6_11

21 E. Steckhan, T. Arns, W. R. Heineman, D. Hoormann, J. Jörissen, L. Kröner, B. Lewall, H. Pütter: Environmental Protection and Economization of Resources by Electroorganic and Electroenzymatic Syntheses. *Chemosphere* **2001**, *43*, 63−73. DOI: 10.1016/S0045-6535(00)00325-8

22 J. Yoshida, S. Suga, S. Suzuki, N. Kinomura, A. Yamamoto, K. Fujiwara: Direct Oxidative Carbon−Carbon Bond Formation Using the "Cation Pool" Method. 1. Generation of Iminium Cation Pools and Their Reaction with Carbon Nucleophiles. *J. Am. Chem. Soc.* **1999**, *121*, 41, 9546–9549. DOI: 10.1021/ja9920112

23 J. Yoshida, A. Shimizu, R. Hayashi: Electrogenerated Cationic Reactive Intermediates: The Pool Method and Further Advances. *Chem. Rev.* **2018**, *118*, 9, 4702–4730. DOI: 10.1021/acs.chemrev.7b00475

24 J. Yoshida: Flash chemistry using electrochemical method and microsystems. *Chem. Commun*. **2005**, 4509−4516.DOI: 10.1039/B508341A

25 S. Kim, K. Hayashi, Y. Kitano, M. Tada, K. Chiba: Anodic Modification of Proline Derivatives Using a Lithium Perchlorate/Nitromethane Electrolyte Solution. *Org. Lett.* **2002**, *4*, 21, 3735–3737. DOI: 10.1021/ol026713z

26 O. Baslé, N. Borduas, P. Dubois, J. M. Chapuzet, T.-H. Chan, J. Lessard, C.-J. Li: Aerobic and Electrochemical Oxidative Cross-Dehydrogenative-Coupling (CDC) Reaction in an Imidazolium-Based Ionic Liquid. *Chem. Eur. J.* **2010**, *16*, 8162–8166. DOI: 10.1002/chem.201000240

27 S. Suga, M. Watanabe, J. Yoshida: Electroauxiliary-Assisted Sequential Introduction of Two Carbon Nucleophiles on the Same α-Carbon of Nitrogen: Application to the Synthesis of Spiro Compounds. *J. Am. Chem. Soc.* **2002**, *124*, 50, 14824–14825. DOI: 10.1021/ja028663z

28 S. Suga, Y. Kageyama, G. Babu, K. Itami, J. Yoshida: Cationic Carbohydroxylation of Alkenes and Alkynes Using the Cation Pool Method. *Org. Lett.* **2004**, *6*, 16, 2709–2711. DOI: 10.1021/ol049049q

29 S. Suga, T. Nishida, D. Yamada, A. Nagaki, J. Yoshida: Three-Component Coupling Based on the "Cation Pool" Method. *J. Am. Chem. Soc.* **2004**, *126*, 44, 14338–14339. DOI: 10.1021/ja0455704

30 S. Suga, A. Nagaki, Y. Tsutsui, J. Yoshida: "N-Acyliminium Ion Pool" as a Heterodiene in [4 + 2] Cycloaddition Reaction. *Org. Lett.* **2003**, *5*, 6, 945–947. DOI: 10.1021/ol0341243

31 A. Nagaki, M. Togai, S. Suga, N. Aoki, K. Mae, J. Yoshida: Control of Extremely Fast Competitive Consecutive Reactions using Micromixing. Selective Friedel–Crafts Aminoalkylation. *J. Am. Chem. Soc.* **2005**, *127*, 33, 11666–11675. DOI: 10.1021/ja0527424

32 S. Suzuki, K. Matsumoto, K. Kawamura, S. Suga, J. Yoshida: Generation of Alkoxycarbenium Ion Pools from Thioacetals and Applications to Glycosylation Chemistry. *Org. Lett.* **2004**, *6*, 21, 3755–3758. DOI: 10.1021/ol048524h

33 T. Nokami, A. Shibuya, H. Tsuyama, S. Suga, A. A. Bowers, D. Crich, J. Yoshida: Electrochemical Generation of Glycosyl Triflate Pools. *J. Am. Chem. Soc.* **2007**, *129*, 35, 10922–10928. DOI: 10.1021/ja072440x

34 T. Nokami, R. Hayashi, Y. Saigusa, A. Shimizu, C.-Y. Liu, K.-K. T. Mong, J. Yoshida: Automated Solution-Phase Synthesis of Oligosaccharides via Iterative Electrochemical Assembly of Thioglycosides. *Org. Lett.* **2013**, *15*, 17, 4520–4523. DOI: 10.1021/ol402034g

35 F. Magno, G. Bontempelli: Electrochemical Behaviour of Diphenyl Sulfide in Acetonitrile Medium at a Platinum Electrode. *J. Electroanal. Chem. Interfacial Electrochem.* **1972**, *36*, 389−397. DOI: 10.1016/S0022-0728(72)80261-4

36 H. Wendt, H. Hoffelner: Arene-Onium Cations V. Preparative Investigation Concerning Yields and Selectivities for the Anodic Formation of Some Selected Trisarene Sulfonium Cations. *Electrochim. Acta* **1983**, *28*, 1465−1472. DOI: 10.1016/0013-4686(83)85202-5

37 K. Matsumoto, Y. Miyamoto, K. Shimada, Y. Morisawa, H. Zipse, S. Suga, J. Yoshida, S. Kashimura, T. Wakabayashi: Low temperature in situ Raman spectroscopy of an electro-generated arylbis(arylthio)sulfonium ion. *Chem. Commun.* **2015**, *51*, 13106−13109. DOI: 10.1039/c5cc03585f

38 K. Matsumoto, T. Sanada, H. Shimazaki, K. Shimada, S. Hagiwara, S. Fujie, Y. Ashikari, S. Suga, S. Kashimura, J. Yoshida: The Addition of ArSSAr to Alkenes: The Implications of a Cationic Chain Mechanism Initiated by Electrogenerated ArS(ArSSAr)$^+$. *Asian J. Org. Chem.* **2013**, *2*, 325−329. DOI: 10.1002/ajoc.201300017

39 S. Fujie, K. Matsumoto, S. Suga, J. Yoshida: Thiofluorination of Carbon–Carbon Multiple Bonds Using Electrochemically Generated ArS(ArSSAr)$^+$BF4$^-$. *Chem. Lett.* **2009**, *38*, 1186−1187. DOI: 10.1246/cl.2009.1186

40 K. Matsumoto, S. Fujie, S. Suga, T. Nokamia, J. Yoshida: Addition of ArSSAr to dienes via intramolecular C–C bond formation initiated by a catalytic amount of ArS$^+$. *Chem. Commun.* **2009**, 5448−5450. DOI: 10.1039/B910821A

41 K. Matsumoto, S. Fujie, K. Ueoka, S. Suga, J. Yoshida: An Electroinitiated Cation Chain Reaction: Intramolecular Carbon–Carbon Bond Formation between Thioacetal and Olefin Groups. *Angew. Chem. Int. Ed.* **2008**, *47*, 2506–2508. DOI: 10.1002/anie.200705748

42 B. Gostevskii, G. Silbert, K. Adear, A. Sivaramakrishna, D. Stalke, S. Deuerlein, N. Kocher, M. G. Voronkov, I. Kalikhman, D. Kost: Donor-Stabilized Silyl Cations. 9. Two Dissociation Patterns of Hexacoordinate Silicon Complexes: A Model Nucleophilic Substitution at Pentacoordinate Silicon. *Organometallics* **2005**, *24*, 12, 2913–2920. DOI: 10.1021/om0500568

43 T. Morofuji, A. Shimizu, J. Yoshida: Electrochemical C−H Amination: Synthesis of Aromatic Primary Amines via N-Arylpyridinium Ions. *J. Am. Chem. Soc.* **2013**, *135*, 13, 5000–5003. DOI: 10.1021/ja402083e

44 T. Takanami, A. Abe, K. Suda, H. Ohmori: Anodic oxidation of triphenylphosphine in the presence of enol silyl ethers or enol esters. Electrochemical one-step preparation of 2-oxocycloalkyltriphenylphosphonium tetrafluoroborates. *J. Chem. Soc., Chem. Commun.* **1990**, 1310–1311. DOI: 10.1039/C39900001310

45 K. Saito, K. Ueoka, K. Matsumoto, S. Suga, T. Nokami, J. Yoshida: Indirect Cation-Flow Method: Flash Generation of Alkoxycarbenium Ions and Studies on the Stability of Glycosyl Cations. *Angew. Chem. Int. Ed.* **2011**, *50*, 5153–5156. DOI: 10.1002/anie.201100854

Chapter 3: Iridium-mediated nitrene-initiated cyclizations

This work has been done with Eleonora Tufano, Matteo Barilli, Emanuele Casali, Marta Morana, and in collaboration with prof. Sukbok Chang and his group members Euijae Lee, Hoimin Jung, Jihye Kang, and Dongwook Kim.

3.1. Introduction

Azacycles can be found in various natural products, synthetic building blocks, pharmaceuticals, or other molecular materials [1]. For example, decahydroquinoline skeleton can be found in several biologically active molecules, some of them are shown in Figure 3.1. Among aza-cycle-containing compounds, aza-steroids are possessing skeletons of ring-fused aza-cycles, where incorporation of the nitrogen atom arises during their biosynthesis, which is catalyzed by cyclases. These frameworks are showing interesting biological properties and therefore new synthetic methodologies for their synthesis are highly desired, especially if they offer stereoselective ring-fused framework construction. Aza-steroids are structurally modified steroids and, therefore, biomimetic cyclization reactions would be of a great interest for their synthesis. One example is Finasteride [2], inhibitor of Type II steroid 5α-reductase, clinically used for the treatment of benign prostatic hyperplasia, and additionally used as an oral drug for treatment of male pattern hair loss. Inspired by the previously described facts, we were trying to explore the possibility of aza-steroidal framework formation in a cyclization cascade.

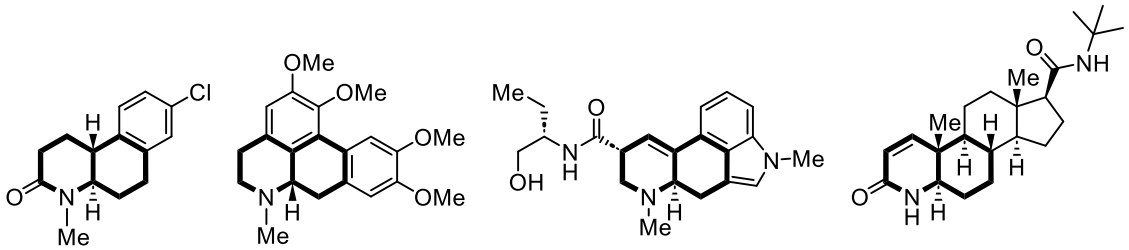

Bexlosteride (+)-Glaucine Methysergide Finasteride

***Figure 3.1**: Decahydroquinoline framework in biologically active compounds.*

Our attention was drawn by Chang's work on nitrenoid transfer within olefinic substrates that leads to allylic lactams [3]. The main interest was focused on reaction mechanism that proceeds through formal carbocation. It has been shown that olefinic dioxazolones serve as as nitrenoid precursors, and a variety of products can be obtained, namely, allylic *γ*-lactams **i2**, *γ*-lactams with enamine motif **i3**, and *δ*-lactams **i4** (Figure 3.2). Transformations were obtained with 10 mol% of iridium catalysts, with addition of $NaBAr^F_4$ in HFIP at 60 °C for 12 h.

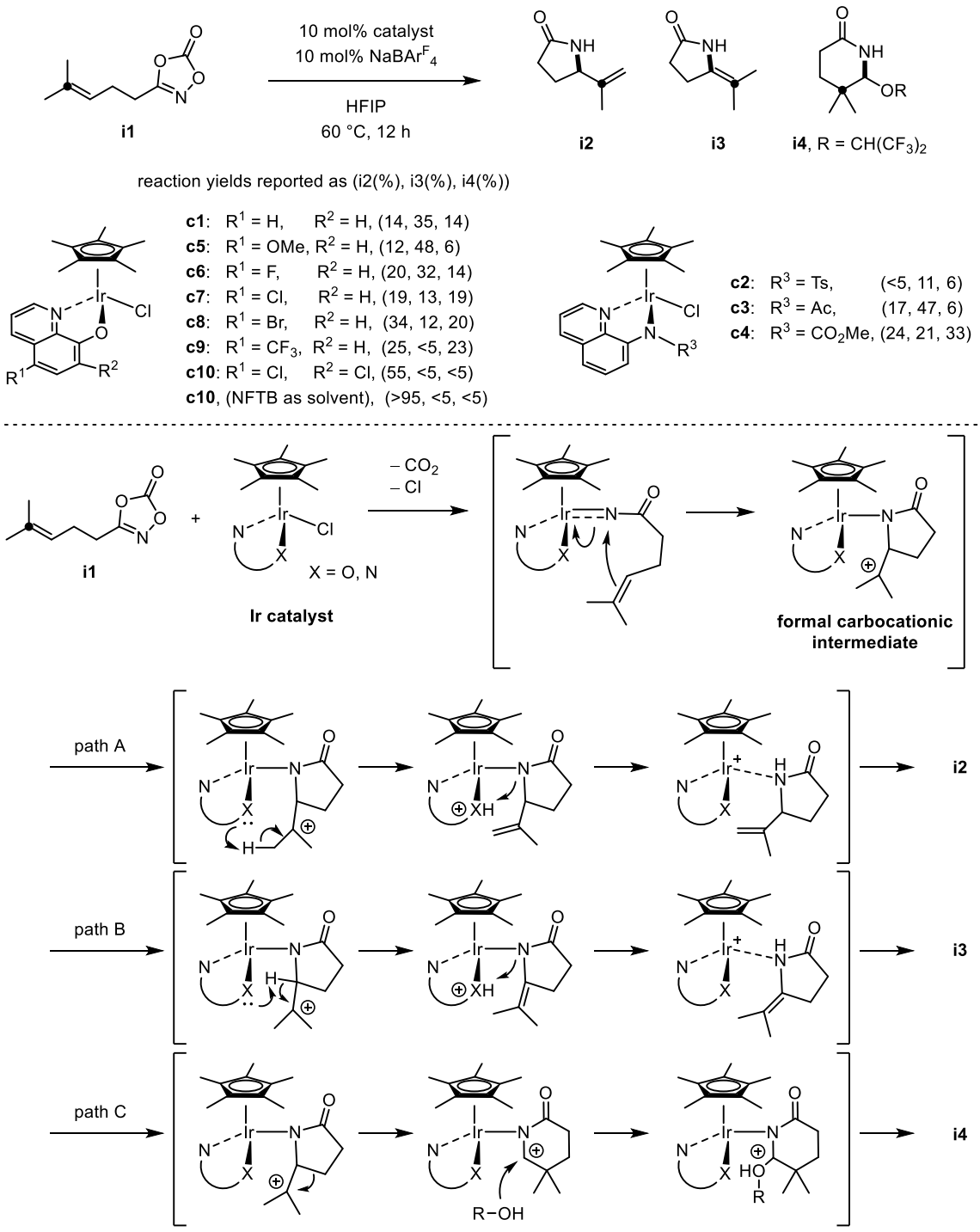

***Figure 3.2**: Acyl nitrenoid transfer in olefinic substrates - ligand design, reaction outcome and proposed reaction mechanism.*

With the optimization of their iridium catalyst by varying the ligand structure (Figure 3.2), highly selective transformations were achieved with major product **i2**. Further substrate scope screening of olefin substituents (Scheme 3.1) has shown that with even lower catalyst loading of **c10** and HFIP or NFTB as solvents, desired products **i6** have been obtained in modest to excellent yields. Results prove that reactivity can be modified by catalyst design.

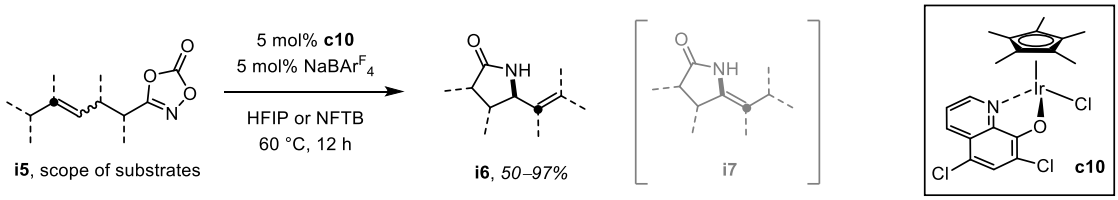

***Scheme 3.1**: Synthesis of allylic lactams from various substrates.*

Further trapping of formal carbocation with external nucleophile, which was used as a solvent, (Scheme 3.2) has given us good grounds to believe that incorporation of nucleophiles is possible. In fact, with their further work [4] they have shown that nucleophiles can be introduced in excess, but not as solvents, and that certain catalysts are able to make the transformations already at room temperature (Scheme 3.3). With (hetero)aryl external nucleophile trapping (Scheme 3.4), we had good grounds to design substrates that would undergo biomimetic cascade cyclization with (hetero)aryl termini.

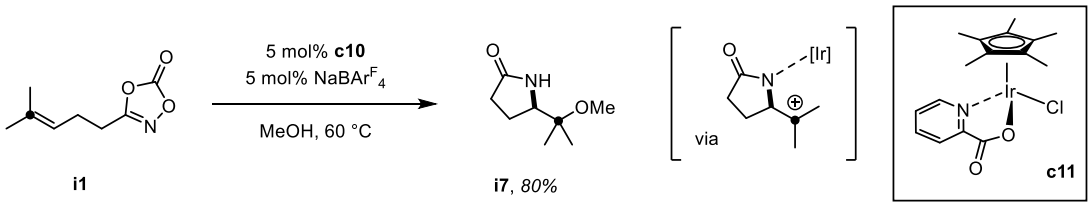

***Scheme 3.2**: Trapping of formal carbocation with external nucleophile which is used as a solvent.*

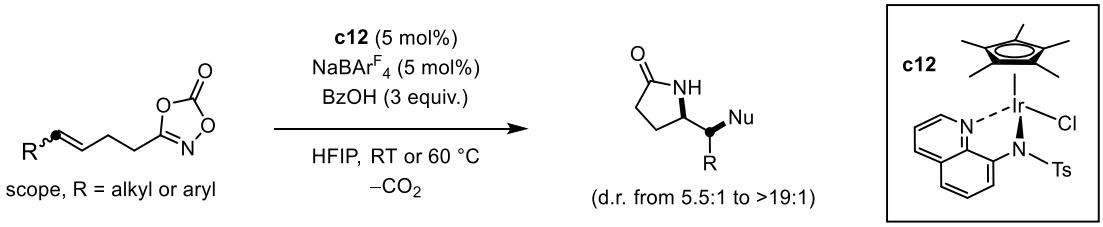

***Scheme 3.3**: Scope of olefinic dioxazolones for alkene difunctionalization.*

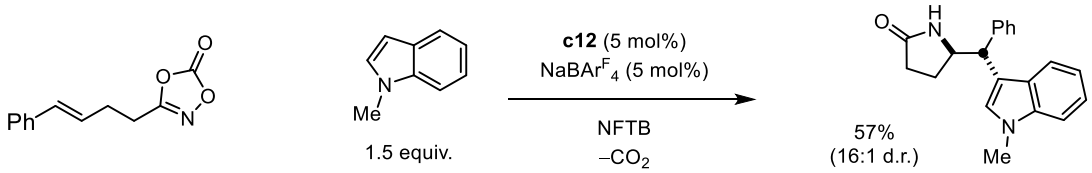

***Scheme 3.4**: Lactam formed after iridium-nitrenoid transfer, resulting in double functionalization of alkene using heteroaryl nucleophile.*

3.2. Results and discussion

3.2.1. Experimental results and observations

We started the research based on our working hypothesis that alkenyl dioxazolones would be suitable substrates to undergo electrophilic iridium-acylnitrenoid transfer to double bonds. This intramolecular process was envisioned not to stop at this stage but rather to continue in a cascade, intramolecularly reacting with nucleophilic moieties. Those could be additional multiple bonds or terminating (hetero)aryl groups, as is observed in several examples of polyene cyclizations. This process would yield polycyclic ring-fused *δ*-lactam compounds.

Suitable dioxazolones had to be designed to test our hypothesis. Having the inspiration from polyene cyclizations, dioxazolones with an alkyl chain bearing double bond and an aryl terminus have been the first choice. With the first substrate (*E*)-phenylalkenyl dioxazolone (**3.1a**) an array of Cp*Ir(III) catalysts was screened (Table 3.1). Reaction of **3.1a** in 1,1,1,3,3,3-hexafluoro-propan-2-ol (HFIP) held at room temperature for 12 h with iridium catalyst **Ir1** (5 mol%), which was bearing unsubstituted 8-hydroxyquinoline ligand, gave 17% yield of the corresponding tricyclic lactam **3.2a** (entry 1). Despite the low yield, we observed that the desired cyclization cascade took place and encouraged us to find better reaction conditions. X-ray crystallographic analysis has unambiguously confirmed that the structure of the tricyclic lactam **3.2a** was having a trans-fused decahydroquinolinone framework.

We observed that variation in substitution of the LX-type co-ligand in the Cp*Ir(III)(κ^2-LX) catalyst system impacted the reaction yield, while the *trans*-diastereoselectivity was maintained in all cases. Catalyst **Ir2** with 5-nitro group in the 8-hydroxyquinoline ligand gave high conversion of the starting material (77%) with increased product yield of 44% (Table 3.1, entry 2). With the incorporation of the halogens in the 8-hydroxiquinoline ligand, corresponding catalysts having halide substituents such as fluoro (**Ir3**), chloro (**Ir4**) and iodo (**Ir5**), were giving lower yields (entries 3–5) compared to nitro-substituted catalyst. Additional methyl group at the C2 position of 8-hyroxyquinoline ligand has significantly improved the reaction yield. With **Ir6** (2-methyl-5-nitro-8-hydroxyquinoline ligand) the product **3.2a** was formed in 65% yield (comparing entries 6 and 2), while **Ir7** (5,7-dichloro-2-methyl-8-hydroxyquinoline) gave 72% yield (comparing entries 7 and 4). When reaction with **Ir7** catalyst was performed in NFTB (nonafluoro-*tert*-butanol) instead of HFIP, the yield was slightly lower but still comparable

(entry 10) which offers NFTB as a possible reaction solvent alternative. In contrast, reaction in dichloromethane under otherwise identical reaction conditions gave the product in only 7% (entry 11), which proved that perfluorinated alcohols are vital for good reaction outcome. Reaction proved to not be operational without catalyst (control experiment) where conversion of the starting material was less than 5% and cyclization product **3.2a** was not detected (entry 9).

***Table 3.1**: Optimization of iridium catalysts in initial cyclization reactions of (E)-olefinic aryldioxazolone **3.1a**.*

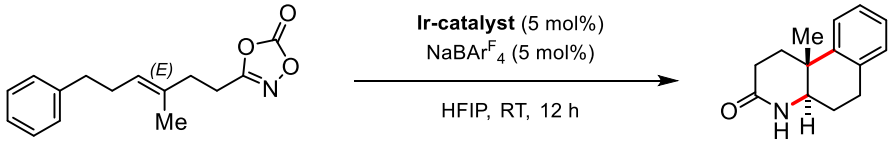

3.1a **3.2a**

Entry	Catalyst	Conversion (%)	Yield (%)
1	**Ir1**	22	17
2	**Ir2**	77	44
3	**Ir3**	73	10
4	**Ir4**	24	16
5	**Ir5**	57	27
6	**Ir6**	> 95	65
7	**Ir7**	> 95	72
8	**Ir8**	11	11
9	**none**	< 5	n.d.
10	**Ir7**	80	68[a]
11	**Ir7**	13	7[b]

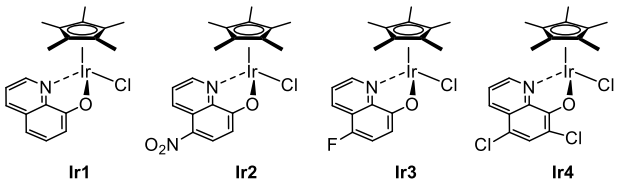

Conditions: substrate **3.1a** (0.1 mmol), catalyst (5 mol %) and NaBAr$^F_4$ (5 mol %) in HFIP (0.5 mL) at room temperature for 12 h. Yields were determined by ^{1}H NMR analysis of the crude reaction mixture. n.d. – not detected. a) NFTB was used as the solvent instead of HFIP. b) Dichloromethane was used as the solvent instead of HFIP.

To expand the scope of substrates and to evaluate generality of the optimal reaction conditions obtained above, we designed a variety of (*E*)-alkenyl dioxazolones with differently substituted arenes as terminating groups (Figure 3.3). Electron rich aryl groups bearing methoxy groups have shown good to excellent yields. Dimethoxy substrate gave the corresponding product **3.2b** in 91% yield even on larger (2 mmol) scale, showing that reaction is operational even when scaled up. 3-methoxy substrate gave a combined yield of 88% of the corresponding two constitutional isomers in 1.3:1 ratio which were separable by silica column chromatography. Cyclization termination event has occurred either at the ortho-position (relative to methoxy group) yielding the product **3.2g*o*** in 38% yield; or at the para-position to give product **3.2g*p*** in 50% yield. Results show that there was a very low selectivity between the relative ortho- and para-position.

Dioxazolone substrate with 4-methoxy group gave 59% yield of the product **3.2c**, and slightly lower cyclization yield (compared to 3-methoxy and 3,5-dimethoxy substrates) could be rationalized with meta-position (relative to formation of the new bond) of the methoxy substituent that cannot as effectively stabilize the transition state after the attack of the electrophile on the aryl ring. Highly substituted bromodimethoxy substrate was able to undergo the cyclization event and gave the corresponding product **3.2f** in 57% yield. Moreover, one-pot reaction – to yield the same product – was performed starting from dioxazolone **3.1b**, where subsequent bromination with NBS in HFIP and further cyclization with iridium catalyst gave the corresponding product **3.2f** in 63% yield. Bromine group can function as a handle for further functionalizations, such as cross-couplings, and demonstrates the possible utility of our protocol for molecular synthesis. Substrates with 4-methylphenyl or even naphthalene termini were viable to give the corresponding products **3.2d** and **3.2e**, respectively, in yields above 80%.

Several terminating groups were successfully participating in the cyclization cascade of monoolefinic substrates and results led us to investigate the cascade cyclization events with substrates possessing additional double bonds, namely, we prepared bisolefinic substrates **3.1h** and **3.1i**, having *E*-configuration at both alkene moieties. General reaction conditions, used in previous cyclizations, readily afforded the corresponding tetracyclic *δ*-lactams (Figure 3.3). Product with unsubstituted phenyl ring **3.2h** was obtained in 59% yield, while dimethoxy substituted product **3.2i** was produced in 68% yield. In both reactions only one diastereoisomer was observed even though four new consecutive stereogenic carbon centers had been formed.

Since (*E*)-olefinic dioxazolones exhibited trans-selectivity and cyclization products had been exclusively obtained as single diastereoisomers, we were interested to see if similar diastereoselectivity can be obtained in the cyclization of (*Z*)-olefinic dioxazolones and if these results can provide us with some information on mechanistic details.

***Figure 3.3**: Cyclization scope of (E)-olefinic dioxazolone substrates.*

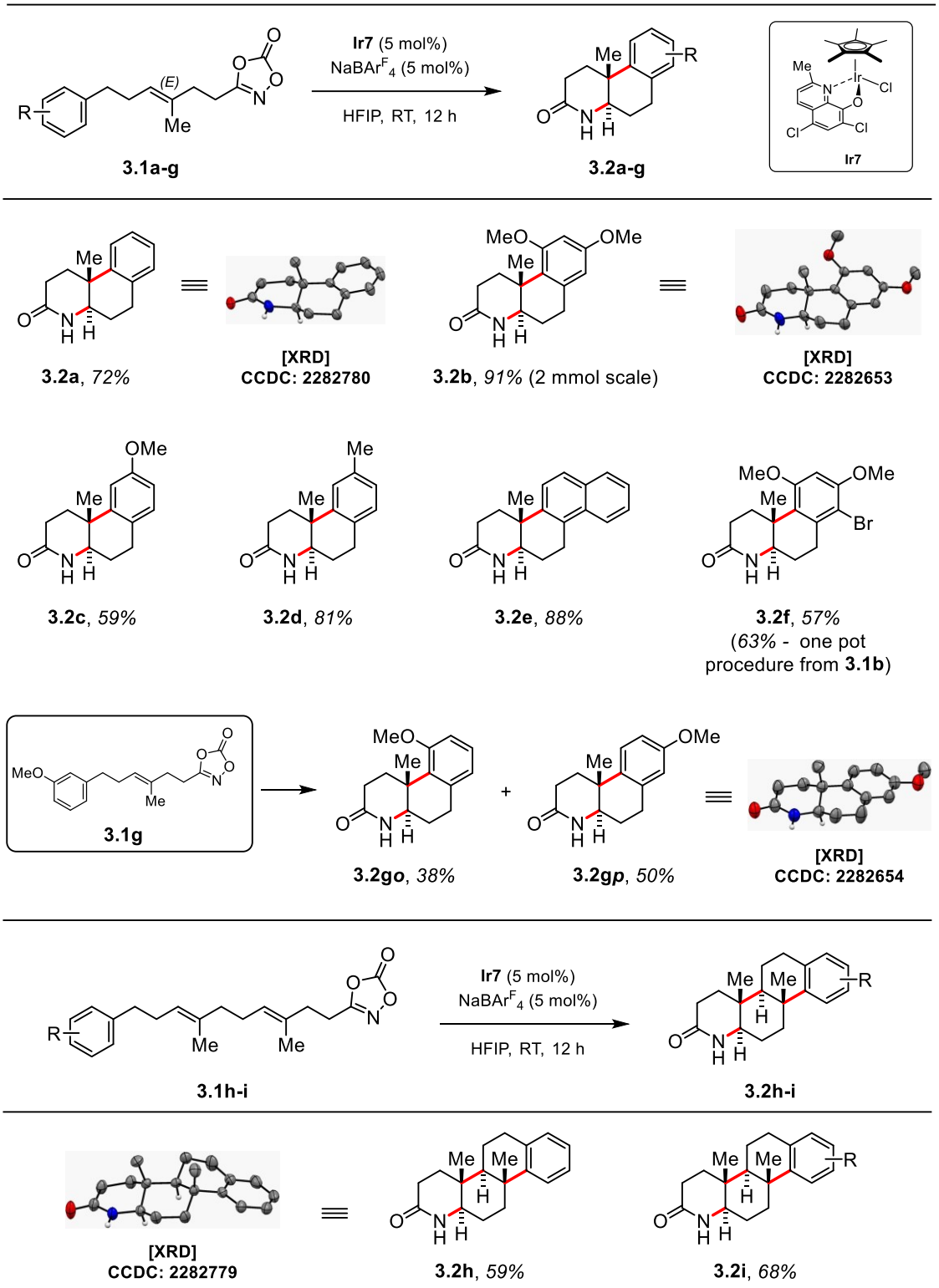

Conditions: substrate **3.1** (0.1 mmol, 1.0 equiv.), **Ir7** (5 mol %), NaBAr$^F_4$ (5 mol %), and HFIP at room temperature for 12 h. Reported isolated yields. The relative *trans* configuration of products **3.2** was determined using NMR spectroscopy and/or single crystal X-ray diffraction (SC-XRD) analysis.

***Table 3.2**: Screening of iridium catalysts in cyclization reactions of (Z)-olefinic aryldioxazolone*

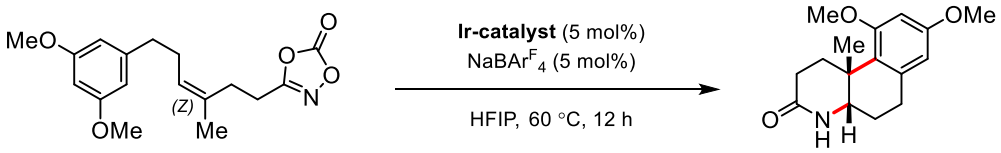

3.3a **3.4a**

Entry	Catalyst	Yield (Conversion) (%)
1	**Ir2**	8 (23)
2	**Ir6**	13 (37)
3	**Ir7**	25 (55)
4	**Ir7**	n.d.[a] (< 5)
5	**Ir8**	58 (72)

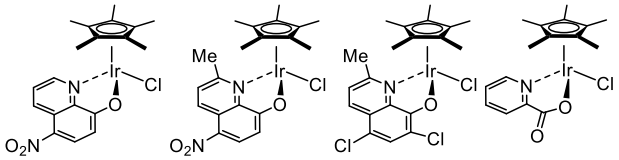

Ir2 **Ir6** **Ir7** **Ir8**

Conditions: **3.3a** (0.1 mmol), catalyst (5 mol %) and NaBAr$^F_4$ (5 mol %) in HFIP at 60°C for 12 h. Yields were determined by ^{1}H NMR analysis of the crude reaction mixture. a) Reaction at room temperature instead of 60°C.

We have prepared the (*Z*)-olefinic dioxazolones with the same aryl terminating groups as in the scope of (*E*)-olefins, except for naphthyl group and bromine containing densely substituted phenyl group. When (*Z*)-olefin **3.3a** was subjected to previous standard conditions (**Ir7** – 5 mol%, NaBAr$^F_4$ – 5 mol%, HFIP, RT, 12 h) no cyclization product was not detected (Table 3.2, entry 4). However, we were delighted that the same reaction conditions at the elevated temperature (60 °C) obtained the cis-fused decahydroquinolinone **3.4a** as the only diastereoisomer, although in low yield of 25% (entry 3). Results of reactions at elevated temperature with catalysts **Ir2** and **Ir6** gave yields of less than 15% (entries 1 and 2, respectively). In contrast, with catalyst **Ir8**, which is bearing a picolinic acid co-ligand, and under elevated reaction temperature (60 °C), we observed a significant improvement in cyclization product yield, reaching 58% (entry 5). We decided to examine the scope of the (*Z*)-olefinic dioxazolones with these new conditions employing **Ir8** catalyst (Figure 3.4). Substrate **3.3b**, with a 4-methoxy substituent on the phenyl ring, gave the corresponding cyclized product **3.4b** in 50% yield. The 3-methoxy substituted substrate **3.3e** exhibited a very good cyclization outcome with 74% combined yield of two constitutional isomers in 1.2:1 ratio, separable by silica column chromatography. Selectivity between the possible cyclization sites was again very low and ortho-cyclized (relative to methoxy group) product **3.4e*o*** was formed in 34% yield, while para-cyclized product **3.4e*p*** was obtained in 40% yield. With less electron rich phenyl termini, either with no substituents or with 4-methyl substituent, corresponding decahydroquinolinones **3.4c** and **3.4d** were isolated in 36% and 38% yields, respectively.

Scopes of (*E*)- and (*Z*)-olefinic aryldioxazolones suggest that in all cases electrophilic nitrenoid-initiated cyclizations proceed through a tight chair-like transition state, based on Stork-Eschenmoser hypothesis [5,6], where relative stereochemistry of the products reflects the initial alkene geometry. Additionally, polyene cyclization strategies that involve *Z*-alkenes in preparation of cis-fused decalin frameworks are rare [7–9]. Therefore, synthesis of such cis-fused systems is rather challenging in terms of polyene cyclizations.

***Figure 3.4**: Cyclization scope of (Z)-olefinic dioxazolone substrates.*

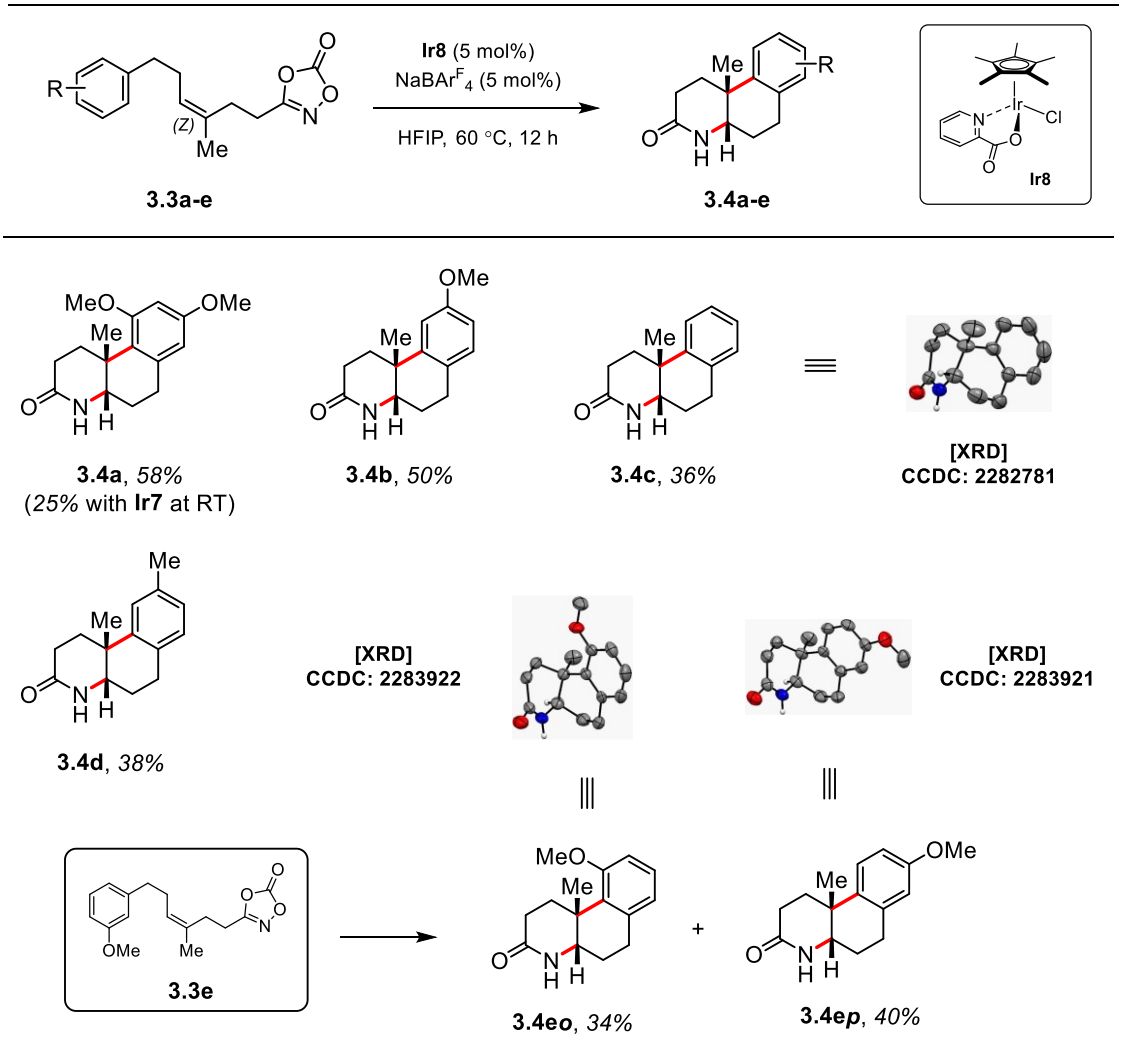

Conditions: substrate **3.3** (0.1 mmol, 1.0 equiv.), **Ir8** (5 mol %), NaBAr$^F_4$ (5 mol %), and HFIP (0.2 M) at 60 °C for 12 h. Reported isolated yields. The relative *cis* configuration of the decahydroquinolinones 3.4 was determined using NMR spectroscopy and/or single crystal X-ray diffraction (SC-XRD) analysis.

***Figure 3.5**: Cyclization scope of dioxazolone substrates with heteroaromatic terminating groups.*

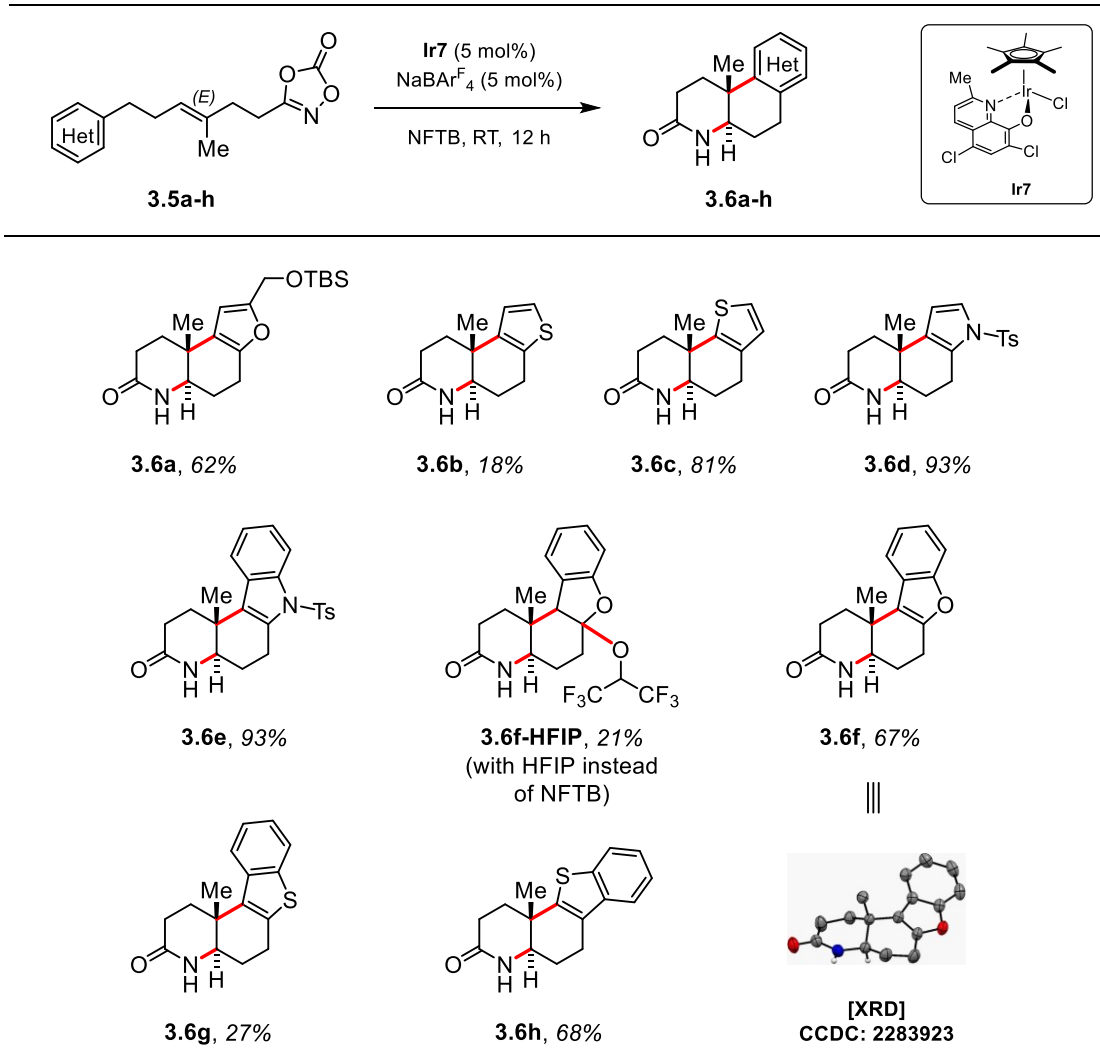

Conditions: substrate **3.5** (0.1 mmol, 1.0 equiv.), **Ir7** (5 mol %), NaBAr$^F_4$ (5 mol %) and NFTB at room temperature for 12 h. Reported isolated yields. The relative trans-configuration of the decahydroquinolinones 3.6 was determined by using NMR spectroscopy and/or single crystal X-ray diffraction (SC-XRD) analysis.

To further expand the scope of substrates participating in iridium-nitrenoid transfer cyclizations we turned to electron rich heterocyclic terminating groups (Figure 3.5). We observed that reaction in HFIP can lead to incorporation of HFIP moiety into the polycyclic product skeleton as shown in the case of the compound **3.6f-HFIP**. Therefore, we have switched the solvent to less nucleophilic NFTB (nonafluoro-*tert*-butanol) which proved to be beneficial as its incorporation into the final products was not observed. Several electron-rich heteroarenes exhibited a good ability to participate in cyclization termination event. Pyrrole and indole delivered excellent yields (93%) of cyclization products that cyclized at position 3 of the heterocycle (products **3.6d** and **3.6e**, respectively). Their oxygen analogues, substrates bearing furan and benzofuran, gave good yields when cyclized at position 3 of the heterocycle (products **3.6a** and **3.6f**, respectively).

However, sulfur analogues, thiofuran and benzothiofuran, yielded low amounts of products cyclized at position 3 (products **3.6b** and **3.6g**, respectively). It is speculated that this might be due to innate regiochemical preference for position 2 to be involved in electrophilic heteroaromatic substitution. Indeed, thiofuran and benzothiofuran substrates with free position 2 for aromatic substitution gave corresponding products **3.6c** and **3.6h**, respectively, in much higher yields (81% and 68%, respectively). These results showed that various heteroarenes can participate in cyclization cascade and corresponding heterocycle-fused decahydroquinolinones can be synthesized.

After a broad scope of (hetero)aromatic termini, we further examined feasibility of alkyne moiety to participate in cyclization termination event (Scheme 3.5). C–C triple bonds are known to participate in cyclization events when they are located at the 5,6-position relative to a newly developing cationic center [10]. We observed that cyclization of the alkynyl substrate **3.7** proceeded only in the presence of water (additive) and intriguing cyclization product **3.8** was obtained in 55% yield. Cyclization is rationalized to proceed through vinyl cation intermediate which is captured by water, serving as an external nucleophile, and yields the final acyl silane.

Possibility of asymmetric cyclization was investigated by preparation of the required chiral dioxazolone substrate **3.11** (Scheme 3.6). It was prepared from the corresponding carboxylic acid using Evans auxiliary to install the methyl group and prepare a chiral amide **3.10** as a single diastereoisomer (^{1}H-NMR analysis) [11]. Further steps yielded optically active α-methyl dioxazolone **3.11** (> 99:1 e.r.). When subjected to standard reaction conditions with **Ir7** catalyst, the desired cyclized product **3.12** was obtained in 74% yield with excellent diastereo- (> 99:1 d.r.) and enantioselectivity (> 99:1 e.r.).

***Scheme 3.5**: Cyclization of alkyne substrate*

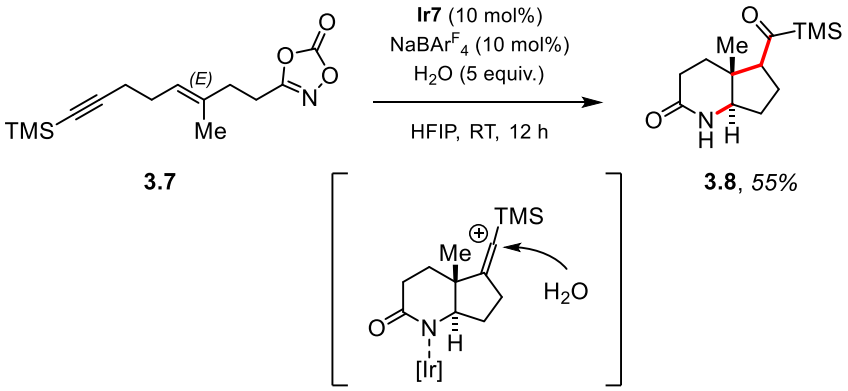

Conditions: substrate **3.7** (0.1 mmol, 1.0 equiv.), **Ir7** (10 mol %), NaBAr$^F_4$ (10 mol %), HFIP, and 5 equiv. of water additive at room temperature for 12 h. [b]Reported isolated yields. The relative configuration of the acyl-silane derivative was determined using NMR spectroscopy - NOESY analysis.

***Scheme 3.6**: Diastereoselective Cyclization of An Optically Active Substrate*

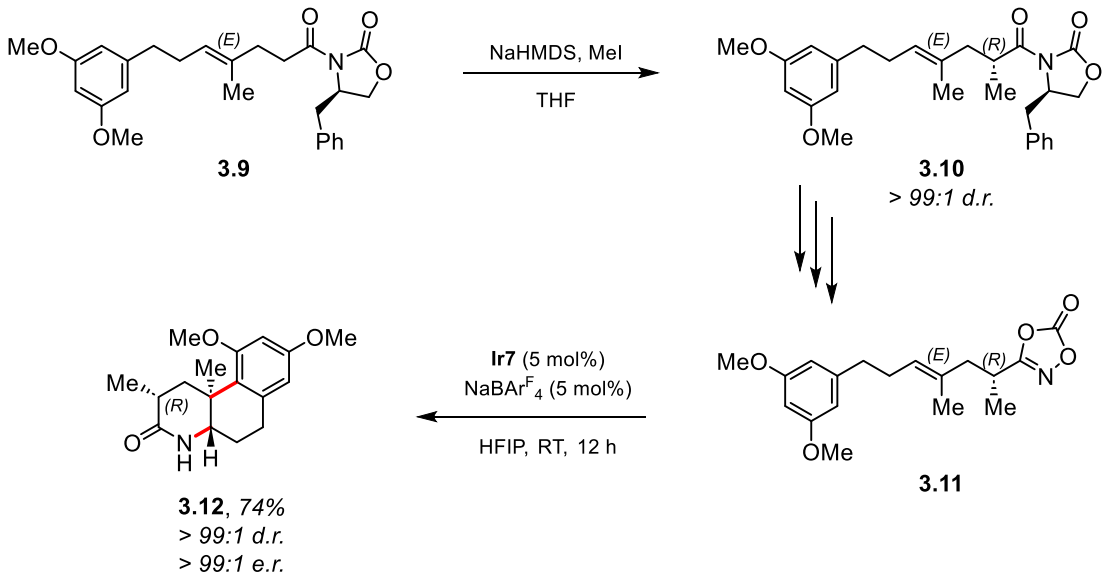

Conditions: substrate **3.11** (0.1 mmol, 1.0 equiv.), **Ir7** (5 mol %), $NaBAr^F_4$ (5 mol %), and HFIP at room temperature for 12 h. Reported isolated yields. Enantiomeric and diastereomeric ratio were determined by HPLC on the chiral stationary phase IC-3 column. The relative configuration of the methyl-decahydroquinolinone **3.12** was determined by using NMR spectroscopy.

Synthetic utility of the decahydroquinolinone products prepared by presented cyclization cascade was also briefly explored (Scheme 3.7). Amide reduction of the tricyclic lactam **3.2b** with $LiAlH_4$ readily afforded amine **3.13** in 67% yield. Alkylation of lactam nitrogen with methyl iodide and sodium hydride gave tertiary amide **3.14** in 72% yield. Desaturation to form α,β-unsaturated amide **3.15** was successfully achieved under DDQ and BSTFA conditions. Such α,β-unsaturated amides with polycyclic frameworks belong to a drug class, e.g. Finasteride and Dutasteride. Finally, electrophilic aromatic bromination of the cyclized product **3.2b** gave an excellent yield (98%) of the corresponding brominated product **3.2f** which would, as mentioned before, serve as a good substrate in further functionalizations, e.g., cross-couplings.

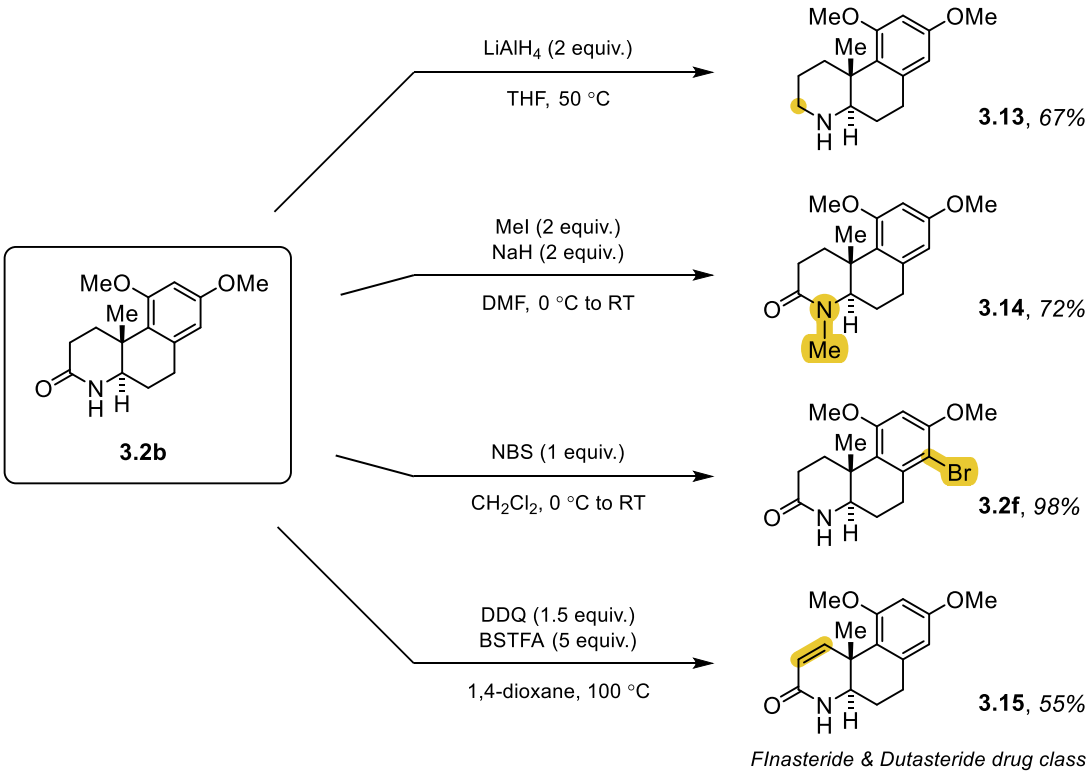

Scheme 3.7: *Synthetic utility of decahydroquinolinone product.*

3.2.2. Strategies for synthesis of dioxazolones – cyclization substrates

Synthesis of dioxazolones, used as substrates for cyclizations, was achieved by using several strategies. Experimental details are presented in the Experimental section. The last step, synthesis of dioxazolones from hydroxamic acids, was common to all substrates and employed simple transformation with CDI as reagent (Scheme 3.8).

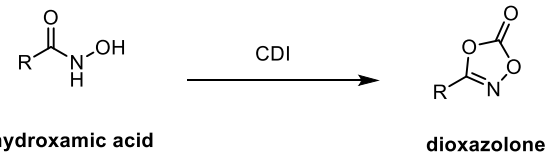

Scheme 3.8*: Common last synthetic step for all substrates – synthesis of dioxazolone from hydroxamic acid with CDI.*

Synthesis of substrates bearing various substituents on the phenyl ring started from geranyl acetate, neryl acetate or *trans*,*trans*-farnesyl acetate (Scheme 3.9). These substrates were prepared as pure *E*- or *Z*-olefins. Shorter substrates were regioselectively epoxidized by *m*CPBA (Scheme 3.9, A), while farnesyl acetate could be regioselectively epoxidized in a 3-step sequence via bromohydrin (Scheme 3.9, B). Epoxidized acetates were then exposed to Grignard reagents in the presence of catalytic amounts of Li_2CuCl_4 which afforded cross-coupled products (Scheme 3.9, C). Resulting epoxides – containing aryl termini – were further cleaved with periodic acid; Malaprade reaction gave the corresponding aldehydes (Scheme 3.9, E). In the next step, Pinnick oxidation afforded carboxylic acids which were transformed to corresponding acyl chlorides in the presence of oxalyl chloride and catalytic amounts of DMF. Addition of hydroxylamine finally yielded hydroxamic acids (Scheme 3.9, E).

The same synthetic sequence, starting from the epoxide cleavage, was used for the substrate containing a triple bond (Scheme 3.9, E). Appropriate epoxide was afforded in two step protocol (Scheme 3.9, D). Geranyl bromide was epoxidized by *m*CPBA and further exposed to lithiated alkyl fragment containing the triple bond to give the corresponding elongated epoxide.

Synthesis of (*E*)-olefinic dioxazolones with plain phenyl or naphthyl terminus started from the corresponding aldehyde with addition of a Grignard reagent to prepare allylic alcohols (Scheme 3.10). Their further reaction with triethyl orthoacetate in acidic medium at elevated temperature proceeded via [3,3]-sigmatropic rearrangement (specifically, Johnson-Claisen rearrangement) which gave final γ,δ-unsaturated esters. Treatment with hydroxylamine in the presence of potassium hydroxide yielded corresponding hydroxamic acids.

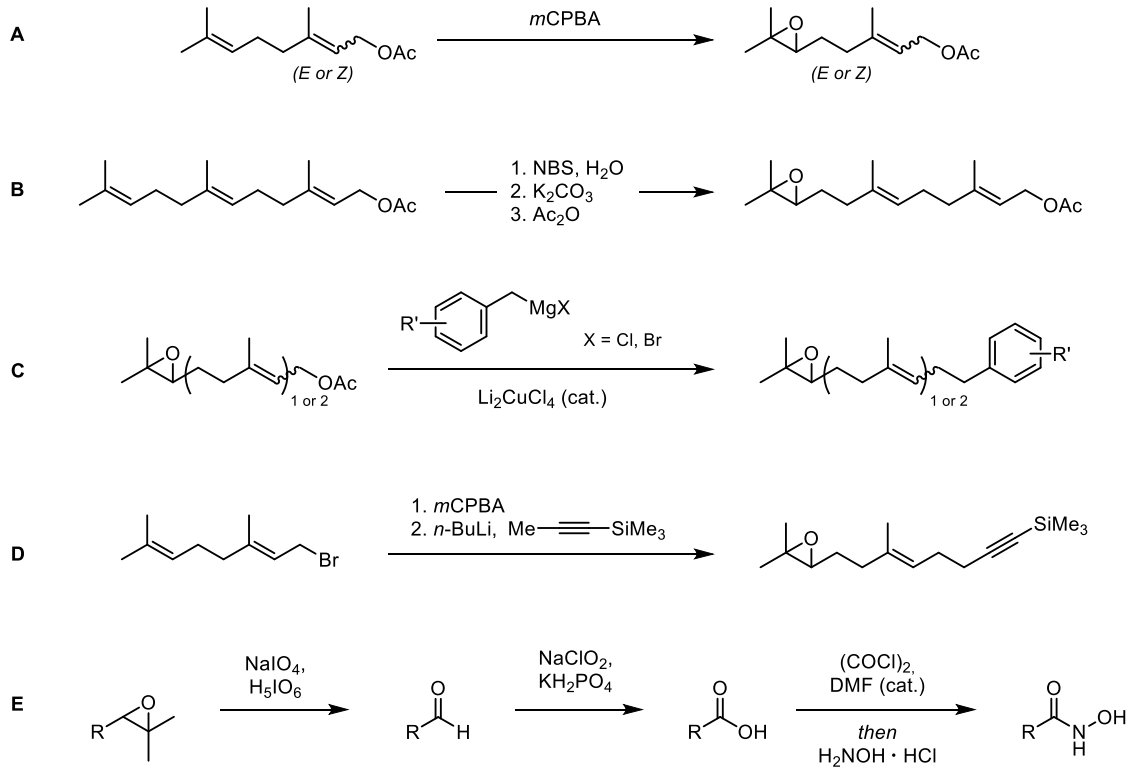

***Scheme 3.9**: Synthetic strategy for synthesis of (E)- and (Z)-olefinic substrates with substituted phenyl or alkyne termini.*

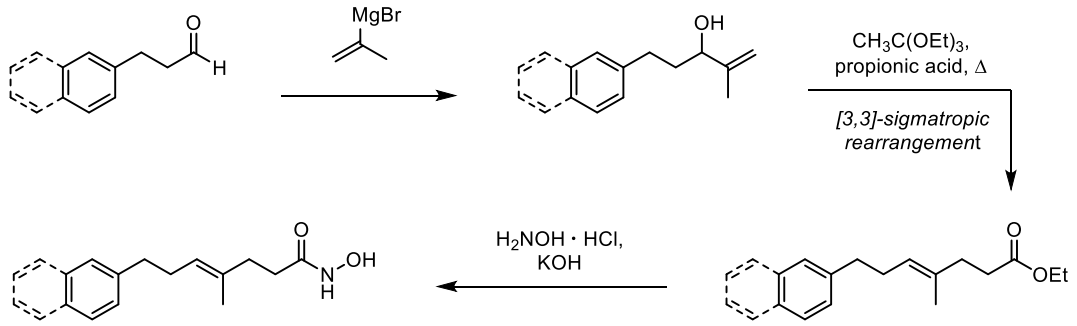

***Scheme 3.10**: Synthetic strategy for synthesis of (E)-olefinic dioxazolones with plain phenyl or naphthyl terminus.*

Substrates with heteroaromatic termini were synthesized by Suzuki cross-coupling strategy (Scheme 3.11). Synthesis of the first fragment started with carboalumination of pent-4-yne-1-ol in the presence of trimethylaluminium and zirconocene dichloride. Further addition of iodine afforded the corresponding vinyl iodide. In the next step, the alcohol was oxidized to carboxylic acid with catalytic amounts of TEMPO and PIDA, and stoichiometric oxidant $NaClO_2$.

Methyl iodide was used to alkylate the carboxylic acid to obtain the methyl ester – the first coupling fragment. The second fragment contained various heteroarenes. Corresponding heteroaryl aldehydes were olefinated by Wittig reaction and then hydroborated with 9-BBN to give the corresponding boranes as the second coupling partners. Suzuki cross-coupling of both fragments afforded corresponding methyl esters which were treated with hydroxylamine in the presence of potassium hydroxide to finally yield the corresponding hydroxamic acids.

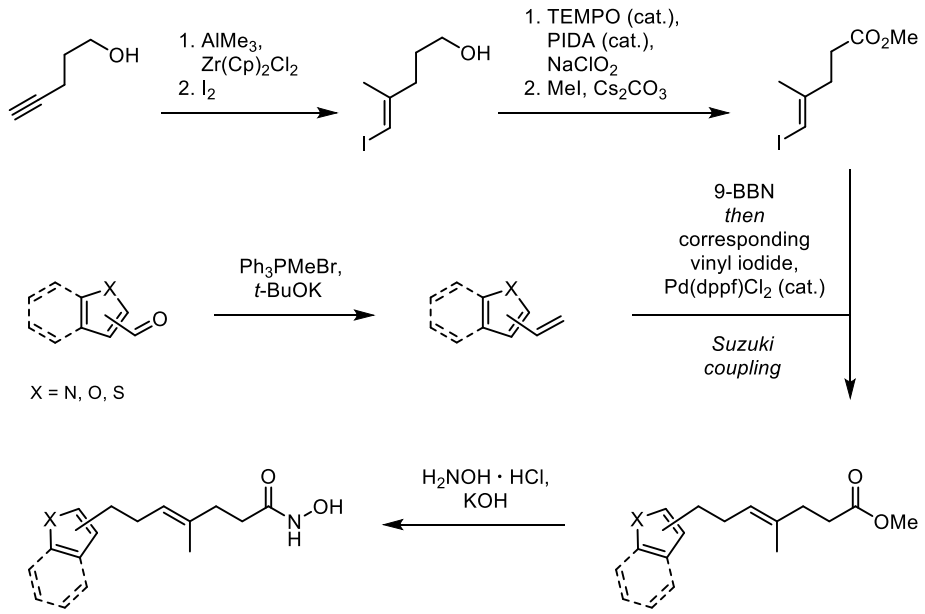

***Scheme 3.11**: Suzuki cross-coupling strategy for synthesis of substrates with heteroaryl termini.*

3.2.3. Computational results

Density functional theory (DFT) computational studies helped us to elucidate mechanistic pathway of cyclization reactions. We used optimal catalyst **Ir7** and (*E*)-dioxazolone substrate **3.1b** for the proposed iridium-nitrenoid-mediated cascade cyclization trajectory calculations (Figure 3.6). Initial coordination of dioxazolone **3.1b** to the cationic iridium species and decarboxylation, with 10.4 kcal/mol barrier, forms the iridium acyl-nitrenoid intermediate **I**. π–π interaction is observed between the ligand and the pendant aryl group of the substrate (distance between the centroids was 3.49 Å) [12,13]. Further interaction of electrophilic acyl-nitrenoid moiety with internal olefin serving as a nucleophile forms aziridine intermediate **II**. This proceeds through transition state **TS-I** with a barrier 7.3 kcal/mol in an overall highly exergonic (ΔG = −23.1 kcal/mol) transformation when reaching intermediate **II**. Change from transition state **TS-I** to intermediate **II** decreases distances between N1 and C5 (from 3.68 Å to 2.21 Å) and between N1 and C6 (from 4.41 Å to 2.60 Å). Aziridination step can be described as an irreversible process in which strained aziridine intermediate **II** is produced stereoselectively. Further conformational rearrangement to **II'** secures the appropriate conformation for the next cyclization step with pendant aromatic ring serving as the nucleophile. Nucleophilic carbon C10 of the aryl ring can approach either carbon C5 or carbon C6 of the iridium-aziridine complex **II'** and forms the corresponding Wheland intermediates **III** or **III'**. Intermediate **III** is generated through a six-membered-ring transition state **II-TS** with a 16.6 kcal/mol barrier. During this process, distance between C10 and C5 decreases (2.34 Å in **II-TS**, and 1.65 Å in **III**) and distance between N1 and C5 increases (2.24 Å in **II-TS** to 2.48 Å in **III**), which are the two key features of **II-TS** collapsing to intermediate **III**. Alternatively, corresponding five-membered-ring analogue (**III'**) exhibits a higher energy barrier ($\Delta\Delta G^{\ddagger}$ = 4.8 kcal/mol) when reaching transition state **II-TS'**. Aziridine ring-opening is observed to proceed with high stereoselectivity, following a concerted S_N2-like pathway. Polycyclic δ-lactam **3.2b** is released together with a cationic iridium species in the final stage of rearomatization of the Wheland intermediate **III**.

Additionally, we examined the intermediacy of aziridine in the cyclization cascade by employing an elongated substrate **3.16**, where the alkyl chain between aryl moiety and olefin has an additional methylene moiety (Figure 3.7). Subjecting substrate **3.16** to the reaction conditions with **Ir8** catalyst yielded tetrahydronaphtalene-substituted γ-lactam **3.17** in 60% yield. In contrast, tricyclic δ-lactam **3.18**, that would arise from opening of the aziridine on the other position, was not observed in the reaction mixture. This experimental outcome is consistent

with computational analysis. The energy barrier from aziridine intermediate **II-16** to transition state **TS-6-5**, which leads to product **3.17**, is 4.0 kcal/mol lower than energy barrier from aziridine intermediate to transition state **TS-7-6**, which would form product **3.18**. Aziridine intermediate **II-16** opening could be rationalized with geometrical preference for formation of six-membered-ring transition state (**TS-6-5**) over seven-membered transition state (**TS-7-6**).

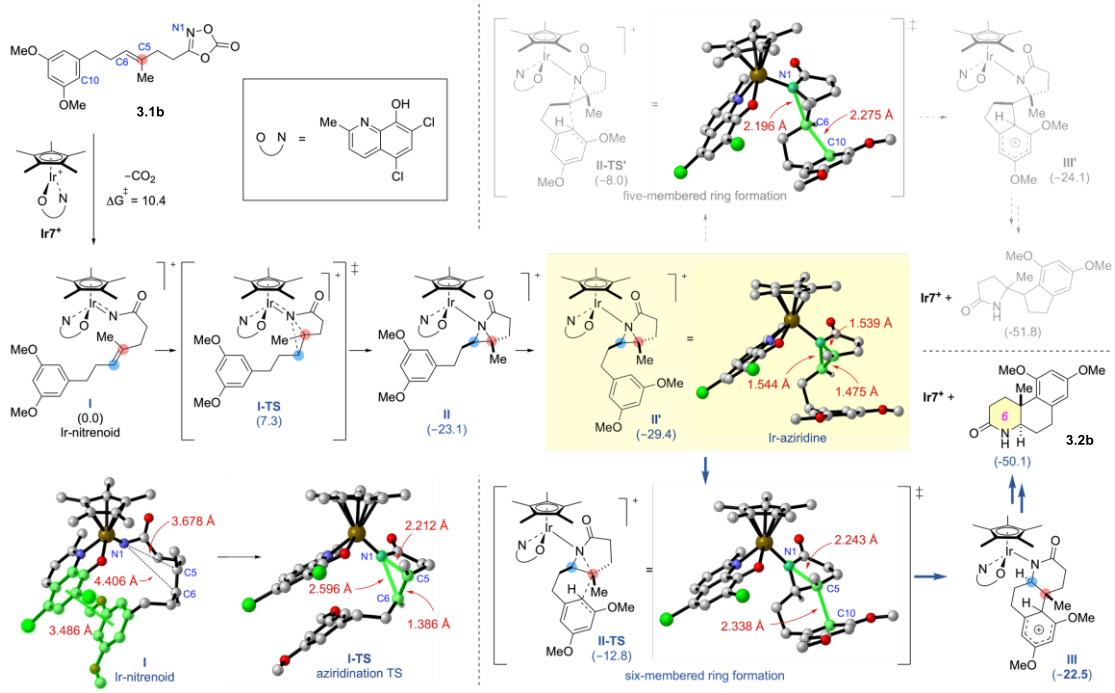

***Figure 3.6**: DFT computational study on Ir-nitrenoid-mediated cyclization cascade. Computational level: SMD(HFIP)-B3LYP-D3/6-311+G**|SDD(Ir)//B3LYP-D3/6-31G**|LANL2DZ(Ir).*

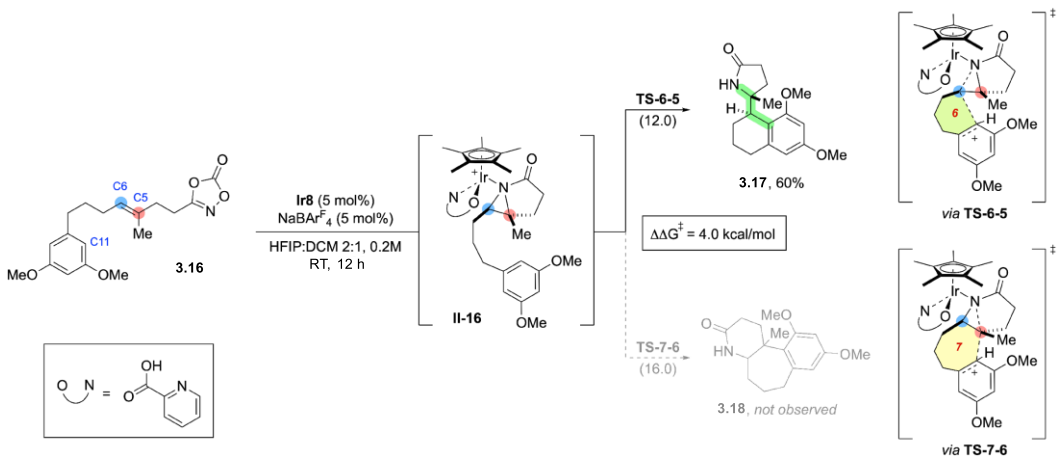

***Figure 3.7**: Experimental mechanistic investigations using modified substrates. Computational level: SMD(HFIP:DCM=2:1)-B3LYP-D3/6-311+G**|SDD(Ir)//B3LYP-D3/6-31G**|LANL2DZ(Ir).*

3.3. Conclusion

In this chapter, we have disclosed a highly diastereoselective cascade cyclization reaction of olefinic aryldioxazolones which furnishes *δ*-lactam products. In situ generated electrophilic iridium-acylnitrenoid initiates the cyclization cascade by an intramolecular transfer to the neighboring alkenyl group forming a key *N*-acylaziridine intermediate. Further intramolecular opening of aziridine by pendant (hetero)arenes or alkynes proceeds in high regioselectivity and yields ring-fused *δ*-lactams. In this process, no other *δ*-lactam derivatives were observed. Initial olefin geometry is well reflected in the final product – *E*-olefins resulted in exclusive formation of *trans*-fused decahydroquinolinone frameworks, while *Z*-olefins resulted in exclusive formation of *cis*-fused decahydroquinolinone frameworks. With this procedure we were able to obtain *cis*-fused polycyclic products, synthesis of which, in terms of polyene cyclizations, is challenging. As terminating groups, a wide range of substituted phenyl rings and other (hetero)arenes were able to participate in cyclization reactions with either synthetically useful or excellent yields. Together with further transformations, these products provide alternative approach to azacyclic compounds synthesis with available diversification having possible applications in synthetic and medicinal chemistry.

3.4. Experimental section

3.4.1. General experimental

Unless otherwise stated, all commercial reagents were used without additional purification. Solvents were purchased from commercial sources. Silica-gel chromatography was performed using a CombiFlash® R_f^+ system with RediSep® R_f Silica columns (230 − 400 mesh) and Silicycle SiliaFlash® P60 (SiO_2, 40–63 µm particle size, 230–400 mesh) using a proper eluent.

^1H NMR spectra were recorded on Agilent Technologies DD2 (600 MHz) and Bruker spectrometer (200–400 MHz). ^{13}C NMR spectra were obtained on Agilent Technologies DD2 (151 MHz) and Bruker spectrometer (101 MHz), also were fully decoupled by broad band proton decoupling. Chemical shifts were quoted in parts per million (ppm) referenced to the residual solvent peak. Coupling constants, *J*, were reported in hertz (Hz).

Infrared (IR) spectra were acquired on Bruker Alpha ATR FT-IR Spectrometer and Perkin-Elmer Spectrum Two FT-IR ATR spectrometer. Frequencies are given in wave numbers (cm^{-1}) and only selected peaks were reported.

High resolution mass spectra were obtained from the Korea Basic Science Institute (Daegu) by using EI method and with High resolution QTOF mass spectrometer AB Sciex X500B by using ESI mode. Data are reported in m/z. Melting point was measured with Buchi Melting Point M-565 and Buchi B-540.

Data collection of parabar-oil-coated single crystals were carried out on:

- a Bruker D8 Quest diffractometer equipped with the IuS 3.0 Mo Kα radiation and PHOTON II area detector. The diffraction data was integrated, scaled, and reduced by using the Bruker APEX3 software. The structure was solved and refined using SHELX programs and SHELXLE.

- Enraf–Nonius CAD4 four-circle diffractometer (Enraf-Nonius, Delft, The Netherlands) equipped with a graphite-monochromatized Mo Kα X-radiation (λ = 0.7107 Å), using a puntual detector for the XRD acquisition.

- Rigaku XtaLab SuperNova (Rigaku Europe SE, Neu-Isenburg, Germany) four-circle diffractometer equipped by a microfocus X-ray source (λ = 0.7107 Å) and a Dectris Pilatus 200K hybrid pixel array detector (DECTRIS AG, Baden-Daettwil, Switzerland).

- a Bruker D8 Venture, equipped with Cu and Mo microfocus X-ray sources, a PHOTON II detector, and Bruker APEX3 program (used λ = 0.71073 Å). The Bruker SAINT software was employed for integration and data reduction, and absorption correction was performed using SADABS-2016/22.

- Rigaku Oxford Diffraction SuperNova diffractometer equipped with a Dectris PILATUS3 R200K-A detector and a micro-focus sealed X-ray tube (λ = 0.71073 Å). X-ray diffraction intensities were integrated with the CrysAlisPro package, while ABSPACK in CrysAlis RED was used for the absorption correction. Crystal structures were solved and refined using SHELXT 2014/5 and SHELXL 2018/3.

3.4.2. Preparation of epoxides

3.4.2.1. Preparation of epoxy acetates

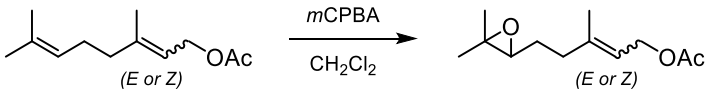

To a solution of the corresponding acetate (1.0 equiv.) in CH_2Cl_2, *m*-chloroperoxybenzoic acid (70%, 1.0 equiv.) was added at 0 °C. The reaction mixture was stirred at 0 °C for 4 h and then filtered over a celite pad. The filtrate was washed with a saturated aqueous $NaHCO_3$ solution, followed by 10% aqueous K_2CO_3 solution. The layers were separated, and the organic phase was dried over $MgSO_4$, filtered, and concentrated under reduced pressure. The crude product was used in the next step without further purification.

(*E*)-5-(3,3-Dimethyloxiran-2-yl)-3-methylpent-2-en-1-yl acetate

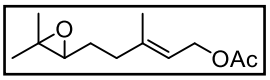

Colorless oil (90%); **^{1}H NMR** (200 MHz, $CDCl_3$): δ 5.38 (t, *J* = 7.0 Hz, 1H), 4.59 (d, *J* = 7.1 Hz, 2H), 2.70 (t, *J* = 6.2 Hz, 1H), 2.31 – 2.09 (m, 2H), 2.05 (s, 3H), 1.82 – 1.52 (m, 5H), 1.30 (s, 3H), 1.26 (s, 3H). *Data consistent with those previously reported [14]*.

(*Z*)-5-(3,3-Dimethyloxiran-2-yl)-3-methylpent-2-en-1-yl acetate

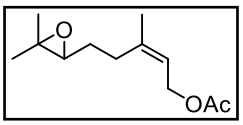

Colorless oil (89%); **^{1}H NMR** (200 MHz, $CDCl_3$): δ 5.40 (t, *J* = 7.2 Hz, 1H), 4.58 (d, *J* = 7.2 Hz, 2H), 2.71 (t, *J* = 6.3 Hz, 1H), 2.25 (t, *J* = 7.8 Hz, 2H), 2.05 (s, 3H), 1.78 (s, 3H), 1.72 – 1.55 (m, 2H), 1.31 (s, 3H), 1.27 (s, 3H).

3.4.2.2. Preparation of epoxy acetate from farnesyl acetate

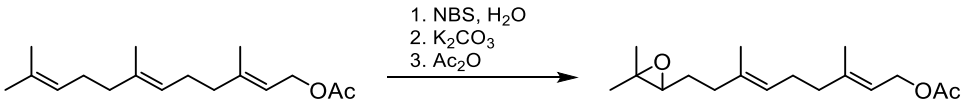

To the solution of farnesyl acetate (6.00 g, 22.7 mmol, 1.0 equiv.) in THF (400 mL) at 0 °C, water (240 mL) was added until the solution became cloudy. *N*-Bromosuccinimide (4.44 g, 25 mmol, 1.1 equiv.) was added in small portions over 1 h at 0 °C, and the reaction mixture was stirred for an additional 2 h at the same temperature. THF was removed under reduced pressure with bath temperature 0 – 5 °C and the aqueous residue was extracted with a solvent mixture 1:1 *n*-hexane/Et_2O. The combined organic phases were dried over $MgSO_4$, filtered, and concentrated under reduced pressure. The crude product was quickly purified by column chromatography (SiO_2, *n*-hexane/EtOAc 9:1 to 4:1) to yield bromohydrin acetate (5.80 g) as a colorless oil.

The purified bromohydrin acetate (5.80 g, 16.0 mmol) was dissolved in anhydrous MeOH (100 mL) and ground K_2CO_3 (6.60 g, 48.0 mmol, 3.0 equiv.) was added and stirred for 2 h at room temperature. The reaction mixture was concentrated under reduced pressure with a bath temperature of 0 – 5 °C, and the residue was diluted with Et_2O (150 mL) and filtered over a celite pad. The filtrate was washed with brine, and the aqueous layer was back-extracted with Et_2O. The combined organic phases were dried oved $MgSO_4$, filtered, and concentrated under reduced pressure to obtain crude epoxy alcohol (3.45 g) as a light-yellow oil.

The epoxy alcohol (3.45 g, 14.5 mmol) was dissolved in CH_2Cl_2 (250 mL) and Et_3N (4.10 mL, 29.0 mmol, 2 equiv.) and 4-(dimethylamino)pyridine (90 mg, 0.73 mmol, 5 mol%) were added, followed by acetic anhydride (2.80 mL, 29.0 mmol, 2 equiv.). The reaction mixture was stirred for 5 h at room temperature, and then ice-cold water (100 mL) was added. The layers were separated, and the aqueous layer was extracted with Et_2O. The combined organic phases were washed with saturated $NaHCO_3$ solution, dried over $MgSO_4$, filtered, and concentrated under reduced pressure. The crude product was purified by column chromatography (SiO_2, *n*-hexane/Et_2O 9:1 to 4:1) to afford the desired product as a colorless oil (3.00 g, 47% yield over 3 steps).

(2*E*,6*E*)-9-(3,3-Dimethyloxiran-2-yl)-3,7-dimethylnona-2,6-dien-1-yl acetate

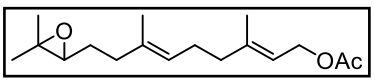

Colorless oil (47% yield over 3 steps); **^{1}H NMR** (200 MHz, $CDCl_3$): δ 5.34 (t, *J* = 7.2 Hz, 1H), 5.20 – 5.08 (m, 1H), 4.58 (d, *J* = 7.1 Hz, 2H), 2.70 (t, *J* = 6.2 Hz, 1H), 2.21 – 1.96 (m, 9H), 1.74 – 1.52 (m, 8H), 1.30 (s, 3H), 1.26 (s, 3H). *Data consistent with those previously reported [15]*.

3.4.2.3. Preparation of aryl epoxides

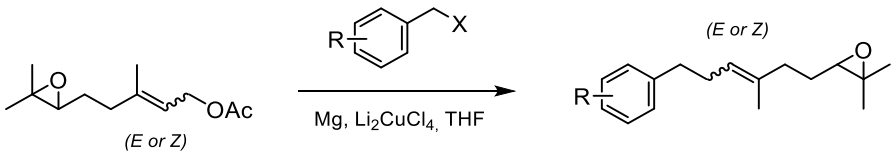

The corresponding halide (2.0 equiv.) was used neat (if liquid) or dissolved in anhydrous THF (if solid) and added dropwise to magnesium turnings (10 equiv.) in anhydrous THF at −10 °C. To initiate the reaction, 1,2-dibromoethane (3 drops) was added after some of the initial halide had already been added. The reaction mixture was stirred at a constant temperature for 1.5 – 3 h. In a separate flask, the corresponding epoxide (1.0 equiv.) was charged with anhydrous THF, which had been dried over 4 Å molecular sieves. This solution was cooled to 0 °C and Li_2CuCl_4 (0.1 M in THF, 10 mol%) was added dropwise. After 15 min, the previously prepared Grignard reagent was added dropwise, and the reaction mixture was stirred for 3 – 5 h at 0 °C. The reaction was quenched by the addition of half-saturated aqueous NH_4Cl solution. The layers were separated, and the aqueous phase was extracted with Et_2O. The combined organic phases were dried over $MgSO_4$, filtered, and concentrated under reduced pressure. The crude product was purified by column chromatography (SiO_2, *n*-hexane/EtOAc 20:1 to 9:1) to obtain the corresponding aryl epoxide.

(*E*)-3-{6-(3,5-Dimethoxyphenyl)-3-methylhex-3-en-1-yl}-2,2-dimethyloxirane

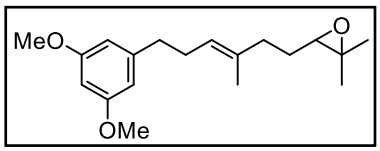

Colorless oil (67%); **^{1}H NMR** (400 MHz, $CDCl_3$): δ 6.35 (d, *J* = 2.2 Hz, 2H), 6.30 (t, *J* = 2.3 Hz, 1H), 5.23 (t, *J* = 7.2 Hz, 1H), 3.78 (s, 6H), 2.69 (t, *J* = 6.3 Hz, 1H), 2.63 – 2.54 (m, 2H), 2.31 (q, *J* = 7.5 Hz, 2H), 2.22 – 2.02 (m, 2H), 1.71 – 1.53 (m, 5H), 1.30 (s, 3H), 1.26 (s, 3H); **^{13}C NMR** (101 MHz, $CDCl_3$): δ 160.8, 144.8, 135.0, 124.3, 106.6, 97.8, 64.3, 58.4, 55.4, 36.4, 36.4, 29.8, 27.6, 25.0, 18.9, 16.1; **IR** (cm^{-1}) 2958, 2929, 2856, 2838, 1596, 1461, 1428, 1377, 1347, 1315, 1293, 1250, 1205, 1153, 1067, 830; **HRMS** (ESI+, *m/z*) $[M+H]^+$ calcd. for $C_{19}H_{29}O_3$: 305.2111, found: 305.2107.

(*Z*)-3-{6-(3,5-Dimethoxyphenyl)-3-methylhex-3-en-1-yl}-2,2-dimethyloxirane

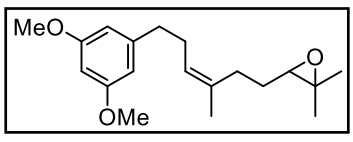

Colorless oil (66%); **^{1}H NMR** (400 MHz, $CDCl_3$): δ 6.35 (d, *J* = 2.2 Hz, 2H), 6.30 (t, *J* = 2.3 Hz, 1H), 5.22 (t, *J* = 7.0 Hz, 1H), 3.78 (s, 6H), 2.69 (t, *J* = 6.3 Hz, 1H), 2.62 – 2.54 (m, 2H), 2.31 (q, *J* = 7.4 Hz, 2H), 2.21 – 2.09 (m, 2H), 1.73 – 1.68 (m, 3H), 1.66 – 1.47 (m, 2H), 1.30 (s, 3H), 1.26 (s, 3H); **^{13}C NMR** (101 MHz, $CDCl_3$): δ 160.8, 144.7, 135.0, 125.2, 106.7, 97.9, 64.2, 58.5, 55.4, 36.7, 29.8, 28.7, 27.5, 25.1, 23.5, 18.9; **IR** (cm^{-1}) 2960, 2929, 2857, 2837, 1596, 1459, 1428, 1377, 1348, 1313, 1293, 1205, 1152, 1068, 830; **HRMS** (ESI+, *m/z*) $[M+H]^+$ calcd. for $C_{19}H_{29}O_3$: 305.2111, found: 305.2098.

(*E*)-3-{6-(4-Methoxyphenyl)-3-methylhex-3-en-1-yl}-2,2-dimethyloxirane

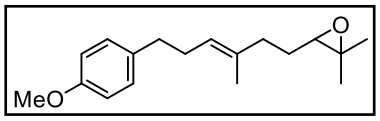

Colorless oil (59%); **^{1}H NMR** (400 MHz, $CDCl_3$): δ 7.13 – 7.07 (m, 2H), 6.85 – 6.79 (m, 2H), 5.22 (t, *J* = 7.1 Hz, 1H), 3.79 (s, 3H), 2.69 (t, *J* = 6.3 Hz, 1H), 2.62 – 2.56 (m, 2H), 2.28 (q, *J* = 7.5 Hz, 2H), 2.20 – 2.03 (m, 2H), 1.70 – 1.53 (m, 5H), 1.30 (s, 3H), 1.26 (s, 3H); **^{13}C NMR** (101 MHz, $CDCl_3$): δ 157.8, 134.9, 134.5, 129.4, 124.4, 113.8, 64.3, 58.5, 55.4, 36.4, 35.2, 30.3, 27.6, 25.0, 18.9, 16.1; **IR** (cm^{-1}) 2958, 2925, 2854, 1612, 1512, 1462, 1377, 1299, 1246, 1177, 1121, 1037, 825; **HRMS** (ESI+, *m/z*) $[M+H]^+$ calcd. for $C_{18}H_{27}O_2$: 275.2006, found: 275.2002.

(*Z*)-3-{6-(4-Methoxyphenyl)-3-methylhex-3-en-1-yl}-2,2-dimethyloxirane

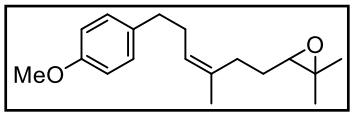

Colorless oil (60%); **^{1}H NMR** (400 MHz, $CDCl_3$): δ 7.13 – 7.07 (m, 2H), 6.86 – 6.79 (m, 2H), 5.22 (t, *J* = 7.1 Hz, 1H), 3.79 (s, 3H), 2.68 (t, *J* = 6.3 Hz, 1H), 2.61 – 2.55 (m, 2H), 2.33 – 2.24 (m, 2H), 2.20 – 2.07 (m, 2H), 1.70 (s, 3H), 1.65 – 1.45 (m, 2H), 1.30 (s, 3H), 1.25 (s, 3H); **^{13}C NMR** (101 MHz, $CDCl_3$): δ 157.9, 134.9, 134.4, 129.4, 125.3, 113.8, 64.2, 58.4, 55.4, 35.5, 30.2, 28.7, 27.5, 25.1, 23.5, 18.9; **IR** (cm^{-1}) 2960, 2926, 2856, 1612, 1512, 1462, 1377, 1299, 1246, 1177, 1121, 1037, 827; **HRMS** (ESI+, *m/z*) $[M+H]^+$ calcd. for $C_{18}H_{27}O_2$: 275.2006, found: 275.2002.

(*E*)-3-{6-(3-Methoxyphenyl)-3-methylhex-3-en-1-yl}-2,2-dimethyloxirane

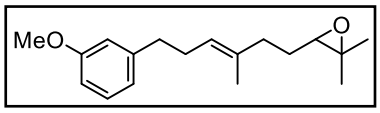

Colorless oil (66%); **^{1}H NMR** (400 MHz, $CDCl_3$): δ 7.22 – 7.16 (m, 1H), 6.78 (d, *J* = 7.8 Hz, 1H), 6.75 – 6.70 (m, 2H), 5.26 – 5.20 (m, 1H), 3.80 (s, 3H), 2.69 (t, *J* = 6.2 Hz, 1H), 2.65 – 2.58 (m, 2H), 2.32 (q, *J* = 7.4 Hz, 2H), 2.21 – 2.03 (m, 2H), 1.70 – 1.55 (m, 5H), 1.30 (s, 3H), 1.26 (s, 3H); **^{13}C NMR** (101 MHz, $CDCl_3$): δ 159.7, 144.0, 135.0, 129.3, 124.3, 121.0, 114.4, 111.1, 64.3, 58.4, 55.3, 36.4, 36.2, 29.9, 27.6, 25.0, 18.9, 16.1; **IR** (cm^{-1}): 2959, 2925, 2856, 1601, 1584, 1488, 1454, 1437, 1377, 1315, 1261, 1152, 1122, 1046, 872; **HRMS** (ESI+, *m/z*) $[M+Na]^+$ calcd. for $C_{18}H_{26}O_2Na$: 297.1825, found: 297.1820.

(*Z*)-3-{6-(3-Methoxyphenyl)-3-methylhex-3-en-1-yl}-2,2-dimethyloxirane

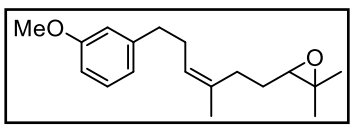

Colorless oil (75%); **^{1}H NMR** (400 MHz, $CDCl_3$): δ 7.23 – 7.16 (m, 1H), 6.78 (d, *J* = 7.6 Hz, 1H), 6.76 – 6.70 (m, 2H), 5.23 (t, *J* = 7.1 Hz, 1H), 3.80 (s, 3H), 2.68 (t, *J* = 6.3 Hz, 1H), 2.64 – 2.59 (m, 2H), 2.32 (q, *J* = 7.6 Hz, 2H), 2.21 – 2.06 (m, 2H), 1.71 (s, 3H), 1.66 – 1.45 (m, 2H), 1.30 (s, 3H), 1.26 (s, 3H); **^{13}C NMR** (101 MHz, $CDCl_3$): δ 159.7, 144.0, 135.0, 129.3, 125.2, 121.0, 114.4, 111.2, 64.2, 58.5, 55.3, 36.5, 29.9, 28.7, 27.5, 25.1, 23.5, 18.9; **IR** (cm^{-1}) 2961, 2926, 2857, 1601, 1584, 1488, 1454, 1437, 1377, 1314, 1260, 1152, 1122, 1052, 866; **HRMS** (ESI+, *m/z*) $[M+H]^+$ calcd. for $C_{18}H_{27}O_2$: 275.2006, found: 275.2003.

3-{(3*E*,7*E*)-10-(3,5-Dimethoxyphenyl)-3,7-dimethyldeca-3,7-dien-1-yl}-2,2-dimethyloxirane

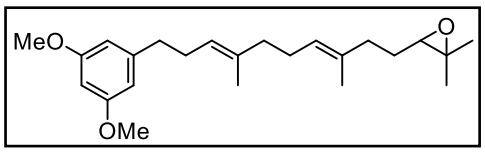

Colorless oil (81%); **^{1}H NMR** (400 MHz, $CDCl_3$): δ 6.36 (d, *J* = 2.2 Hz, 2H), 6.31 (d, *J* = 2.2 Hz, 1H), 5.22 – 5.12 (m, 2H), 3.78 (s, 6H), 2.70 (t, *J* = 6.2 Hz, 1H), 2.61 – 2.54 (m, 2H), 2.34 – 2.25 (m, 2H), 2.20 – 2.03 (m, 4H), 2.03 – 1.96 (m, 2H), 1.72 – 1.59 (m, 5H), 1.58 (s, 3H), 1.30 (s, 3H), 1.26 (s, 3H); **^{13}C NMR** (101 MHz, $CDCl_3$): δ 160.8, 145.0, 135.8, 134.2, 125.0, 123.8, 106.6, 97.8, 64.3, 58.4, 55.4, 39.8, 36.6, 36.4, 29.9, 27.6, 26.8, 25.0, 18.9, 16.2, 16.1; **IR** (cm^{-1}) 2967, 2918, 2855, 2833, 1601, 1459, 1423, 1372, 1345, 1313, 1299, 1252, 1201, 1150, 1070, 832; **HRMS** (ESI+, *m/z*) $[M+H]^+$ calcd. for $C_{24}H_{37}O_3$: 373.2738, found: 373.2724.

3.4.2.4. Preparation of alkynyl epoxide

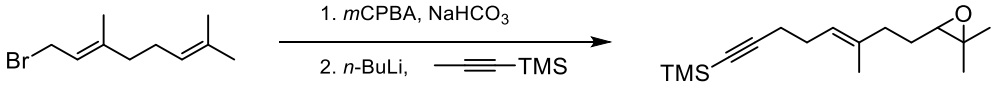

To the suspension of $NaHCO_3$ (4.64 g, 55.3 mmol, 1.5 equiv.) in CH_2Cl_2 at 0 °C, geranyl bromide (7.31 mL, 36.8 mmol, 1.0 equiv.) was added, followed by *m*CPBA (70%, 10.0 g, 40.5 mmol, 1.1 equiv.). The reaction mixture was stirred at 0 °C for 1.5 h and then diluted with water. The layers were separated, and the organic phase was washed with saturated aqueous $NaHCO_3$ solution. The combined aqueous phases were extracted with a solvent mixture of *n*-hexane/Et_2O 1:1. The combined organic phases were dried over $MgSO_4$, filtered, and concentrated under reduced pressure. The crude epoxy bromide was used without further purification.

In a separate flask, 1-trimethylsilyl-1-propyne (6.0 mL, 41 mmol, 1.1 equiv.) in anhydrous THF was cooled to −78 °C, and *n*-BuLi (2.5 M in *n*-hexane, 15 mL, 37 mmol, 1.0 equiv.) was added dropwise. The reaction mixture was warmed up to −40 °C and stirred for 30 min. After that, the above-mentioned epoxy bromide (1.0 equiv.) in anhydrous THF was added dropwise. After addition, the reaction mixture was stirred at 0 °C for 2 h and then quenched with saturated aqueous NH_4Cl solution. The layers were separated, and the aqueous layer was extracted with Et_2O. The combined organic phases were dried over $MgSO_4$, filtered, and concentrated under reduced pressure. The crude product was purified by column chromatography (SiO_2, *n*-hexane/EtOAc 40:1) to obtain the corresponding alkynyl epoxide as a colorless oil (4.91 g, 51% yield over 2 steps).

(*E*)-{8-(3,3-Dimethyloxiran-2-yl)-6-methyloct-5-en-1-yn-1-yl}trimethylsilane

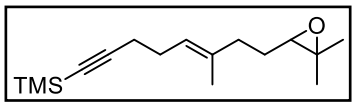

Colorless oil (51% yield over 2 steps); **^{1}H NMR** (400 MHz, $CDCl_3$): δ 5.25 – 5.17 (m, 1H), 2.71 (t, *J* = 6.3 Hz, 1H), 2.26 – 2.20 (m, 4H), 2.20 – 2.05 (m, 2H), 1.76 – 1.55 (m, 5H), 1.30 (s, 3H), 1.26 (s, 3H), 0.14 (s, 9H); **^{13}C NMR** (101 MHz, $CDCl_3$): δ 135.9, 123.3, 107.4, 84.5, 64.3, 58.5, 36.4, 27.6, 27.5, 25.0, 20.4, 18.9, 16.3, 0.3; **IR** (cm^{-1}) 2960,2923, 2174, 1449, 1377, 1249, 1122, 898, 842; **HRMS** (ESI+, *m/z*) $[M+H]^+$ calcd. for $C_{16}H_{29}OSi$: 265.1982, found: 265.1980.

3.4.3. Preparation of aldehydes from epoxides

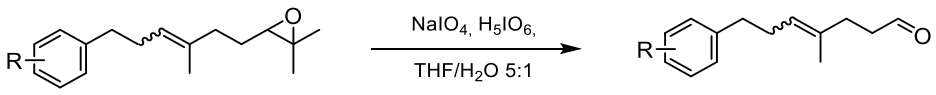

The corresponding epoxide (1.0 equiv.) was dissolved in a mixture of solvents THF/H_2O 5:1 and cooled to 0 °C. $NaIO_4$ (0.5 equiv.) and H_5IO_6 (1.1 equiv.) were added, and the reaction mixture was left to warm up to room temperature. After completion (ca. 4–6 h), the reaction was quenched with saturated aqueous $NaHCO_3$ solution and extracted with EtOAc. The combined organic phases were dried over $MgSO_4$, filtered, and concentrated under reduced pressure. The crude product was then purified by column chromatography (SiO_2, *n*-hexane/EtOAc 20:1 to 9:1) to obtain the corresponding aldehyde.

(*E*)-7-(3,5-Dimethoxyphenyl)-4-methylhept-4-enal

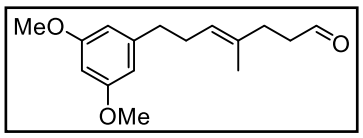

Colorless oil (80%); **^{1}H NMR** (400 MHz, $CDCl_3$): δ 9.74 (t, *J* = 1.9 Hz, 1H), 6.34 (d, *J* = 2.2 Hz, 2H), 6.30 (t, *J* = 2.2 Hz, 1H), 5.24 – 5.17 (m, 1H), 3.78 (s, 6H), 2.60 – 2.54 (m, 2H), 2.53 – 2.47 (m, 2H), 2.35 – 2.25 (m, 4H), 1.58 (s, 3H). **^{13}C NMR** (101 MHz, $CDCl_3$): δ 202.8, 160.8, 144.7, 133.9, 124.8, 106.7, 97.8, 55.4, 42.3, 36.3, 31.9, 29.8, 16.2. *Data consistent with those previously reported [16]*.

(*Z*)-7-(3,5-Dimethoxyphenyl)-4-methylhept-4-enal

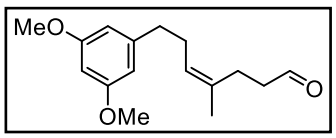

Colorless oil (81%); **^{1}H NMR** (400 MHz, $CDCl_3$): δ 9.72 (t, *J* = 1.6 Hz, 1H), 6.34 (d, *J* = 2.2 Hz, 2H), 6.30 (t, *J* = 2.2 Hz, 1H), 5.23 (t, *J* = 7.2 Hz, 1H), 3.78 (s, 6H), 2.58 (t, *J* = 7.7 Hz, 2H), 2.41 – 2.35 (m, 2H), 2.34 – 2.26 (m, 4H), 1.70 – 1.65 (m, 3H); **^{13}C NMR** (101 MHz, $CDCl_3$): δ 202.3, 160.9, 144.6, 133.9, 125.8, 106.7, 97.9, 55.4, 42.4, 36.5, 29.8, 24.4, 23.2; **IR** (cm^{-1}) 2935, 2838, 2724, 1722, 1596, 1461, 1429, 1348, 1312, 1293, 1205, 1151, 1068, 832; **HRMS** (ESI+, *m/z*) $[M+H]^+$ calcd. for $C_{16}H_{23}O_3$: 263.1642, found: 263.1641.

(*E*)-7-(4-Methoxyphenyl)-4-methylhept-4-enal

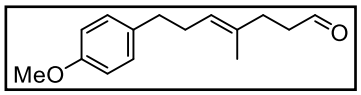

Colorless oil (74%); **^{1}H NMR** (400 MHz, $CDCl_3$): δ 9.74 (t, *J* = 1.9 Hz, 1H), 7.12 – 7.04 (m, 2H), 6.86 – 6.78 (m, 2H), 5.20 (t, *J* = 7.0 Hz, 1H), 3.79 (s, 3H), 2.61 – 2.54 (m, 2H), 2.53 – 2.46 (m, 2H), 2.35 – 2.23 (m, 4H), 1.55 (s, 3H); **^{13}C NMR** (101 MHz, $CDCl_3$): δ 202.8, 157.9, 134.3, 133.8, 129.5, 124.9, 113.8, 55.4, 42.2, 35.1, 31.9, 30.2, 16.2; **IR** (cm^{-1}) 2931, 2915, 2854, 2835, 2720, 1723, 1611, 1583, 1511, 1464, 1442, 1299, 1177, 1107, 1036, 827; **HRMS** (ESI+, *m/z*) $[M+H]^+$ calcd. for $C_{15}H_{21}O_2$: 233.1536, found: 233.1534. *Data consistent with those previously reported [17].*

(*Z*)-7-(4-Methoxyphenyl)-4-methylhept-4-enal

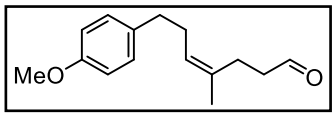

Colorless oil (67%); **^{1}H NMR** (400 MHz, $CDCl_3$): δ 9.73 – 9.69 (m, 1H), 7.13 – 7.05 (m, 2H), 6.86 – 6.79 (m, 2H), 5.22 (t, *J* = 7.2 Hz, 1H), 3.79 (s, 3H), 2.58 (t, *J* = 7.6 Hz, 2H), 2.40 – 2.33 (m, 2H), 2.32 – 2.24 (m, 4H), 1.68 (s, 3H); **^{13}C NMR** (101 MHz, $CDCl_3$): δ 202.3, 157.9, 134.3, 133.7, 129.5, 126.0, 113.8, 55.4, 42.3, 35.3, 30.2, 24.4, 23.2; **IR** (cm^{-1}) 2961, 2929, 2854, 2834, 2722, 1721, 1611, 1583, 1511, 1458, 1442, 1299, 1245, 1177, 1036, 827; **HRMS** (ESI+, *m/z*) $[M+H]^+$ calcd. for $C_{15}H_{21}O_2$: 233.1536, found: 233.1532.

(*E*)-7-(3-Methoxyphenyl)-4-methylhept-4-enal

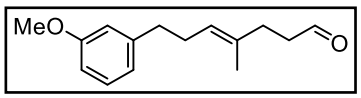

Colorless oil (75%); **^{1}H NMR** (400 MHz, $CDCl_3$): δ 9.74 (t, *J* = 1.8 Hz, 1H), 7.22 – 7.16 (m, 1H), 6.77 (d, *J* = 7.6 Hz, 1H), 6.75 – 6.71 (m, 2H), 5.21 (t, *J* = 6.5 Hz, 1H), 3.80 (s, 3H), 2.64 – 2.58 (m, 2H), 2.53 – 2.46 (m, 2H), 2.34 – 2.26 (m, 4H), 1.57 (s, 3H); **^{13}C NMR** (101 MHz, $CDCl_3$): δ 202.7, 159.7, 143.9, 133.9, 129.3, 124.8, 121.0, 114.4, 111.1, 55.3, 42.3, 36.1, 32.0, 29.9, 16.2; **IR** (cm^{-1}) 2935, 2919, 2855, 2835, 2720, 1723, 1601, 1584, 1488, 1453, 1437, 1261, 1152, 1044, 872; **HRMS** (ESI+, *m/z*) $[M+MeOH+Na]^+$ calcd. for $C_{16}H_{25}O_3Na$: 287.1618, found: 287.1605.

(*Z*)-7-(3-Methoxyphenyl)-4-methylhept-4-enal

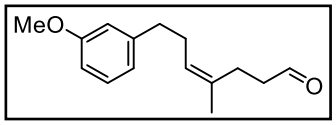

Colorless oil (82%); **^{1}H NMR** (400 MHz, $CDCl_3$): δ 9.71 (t, *J* = 1.6 Hz, 1H), 7.22 – 7.16 (m, 1H), 6.79 – 6.76 (m, 1H), 6.75 – 6.71 (m, 2H), 5.23 (t, *J* = 7.1 Hz, 1H), 3.80 (s, 3H), 2.62 (t, *J* = 7.7 Hz, 2H), 2.39 – 2.25 (m, 6H), 1.69 – 1.66 (m, 3H); **^{13}C NMR** (101 MHz, $CDCl_3$): δ 202.3, 159.7, 143.8, 133.8, 129.4, 125.8, 121.1, 114.4, 111.2, 55.3, 42.3, 36.3, 29.9, 24.3, 23.2; **IR** (cm^{-1}) 2962, 2932, 2856, 2835, 2723, 1723, 1601, 1584, 1488, 1453, 1438, 1313, 1261, 1152, 1053, 874; **HRMS** (ESI+, *m/z*) $[M+H]^+$ calcd. for $C_{15}H_{21}O_2$: 233.1536, found: 233.1534**.**

(4*E*,8*E*)-11-(3,5-Dimethoxyphenyl)-4,8-dimethylundeca-4,8-dienal

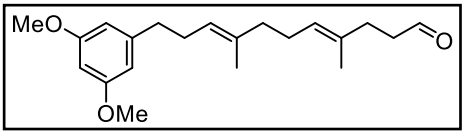

Colorless oil (79%); **^{1}H NMR** (400 MHz, $CDCl_3$): δ 9.74 (t, *J* = 1.9 Hz, 1H), 6.36 (d, *J* = 2.2 Hz, 2H), 6.30 (t, *J* = 2.3 Hz, 1H), 5.20 – 5.10 (m, 2H), 3.78 (s, 6H), 2.61 – 2.55 (m, 2H), 2.52 – 2.47 (m, 2H), 2.34 – 2.25 (m, 4H), 2.11 – 2.04 (m, 2H), 2.02 – 1.95 (m, 2H), 1.61 (s, 3H), 1.57 (s, 3H); **^{13}C NMR** (101 MHz, $CDCl_3$): δ 202.8, 160.8, 144.9, 135.6, 133.1, 125.4, 123.9, 106.6, 97.8, 55.3, 42.3, 39.6, 36.5, 32.0, 29.8, 26.6, 16.2, 16.1; **IR** (cm^{-1}) 3005, 2942, 2833, 2725, 1719, 1556, 1458, 1434, 1399, 1341, 1307, 1285, 1211, 1146, 1061, 911, 836; **HRMS** (ESI+, *m/z*) $[M+H]^+$ calcd. for $C_{21}H_{31}O_3$: 331.2268, found: 331.2264.

(*E*)-4-Methyl-9-(trimethylsilyl)non-4-en-8-ynal

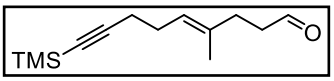

Colorless oil (69%); **^{1}H NMR** (400 MHz, $CDCl_3$): δ 9.76 (t, *J* = 1.8 Hz, 1H), 5.24 – 5.16 (m, 1H), 2.52 (td, *J* = 7.5, 1.6 Hz, 2H), 2.33 (t, *J* = 7.5 Hz, 2H), 2.25 – 2.18 (m, 4H), 1.64 (s, 3H), 0.14 (s, 9H); **^{13}C NMR** (101 MHz, $CDCl_3$): δ 202.6, 134.8, 123.8, 107.2, 84.7, 42.2, 31.9, 27.3, 20.3, 16.4, 0.3; **IR** (cm^{-1}) 3430, 2960, 2932, 2174, 1725, 1447, 1430, 1383, 1249, 1086, 1045, 997, 898, 847; **HRMS** (ESI+, *m/z*) $[M+MeOH+Na]^+$ calcd. for $C_{14}H_{26}O_2SiNa$: 277.1594, found: 277.1588.

(*Z*)-4-Methyl-7-phenylhept-4-enal

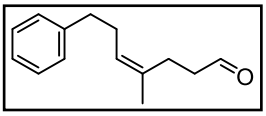

Pale yellow oil (78%, crude aryl epoxide was used without purification for next step); **^{1}H NMR** (600 MHz, $CDCl_3$): δ 9.69 (s, 1H), 7.30 – 7.26 (m, 2H), 7.20 – 7.15 (m, 3H), 5.23 (t, *J* = 7.2 Hz, 1H), 2.64 (t, *J* = 7.6 Hz, 2H), 2.36 – 2.29 (m, 4H), 2.29 – 2.24 (m, 2H), 1.67 (s, 3H). *Data consistent with those previously reported [18]*.

(*E*)-4-Methyl-7-(*p*-tolyl)hept-4-enal

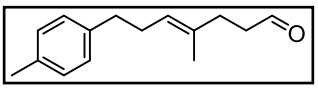

Colorless oil (60%, crude aryl epoxide was used without purification for next step); **^{1}H NMR** (600 MHz, $CDCl_3$): δ 9.74 (t, *J* = 1.9 Hz, 1H), 7.10 – 7.05 (m, 4H), 5.23 – 5.19 (m, 1H), 2.61 – 2.57 (m, 2H), 2.50 (td, *J* = 7.5, 1.8 Hz, 2H), 2.35 – 2.26 (m, 7H), 1.57 (s, 3H); **^{13}C NMR** (151 MHz, $CDCl_3$): δ 202.8, 139.1, 135.3, 133.8, 129.1, 128.5, 125.0, 42.3, 35.6, 32.0, 30.1, 21.1, 16.2; **IR** (cm^{-1}) 2919, 2856, 1723, 1514, 1446, 1383, 1109, 809; **HRMS** (EI, *m/z*) $[M]^+$ calcd. for $C_{15}H_{20}O$: 216.1514, found: 216.1517.

(*Z*)-4-Methyl-7-(*p*-tolyl)hept-4-enal

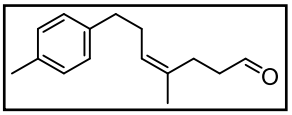

Colorless oil (37%, crude aryl epoxide was used without purification for next step); **^{1}H NMR** (600 MHz, $CDCl_3$): δ 9.70 (s, 1H), 7.12 – 7.04 (m, 4H), 5.23 (t, *J* = 7.3 Hz, 1H), 2.62 – 2.56 (m, 2H), 2.36 – 2.26 (m, 9H), 1.67 (d, *J* = 1.2 Hz, 3H); **^{13}C NMR** (151 MHz, $CDCl_3$): δ 202.3, 139.1, 135.4, 133.7, 129.1, 128.5, 126.0, 42.3, 35.8, 30.1, 24.4, 23.2, 21.1; **IR** (cm^{-1}) 2919, 1723, 1514, 1447, 807; **HRMS** (EI, *m/z*) $[M]^+$ calcd. for $C_{15}H_{20}O$: 216.1514, found: 216.1510.

3.4.4. Preparation of carboxylic acids from aldehydes

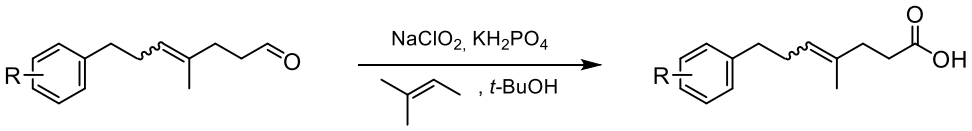

To a solution of corresponding aldehyde (1.0 equiv.) in *t*-BuOH, 2-methyl-2-butene (10 equiv.) was added, followed by an aqueous solution of $NaClO_2$ (4.0 equiv.) and KH_2PO_4 (4.0 equiv.). The reaction mixture was stirred for 4 – 6 h at room temperature, then diluted with water, followed by removal of *t*-BuOH under reduced pressure. The remaining solution was extracted with EtOAc. The combined organic phases were dried over $MgSO_4$, filtered, and concentrated under reduced pressure. The crude product was purified by column chromatography (SiO_2, *n*-hexane/EtOAc 9:1 to 2:1) to obtain the corresponding carboxylic acid.

(*E*)-7-(3,5-Dimethoxyphenyl)-4-methylhept-4-enoic acid

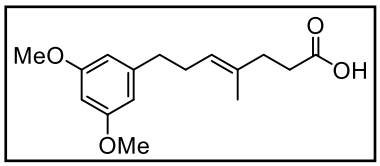

White solid (78%); **m. p.** 44 – 46 °C; **^{1}H NMR** (400 MHz, $CDCl_3$): δ 6.35 (d, *J* = 2.3 Hz, 2H), 6.31 (t, *J* = 2.3 Hz, 1H), 5.26 – 5.19 (m, 1H), 3.78 (s, 6H), 2.61 – 2.54 (m, 2H), 2.48 – 2.41 (m, 2H), 2.35 – 2.25 (m, 4H), 1.59 (s, 3H); **^{13}C NMR** (101 MHz, $CDCl_3$): δ 179.7, 160.8, 144.7, 133.9, 124.8, 106.7, 97.8, 55.4, 36.3, 34.4, 33.0, 29.8, 16.0; **IR** (cm^{-1}) 2936, 2838, 2659, 1708, 1596, 1460, 1428, 1347, 1294, 1205, 1152, 1067, 924, 831; **HRMS** (ESI+, *m/z*) $[M+H]^+$ calcd. for $C_{16}H_{23}O_4$: 279.1591 found: 279.1587.

(*Z*)-7-(3,5-Dimethoxyphenyl)-4-methylhept-4-enoic acid

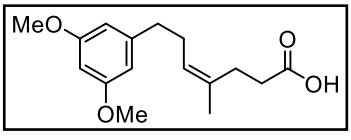

Pale-yellow oil (86%); **^{1}H NMR** (400 MHz, $CDCl_3$): δ 6.34 (d, *J* = 2.3 Hz, 2H), 6.30 (t, *J* = 2.2 Hz, 1H), 5.27 – 5.19 (m, 1H), 3.78 (s, 6H), 2.60 – 2.54 (m, 2H), 2.32 (s, 6H), 1.70 – 1.67 (m, 3H); **^{13}C NMR** (101 MHz, $CDCl_3$): δ 178.5, 160.8, 144.6, 133.7, 126.1, 106.7, 98.0, 55.4, 36.6, 32.4, 29.7, 27.0, 23.0; **IR** (cm^{-1}) 2936, 2838, 2675, 1708, 1596, 1460, 1429, 1348, 1293, 1205, 1152, 1068, 924, 831; **HRMS** (ESI+, *m/z*) $[M+H]^+$ calcd. for $C_{16}H_{23}O_4$: 279.1591, found: 279.1583.

(*E*)-7-(4-Methoxyphenyl)-4-methylhept-4-enoic acid

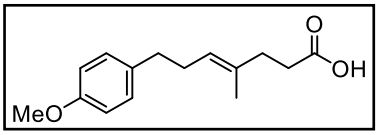

White solid (72%); **m. p.** 47 – 49 °C **^{1}H NMR** (400 MHz, $CDCl_3$): δ 7.11 – 7.06 (m, 2H), 6.86 – 6.79 (m, 2H), 5.22 (t, *J* = 7.0 Hz, 1H), 3.79 (s, 3H), 2.57 (t, *J* = 7.7 Hz, 2H), 2.48 – 2.41 (m, 2H), 2.35 – 2.23 (m, 4H), 1.56 (s, 3H); **^{13}C NMR** (101 MHz, $CDCl_3$): δ 179.8, 157.8, 134.4, 133.8, 129.5, 124.8, 113.8, 55.4, 35.1, 34.4, 33.0, 30.3, 16.0; **IR** (cm^{-1}) 2932, 2918, 2856, 2664, 1708, 1612, 1512, 1442, 1300, 1245, 1177, 1037, 940, 825; **HRMS** (ESI+, *m/z*) $[M+Na]^+$ calcd. for $C_{15}H_{20}O_3Na$: 271.1305, found: 271.1294.

(*Z*)-7-(4-Methoxyphenyl)-4-methylhept-4-enoic acid

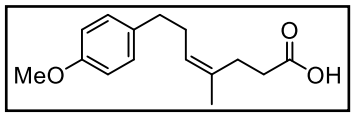

Colorless oil (74%); **^{1}H NMR** (400 MHz, $CDCl_3$): δ 7.13 – 7.05 (m, 2H), 6.86 – 6.78 (m, 2H), 5.27 – 5.18 (m, 1H), 3.78 (s, 3H), 2.60 – 2.54 (m, 2H), 2.34 – 2.24 (m, 6H), 1.72 – 1.64 (m, 3H); **^{13}C NMR** (101 MHz, $CDCl_3$): δ 179.1, 157.9, 134.3, 133.6, 129.5, 126.2, 113.8, 55.4, 35.4, 32.5, 30.2, 27.0, 23.0; **IR** (cm^{-1}) 2963, 2931, 2856, 2678, 1709, 1612, 1512, 1442, 1299, 1246, 1177, 1037, 937, 826; **HRMS** (ESI+, *m/z*) $[M+Na]^+$ calcd. for $C_{15}H_{20}O_3Na$: 271.1305, found: 271.1302.

(*E*)-7-(3-Methoxyphenyl)-4-methylhept-4-enoic acid

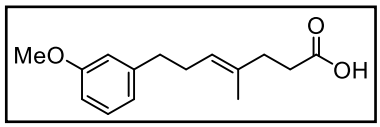

Colorless oil (72%); **^{1}H NMR** (400 MHz, $CDCl_3$): δ 7.23 – 7.16 (m, 1H), 6.78 (d, *J* = 7.6 Hz, 1H), 6.76 – 6.71 (m, 2H), 5.23 (t, *J* = 6.6 Hz, 1H), 3.80 (s, 3H), 2.65 – 2.57 (m, 2H), 2.48 – 2.41 (m, 2H), 2.35 – 2.26 (m, 4H), 1.57 (s, 3H); **^{13}C NMR** (101 MHz, $CDCl_3$). δ 179.6, 159.7, 143.9, 133.9, 129.3, 124.8, 121.1, 114.5, 111.1, 55.3, 36.1, 34.4, 33.0, 29.9, 16.0; **IR** (cm^{-1}) 2936, 2920, 2857, 2662, 1708, 1601, 1584, 1488, 1453, 1437, 1261, 1152, 1051, 930, 873, 850; **HRMS** (ESI+, *m/z*) $[M+Na]^+$ calcd. for $C_{15}H_{20}O_3Na$: 271.1305, found: 271.1301.

(*Z*)-7-(3-Methoxyphenyl)-4-methylhept-4-enoic acid

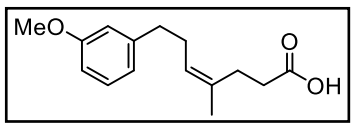

Colorless oil (82%); **^{1}H NMR** (400 MHz, $CDCl_3$): δ 7.22 – 7.15 (m, 1H), 6.77 (d, *J* = 7.6 Hz, 1H), 6.76 – 6.69 (m, 2H), 5.28 – 5.19 (m, 1H), 3.79 (s, 3H), 2.64 – 2.57 (m, 2H), 2.37 – 2.27 (m, 6H), 1.70 – 1.66 (m, 3H); **^{13}C NMR** (101 MHz, $CDCl_3$): δ 178.9, 159.7, 143.9, 133.7, 129.4, 126.1, 121.1, 114.4, 111.2, 55.3, 36.3, 32.5, 29.8, 27.0, 23.0; **IR** (cm^{-1}) 2935, 2857, 2677, 1708, 1601, 1584, 1488, 1453, 1437, 1261, 1152, 1085, 1052, 931, 873, 850; **HRMS** (ESI+, *m/z*) $[M+Na]^+$ calcd. for $C_{15}H_{20}O_3Na$: 271.1305, found: 271.1302.

(4*E*,8*E*)-11-(3,5-Dimethoxyphenyl)-4,8-dimethylundeca-4,8-dienoic acid

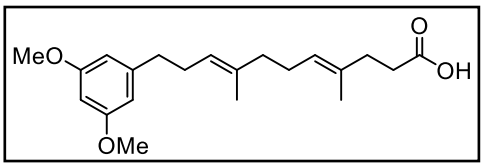

Colorless oil (67%); **^{1}H NMR** (400 MHz, $CDCl_3$): δ 6.37 (d, *J* = 2.2 Hz, 2H), 6.31 (t, *J* = 2.2 Hz, 1H), 5.22 – 5.12 (m, 2H), 3.78 (s, 6H), 2.63 – 2.55 (m, 2H), 2.49 – 2.42 (m, 2H), 2.35 – 2.26 (m, 4H), 2.12 – 2.04 (m, 2H), 2.03 – 1.95 (m, 2H), 1.62 (s, 3H), 1.58 (s, 3H); **^{13}C NMR** (101 MHz, $CDCl_3$): δ 179.9, 160.8, 144.9, 135.7, 133.1, 125.4, 123.9, 106.7, 97.8, 55.3, 39.6, 36.5, 34.4, 33.1, 29.8, 26.7, 16.1, 16.0; **IR** (cm^{-1}) 3033, 2896, 2655, 1719, 1595, 1455, 1432, 1336, 1288, 1199, 1147, 1061, 921, 837; **HRMS** (ESI+, *m/z*) $[M+H]^+$ calcd. for $C_{21}H_{31}O_4$: 347.2217, found: 347.2208.

(*E*)-4-Methyl-9-(trimethylsilyl)non-4-en-8-ynoic acid

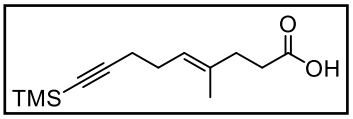

Colorless oil (83%); **^{1}H NMR** (400 MHz, $CDCl_3$): δ 5.25 – 5.17 (m, 1H), 2.49 – 2.43 (m, 2H), 2.35 – 2.30 (m, 2H), 2.26 – 2.17 (m, 4H), 1.64 (s, 3H), 0.14 (s, 9H); **^{13}C NMR** (101 MHz, $CDCl_3$): δ 179.6, 134.7, 123.8, 107.3, 84.6, 34.4, 33.0, 27.4, 20.3, 16.2, 0.3; **IR** (cm^{-1}) 3028, 2960, 2664, 2174, 1709, 1412, 1300, 1249, 1212, 1167, 1095, 1043, 897, 841; **HRMS** (ESI+, *m/z*) $[M+Na]^+$ calcd. for $C_{13}H_{22}O_2SiNa$: 261.1281, found: 261.1276.

(*Z*)-4-Methyl-7-phenyl-4-heptenoic acid

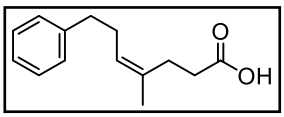

Colorless liquid (98%); **^{1}H NMR** (600 MHz, CD_2Cl_2): δ 7.30 – 7.26 (m, 2H), 7.21 – 7.15 (m, 3H), 5.24 (t, *J* = 7.2 Hz, 1H), 2.67 – 2.59 (m, 2H), 2.37 – 2.26 (m, 6H), 1.68 (d, *J* = 1.2 Hz, 3H); **^{13}C NMR** (151 MHz, $CDCl_3$): δ 179.4, 142.2, 133.7, 128.6, 128.4, 126.2, 125.9, 36.3, 32.5, 29.9, 27.0, 23.0; **IR** (cm^{-1}) 2920, 1704, 1452, 1281, 1211, 933, 746, 697, 475; **HRMS** (EI, *m/z*) $[M]^+$ calcd. for $C_{14}H_{18}O_2$: 218.1307, found: 218.1305.

(*E*)-4-Methyl-7-(*p*-tolyl)hept-4-enoic acid

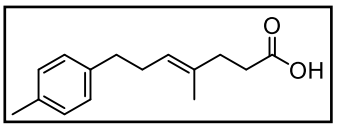

White solid (77%); **m. p.** 45 – 47 °C; **^{1}H NMR** (600 MHz, $CDCl_3$): δ 7.10 – 7.05 (m, 4H), 5.23 (t, *J* = 7.0 Hz, 1H), 2.61 – 2.57 (m, 2H), 2.46 – 2.43 (m, 2H), 2.34 – 2.25 (m, 7H), 1.57 (s, 3H); **^{13}C NMR** (151 MHz, $CDCl_3$): δ 179.1, 139.2, 135.3, 133.8, 129.1, 128.5, 124.9, 35.6, 34.4, 32.9, 30.2, 21.1, 16.0; **IR** (cm^{-1}) 2963, 2921, 1694, 1514, 1428, 1407, 1305, 1216, 915, 798, 678, 522, 494, 457; **HRMS** (EI, *m/z*) $[M]^+$ calcd. for $C_{15}H_{20}O_2$: 232.1463, found: 232.1464.

(*Z*)-4-Methyl-7-(*p*-tolyl)hept-4-enoic acid

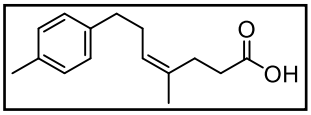

Colorless liquid (77%); **^{1}H NMR** (600 MHz, $CDCl_3$): δ 7.11 – 7.05 (m, 4H), 5.24 (t, *J* = 7.2 Hz, 1H), 2.59 (t, *J* = 7.7 Hz, 2H), 2.34 – 2.26 (m, 9H), 1.68 (s, 3H); **^{13}C NMR** (151 MHz, $CDCl_3$): δ 179.1, 139.1, 135.4, 133.6, 129.1, 128.5, 126.3, 35.9, 32.5, 30.0, 27.0, 23.0, 21.1; **IR** (cm^{-1}) 2919, 1707, 1515, 1447, 1412, 1282, 1211, 935, 807; **HRMS** (EI, *m/z*) $[M]^+$ calcd. for $C_{15}H_{20}O_2$: 232.1463, found: 232.1466.

3.4.5. Preparation of α-methyl carboxylic acid derivatives

3.4.5.1. Synthesis of chiral substrates

Synthesis of (*R*,*E*)-4-Benzyl-3-{7-(3,5-dimethoxyphenyl)-4-methylhept-4-enoyl}oxazolidin-2-one (9)

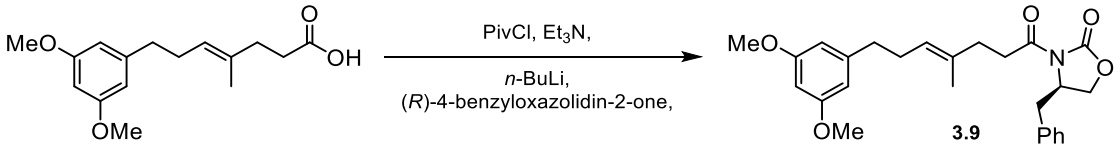

To the solution of (*E*)-7-(3,5-dimethoxyphenyl)-4-methylhept-4-enoic acid (2.00 g, 7.10 mmol, 1.0 equiv.) in anhydrous THF, Et_3N (1.20 mL, 8.62 mmol, 1.2 equiv.) was added, and the solution was cooled to −78 °C. Then, pivaloyl chloride (0.93 mL, 7.54 mmol, 1.05 equiv.) was added, and the reaction mixture was stirred for 30 min at the same temperature. In a separate flask, (*R*)-4-benzyloxazolidin-2-one (1.21 g, 6.83 mmol, 0.95 equiv.) in anhydrous THF was cooled to −78 °C, and *n*-BuLi (2.5 M in *n*-hexane, 2.73 mL, 6.83 mmol, 0.95 equiv.) was added dropwise and stirred for 10 min. After that, this solution was added to the solution of anhydride prepared above, and the reaction mixture was stirred for 30 min at 0 °C. The reaction was quenched with saturated aqueous NH_4Cl solution, the layers were separated, and the aqueous layer was extracted with Et_2O. The combined organic phases were dried over $MgSO_4$, filtered, and concentrated under reduced pressure. The crude product was purified by column chromatography (SiO_2, *n*-hexane/EtOAc 9:1 to 6:1) to obtain **3.9** (2.47 g, 79%) as a viscous colorless oil.

(*R*,*E*)-4-Benzyl-3-{7-(3,5-dimethoxyphenyl)-4-methylhept-4-enoyl}oxazolidin-2-one (3.9)

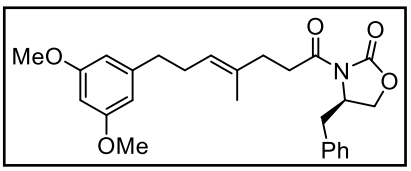

Colorless oil (79%); **^{1}H NMR** (400 MHz, $CDCl_3$): δ 7.37 – 7.31 (m, 2H), 7.30 – 7.26 (m, 1H), 7.24 – 7.19 (m, 2H), 6.35 (d, *J* = 2.2 Hz, 2H), 6.30 (t, *J* = 2.2 Hz, 1H), 5.27 (t, *J* = 6.8 Hz, 1H), 4.66 (ddt, *J* = 10.3, 6.8, 3.4 Hz, 1H), 4.21 – 4.13 (m, 2H), 3.77 (s, 6H), 3.29 (dd, *J* = 13.3, 3.3 Hz, 1H), 3.14 – 2.96 (m, 2H), 2.75 (dd, *J* = 13.3, 9.7 Hz, 1H), 2.62 – 2.55 (m, 2H), 2.38 (t, *J* = 7.8 Hz, 2H), 2.31 (q, *J* = 7.4 Hz, 2H), 1.64 (s, 3H); **^{13}C NMR** (101 MHz, $CDCl_3$): δ 173.0, 160.8, 153.5, 144.7, 135.4, 134.2, 129.5, 129.1, 127.4, 124.8, 106.6, 97.9, 66.3, 55.4, 55.3, 38.0, 36.3, 34.4, 34.1, 29.8, 16.2; **IR** (cm^{-1}) 2936, 2838, 1781, 1699, 1595, 1456, 1429, 1385, 1352, 1307, 1294, 1206, 1152, 1110, 1066, 923, 833; **HRMS** (ESI+, *m/z*) $[M+H]^+$ calcd. for $C_{26}H_{32}NO_5$: 438.2275, found: 438.2265; **Specific Rotation** $[\alpha]_D^{22}$ −43.7 (c = 1.0, CH_2Cl_2).

Synthesis of (*R*)-4-Benzyl-3-{(*R*,*E*)-7-(3,5-dimethoxyphenyl)-2,4-dimethylhept-4-enoyl}oxazolidin-2-one (3.10)

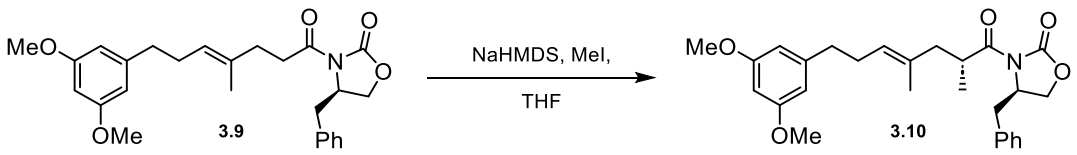

To the solution of **3.9** (2.32 g, 5.30 mmol, 1.0 equiv.) in anhydrous THF at −78 °C, NaHMDS (1 M in THF, 6.36 mL, 6.36 mmol, 1.2 equiv.) was added, and the reaction mixture was stirred for 30 min. Then, iodomethane (1.66 mL, 26.5 mL, 5.0 equiv.) was added, and the reaction mixture was stirred at −78 °C for 5 h. After completion, the reaction was quenched with saturated aqueous NH_4Cl solution, the layers were separated, and the aqueous layer was extracted with Et_2O. The combined organic phases were dried over $MgSO_4$, filtered, and concentrated under reduced pressure. The crude product was purified by column chromatography (SiO_2, *n*-hexane/EtOAc 15:1 to 10:1) to obtain **3.10** (1.69 g, 71%) as a viscous colorless oil.

(*R*)-4-Benzyl-3-{(*R*,*E*)-7-(3,5-dimethoxyphenyl)-2,4-dimethylhept-4-enoyl}oxazolidin-2-one (3.10)

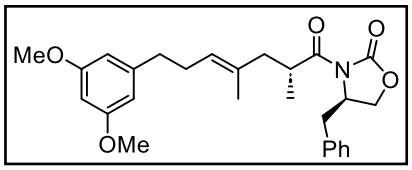

Colorless oil (71%); **^{1}H NMR** (400 MHz, $CDCl_3$): δ 7.36 – 7.30 (m, 2H), 7.30 – 7.27 (m, 1H), 7.23 – 7.19 (m, 2H), 6.34 (d, *J* = 2.2 Hz, 2H), 6.28 (t, *J* = 2.2 Hz, 1H), 5.22 (t, *J* = 6.7 Hz, 1H), 4.60 (ddt, *J* = 9.7, 7.3, 3.2 Hz, 1H), 4.17 – 4.10 (m, 2H), 3.93 (h, *J* = 7.0 Hz, 1H), 3.77 (s, 6H), 3.26 (dd, *J* = 13.3, 3.3 Hz, 1H), 2.76 (dd, *J* = 13.3, 9.5 Hz, 1H), 2.57 (t, *J* = 7.7 Hz, 2H), 2.44 (dd, *J* = 13.5, 6.7 Hz, 1H), 2.38 – 2.21 (m, 2H), 2.03 (dd, *J* = 13.5, 7.8 Hz, 1H), 1.60 (s, 3H), 1.15 (d, *J* = 6.8 Hz, 3H); **^{13}C NMR** (101 MHz, $CDCl_3$): δ 177.2, 160.8, 153.2, 144.7, 135.5, 133.1, 129.6, 129.1, 127.5, 126.4, 106.6, 97.9, 66.1, 55.5, 55.4, 43.5, 38.0, 36.3, 35.9, 29.8, 16.9, 16.1; **IR** (cm^{-1}) 2934, 2838, 1779, 1695, 1595, 1454, 1384, 1349, 1292, 1205, 1152, 1068, 1014, 971, 923, 832; **HRMS** (ESI+, *m/z*) $[M+H]^+$ calcd. for $C_{27}H_{34}NO_5$: 452.2431, found: 452.2427; **Specific Rotation** $[\alpha]_D^{22}$ −64.5 (c = 1.0, CH_2Cl_2).

Preparation of chiral α-methyl carboxylic acid from 3.10

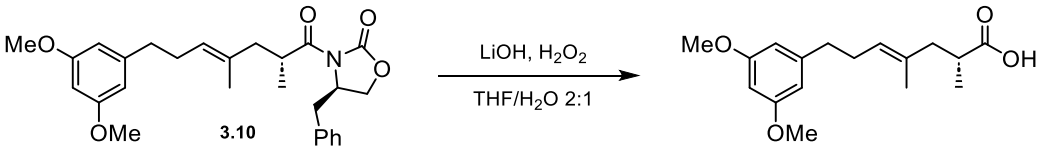

To the solution of **3.10** (1.60 g, 3.54 mmol, 1.0 equiv.) in a solvent mixture of THF/H_2O 2:1 at 0 °C, H_2O_2 (30% in H_2O, 1.81 mL, 17.7 mmol, 5.0 equiv.) was added, followed by the addition of LiOH (127 mg, 5.31 mmol, 1.5 equiv.). The reaction mixture was stirred for 2 h at the same temperature and then quenched by the addition of $Na_2S_2O_3{\cdot}5H_2O$ (10 equiv.) and stirred for an additional 2h. The reaction mixture was basified by the addition of 1 M NaOH to reach a pH of

around 10–11 and extracted with Et_2O. The organic phase was discarded, and the aqueous solution was acidified with $NaHSO_4$ to reach a pH of around 3 and then extracted with EtOAc. The combined organic phases were dried over $MgSO_4$, filtered, and concentrated under reduced pressure. The crude product was purified by column chromatography (SiO_2, *n*-hexane/EtOAc 4:1) to give (*R*,*E*)-7-(3,5-dimethoxyphenyl)-2,4-dimethylhept-4-enoic acid (800 mg, 77%) as a viscous colorless oil.

(*R*,*E*)-7-(3,5-Dimethoxyphenyl)-2,4-dimethylhept-4-enoic acid

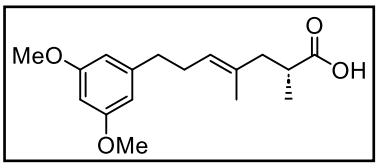

Colorless oil (77%); **^{1}H NMR** (400 MHz, $CDCl_3$): δ 6.35 (d, *J* = 2.2 Hz, 2H), 6.30 (t, *J* = 2.1 Hz, 1H), 5.23 (t, *J* = 7.0 Hz, 1H), 3.78 (s, 6H), 2.67 – 2.54 (m, 3H), 2.40 (dd, *J* = 13.6, 6.8 Hz, 1H), 2.30 (q, *J* = 7.5 Hz, 2H), 2.05 (dd, *J* = 13.6, 8.0 Hz, 1H), 1.57 (s, 3H), 1.10 (d, *J* = 6.8 Hz, 3H); **^{13}C NMR** (101 MHz, $CDCl_3$): δ 182.6, 160.8, 144.7, 132.7, 126.7, 106.7, 97.9, 55.4, 43.7, 37.8, 36.3, 29.8, 16.4, 15.8; **IR** (cm^{-1}) 2937, 2838, 1705, 1596, 1461, 1428, 1347, 1293, 1240, 1205, 1153, 1068, 924, 831; **HRMS:** (ESI+, *m/z*) $[M+H]^+$ calcd. for $C_{17}H_{25}O_4$: 293.1747, found: 293.1744; **Specific Rotation** $[\alpha]_D^{22}$ +2.5 (c = 1.0, CH_2Cl_2).

3.4.5.2. Preparation of methyl (*E*)-7-(3,5-dimethoxyphenyl)-4-methylhept-4-enoate

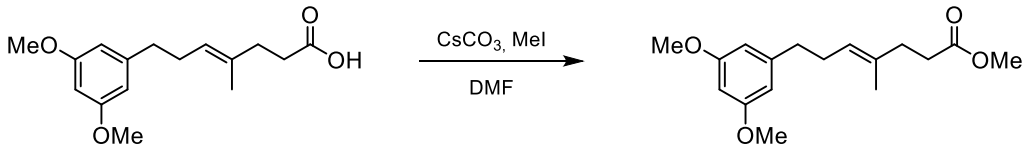

To a flame-dried flask and stir bar under an argon atmosphere, Cs_2CO_3 (1.29 g, 3.95 mmol, 1.1 equiv.), anhydrous DMF (24 mL), and (*E*)-7-(3,5-dimethoxyphenyl)-4-methylhept-4-enoic acid (1.0 g, 3.6 mmol, 1 equiv.) were added. Then, iodomethane (0.34 mL, 5.4 mmol, 1.5 equiv.) was added dropwise and stirred for 12 h. After completion, the reaction mixture was diluted with *n*-hexanes (15 mL) and water (15 mL). The aqueous layer was extracted with *n*-hexane (2 × 20 mL). The combined organic phases were washed with brine, dried over $MgSO_4$, filtered, and concentrated under reduced pressure to obtain methyl (*E*)-7-(3,5-dimethoxyphenyl)-4-methylhept-4-enoate as a colorless oil (1.00 g, 95%).

Methyl (*E*)-7-(3,5-dimethoxyphenyl)-4-methylhept-4-enoate

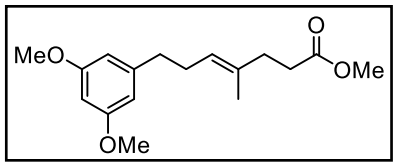

Colorless oil (95%); **^{1}H NMR** (400 MHz, $CDCl_3$): δ 6.34 (d, *J* = 2.3 Hz, 2H), 6.30 (t, *J* = 2.3 Hz, 1H), 5.20 (t, *J* = 7.1, 1.3 Hz, 1H), 3.78 (s, 6H), 3.66 (s, 3H), 2.56 (t, *J* = 8.9, 6.7 Hz, 2H), 2.44 – 2.37 (m, 2H), 2.33 – 2.24 (m, 4H), 1.58 (s, *J* = 1.3 Hz, 3H); **^{13}C NMR** (101 MHz, $CDCl_3$): δ 174.0, 160.8, 144.7, 134.2, 124.5, 106.6, 97.8, 55.4, 51.6, 36.4, 34.7, 33.1, 29.8, 16.1; **IR** (cm^{-1}) 2933, 2856, 2838, 1734, 1593, 1466, 1339, 1325, 1266, 1207, 1154, 1065, 910, 832; **HRMS** (ESI+, *m/z*) $[M+H]^+$ calcd. for $C_{17}H_{25}O_4$: 293.1747, found: 293.1751.

3.4.5.3. Preparation of racemic α-methyl ester

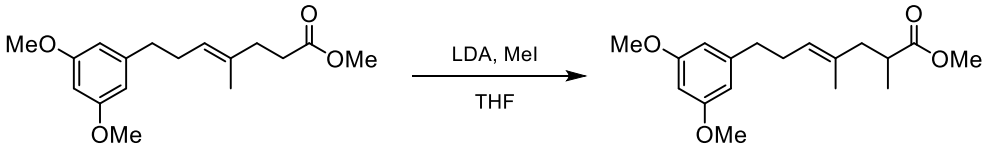

To a flamed-dried flask under an argon atmosphere, diisopropylamine (0.58 ml, 4.10 mmol, 1.2 equiv.) was dissolved in anhydrous THF (4 mL). The solution was cooled to 0 °C, and a solution of *n*-BuLi (1.6 M in *n*-hexane, 2.57 ml, 4.10 mmol, 1.2 equiv.) was added dropwise. The reaction mixture was stirred at 0 °C for 10 min. A solution of methyl (*E*)-7-(3,5-dimethoxyphenyl)-4-methylhept-4-enoate (1.00 g, 3.42 mmol, 1.0 equiv.) in anhydrous THF (6.6 mL) was added to the lithium diisopropyl amide mixture at −78 °C. The reaction was stirred for 30 min at the same temperature, and then iodomethane (0.32 ml, 5.13 mmol, 1.5 equiv.) was added. The mixture was stirred for 1 h at room temperature. After completion, the reaction was quenched with a saturated aqueous NH_4Cl solution (10 mL). The aqueous phase was extracted with Et_2O (3 × 30 mL). The combined organic phases were washed with brine, dried over Na_2SO_4, filtered, and concentrated under reduced pressure. The crude product was purified by column chromatography (SiO_2, *n*-hexane/EtOAc 9:1) to give (*E*)-7-(3,5-dimethoxyphenyl)-2,4-dimethylhept-4-enoate (729 mg, 69%) as a viscous colorless oil.

Methyl (*E*)-7-(3,5-dimethoxyphenyl)-2,4-dimethylhept-4-enoate

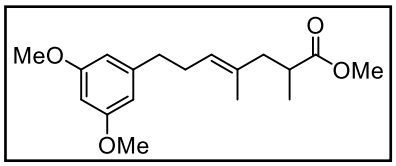

Colorless oil (69%); **^{1}H NMR** (400 MHz, $CDCl_3$): δ 6.35 (d, *J* = 2.3 Hz, 2H), 6.30 (t, *J* = 2.3 Hz, 1H), 5.20 (m, *J* = 7.1, 1.3 Hz, 1H), 3.78 (s, 6H), 3.64 (s, 3H), 2.65 – 2.53 (m, 3H), 2.43 – 2.24 (m, 3H), 2.03 (ddd, *J* = 13.5, 7.8, 0.9 Hz, 1H), 1.59 – 1.55 (s, 3H), 1.08 (d, *J* = 6.9 Hz, 3H); **^{13}C NMR** (101 MHz, $CDCl_3$): δ 177.2, 160.8, 144.8, 133.0, 126.4, 106.6, 97.9, 55.4, 51.6, 44.0, 38.0, 36.4, 29.8, 16.7, 15.8; **IR** (cm^{-1}) 2939, 2855, 2839, 1735, 1594, 1462, 1346, 1327, 1262, 1204, 1155, 1068, 830; **HRMS** (ESI+, *m/z*) $[M+H]^+$ calcd. for $C_{18}H_{27}O_4$: 307.1904, found: 307.1901.

3.4.6. Preparation of esters with heteroaryl group

3.4.6.1. Preparation of iodoalkene

This procedure was adapted from the literature [19].

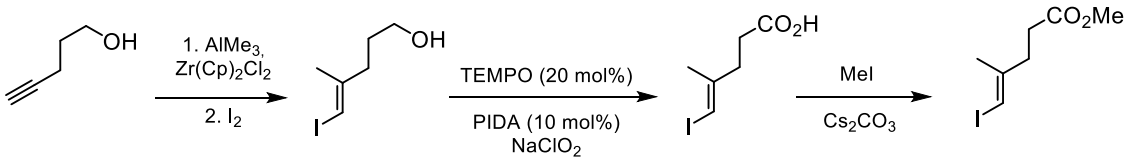

Step 1: A flame-dried two-necked flask, containing zirconocene dichloride (4.17 g, 14.3 mmol, 0.4 equiv.), was evacuated and backfilled three times with argon. Anhydrous CH_2Cl_2 (80 mL) was added, followed by a solution of trimethyl aluminum (53.5 mL, 107 mmol, 3.0 equiv., 2.0 M in toluene), and stirred for 15 min. After the addition of trimethyl aluminum, the flask was placed in an ice bath and allowed to cool before 4-pentyn-1-ol (3.00 g, 3.32 mL, 35.7 mmol, 1 equiv.) was added dropwise (*Notes*). The reaction mixture was allowed to warm to room temperature and stirred for 12 h.

Next, the reaction was cooled to 0 °C, and a solution of iodine (11.8 g, 46.4 mmol, 1.3 equiv.) in anhydrous THF (40 mL) was added. The reaction was stirred at 0 °C for 1 h until it turned bright yellow. Then, CH_2Cl_2 (50 mL) was added slowly, followed by the dropwise addition of water (10 mL) (*Notes*). The addition of water was continued until the bubbling stopped. The resulting slurry was filtered through a celite pad and washed with CH_2Cl_2. The solution was further washed with aqueous 1 M HCl (50 mL), saturated aqueous $NaHCO_3$ (50 mL), saturated aqueous sodium thiosulfate (50 mL), and finally with brine (20 mL). The combined organic phases were dried over $MgSO_4$, filtered, and concentrated under reduced pressure. The reaction mixture was not heated above 30 °C and was shielded from light. The crude (*E*)-5-iodo-4-methylpent-4-en-1-ol was used without purification in the next step.

Notes: The addition of 4-pentyn-1-ol is exothermic. Also, the addition of water is extremely exothermic and generates a lot of bubbling in the reaction mixture.

Step 2: The crude (*E*)-5-iodo-4-methylpent-4-en-1-ol was dissolved in a 1:1 solution of acetonitrile and aqueous 1 M sodium phosphate buffer with pH = 7 (total volume 350 mL), cooled to 0 °C. Then, 2,2,6,6-tetramethylpiperidine 1-oxyl (1.12 g, 7.14 mmol, 0.2 equiv.) and (diacetoxyiodo)benzene (1.15 g, 3.57 mmol, 0.1 equiv.) were added, followed by addition of sodium chlorite (12.1 g, 107 mmol, 3.0 equiv.). After completed addition, the reaction mixture turned deep purple and was allowed to warm to room temperature and stirred for 12 h. After reaction completion, the flask was cooled to 0 °C, diluted with distilled water, and sodium sulfite was added portion-wise until the reaction became colorless. The pH was adjusted to 1 with addition of aqueous 3 M HCl. The aqueous layer was extracted with Et_2O (3 × 50 mL), and the combined organic phases were washed with aqueous 1 M HCl (50 mL). Combined organic phases were further extracted with aqueous 1 M NaOH (4 × 50ml). The combined aqueous phases were washed with hexane (50 mL) and acidified with aqueous 3 M HCl to reach pH 1. The aqueous phase turned into a cloudy suspension, and was extracted with *n*-hexane (5 × 50 mL). The combined organic phases were washed with water and brine, then dried over $MgSO_4$, filtered, and concentrated to yield (*E*)-5-iodo-4-methylpent-4-enoic acid as a clear, colorless oil (4.2 g, 49% yield over two steps) that was stored at −20 °C. (*E*)-5-iodo-4-methylpent-4-enoic acid was used in the next step without any further purification.

(*E*)-5-Iodo-4-methylpent-4-enoic acid

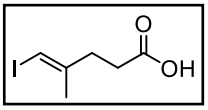

Colorless oil (49% yield over two steps); **^{1}H NMR** (400 MHz, $CDCl_3$): δ 11.14 (s, 1H), 6.01 (s, 1H), 2.56 – 2.50 (m, 4H), 1.86 (s, 3H). *Data consistent with those previously reported [19]*.

Step 3: To a flame-dried flask under an argon atmosphere, Cs_2CO_3 (6.3 g, 19 mmol, 1.1 equiv.) was added, followed by an anhydrous DMF (120 mL; 0.15 M), and (*E*)-5-iodo-4-methylpent-4-enoic acid (4.2 g, 17 mmol, 1.0 equiv.). Then, iodomethane (1.6 mL, 26 mmol, 1.5 equiv.) was added dropwise. The reaction mixture was stirred for 12 h.

After completion, the reaction mixture was diluted with *n*-hexane (80 mL) and water (80 mL). The aqueous layer was extracted with *n*-hexane (2 × 30 mL). The combined organic phases were washed with brine and dried over $MgSO_4$. The solvent was removed under reduced pressure to obtain methyl (*E*)-5-iodo-4-methylpent-4-enoate as a colorless oil (3.62 g, 81%).

Methyl (*E*)-5-iodo-4-methylpent-4-enoate

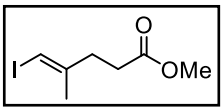

Colorless oil (81%); **^{1}H NMR** (400 MHz, $CDCl_3$): δ 5.97 (s, 1H), 3.68 (s, 3H), 2.55 – 2.50 (m, 2H), 2.48 – 2.41 (m, 2H), 1.85 (s, 3H). *Data consistent with those previously reported [19]*.

3.4.6.2. Preparation of vinyl-substituted heteroarenes

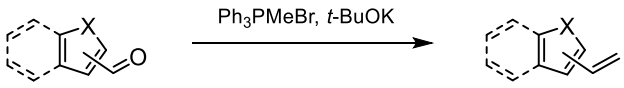

A flamed-flask was charged with methyltriphenylphosphonium bromide (1.7 equiv.) and potassium tert-butoxide (1.5 equiv.), and the mixture was stirred in anhydrous Et_2O (0.7M) at 0 °C for 15 min until the reaction turned bright yellow. After that, a solution of the aldehyde (1.0 equiv.) in Et_2O (0.75M) was added dropwise to the mixture at the same temperature. Cooling was then removed and reaction mixture was stirred at room temperature for 12 h. After completion, the reaction mixture was cooled to 0 °C and quenched with a saturated aqueous NH_4Cl solution (80 mL). The aqueous phase was extracted with Et_2O (3 × 50 mL). The combined organic phases were washed with brine, dried over $MgSO_4$, filtered, and concentrated under reduced pressure. The crude product was purified by column chromatography (SiO_2, *n*-pentane/CH_2Cl_2 20:1) to give the desired alkene.

1-Methyl-2-vinyl-1*H*-indole

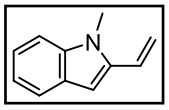

White solid (50%); **^{1}H NMR** (400 MHz, CD_2Cl_2): δ 7.54 (dt, *J* = 7.9, 1.0 Hz, 1H), 7.30 (dq, *J* = 8.2, 0.9 Hz, 1H), 7.17 (ddd, *J* = 8.3, 7.0, 1.2 Hz, 1H), 7.06 (ddd, *J* = 8.0, 7.0, 1.0 Hz, 1H), 6.84 (ddd, *J* = 17.5, 11.2, 0.6 Hz, 1H), 6.68 (s, 1H), 5.84 (dd, *J* = 17.5, 1.4 Hz, 1H), 5.37 (dd, *J* = 11.2, 1.4 Hz, 1H), 3.75 (s, 3H). *Data consistent with those previously reported [20]*.

2-Vinylbenzofuran

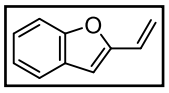

Colorless liquid (73%); **^{1}H NMR** (200 MHz, $CDCl_3$): δ 7.52 (d, *J* = 7.7 Hz, 1H), 7.45 (d, *J* = 8.2 Hz, 1H), 7.27 (t, *J* = 7.8 Hz, 1H), 7.20 (t, *J* = 7.4 Hz, 1H), 6.64 (dd, *J* = 11.2, 17.5 Hz, 1H), 6.60 (s, 1H), 5.96 (d, *J* = 17.2 Hz, 1H), 5.39 (dd, *J* = 11.2, 0.9 Hz, 1H). *Data consistent with those previously reported [9]*.

1-Tosyl-2-vinyl-1*H*-pyrrole

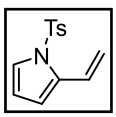

Dark red solid (41%); **^{1}H NMR** (200 MHz, CD_2Cl_2): δ 7.65 (d, *J* = 3.6 Hz 2H), 7.27 – 7.22 (m, 3 H), 7.12 – 7.02 (m, 1H), 6.44 (d, *J* = 3.4 Hz, 1H), 6.23 (t, *J* = 3.4 Hz, 1H), 5.49 (dd, *J* = 17.5, 1.3 Hz, 1H), 5.09 (dd, *J* = 11.2, 1.2 Hz, 1 H), 2.36 (s, 3H). *Data consistent with those previously reported [21]*.

2-Vinylbenzo[*b*]thiophene

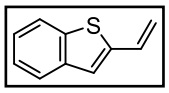

Pale yellow solid (70%); **^{1}H NMR** (200 MHz, $CDCl_3$) δ 7.74 (m, 1H), 7.67 (dd, *J* = 5.1, 3.8 Hz, 1H), 7.30 – 7.25 (m, 2H), 7.14 (s, 1H), 6.90 (dd, *J* = 17.3, 10.8 Hz, 1H), 5.66 (d, *J* = 17.3 Hz, 1H), 5.29 (d, *J* = 10.8 Hz, 1H). *Data consistent with those previously reported [21]*.

***tert*-Butyldimethyl{(5-vinylfuran-2-yl)methoxy}silane**

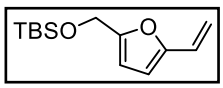

Colorless oil (60%); **^{1}H NMR** (400 MHz, CD_2Cl_2): δ 6.46 (dd, *J* = 17.5, 11.3 Hz, 1H), 6.22 – 6.17 (m, 2H), 5.64 (dd, *J* = 16.2, 1.2 Hz, 1H), 5.12 (dd, *J* = 11.2, 1.4 Hz, 1H), 4.64 (s, 2H), 0.91 (s, 9H), 0.10 (s, 6H). *Data consistent with those previously reported [22]*.

3-Vinylbenzo[*b*]thiophene

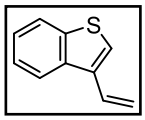

Pale yellow solid (30%); **^{1}H NMR** (200 MHz, CD_2Cl_2): δ 7.93 – 7.92 (m, 2H), 7.44 (s, 1H), 7.37 (m, 2H), 7.05 (s, 1H), 5.82 (dd, *J* = 17.6, 1.3 Hz, 1H), 5.34 (dd, *J* = 11.1, 1.3 Hz, 1H). *Data consistent with those previously reported [23]*.

3-Vinylthiophene

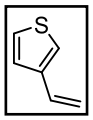

Colorless oil (22%); **^{1}H NMR** (400 MHz, $CDCl_3$): δ 7.30 – 7.23 (m, 2H), 7.18 (dd, *J* = 2.8, 1.4 Hz, 1H), 6.77 – 6.68 (m, 1H), 5.59 (dd, *J* = 17.6, 1.2 Hz, 1H), 5.20 (dd, *J* = 10.8, 1.2 Hz, 1H). *Data consistent with those previously reported [24]*.

3.4.6.3. Preparation of esters with heteroaryl group *via* Suzuki coupling

To a solution of the corresponding alkene (2.0 equiv.) in THF, 9-borabicyclo[3.3.1]nonane (2.0 equiv.) in THF (0.2 M) was added at 0 °C, and the mixture was stirred for 3 h at room temperature. After that, the reaction was diluted with DMF (0.1 M), and an aqueous solution of K_3PO_4 (2.5 equiv., 3.0 M) was added. Then $Pd(dppf)Cl_2$ (0.1 equiv.) and methyl (*E*)-5-iodo-4-methylpent-4-enoate (1.0 equiv.) were added consecutively, and the reaction mixture was stirred for 12 h at room temperature. After the reaction was completed, it was diluted with *n*-hexane (20-30 mL) and quenched with a saturated aqueous solution of NH_4Cl (20–30 mL). The aqueous layer was extracted with *n*-hexane (3 × 20 mL). The combined organic phases were washed with brine, dried over $MgSO_4$, filtered, and concentrated under reduced pressure. The crude product was purified by column chromatography (SiO_2, *n*-hexane/EtOAc 10:1) to give the desired product.

Methyl (*E*)-4-methyl-7-(1-methyl-1*H*-indol-2-yl)hept-4-enoate

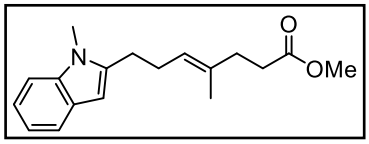

Colorless oil (81%); **^{1}H NMR** (400 MHz, CD_2Cl_2): δ 7.48 (dt, *J* = 7.8, 1.0 Hz, 1H), 7.26 (dt, *J* = 8.2, 1.0 Hz, 1H), 7.11 (ddd, *J* = 8.2, 7.0, 1.2 Hz, 1H), 7.02 (ddd, *J* = 8.0, 7.0, 1.0 Hz, 1H), 6.22 (s, 1H), 5.35 – 5.25 (m, 1H), 3.66 (s, 3H), 3.62 (s, 3H), 2.83 – 2.73 (m, 2H), 2.50 – 2.32 (m, 4H), 2.36 – 2.26 (m, 2H), 1.64 (s, 3H); **^{13}C NMR** (101 MHz, CD_2Cl_2): δ 174.1, 141.7, 138.0, 135.3, 128.6, 124.6, 120.9, 120.1, 119.6, 109.3, 99.1, 51.9, 35.1, 33.4, 29.9, 27.6, 27.4, 16.3; **IR** (cm^{-1}) 2946, 2854, 1737, 1544, 1467, 1436, 1400, 1344, 1313, 1159, 773, 747; **HRMS** (ESI+, *m/z*) $[M+H]^+$ calcd. for $C_{18}H_{24}NO_2$: 286.1802, found: 286.1804.

Methyl (*E*)-7-(furan-2-yl)-4-methylhept-4-enoate

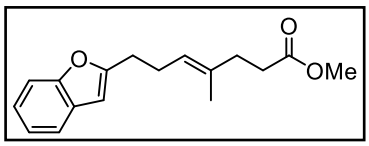

Colorless oil (84%); **^{1}H NMR** (400 MHz, $CDCl_3$): δ 7.49 – 7.46 (m, 1H), 7.43 – 7.39 (m, 1H), 7.23 – 7.15 (m, 2H), 6.37 (q, *J* = 1.0 Hz, 1H), 5.23 (tq, *J* = 7.1, 1.3 Hz, 1H), 3.64 (s, 3H), 2.79 (t, *J* = 7.8 Hz, 2H), 2.48 – 2.37 (m, 4H), 2.34 – 2.28 (m, 2H), 1.62 (s, 3H); **^{13}C NMR** (101 MHz, $CDCl_3$): δ 173.9, 159.1, 154.7, 134.9, 129.1, 123.8, 123.2, 122.5, 120.3, 110.8, 102.2, 51.6, 34.7, 33.1, 28.7, 26.3, 16.1; **IR** (cm^{-1}) 2950, 2854, 1738, 1601, 1587, 1455, 1436, 1350, 1293, 1164, 1009, 943; **HRMS** (ESI+, *m/z*) $[M+H]^+$ calcd. for $C_{17}H_{21}O_3$: 273.1485, found: 273.1483.

Methyl (*E*)-4-methyl-7-(1-tosyl-1*H*-pyrrol-2-yl)hept-4-enoate

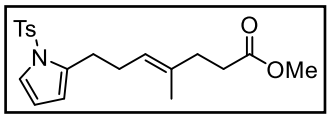

Colorless oil (84%); **^{1}H NMR** (400 MHz, CD_2Cl_2): δ 7.63 (d, *J* = 8.4 Hz, 2H), 7.31 (d, *J* = 8.1 Hz, 2H), 7.25 (dd, *J* = 3.4, 1.8 Hz, 1H), 6.20 (t, *J* = 3.4 Hz, 1H), 5.99 (m, 1H), 5.11 (m, 1H), 3.62 (s, 3H), 2.67 (t, *J* = 7.6 Hz, 2H), 2.44 – 2.31 (m, 5H), 2.29 – 2.19 (m, 4H), 1.55 (s, 3H); **^{13}C NMR** (101 MHz, CD_2Cl_2): δ 174.1, 145.7, 136.9, 135.9, 135.2, 130.5, 127.2, 124.4, 122.7, 112.7, 111.9, 51.8, 35.1, 33.4, 32.6, 27.7, 26.8, 22.6, 21.8, 16.2; **IR** (cm^{-1}) 2954, 2850, 1734, 1604, 1550, 1450, 1422, 1262, 1175, 1155, 985; **HRMS** (ESI+, *m/z*) $[M+H]^+$ calcd. for $C_{20}H_{26}NO_4S$: 376.1577, found: 376.1579.

Methyl (*E*)-7-(benzo[b]thiophen-2-yl)-4-methylhept-4-enoate

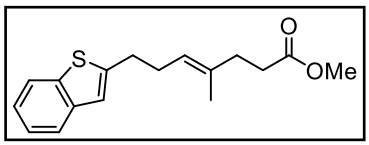

Colorless oil (77%); **^{1}H NMR** (400 MHz, CD_2Cl_2): δ 7.88 – 7.70 (d, 1H), 7.67 (d, *J* = 8.2, 0.9 Hz, 1H), 7.48 – 7.14 (m, 2H), 7.02 (s, *J* = 1.0 Hz, 1H), 5.25 (tq, *J* = 7.1, 1.4 Hz, 1H), 3.61 (s, 3H), 2.93 (t, *J* = 7.8 Hz, 2H), 2.59 – 2.35 (m, 4H), 2.36 – 2.11 (m, 2H), 1.76 – 1.40 (s, 3H); **^{13}C NMR** (101 MHz, CD_2Cl_2): δ 174.0, 146.8, 140.8, 139.9, 135.6, 124.5, 124.2, 123.9, 123.2, 122.5, 121.1, 51.8, 35.1, 33.3, 31.3, 30.0, 16.3; **IR** (cm^{-1}) 2948, 2854, 1737, 1602, 1549, 1434, 1358, 1293, 1242, 1195, 1081, 1019, 936; **HRMS** (ESI+, *m/z*) $[M+H]^+$ calcd. for $C_{17}H_{21}O_2S$: 289.1257, found: 289.1259.

Methyl (*E*)-7-(5-[{(*tert*-butyldimethylsilyl)oxy}methyl]furan-2-yl)-4-methylhept-4-enoate

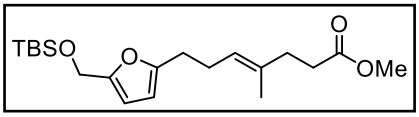

Colorless oil (90%); **^{1}H NMR** (400 MHz, $CDCl_3$): δ 6.09 (d, *J* = 3.0 Hz, 1H), 5.88 (d, *J* = 3.0 Hz, 1H), 5.18 (tq, *J* = 7.1, 1.3 Hz, 1H), 4.58 (s, 2H), 3.65 (s, 3H), 2.64 – 2.58 (m, 2H), 2.42 – 2.37 (m, 2H), 2.34 – 2.26 (m, 4H), 1.60 (s, 3H), 0.90 (s, 9H), 0.08 (s, 6H); **^{13}C NMR** (101 MHz, $CDCl_3$): δ 174.0, 155.6, 152.6, 134.5, 124.1, 108.1, 105.6, 58.4, 51.6, 34.7, 33.1, 28.3, 26.6, 26.1, 18.6, 16.0, −5.0; **IR** (cm^{-1}) 2937, 2855, 1741, 1618, 1458, 1389, 1372, 1300, 1252, 1071, 1042, 841; **HRMS** (ESI+, *m/z*) $[M+H]^+$ calcd. for $C_{20}H_{35}O_4Si$: 367.2299, found: 367.2302.

Methyl (*E*)-7-(benzo[*b*]thiophen-3-yl)-4-methylhept-4-enoate

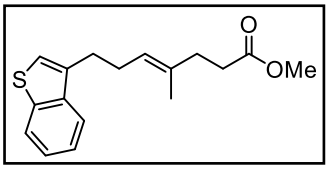

Colorless oil (95%); **^{1}H NMR** (400 MHz, CD_2Cl_2): δ 7.87 – 7.84 (d, 1H), 7.77 (d, *J* = 7.3 Hz, 1H), 7.41 – 7.31 (m, 2H), 7.11 (s, 1H), 5.28 (t, *J* = 6.5 Hz, 1H), 3.62 (s, 3H), 2.87 (t, *J* = 7.6 Hz, 2H), 2.44 (q, *J* = 7.4 Hz, 2H), 2.41 – 2.35 (m, 2H), 2.31 – 2.26 (m, 2H), 1.57 (s, 3H); **^{13}C NMR** (101 MHz, CD_2Cl_2): δ 174.1, 140.9, 139.7, 137.2, 135.2, 124.8, 124.6, 124.3, 123.3, 122.2, 121.7, 51.8, 35.1, 33.4, 29.0, 28.0, 16.2; **IR** (cm^{-1}) 2945, 2852, 1736, 1604, 1551, 1432, 1357, 1294, 1244, 1193, 1079, 1021, 933; **HRMS** (ESI+, *m/z*) $[M+H]^+$ calcd. for $C_{17}H_{21}O_2S$: 289.1257, found: 289.1260.

Methyl (*E*)-4-methyl-7-(thiophen-3-yl)hept-4-enoate

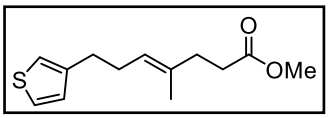

Colorless oil (98%); **^{1}H NMR** (400 MHz, $CDCl_3$): δ 7.23 (dd, *J* = 4.9, 3.0 Hz, 1H), 6.94 – 6.91 (m, 2H), 5.23 – 5.18 (m, 1H), 3.66 (s, 3H), 2.68 – 2.63 (m, 2H), 2.43 – 2.38 (m, 2H), 2.31 (q, *J* = 6.7 Hz, 4H), 1.57 (s, 3H); **^{13}C NMR** (101 MHz, $CDCl_3$): δ 174.0, 142.7, 134.3, 128.4, 125.2, 124.6, 120.2, 51.6, 34.4, 32.9, 30.4, 29.0, 16.0; **IR** (cm^{-1}) 2949, 2854, 1737, 1645, 1436, 1352, 1293, 1253, 1196, 1160, 836; **HRMS** (ESI+, *m/z*) $[M+H]^+$ calcd. for $C_{13}H_{19}O_2S$: 239.1100, found: 239.1097.

Methyl (*E*)-4-methyl-7-(thiophen-2-yl)hept-4-enoate

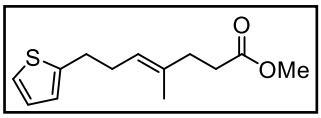

Colorless oil (80%); **^{1}H NMR** (400 MHz, $CDCl_3$): δ 7.10 (dd, *J* = 5.1, 1.2 Hz, 1H), 6.91 (dd, *J* = 5.1, 3.4 Hz, 1H), 6.79 – 6.77 (m, 1H), 5.22 (tq, *J* = 7.1, 1.4 Hz, 1H), 3.66 (s, 3H), 2.85 (t, *J* = 7.5 Hz, 2H), 2.45 – 2.27 (m, 6H), 1.59 (s, 3H); **^{13}C NMR** (101 MHz, $CDCl_3$): δ 174.0, 145.1, 134.9, 126.8, 124.3, 124.1, 123.1, 51.7, 34.7, 33.1, 30.3, 30.1, 16.1; **IR** (cm^{-1}) 2951, 2852, 1735, 1645, 1435, 1354, 1291, 1255, 1199, 1158, 833; **HRMS** (ESI+, *m/z*) $[M+H]^+$ calcd. for $C_{13}H_{19}O_2S$: 239.1100, found: 239.1097.

3.4.7. Preparation of elongated ester

3.4.7.1. Preparation of elongated ester with vinyl group

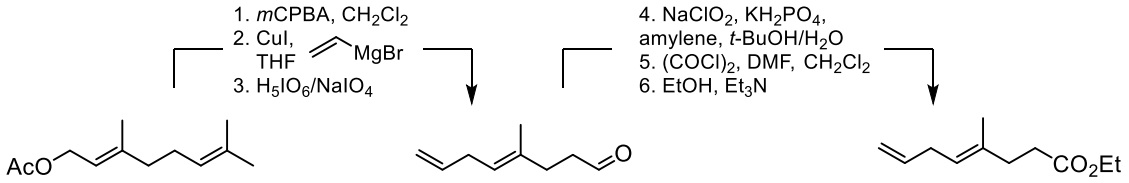

Step 1: To a solution of geranyl acetate (8.00 g, 40.8 mmol, 1.0 equiv.) in CH_2Cl_2, *m*-chloroperoxybenzoic acid (70%, 11.0 g, 44.8 mmol, 1.1 equiv.) was added at 0 °C. The reaction mixture was stirred at 0 °C for 4 h and then filtered over a celite pad. The filtrate was washed with saturated aqueous $NaHCO_3$ solution, followed by 10% aqueous K_2CO_3 solution. The layers were separated, and the organic phase was dried over $MgSO_4$, filtered, and concentrated under reduced pressure. The crude product was used in the next step without further purification.

Step 2: A separate flask was charged with a solution of the corresponding epoxide (1.0 equiv., 40.8 mmol) in anhydrous THF (140 mL). This solution was cooled to −30 °C, and copper iodide (776 mg, 4.07 mmol, 0.1 equiv.) was added. After 5 min, a solution of vinylmagnesium bromide (1.0 M in THF, 81.5 mmol, 2.0 equiv.) was added dropwise, and the reaction mixture was stirred for 1 h at −30 °C. The reaction was quenched by the addition of saturated aqueous NH_4Cl solution (80 mL). The layers were separated, and the aqueous phase was extracted with THF (160 mL). The combined organic phases were dried over $MgSO_4$, filtered, and the product was used in the next step without further purification.

Step 3: To the THF (400 mL) solution of the previous epoxide (40.8 mmol, 1.0 equiv.), a mixture of $NaIO_4$ (4.38 g, 20.4 mmol, 0.5 equiv.) and H_5IO_6 (10.2 g, 44.9 mmol, 1.1 equiv.) in water (50 mL) was added at 0 °C. The reaction mixture was stirred and allowed to warm up to room temperature. Upon completion (monitored by TLC), the reaction was quenched with saturated aqueous $NaHCO_3$ solution and extracted with Et_2O (50 mL). The combined organic phases were dried over $MgSO_4$, filtered, and concentrated under reduced pressure. (*Note: the aldehyde is fairly volatile*). The crude product was purified by column chromatography (SiO_2, *n*-hexane/EtOAc 98:2) to obtain the corresponding aldehyde as a colorless oil (2.82 g, 50% yield over 3 steps).

(*E*)-4-Methylocta-4,7-dienal

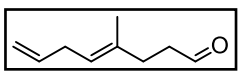

Colorless oil (50% yield over 3 steps); **^{1}H NMR** (400 MHz, $CDCl_3$): δ 9.77 (t, *J* = 1.9 Hz, 1H), 5.78 (ddt, *J* = 17.2, 10.1, 6.2 Hz, 1H), 5.20 (tq, *J* = 7.2, 1.3 Hz, 1H), 5.03 – 4.90 (m, 2H), 2.75 (t, *J* = 6.8 Hz, 2H), 2.57 – 2.50 (m, 2H), 2.35 (t, *J* = 7.5 Hz, 2H), 1.63 (s, 3H). *Data consistent with those previously reported [25]*.

Step 4: To the solution of the corresponding aldehyde (2.82 g, 20.4 mmol, 1.0 equiv.) in *t*-BuOH (200 mL), 2-methyl-2-butene (11 ml, 102 mmol, 5 equiv.) was added, followed by an aqueous solution of $NaClO_2$ (3.7 g, 40.8 mmol, 2.0 equiv.) and KH_2PO_4 (5.5 g, 40.8 mmol, 2.0 equiv.). The reaction mixture was stirred for 3 h at room temperature, then diluted with water (20 mL) and *t*-BuOH was removed under reduced pressure. The crude reaction mixture was diluted with *n*-hexane (100 mL) and extracted with 0.1 M aqueous NaOH solution (3 × 50 mL). The aqueous phases were combined and then acidified with 1 M aqueous HCl solution to reach pH 1. This aqueous phase was extracted with EtOAc (5 × 50 mL). The combined organic phases were dried over $MgSO_4$, filtered, and concentrated under reduced pressure. The carboxylic acid (2.61 g) was used in the next step without further purification.

Step 5 and 6: To a solution of the corresponding carboxylic acid (2.61 g, 16.9 mmol, 1.0 equiv.) in anhydrous CH_2Cl_2 (170 mL) at 0 °C, a drop of DMF was added, followed by oxalyl chloride (1.78 mL, 20.3 mmol, 1.2 equiv.). The reaction mixture was stirred for 4 h at room temperature and then concentrated under reduced pressure. The concentrated residue was dissolved in minimal amount of EtOAc and added to an ice-cold mixture of Et_3N (9.44 mL, 67.7 mmol, 4.0 equiv.) and ethanol (3.95 mL, 67.7 mmol, 4 equiv.). The reaction mixture was allowed to warm up to room temperature and after 12 h it was quenched with 1 M aqueous HCl solution (70 mL). The reaction mixture was extracted with Et_2O. The combined organic phases were dried over $MgSO_4$, filtered, and concentrated under reduced pressure. The crude product was purified by column chromatography (SiO_2, *n*-pentane/Et_2O 50:1) to obtain the corresponding ethyl (*E*)-4-methylocta-4,7-dienoate (1.41 g, 46% yield over 3 steps) as a colorless oil.

Ethyl (*E*)-4-methylocta-4,7-dienoate

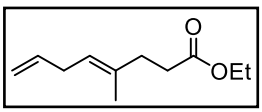

Colorless oil (46% yield over 3 steps); **^{1}H NMR** (400 MHz, $CDCl_3$): δ 5.84 – 5.72 (m, 1H), 5.20 (tq, *J* = 7.2, 1.1 Hz, 1H), 5.04 – 4.92 (m, 2H), 4.12 (q, *J* = 7.1 Hz, 2H), 2.74 (t, *J* = 6.7 Hz, 2H), 2.46 – 2.38 (m, 2H), 2.37 – 2.30 (m, 2H), 1.63 (s, 3H), 1.25 (t, *J* = 6.9 Hz, 3H). *Data consistent with those previously reported [26]*.

3.4.7.2. Preparation of elongated ester *via* Suzuki coupling

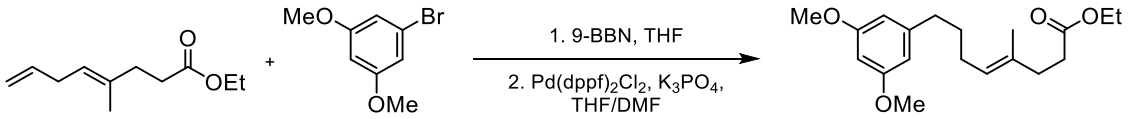

A flamed-dried two-necked flask was charged with ethyl (*E*)-4-methylocta-4,7-dienoate (806 mg, 4.42 mmol, 1.2 equiv.) and dissolved in THF (15 mL), then the mixture was cooled to 0 °C. Further, a 9-borabicyclo[3.3.1]nonane solution (8.8 mL, 0.5 M in THF, 4.42 mmol, 1.2 equiv.) was added, and the mixture was stirred for 3 h at room temperature. After that, the reaction was diluted with DMF (10 mL), and a 3.0 M aqueous K_3PO_4 solution (5.53 mmol, 1.5 equiv.) was added. $Pd(dppf)Cl_2$ (270 mg, 0.37 mmol, 0.1 equiv.) and 1-bromo-3,5-dimethoxybenzene (800 mg, 3.69 mmol, 1.0 equiv.) were then added to the mixture, which was stirred for 12 h at room temperature. After completion of the reaction, mixture was diluted with *n*-hexane (20 mL) and quenched with a saturated aqueous solution of NH_4Cl (20 mL). The aqueous layer was extracted with *n*-hexane (3 × 40 mL). The combined organic phases were washed with brine, dried over $MgSO_4$, and concentrated under reduced pressure. The crude product was purified by column chromatography (SiO_2, toluene/acetone 40:1 to 20:1) to obtain the ethyl (*E*)-8-(3,5-dimethoxyphenyl)-4-methyloct-4-enoate (0.44 g, 37%) as a colorless oil.

Ethyl (*E*)-8-(3,5-dimethoxyphenyl)-4-methyloct-4-enoate

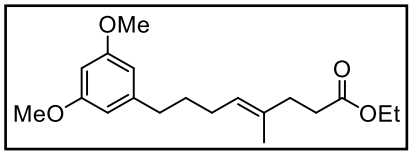

Colorless oil (37%); **^{1}H NMR** (400 MHz, $CDCl_3$): δ 6.34 (d, *J* = 2.3 Hz, 2H), 6.29 (t, *J* = 2.3 Hz, 1H), 5.18 (tq, *J* = 7.2, 1.3 Hz, 1H), 4.12 (q, *J* = 7.1 Hz, 2H), 3.78 (s, 6H), 2.58 – 2.49 (m, 2H), 2.44 – 2.37 (m, 2H), 2.35 – 2.28 (m, 2H), 2.02 (q, *J* = 7.3 Hz, 2H), 1.70 – 1.59 (m, 5H), 1.25 (t, *J* = 7.1 Hz, 3H); **^{13}C NMR** (101 MHz, $CDCl_3$): δ 173.6, 160.8, 145.2, 133.9, 125.2, 106.6, 97.8, 60.4, 55.4, 35.9, 34.9, 33.4, 31.3, 27.6, 16.1, 14.4; **IR** (cm^{-1}) 2935, 2857, 2838, 1733, 1596, 1461, 1344, 1323, 1265, 1205, 1154, 1068, 911, 830; **HRMS** (ESI+, *m/z*) $[M+H]^+$ calcd. for $C_{19}H_{29}O_4$: 321.2060, found: 321.2062.

3.4.8. Preparation of hydroxamic acids

3.4.8.1. Preparation of hydroxamic acids from esters

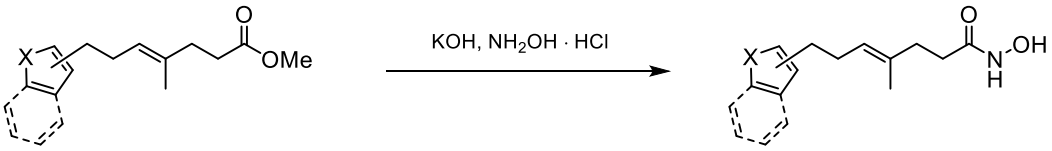

The corresponding ester (1.0 equiv.) was dissolved in MeOH (0.15 M), and then potassium hydroxide (12 equiv.) and hydroxylamine hydrochloride salt (10 equiv.) were added to the solution. The reaction mixture was stirred for 12 h at room temperature. After completion, the pH was adjusted to 4 using a 0.1 M aqueous HCl solution. Then, MeOH was removed under reduced pressure, and the resulting aqueous mixture was extracted with EtOAc (5 × 20 mL). The combined organic phases were washed with brine, dried over $MgSO_4$, filtered, and concentrated under reduced pressure. The crude product was purified by column chromatography (SiO_2, *n*-hexane/EtOAc 1:1) to give the desired hydroxamic acid.

(*E*)-*N*-Hydroxy-4-methyl-7-(1-methyl-1*H*-indol-2-yl)hept-4-enamide

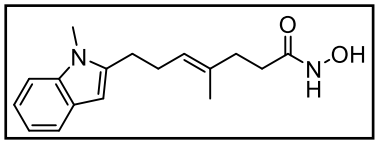

White solid (55%); **m. p.** 78 – 80 °C; **^{1}H NMR** (400 MHz, CD_2Cl_2): δ 7.49 (dt, *J* = 7.8, 1.0 Hz, 1H), 7.27 (dt, *J* = 8.0, 0.9 Hz, 1H), 7.12 (ddd, *J* = 8.2, 7.1, 1.2 Hz, 1H), 7.02 (ddd, *J* = 8.0, 7.0, 1.0 Hz, 1H), 6.22 (s, 1H), 5.32 – 5.28 (m, 1H), 3.66 (s, 3H), 2.78 (t, *J* = 7.9 Hz, 2H), 2.44 (q, *J* = 7.4 Hz, 2H), 2.36 – 2.20 (m, 4H), 1.63 (s, 3H); **^{13}C NMR** (101 MHz, CD_2Cl_2): δ 171.6, 141.0, 137.4, 134.5, 127.9, 124.7, 120.4, 119.5, 119.0, 108.7, 98.6, 34.7, 31.6, 29.3, 26.9, 26.7, 15.7; **IR** (cm^{-1}) 3213, 2947, 2850, 1648, 1544, 1466, 1433, 1399, 1342, 1315, 1162, 772, 747; **HRMS** (ESI+, *m/z*) $[M+H]^+$ calcd. for $C_{17}H_{23}N_2O_2$: 287.1754, found: 287.1758.

(*E*)-7-(Furan-2-yl)-*N*-hydroxy-4-methylhept-4-enamide

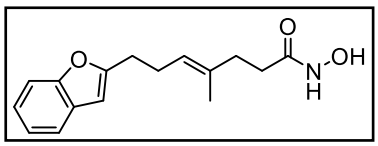

Colorless oil (84%); **^{1}H NMR** (400 MHz, $CDCl_3$): δ 8.30 (s, 2H), 7.48 (dd, *J* = 6.8, 2.1 Hz, 1H), 7.24 – 7.13 (m, 2H), 6.37 (s, 1H), 5.24 (t, *J* = 7.2 Hz, 1H), 2.79 (t, *J* = 7.4 Hz, 2H), 2.44 (q, *J* = 7.3 Hz, 2H), 2.37 – 2.16 (m, 4H), 1.58 (s, 3H); **^{13}C NMR** (101 MHz, $CDCl_3$) δ 171.1, 158.8, 154.6, 134.6, 128.9, 124.5, 123.2, 122.5, 120.3, 110.7, 102.2, 34.7, 31.7, 30.9, 28.4, 26.2, 15.9; **IR** (cm^{-1}) 3210, 2949, 2855, 1648, 1599, 1589, 1454, 1434, 1347, 1301 1160, 1010, 942; **HRMS** (ESI+, *m/z*) $[M+H]^+$ calcd. for $C_{16}H_{20}NO_3$: 274.1438, found: 274.1435.

(*E*)-*N*-Hydroxy-4-methyl-7-(1-tosyl-1*H*-pyrrol-2-yl)hept-4-enamide

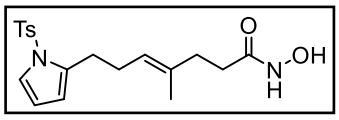

Colorless oil (60%); **^{1}H NMR** (400 MHz, CD_2Cl_2): δ 8.21 (s, 2H), 7.63 (d, *J* = 8.4 Hz, 2H), 7.31 (d, *J* = 8.0 Hz, 2H), 7.25 (dd, *J* = 3.4, 1.8 Hz, 1H), 6.20 (t, *J* = 3.3 Hz, 1H), 6.01 – 5.98 (m, 1H), 5.15 (t, *J* = 6.5 Hz, 1H), 2.69 (t, *J* = 7.6 Hz, 2H), 2.40 (s, 3H), 2.29 – 2.21 (m, 6H), 1.56 (s, 3H); **^{13}C NMR** (101 MHz, CD_2Cl_2) δ 171.5, 145.7, 136.9, 135.9, 135.0, 130.5, 127.2, 125.2, 122.8, 112.7, 111.9, 35.2, 32.2, 27.9, 27.7, 21.9, 16.1; **IR** (cm^{-1}) 3213, 2948, 2847, 1649, 1599, 1547, 1447, 1412, 1251, 1172, 1151, 982; **HRMS** (ESI+, *m/z*) $[M+H]^+$ calcd. for $C_{19}H_{25}N_2O_4S$: 377.1530, found: 377.1530.

(*E*)-7-(Benzo[*b*]thiophen-2-yl)-*N*-hydroxy-4-methylhept-4-enamide

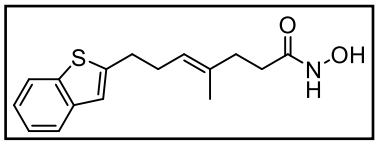

Colorless oil (66%); **^{1}H NMR** (400 MHz, CD_2Cl_2): δ 8.12 (s, 2H), 7.85 – 7.59 (m, 2H), 7.47 – 7.12 (m, 2H), 7.02 (d, *J* = 0.8 Hz, 1H), 5.28 (t, *J* = 7.1 Hz, 1H), 2.94 (t, *J* = 7.4 Hz, 2H), 2.45 (q, *J* = 7.4 Hz, 2H), 2.34 – 2.20 (m, 4H), 1.62 (s, 3H); **^{13}C NMR** (101 MHz, CD_2Cl_2): δ 171.3, 146.7, 140.7, 139.9, 135.4, 124.9, 124.6, 123.9, 123.2, 122.6, 121.3, 35.2, 32.1, 31.3, 29.9, 16.3; **IR** (cm^{-1}) 3218, 2951, 2849, 1644, 1606, 1545, 1431, 1361, 1295, 1238, 1194, 1078, 1021, 938; **HRMS** (ESI+, *m/z*) $[M+H]^+$ calcd. for $C_{16}H_{20}NO_2S$: 290.1209, found: 290.1205.

(*E*)-7-(5-[{(*tert*-Butyldimethylsilyl)oxy}methyl]furan-2-yl)-*N*-hydroxy-4-methylhept-4-enamide

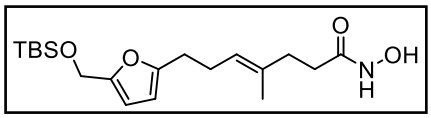

Colorless oil (70%); **^{1}H NMR** (400 MHz, $CDCl_3$): δ 8.44 – 8.28 (m, 1H), 7.91 (s, 1H), 6.11 (d, *J* = 3.0 Hz, 1H), 5.90 (d, *J* = 3.0 Hz, 1H), 5.20 (t, *J* = 6.6 Hz, 1H), 4.59 (s, 2H), 2.64 (t, *J* = 7.3 Hz, 2H), 2.36 – 2.21 (m, 6H), 1.57 (s, 3H), 0.91 (s, 9H), 0.09 (s, 6H); **^{13}C NMR** (101 MHz, $CDCl_3$): δ 170.7, 155.6, 152.4, 134.4, 124.8, 108.2, 105.7, 58.3, 34.6, 31.8, 28.0, 26.6, 25.9, 18.5, 15.9, -5.2; **IR** (cm^{-1}) 3211, 2944, 2856, 1644, 1610, 1458, 1391, 1372, 1294, 1251, 1061, 1038, 840; **HRMS** (ESI+, *m/z*) $[M+H]^+$ calcd. for $C_{19}H_{34}NO_4Si$: 368.2252, found: 368.2255.

(*E*)-7-(Benzo[*b*]thiophen-3-yl)-*N*-hydroxy-4-methylhept-4-enamide

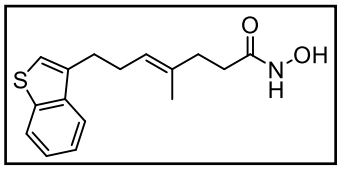

Colorless oil (48%); **^{1}H NMR** (400 MHz, CD_2Cl_2): δ 8.20 (s, 2H), 7.87 – 7.83 (m, 1H), 7.76 (dd, *J* = 7.3, 1.2 Hz, 1H), 7.41 – 7.31 (m, 2H), 7.11 (s, 1H), 5.29 (t, *J* = 7.1 Hz, 1H), 2.88 (t, *J* = 7.5 Hz, 2H), 2.44 (q, *J* = 7.3 Hz, 2H), 2.31 – 2.25 (m, 2H), 2.23 – 2.16 (m, 2H), 1.54 (s, 3H); **^{13}C NMR** (101 MHz, CD_2Cl_2): δ 171.6, 140.9, 139.7, 137.1, 134.9, 125.5, 124.6, 124.3, 123.3, 122.2, 121.8, 35.3, 32.2, 28.9, 28.1, 16.1; **IR** (cm^{-1}) 3215, 2954, 2849, 1645, 1607, 1545, 1433, 1364, 1292, 1238, 1190, 1081, 1021, 936; **HRMS** (ESI+, *m/z*) $[M+H]^+$ calcd. for $C_{16}H_{20}NO_2S$: 290.1209, found: 290.1205.

(*E*)-*N*-Hydroxy-4-methyl-7-(thiophen-3-yl)hept-4-enamide

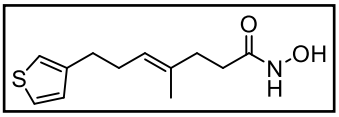

Colorless oil (70%); **^{1}H NMR** (400 MHz, $CDCl_3$): δ 8.23 (s, 2H), 7.24 (dd, *J* = 4.8, 3.0 Hz, 1H), 6.96 – 6.90 (m, 2H), 5.22 (t, *J* = 6.7 Hz, 1H), 2.66 (t, *J* = 7.6 Hz, 2H), 2.39 – 2.19 (m, 6H), 1.56 (s, 3H). **^{13}C NMR** (101 MHz, $CDCl_3$): δ 171.2, 142.5, 134.1, 128.4, 125.5, 125.3, 120.3, 34.9, 31.9, 30.3, 29.0, 16.0. **IR** (cm^{-1}): 3208, 2949, 2851, 1648, 1630, 1436, 1351, 1295, 1250, 1198, 1158, 833 **HRMS** (ESI+, *m/z*): $[M+H]^+$ calcd. for $C_{12}H_{18}NO_2S$, 240.1053; found, 240.1055.

(*E*)-*N*-Hydroxy-4-methyl-7-(thiophen-2-yl)hept-4-enamide

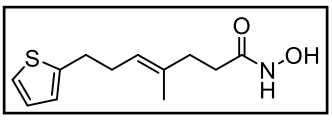

Colorless oil (65%); **^{1}H NMR** (400 MHz, CD_2Cl_2): δ 8.12 (s, 1H), 7.32 (s, 1H), 7.12 (dd, *J* = 5.1, 1.2 Hz, 1H), 6.91 (dd, *J* = 5.1, 3.4 Hz, 1H), 6.79 (dq, *J* = 3.3, 1.0 Hz, 1H), 5.24 (tq, *J* = 7.1, 1.3 Hz, 1H), 2.86 (t, *J* = 7.5 Hz, 2H), 2.40 – 2.20 (m, 6H), 1.59 (s, 3H); **^{13}C NMR** (101 MHz, CD_2Cl_2): δ 171.4, 145.6, 135.3, 127.2, 125.2, 124.8, 123.5, 35.2, 32.2, 30.7, 30.4, 16.2; **IR** (cm^{-1}) 3211, 2951, 2847, 1648, 1629, 1437, 1349, 1293, 1247, 1194, 1154, 837; **HRMS** (ESI+, *m/z*) $[M+H]^+$ calcd. for $C_{12}H_{18}NO_2S$: 240.1053, found: 240.1058.

(*E*)-8-(3,5-Dimethoxyphenyl)-*N*-hydroxy-4-methyloct-4-enamide

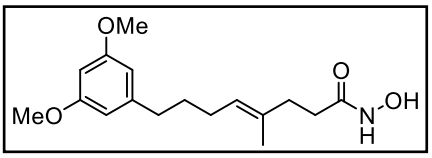

Colorless oil (160 mg, 38%); **^{1}H NMR** (400 MHz, $CDCl_3$): δ 8.28 (s, 2H), 6.34 (d, *J* = 2.3 Hz, 2H), 6.30 (t, *J* = 2.3 Hz, 1H), 5.24 – 5.17 (m, 1H), 3.78 (s, 6H), 2.54 (t, *J* = 7.7 Hz, 2H), 2.38 – 2.21 (m, 4H), 2.02 (q, *J* = 7.3 Hz, 2H), 1.65 (p, *J* = 7.4 Hz, 2H), 1.59 (s, 3H); **^{13}C NMR** (101 MHz $CDCl_3$): δ 171.1, 160.8, 145.0, 133.6, 126.1, 106.7, 97.8, 55.4, 35.9, 35.0, 31.9, 31.1, 27.6, 16.0; **IR** (cm^{-1}) 3197, 2925, 2849, 2837, 1641, 1583, 1412, 1403, 1352, 1322, 1303, 1198, 1153, 1047, 829; **HRMS** (ESI+, *m/z*) $[M+H]^+$ calcd. for $C_{17}H_{26}NO_4$: 308.1856, found: 308.1860.

(*E*)-7-(3,5-Dimethoxyphenyl)-*N*-hydroxy-2,4-dimethylhept-4-enamide

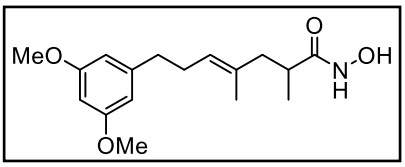

White solid (55 %); **m. p.** 64 – 66 °C; **^{1}H NMR** (400 MHz, $CDCl_3$): δ 8.21 (s, 2H), 6.34 (d, *J* = 2.25 Hz, 2H), 6.32 – 6.30 (m, 1H), 5.22 (t, *J* = 6.75 Hz, 1H), 3.78 (s, 6H), 2.63 – 2.54 (m, 2H), 2.38 – 2.23 (m, 4H), 2.04 (s, 1H), 1.51 (s, 3H), 1.11 (d, *J* = 6.75 Hz, 3H); **^{13}C NMR** (101 MHz, $CDCl_3$): δ 160.7, 144.6, 133.1, 127.1, 106.9, 97.7, 60.5, 55.4, 43.8, 37.1, 36.1, 29.6, 17.4, 16.1; **IR** (cm^{-1}) 3199, 3027, 2928, 2835, 1628, 1593,0 1535, 1464, 1433, 1352, 1296, 1198, 1152, 1057, 955, 829; **HRMS** (ESI+, *m/z*) $[M+H]^+$ calcd. for $C_{17}H_{26}O_4$: 308.1856, found: 308.1858.

(4*E*,8*E*)-*N*-Hydroxy-4,8-dimethyl-11-phenylundeca-4,8-dienamide

The precursor ethyl ester was prepared according to the reported literature [17].

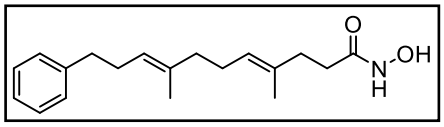

White solid (72%); **m. p.** 47 – 49 °C; **^{1}H NMR** (600 MHz, $CDCl_3$): δ 8.86 (br, 2H), 7.28 (t, *J* = 7.6 Hz, 2H), 7.21 – 7.16 (m, 3H), 5.22 – 5.12 (m, 2H), 2.66 – 2.61 (m, 2H), 2.34 – 2.26 (m, 4H), 2.26 – 2.21 (m, 2H), 2.10 – 2.03 (m, 2H), 2.01 – 1.95 (m, 2H), 1.60 (s, 3H), 1.56 (s, 3H); **^{13}C NMR** (151 MHz, $CDCl_3$) δ 171.7, 142.5, 135.6, 133.3, 128.6, 128.3, 126.0, 125.8, 123.9, 39.6, 36.2, 35.0, 32.1, 30.0, 26.7, 16.1, 16.0; **IR** (cm^{-1}) 3256, 2959, 2936, 1618, 1537, 1494, 1378, 1091, 1076, 982, 742, 679, 522, 511; **HRMS** (EI, *m/z*) $[M]^+$ calcd. for $C_{19}H_{27}NO_2$: 301.2042, found: 301.2047.

3.4.8.2. Preparation of hydroxamic acids *via* [3,3] rearrangement

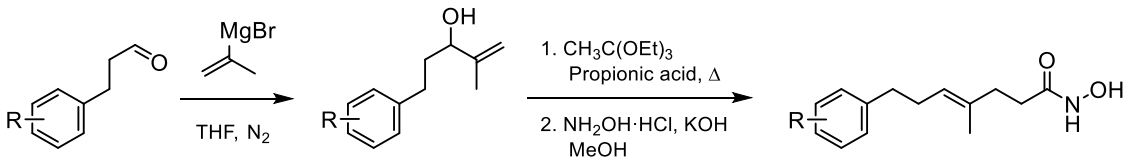

To a solution of the corresponding aldehyde in THF (1.0 M) at 0 °C was added prop-1-en-2-ylmagnesium bromide (0.5 M in THF, 1.5 equiv.) dropwise under nitrogen and the reaction mixture was stirred for 1 h at room temperature. The reaction mixture was quenched with saturated aqueous NH_4Cl solution and extracted with EtOAc. The combined organic layers were dried over $MgSO_4$, filtered, and concentrated under reduced pressure. Crude product was purified by column chromatography (SiO_2, *n*-hexane/EtOAc 10:1) to afford the corresponding allylic alcohol.

A solution of the corresponding allylic alcohol and propanoic acid (0.1 equiv.) in triethyl orthoacetate (5.0 equiv.) was refluxed at 150 °C and stirred for 4 h. After the reaction was completed, the solution was cooled to room temperature and solvents were removed under reduced pressure. The crude reaction mixture was dissolved in EtOAc and quenched with saturated aqueous $NaHCO_3$ solution and extracted with EtOAc. Combined organic phases were washed with brine, and dried over $MgSO_4$. The crude mixture was filtered through a pad of silica and washed with CH_2Cl_2 and concentrated under reduced pressure. The crude mixture was then added to the mixture of hydroxylamine hydrochloride (3.0 equiv.) and potassium hydroxide (6.0 equiv.) in MeOH (0.2 M). The mixture was allowed to stir at room temperature for 12 h and was then concentrated under reduced pressure to remove methanol. The resultant mixture was acidified with 1 M aqueous HCl solution to pH 4 and extracted with EtOAc. The combined organic phases were washed with brine, dried over $MgSO_4$, filtered, and concentrated under reduced pressure. The crude product was purified by column chromatography (SiO_2, *n*-hexane/EtOAc 3:1 to 1:2) to obtain the corresponding hydroxamic acid.

2-Methyl-5-phenylpent-1-en-3-ol

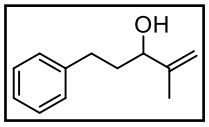

Colorless liquid (49%); **^{1}H NMR** (600 MHz, $CDCl_3$): δ 7.31 – 7.27 (m, 2H), 7.24 – 7.17 (m, 3H), 4.98 (s, 1H), 4.88 (s, 1H), 4.10 (t, *J* = 6.1 Hz, 1H), 2.77 – 2.69 (m, 1H), 2.68 – 2.60 (m, 1H), 1.94 – 1.83 (m, 2H), 1.75 (s, 3H); *Data consistent with those previously reported [18]*.

2-Methyl-5-(naphthalen-1-yl)pent-1-en-3-ol

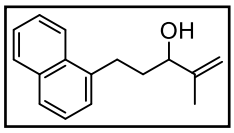

Colorless liquid (64%); **^{1}H NMR** (600 MHz, $CDCl_3$): δ 8.07 (d, *J* = 8.3 Hz, 1H), 7.86 (d, *J* = 8.0 Hz, 1H), 7.72 (d, *J* = 8.0 Hz, 1H), 7.52 (t, *J* = 7.5 Hz, 1H), 7.48 (t, *J* = 7.4 Hz, 1H), 7.40 (t, *J* = 7.5 Hz, 1H), 7.36 (d, *J* = 6.9 Hz, 1H), 5.03 (s, 1H), 4.91 (s, 1H), 4.20 (t, *J* = 6.2 Hz, 1H), 3.26 – 3.19 (m, 1H), 3.14 – 3.06 (m, 1H), 2.07 – 1.94 (m, 2H), 1.77 (s, 3H); **^{13}C NMR** (151 MHz, $CDCl_3$): δ 147.6, 138.4, 134.1, 132.0, 128.9, 126.8, 126.1, 126.0, 125.7, 125.6, 123.9, 111.4, 75.7, 36.1, 29.1, 18.0; **IR** (cm^{-1}) 3356, 2942, 1596, 1510, 1444, 1059, 902, 798, 779; **HRMS** (EI, *m/z*) $[M]^+$ calcd. for $C_{16}H_{18}O$: 226.1358, found: 226.1357.

(*E*)-*N*-Hydroxy-4-methyl-7-phenylhept-4-enamide

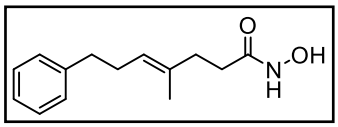

White solid (72%); **m. p.** 51 – 53 °C; **^{1}H NMR** (600 MHz, $CDCl_3$): δ 8.48 (br, 2H), 7.27 (t, *J* = 7.7 Hz, 2H), 7.20 – 7.15 (m, 3H), 5.23 (t, *J* = 6.9 Hz, 1H), 2.63 (t, *J* = 7.7 Hz, 2H), 2.35 – 2.26 (m, 4H), 2.25 – 2.18 (m, 2H), 1.53 (s, 3H); **^{13}C NMR** (151 MHz, $CDCl_3$): δ 171.5, 142.2, 134.1, 128.6, 128.4, 125.9, 125.4, 36.0, 35.0, 32.1, 29.9, 16.0; **IR** (cm^{-1}) 3262, 2915, 1619, 1541, 1452, 1077, 1065, 982, 743, 696, 480; **HRMS** (EI, *m/z*) $[M]^+$ calcd. for $C_{14}H_{19}NO_2$: 233.1416, found: 233.1413.

(*E*)-*N*-Hydroxy-4-methyl-7-(naphthalen-1-yl)hept-4-enamide

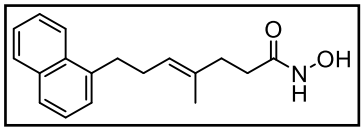

White solid (75%); **m. p.** 78 – 80 °C; **^{1}H NMR** (600 MHz, $CDCl_3$): δ 8.45 (s, 1H), 8.04 (d, *J* = 8.3 Hz, 1H), 7.85 (d, *J* = 7.9 Hz, 1H), 7.71 (d, *J* = 8.2 Hz, 1H), 7.50 (t, *J* = 7.0 Hz, 1H), 7.47 (t, *J* = 7.2 Hz, 1H), 7.39 (t, *J* = 7.6 Hz, 1H), 7.29 (d, *J* = 6.9 Hz, 1H), 5.31 (t, *J* = 6.9 Hz, 1H), 3.12 – 3.06 (m, 2H), 2.44 (q, *J* = 7.4 Hz, 2H), 2.28 (t, *J* = 7.5 Hz, 2H), 2.17 (t, *J* = 7.5 Hz, 2H), 1.48 (s, 3H); **^{13}C NMR** (151 MHz, $CDCl_3$): δ 171.3, 138.0, 134.0, 133.8, 131.9, 128.8, 126.6, 126.0, 125.7, 125.5, 125.4, 125.3, 123.8, 34.8, 32.8, 31.8, 29.1, 15.8; **IR** (cm^{-1}) 3266, 2918, 1616, 1598, 1367, 1067, 984, 791, 774, 542, 420; **HRMS** (EI, *m/z*) $[M]^+$ calcd. for $C_{18}H_{21}NO_2$: 283.1572, found: 283.1575.

3.4.8.3. Preparation of hydroxamic acids from carboxylic acids

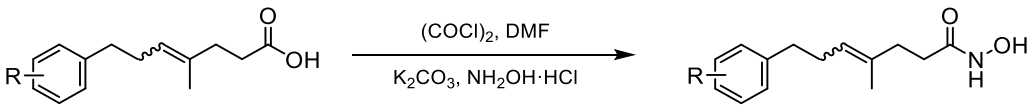

To a solution of the corresponding carboxylic acid (1.0 equiv.) in anhydrous CH_2Cl_2 at 0 °C, a drop of DMF was added, followed by oxalyl chloride (3.0 equiv.). The reaction mixture was stirred for 4 h at room temperature and then concentrated under reduced pressure. The concentrated residue was dissolved in minimal amount of EtOAc and added to an ice-cold biphasic mixture of EtOAc/H_2O (1:1) containing K_2CO_3 (3.0 equiv.) and hydroxylamine hydrochloride (1.5 equiv.). The reaction mixture was allowed to warm up to room temperature and stirred for 12–22 h. The layers were separated and aqueous phase was extracted with EtOAc. The combined organic phases were dried over $MgSO_4$, filtered, and concentrated under reduced pressure. The crude product was purified by column chromatography (SiO_2, *n*-hexane/EtOAc 2:1: to 1:4) to obtain the corresponding hydroxamic acid.

(*E*)-7-(3,5-Dimethoxyphenyl)-*N*-hydroxy-4-methylhept-4-enamide

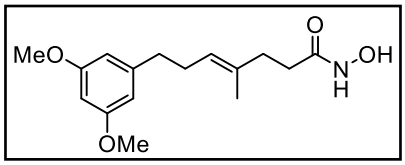

Off-white solid (77%); **m. p.** 77 – 79 °C; **^{1}H NMR** (400 MHz, $CDCl_3$): δ 6.34 (d, *J* = 2.1 Hz, 2H), 6.30 (t, *J* = 2.1 Hz, 1H), 5.20 (t, *J* = 6.9 Hz, 1H), 3.77 (s, 6H), 2.56 (t, *J* = 7.6 Hz, 2H), 2.35 – 2.16 (m, 6H), 1.54 (s, 3H); **^{13}C NMR** (101 MHz, $CDCl_3$): δ 171.6, 160.7, 144.6, 134.2, 125.1, 106.8, 97.7, 55.4, 36.2, 35.0, 32.1, 29.7, 16.0; **IR** (cm^{-1}) 3213, 2935, 2856, 2838, 1645, 1596, 1461, 1429, 1347, 1314, 1293, 1204, 1151, 1067, 832; **HRMS** (ESI+, *m/z*) $[M+H]^+$ calcd. for $C_{16}H_{24}NO_4$: 294.1700, found: 294.1689.

(*Z*)-7-(3,5-Dimethoxyphenyl)-*N*-hydroxy-4-methylhept-4-enamide

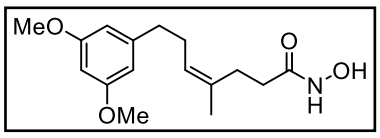

Off-white solid (57%); **m. p.** 60 – 62 °C; **^{1}H NMR** (400 MHz, $CDCl_3$): δ 8.95 (brs, 1H), 6.34 (d, *J* = 2.2 Hz, 2H), 6.30 (t, *J* = 2.2 Hz, 1H), 5.18 (t, *J* = 7.0 Hz, 1H), 3.76 (s, 6H), 2.56 (t, *J* = 7.4 Hz, 2H), 2.35 – 2.21 (m, 4H), 2.00 – 1.91 (m, 2H), 1.62 (s, 3H); **^{13}C NMR** (101 MHz, $CDCl_3$): δ 171.5, 160.7, 144.7, 134.0, 126.1, 106.9, 97.8, 55.4, 36.3, 31.6, 29.5, 27.7, 23.1; **IR** (cm^{-1}) 3210, 2936, 2839, 1650, 1596, 1530, 1462, 1429, 1348, 1311, 1293, 1204, 1151, 1091, 1067, 981, 923, 832; **HRMS** (ESI+, *m/z*) $[M+Na]^+$ calcd. for $C_{16}H_{23}NO_4Na$: 316.1519, found: 316.1517.

(*E*)-*N*-Hydroxy-7-(4-methoxyphenyl)-4-methylhept-4-enamide

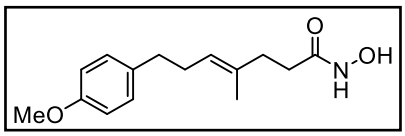

White solid (72%); **m. p.** 64 – 66 °C; **^{1}H NMR** (400 MHz, $CDCl_3$): δ 8.96 (brs, 1H), 8.55 (brs, 1H), 7.10 – 7.05 (m, 2H), 6.84 – 6.80 (m, 2H), 5.21 (t, *J* = 6.7 Hz, 1H), 3.78 (s, 3H), 2.61 – 2.53 (m, 2H), 2.31 – 2.18 (m, 6H), 1.53 (s, 3H); **^{13}C NMR** (101 MHz, $CDCl_3$): δ 171.5, 157.9, 134.3, 133.9, 129.5, 125.4, 113.8, 55.4, 35.0, 34.9, 32.0, 30.2, 16.0; **IR** (cm^{-1}) 3307, 3059, 2952, 2936, 2914, 2852, 1663, 1626, 1614, 1513, 1450, 1252, 1176, 1108, 1030, 981, 827; **HRMS** (ESI+, *m/z*) $[M+H]^+$ calcd. for $C_{15}H_{22}NO_3$: 264.1594, found: 264.1587.

(*Z*)-*N*-Hydroxy-7-(4-methoxyphenyl)-4-methylhept-4-enamide

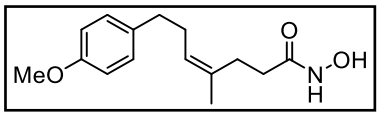

Off-white solid (79%); **m. p.** 48 – 50 °C; **^{1}H NMR** (400 MHz, $CDCl_3$): δ 9.32 (brs, 1H), 7.10 (d, *J* = 8.4 Hz, 2H), 6.83 (d, *J* = 8.4 Hz, 2H), 5.21 (t, *J* = 7.0 Hz, 1H), 3.77 (s, 3H), 2.57 (t, *J* = 7.5 Hz, 2H), 2.32 – 2.22 (m, 4H), 2.07 – 1.98 (m, 2H), 1.65 (s, 3H); **^{13}C NMR** (101 MHz, $CDCl_3$): δ 171.6, 157.7, 134.2, 133.7, 129.5, 126.1, 113.7, 55.2, 35.1, 31.4, 29.9, 27.5, 23.0; **IR** (cm^{-1}) 3203, 2961, 2930, 2912, 2855, 1647, 1612, 1511, 1451, 1245, 1177, 1035, 828; **HRMS** (ESI+, *m/z*) $[M+H]^+$ calcd. for $C_{15}H_{22}NO_3$: 264.1594, found: 264.1591.

(*E*)-*N*-Hydroxy-7-(3-methoxyphenyl)-4-methylhept-4-enamide

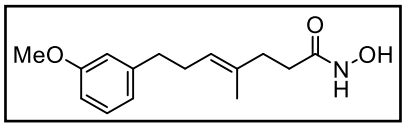

Pale-yellow oil (81%); **^{1}H NMR** (400 MHz, $CDCl_3$): δ 9.17 (s, 1H), 7.22 – 7.15 (m, 1H), 6.77 (d, *J* = 7.6 Hz, 1H), 6.75 – 6.70 (m, 2H), 5.21 (t, *J* = 6.8 Hz, 1H), 3.79 (s, 3H), 2.63 – 2.56 (m, 2H), 2.33 – 2.17 (m, 6H), 1.53 (s, 3H); **^{13}C NMR** (101 MHz, $CDCl_3$) δ 171.7, 159.6, 143.8, 134.1, 129.3, 125.1, 121.1, 114.5, 111.0, 55.3, 35.9, 35.1, 32.1, 29.8, 15.9; **IR** (cm^{-1}) 3211, 2934, 2856, 1639, 1610, 1488, 1452, 1262, 1152, 1050, 982, 872, 849; **HRMS** (ESI+, *m/z*) $[M+Na]^+$ calcd. for $C_{15}H_{21}NO_3Na$: 286.1414, found: 286.1411.

(*Z*)-*N*-Hydroxy-7-(3-methoxyphenyl)-4-methylhept-4-enamide

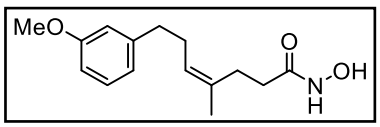

Pale-yellow oil (66%); **^{1}H NMR** (400 MHz, $CDCl_3$): δ 9.20 (brs, 1H), 7.19 (t, *J* = 7.7 Hz, 1H), 6.81 – 6.70 (m, 3H), 5.20 (t, *J* = 7.0 Hz, 1H), 3.79 (s, 3H), 2.60 (t, *J* = 7.5 Hz, 2H), 2.34 – 2.22 (m, 4H), 2.01 – 1.94 (m, 2H), 1.64 (s, 3H); **^{13}C NMR** (101 MHz, $CDCl_3$): δ 171.5, 159.5, 143.9, 133.9, 129.2, 126.0, 121.2, 114.5, 111.0, 55.2, 36.0, 31.5, 29.5, 27.6, 23.0; **IR** (cm^{-1}) 3208, 2962, 2933, 2857, 1644, 1602, 1488, 1453, 1260, 1151, 1091, 1052, 982; **HRMS** (ESI+, *m/z*) $[M+H]^+$ calcd. for $C_{15}H_{22}NO_3$: 264.1594, found: 264.1587.

(4*E*,8*E*)-11-(3,5-Dimethoxyphenyl)-*N*-hydroxy-4,8-dimethylundeca-4,8-dienamide

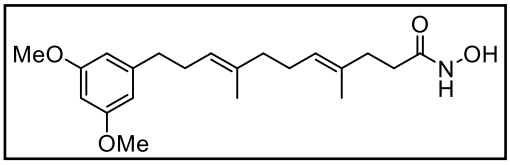

Colorless oil (60%); **^{1}H NMR** (400 MHz, $CDCl_3$): δ 8.49 (s, 1H), 6.36 (d, *J* = 2.3 Hz, 2H), 6.31 (t, *J* = 2.3 Hz, 1H), 5.20 – 5.10 (m, 2H), 3.78 (s, 6H), 2.58 (t, *J* = 7.7 Hz, 2H), 2.34 – 2.21 (m, 6H), 2.11 – 2.03 (m, 2H), 2.02 – 1.95 (m, 2H), 1.59 (s, 3H), 1.57 (s, 3H); **^{13}C NMR** (101 MHz, $CDCl_3$): δ 171.3, 160.8, 144.9, 135.5, 133.3, 125.9, 124.0, 106.8, 97.8, 55.4, 39.5, 36.4, 34.9, 32.0, 29.6, 26.5, 16.1, 16.0; **IR** (cm^{-1}) 3211, 2927, 2861, 2831, 1648, 1599, 1465, 1431, 1339, 1311, 1290, 1201, 1147, 1051, 829; **HRMS** (ESI+, *m/z*) $[M+H]^+$ calcd. for $C_{21}H_{32}NO_4$: 362.2326, found: 362.2320.

(*E*)-*N*-Hydroxy-4-methyl-9-(trimethylsilyl)non-4-en-8-ynamide

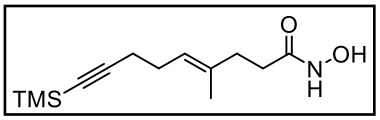

Colorless oil (79%); **^{1}H NMR** (400 MHz, $CDCl_3$): δ 8.66 (brs, 1H), 5.25 – 5.17 (m, 1H), 2.34 – 2.16 (m, 8H), 1.64 (s, 3H), 0.14 (s, 9H); **^{13}C NMR** (101 MHz, $CDCl_3$): δ 171.5, 135.0, 124.5, 107.3, 84.8, 35.1, 32.1, 27.3, 20.3, 16.2, 0.3; **IR** (cm^{-1}) 3206, 2960, 2174, 1646, 1532, 1448, 1385, 1326, 1249, 1167, 1097, 1067, 1040, 985, 896, 847; **HRMS** (ESI+, *m/z*) $[M+H]^+$ calcd. for $C_{13}H_{24}NO_2Si$: 254.1571, found: 254.1569.

(*R*,*E*)-7-(3,5-Dimethoxyphenyl)-*N*-hydroxy-2,4-dimethylhept-4-enamide

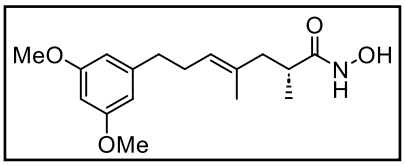

Off-white solid (57%); **m. p.** 67 – 69 °C; **^{1}H NMR** (400 MHz, $CDCl_3$): δ 8.17 (brs, 1H), 6.34 (d, *J* = 2.2 Hz, 2H), 6.31 (t, *J* = 2.3 Hz, 1H), 5.22 (t, *J* = 6.8 Hz, 1H), 3.78 (s, 6H), 2.67 – 2.51 (m, 2H), 2.36 – 2.21 (m, 4H), 2.05 (dd, *J* = 12.7, 5.8 Hz, 1H), 1.51 (s, 3H), 1.10 (d, *J* = 6.7 Hz, 3H); **^{13}C NMR** (101 MHz, $CDCl_3$): δ 174.5, 160.8, 144.6, 133.1, 127.1, 106.9, 97.8, 55.5, 43.8, 37.1, 36.1, 29.6, 17.4, 16.1; **IR** (cm^{-1}) 3197, 3029, 2930, 2838, 1626, 1595, 1537, 1459, 1427, 1347, 1293, 1203, 1149, 1058, 952, 830; **HRMS** (ESI+, *m/z*) $[M+H]^+$ calcd. for $C_{17}H_{26}NO_4$: 308.1856, found: 308.1856; **Specific Rotation** $[\alpha]_D^{22}$ −21.4 (c = 1.0, CH_2Cl_2).

(*E*)-*N*-Hydroxy-4-methyl-7-phenylhept-4-enamide

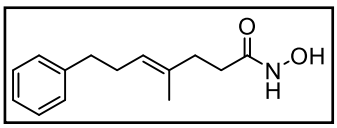

White solid (72%); **m. p.** 51 – 53 °C; **^{1}H NMR** (600 MHz, $CDCl_3$): δ 8.48 (br, 2H), 7.27 (t, *J* = 7.7 Hz, 2H), 7.20 – 7.15 (m, 3H), 5.23 (t, *J* = 6.9 Hz, 1H), 2.63 (t, *J* = 7.7 Hz, 2H), 2.35 – 2.26 (m, 4H), 2.25 – 2.18 (m, 2H), 1.53 (s, 3H); **^{13}C NMR** (151 MHz, $CDCl_3$): δ 171.5, 142.2, 134.1, 128.6, 128.4, 125.9, 125.4, 36.0, 35.0, 32.1, 29.9, 16.0; **IR** (cm^{-1}) 3262, 2915, 1619, 1541, 1452, 1077, 1065, 982, 743, 696, 480; **HRMS** (EI, *m/z*) $[M]^+$ calcd. for $C_{14}H_{19}NO_2$: 233.1416, found: 233.1413.

(*Z*)-*N*-Hydroxy-4-methyl-7-phenylhept-4-enamide

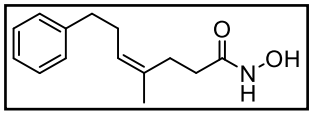

Pale yellow solid (68%) **m. p.** 61 – 63 °C; **^{1}H NMR** (600 MHz, $CDCl_3$): δ 7.28 (t, *J* = 7.4 Hz, 2H), 7.21 – 7.16 (m, 3H), 5.26 – 5.18 (m, 1H), 2.63 (t, *J* = 7.4 Hz, 2H), 2.29 (q, *J* = 7.2 Hz, 2H), 2.23 (t, *J* = 7.3 Hz, 2H), 1.97 – 1.87 (m, 2H), 1.64 (s, 3H); **^{13}C NMR** (151 MHz, $CDCl_3$): δ 171.2, 142.2, 133.7, 128.7, 128.3, 126.2, 125.8, 36.0, 31.4, 29.8, 27.4, 23.1; **IR** (cm^{-1}) 3257, 2959, 2911, 2856, 1616, 1537, 1451, 1091, 1029, 982, 741, 696, 518, 489; **HRMS** (EI, *m/z*) $[M]^+$ calcd. for $C_{14}H_{19}NO_2$: 233.1416, found: 233.1417.

(*E*)-*N*-Hydroxy-4-methyl-7-(*p*-tolyl)hept-4-enamide

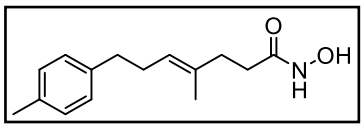

White solid (88%); **m. p.** 75 – 77 °C; **^{1}H NMR** (600 MHz, $CDCl_3$): δ 7.10 – 7.04 (m, 4H), 5.23 (t, *J* = 6.8 Hz, 1H), 2.59 (t, *J* = 7.7 Hz, 2H), 2.34 – 2.22 (m, 9H), 1.55 (s, 3H); **^{13}C NMR** (151 MHz, $CDCl_3$) δ 171.5, 139.1, 135.4, 133.9, 129.1, 128.5, 125.6, 35.5, 35.0, 31.9, 30.1, 21.1, 16.0; **IR** (cm^{-1}) 3301, 2914, 1617, 1537, 1513, 985, 538, 520, 486; **HRMS** (EI, *m/z*) $[M]^+$ calcd. for $C_{15}H_{21}NO_2$: 247.1572, found: 247.1569.

(*Z*)-*N*-Hydroxy-4-methyl-7-(*p*-tolyl)hept-4-enamide

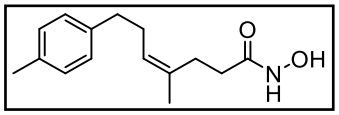

White solid (93%); **m. p.** 76 – 78 °C; **^{1}H NMR** (600 MHz, $CDCl_3$): δ 7.10 (d, *J* = 7.9 Hz, 2H), 7.06 (d, *J* = 8.0 Hz, 2H), 5.23 (t, *J* = 7.1 Hz, 1H), 2.59 (t, *J* = 7.4 Hz, 2H), 2.32 (s, 3H), 2.30 – 2.22 (m, 4H), 1.98 (t, *J* = 6.5 Hz, 2H), 1.65 (s, 3H); **^{13}C NMR** (151 MHz, $CDCl_3$): δ 171.2, 139.2, 135.5, 133.7, 129.1, 128.8, 126.6, 35.7, 31. 5, 30.1, 27.5, 23.2, 21.1; **IR** (cm^{-1}) 3260, 2917, 1617, 1538, 1514, 1470, 1444, 1089, 982, 807, 566, 523, 484; **HRMS** (EI, *m/z*) $[M]^+$ calcd. for $C_{15}H_{21}NO_2$: 247.1572, found: 247.1575.

3.4.9. Preparation of dioxazolones from hydroxamic acids

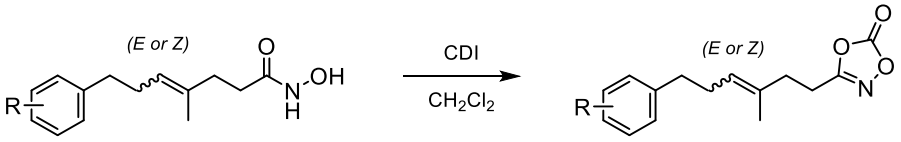

To a solution of the corresponding hydroxamic acid (1.0 equiv.) in anhydrous CH_2Cl_2, 1,1'-carbonyldiimidazole (1.5 equiv.) was added. The reaction mixture was stirred for 4–10 h at room temperature and quenched with 0.5 M $HCl_{(aq)}$. The layers were separated, and the aqueous phase was extracted with CH_2Cl_2. The combined organic phases were dried over $MgSO_4$, filtered, and concentrated under reduced pressure. The crude mixture was filtered through a pad of silica and washed with CH_2Cl_2. The filtrate was concentrated under reduced pressure to afford desired 1,4,2-dioxazol-5-ones.

(*E*)-3-{6-(3,5-Dimethoxyphenyl)-3-methylhex-3-en-1-yl}-1,4,2-dioxazol-5-one (3.1b)

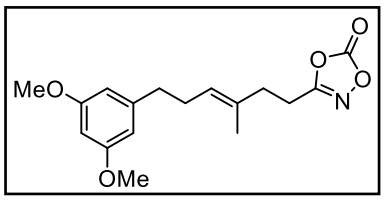

Colorless oil (73%); **^{1}H NMR** (400 MHz, $CDCl_3$): δ 6.33 (d, *J* = 2.2 Hz, 2H), 6.31 (t, *J* = 2.2 Hz, 1H), 5.27 (t, *J* = 6.7 Hz, 1H), 3.78 (s, 6H), 2.71 (t, *J* = 7.6 Hz, 2H), 2.60 – 2.54 (m, 2H), 2.42 – 2.26 (m, 4H), 1.61 (s, 3H); **^{13}C NMR** (101 MHz, $CDCl_3$): δ 166.4, 160.9, 154.3, 144.3, 132.1, 126.7, 106.7, 97.9, 55.4, 36.1, 34.3, 29.6, 23.8, 15.8; **IR** (cm^{-1}) 2937, 2839, 1868, 1830, 1634, 1596, 1460, 1429, 1349, 1314, 1205, 1151, 1066, 983, 929, 833; **HRMS** (ESI+, *m/z*) $[M+MeOH+Na]^+$ calcd. for $C_{18}H_{25}NO_5Na$: 374.1574, found: 374.1556.

(*Z*)-3-{6-(3,5-Dimethoxyphenyl)-3-methylhex-3-en-1-yl}-1,4,2-dioxazol-5-one (3.3a)

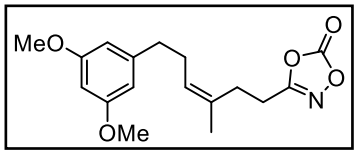

Colorless oil (57%); **^{1}H NMR** (400 MHz, $CDCl_3$): δ 6.33 (d, *J* = 2.2 Hz, 2H), 6.30 (t, *J* = 2.3 Hz, 1H), 5.31 (t, *J* = 7.3 Hz, 1H), 3.77 (s, 6H), 2.58 (t, *J* = 7.5 Hz, 2H), 2.50 – 2.44 (m, 2H), 2.37 – 2.26 (m, 4H), 1.72 – 1.68 (m, 3H); **^{13}C NMR** (101 MHz, $CDCl_3$): δ 166.4, 160.8, 154.2, 144.2, 131.9, 127.5, 106.7, 97.9, 55.3, 36.3, 29.7, 26.6, 23.2, 22.7; **IR** (cm^{-1}) 2960, 2927, 2839, 1867, 1828, 1631, 1595, 1459, 1428, 1351, 1293, 1204, 1149, 1066, 978, 832; **HRMS** (ESI+, *m/z*) $[M+MeOH+Na]^+$ calcd. for $C_{18}H_{25}NO_6Na$: 374.1574, found: 374.1567.

(*E*)-3-{6-(4-Methoxyphenyl)-3-methylhex-3-en-1-yl}-1,4,2-dioxazol-5-one (3.1c)

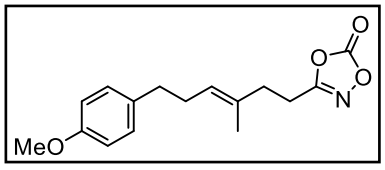

Colorless oil (79%); **^{1}H NMR** (400 MHz, $CDCl_3$): δ 7.10 – 7.05 (m, 2H), 6.86 – 6.80 (m, 2H), 5.29 – 5.22 (m, 1H), 3.79 (s, 3H), 2.74 – 2.68 (m, 2H), 2.60 – 2.55 (m, 2H), 2.37 (t, *J* = 7.5 Hz, 2H), 2.29 (q, *J* = 7.5 Hz, 2H), 1.58 (s, 3H); **^{13}C NMR** (101 MHz, $CDCl_3$): δ 166.4, 157.9, 154.3, 134.0, 131.9, 129.4, 126.8, 113.8, 55.4, 34.9, 34.3, 30.1, 23.7, 15.7; **IR** (cm^{-1}): 2933, 2919, 2856, 2837, 1868, 1830, 1636, 1612, 1512, 1443, 1362, 1301, 1245, 1177, 1149, 1035, 983, 828; **HRMS** (ESI+, *m/z*) $[M+MeOH+Na]^+$ calcd. for $C_{17}H_{23}NO_5Na$: 344.1468, found: 344.1463.

(*Z*)-3-{6-(4-Methoxyphenyl)-3-methylhex-3-en-1-yl}-1,4,2-dioxazol-5-one (3.3b)

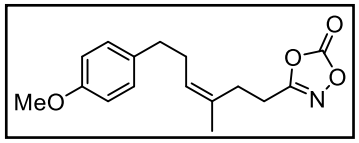

Colorless oil (75%); **^{1}H NMR** (400 MHz, $CDCl_3$) δ 7.10 – 7.05 (m, 2H), 6.85 – 6.80 (m, 2H), 5.31 (t, *J* = 7.2 Hz, 1H), 3.79 (s, 3H), 2.58 (t, *J* = 7.5 Hz, 2H), 2.52 – 2.45 (m, 2H), 2.37 – 2.22 (m, 4H), 1.70 (s, 3H); **^{13}C NMR** (101 MHz, $CDCl_3$) δ 166.4, 158.0, 154.2, 133.9, 131.7, 129.6, 127.8, 113.9, 55.4, 35.1, 30.3, 26.8, 23.3, 22.8; **IR** (cm^{-1}) 2964, 2932, 2856, 2837, 1867, 1829, 1634, 1612, 1583, 1512, 1455, 1380, 1357, 1300, 1178, 1150, 1036, 983, 941, 930, 828; **HRMS** (ESI+, *m/z*) $[M+MeOH+H]^+$ calcd. for $C_{17}H_{24}NO_5$: 322.1654, found: 322.1641.

(*E*)-3-{6-(3-Methoxyphenyl)-3-methylhex-3-en-1-yl}-1,4,2-dioxazol-5-one (3.1g)

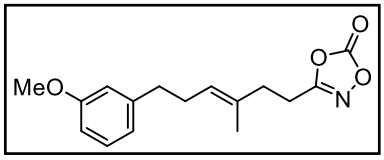

Colorless oil (66%); **^{1}H NMR** (400 MHz, $CDCl_3$): δ 7.20 (t, *J* = 7.8 Hz, 1H), 6.78 – 6.70 (m, 3H), 5.27 (t, *J* = 6.6 Hz, 1H), 3.80 (s, 3H), 2.71 (t, *J* = 7.6 Hz, 2H), 2.64 – 2.58 (m, 2H), 2.40 – 2.28 (m, 4H), 1.60 (s, 3H); **^{13}C NMR** (101 MHz, $CDCl_3$): δ 166.4, 159.8, 154.3, 143.5, 132.1, 129.4, 126.7, 121.0, 114.4, 111.2, 55.3, 35.8, 34.3, 29.8, 23.8, 15.7; **IR** (cm^{-1}) 2937, 2924, 2857, 2837, 1868, 1829, 1636, 1601, 1584, 1488, 1453, 1363, 1310, 1261, 1150, 1093, 1051, 983, 930, 874; **HRMS** (ESI+, *m/z*) $[M+MeOH+Na]^+$ calcd. for $C_{17}H_{23}NO_5Na$: 344.1468, found: 344.1467.

(*Z*)-3-{6-(3-Methoxyphenyl)-3-methylhex-3-en-1-yl}-1,4,2-dioxazol-5-one (3.3e)

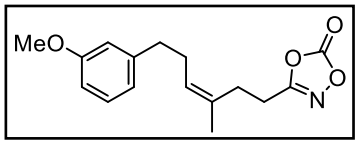

Colorless oil (86%); **^{1}H NMR** (400 MHz, $CDCl_3$): δ 7.19 (t, *J* = 7.8 Hz, 1H), 6.79 – 6.70 (m, 3H), 5.32 (t, *J* = 7.3 Hz, 1H), 3.80 (s, 3H), 2.62 (t, *J* = 7.5 Hz, 2H), 2.50 – 2.43 (m, 2H), 2.37 – 2.27 (m, 4H), 1.72 – 1.69 (m, 3H); **^{13}C NMR** (101 MHz, $CDCl_3$): δ 166.4, 159.8, 154.2, 143.5, 131.9, 129.4, 127.6, 121.1, 114.5, 111.4, 55.3, 36.1, 29.9, 26.7, 23.3, 22.8; **IR** (cm^{-1}) 2965, 2936, 2858, 2837, 1867, 1828, 1634, 1601, 1488, 1454, 1380, 1358, 1261, 1151, 1052, 983; **HRMS** (ESI+, *m/z*) $[M+MeOH+Na]^+$ calcd. for $C_{17}H_{23}NO_5Na$: 344.1468, found: 344.1466.

3-{(3*E*,7*E*)-10-(3,5-Dimethoxyphenyl)-3,7-dimethyldeca-3,7-dien-1-yl}-1,4,2-dioxazol-5-one (3.1i)

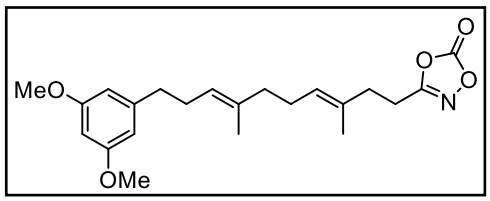

Colorless oil (68%); **^{1}H NMR** (400 MHz, $CDCl_3$): δ 6.36 (d, *J* = 2.3 Hz, 1H), 6.30 (t, *J* = 2.3 Hz, 1H), 5.17 (dtq, *J* = 9.7, 7.0, 1.3 Hz, 1H), 3.78 (s, 3H), 2.71 (dd, *J* = 8.0, 7.1 Hz, 1H), 2.58 (dd, *J* = 8.9, 6.7 Hz, 1H), 2.36 (t, *J* = 7.5 Hz, 1H), 2.30 (q, *J* = 7.5 Hz, 1H), 2.12 – 2.04 (m, 1H), 2.01 – 1.95 (m, 1H), 1.63 (s, 1H), 1.57 (s, 1H); **^{13}C NMR** (101 MHz, $CDCl_3$): δ 166.5, 160.8, 154.3, 144.9, 135.3, 131.2, 127.4, 124.1, 106.7, 97.8, 55.4, 39.4, 36.5, 34.4, 29.7, 26.6, 23.8, 16.1, 15.8; **IR** (cm^{-1}) 2987, 2922, 2836, 1869, 1829, 1627, 1592, 1463, 1425, 1347, 1296, 1204, 1151, 1061, 982, 830; **HRMS:** (ESI+, *m/z*) $[M+MeOH+Na]^+$ calcd. for $C_{17}H_{23}NO_5Na$: 442.2381, found: 442.2377.

(*E*)-3-{3-Methyl-8-(trimethylsilyl)oct-3-en-7-yn-1-yl}-1,4,2-dioxazol-5-one (3.7)

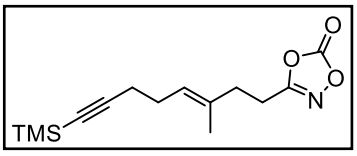

Colorless oil (78%); **^{1}H NMR** (400 MHz, $CDCl_3$): δ 5.31 – 5.24 (m, 1H), 2.77 – 2.71 (m, 2H), 2.40 (t, *J* = 7.6 Hz, 2H), 2.27 – 2.19 (m, 4H), 1.67 (s, 3H), 0.14 (s, 9H); **^{13}C NMR** (101 MHz, $CDCl_3$): δ 166.4, 154.2, 132.9, 125.7, 106.8, 84.9, 34.4, 27.3, 23.8, 20.2, 16.0, 0.2; **IR** (cm^{-1}) 2959, 2919, 2860, 2173, 1869, 1830, 1638, 1446, 1430, 1363, 1330, 1306, 1249, 1146, 1042, 982, 842; **HRMS** (ESI+, *m/z*) $[M+MeOH+Na]^+$ calcd. for $C_{15}H_{25}NO_4SiNa$: 334.1445, found: 334.1442.

(*R*,*E*)-3-{7-(3,5-Dimethoxyphenyl)-4-methylhept-4-en-2-yl}-1,4,2-dioxazol-5-one (3.11)

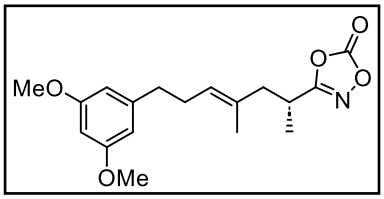

Colorless oil (74%); **^{1}H NMR** (400 MHz, $CDCl_3$): δ 6.33 (d, *J* = 2.2 Hz, 2H), 6.30 (t, *J* = 2.2 Hz, 1H), 5.26 (t, *J* = 6.7 Hz, 1H), 3.78 (s, 6H), 2.97 (h, *J* = 7.1 Hz, 1H), 2.63 – 2.50 (m, 2H), 2.40 (dd, *J* = 13.6, 7.5 Hz, 1H), 2.31 (q, *J* = 7.5 Hz, 2H), 2.19 (dd, *J* = 13.6, 7.8 Hz, 1H), 1.59 (s, 3H), 1.24 (d, J = 7.1 Hz, 3H); **^{13}C NMR** (101 MHz, $CDCl_3$): δ 169.6, 160.9, 154.4, 144.3, 131.0, 128.4, 106.6, 97.9, 55.4, 43.1, 36.1, 29.9, 29.7, 16.0, 15.7; **IR** (cm^{-1}) 2938, 2839, 1871, 1828, 1596, 1460, 1429, 1384, 1349, 1314, 1293, 1253, 1204, 1151, 1113, 1068, 975, 935, 833; **HRMS** (ESI+, *m/z*) $[M+H]^+$ calcd. for $C_{18}H_{24}NO_5$: 334.1649, found: 334.1656; **Specific Rotation** $[\alpha]_D^{25}$ −11.4 (c = 1.0, CH_2Cl_2).

(*E*)-3-{3-Methyl-6-(1-methyl-1*H*-indol-2-yl)hex-3-en-1-yl}-1,4,2-dioxazol-5-one (3.5e)

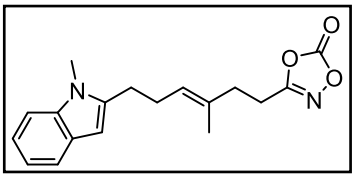

White solid (75%); **m. p.** 75 – 77 °C; **^{1}H NMR** (400 MHz, CD_2Cl_2): δ 7.47 (dt, *J* = 7.8, 1.0 Hz, 1H), 7.25 (dq, *J* = 8.0, 0.8 Hz, 1H), 7.11 (ddd, *J* = 8.2, 7.1, 1.2 Hz, 1H), 7.01 (ddd, *J* = 8.0, 7.0, 1.0 Hz, 1H), 6.20 (d, *J* = 0.9 Hz, 1H), 5.36 (tq, *J* = 7.0, 1.3 Hz, 1H), 3.65 (s, 3H), 2.79 – 2.71 (m, 4H), 2.49 – 2.36 (m, 4H), 1.66 (s, 3H); **^{13}C NMR** (101 MHz, CD_2Cl_2): δ 167.2, 154.9, 141.3, 138.0, 133.2, 128.5, 126.7, 121.0, 120.1, 119.6, 109.3, 99.1, 34.7, 29.9, 27.5, 27.2, 24.2, 16.0; **IR** (cm^{-1}) 2947, 2855, 1866, 1830, 1542, 1462, 1433, 1397, 1342, 1311, 1157, 772; **HRMS** (ESI+, *m/z*) $[M+MeOH+Na]^+$ calcd. for $C_{19}H_{24}N_2O_4Na$: 367.1628, found: 367.1632.

(*E*)-3-{6-(Benzofuran-2-yl)-3-methylhex-3-en-1-yl}-1,4,2-dioxazol-5-one (3.5f)

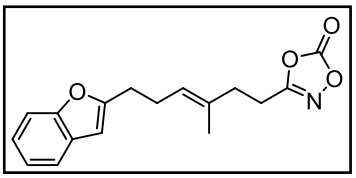

Colorless oil (63%); **^{1}H NMR** (400 MHz, $CDCl_3$): δ 7.50 – 7.47 (m, 1H), 7.41 (m, *J* = 8.0, 1.0 Hz, 1H), 7.24 – 7.15 (m, 2H), 6.36 (q, *J* = 1.0 Hz, 1H), 5.29 (tq, *J* = 7.1, 1.3 Hz, 1H), 2.83 – 2.77 (t, 2H), 2.71 (t, *J* = 8.0, 7.1 Hz, 2H), 2.50 – 2.43 (m, 2H), 2.38 (t, *J* = 7.6 Hz, 2H), 1.64 (s, 3H); **^{13}C NMR** (101 MHz, $CDCl_3$) δ 166.4, 158.7, 154.8, 154.2, 132.8, 129.0, 126.0, 123.4, 122.6, 120.4, 110.8, 102.4, 34.3, 28.5, 26.3, 23.7, 15.8; **IR** (cm^{-1}) 2952, 2852, 1866, 1827, 1599, 1585, 1450, 1440, 1348, 1292, 1163, 1007, 944; **HRMS** (ESI+, *m/z*) $[M+MeOH+Na]^+$ calcd. for $C_{18}H_{21}NO_5Na$: 354.1312, found: 354.1316.

(*E*)-3-{3-Methyl-6-(1-tosyl-1*H*-pyrrol-2-yl)hex-3-en-1-yl}-1,4,2-dioxazol-5-one (3.5d)

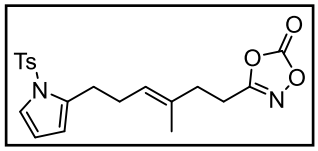

White solid (64%); **m. p.** 66 – 68 °C; **^{1}H NMR** (400 MHz, CD_2Cl_2): δ 7.63 (d, *J* = 8.4 Hz, 2H), 7.32 (d, *J* = 8.1 Hz, 2H), 7.25 (dd, *J* = 3.3, 1.7 Hz, 1H), 6.20 (t, *J* = 3.4 Hz, 1H), 5.98 – 5.96 (m, 1H), 5.19 (t, *J* = 6.4 Hz, 1H), 2.73 (t, *J* = 7.6 Hz, 2H), 2.67 (t, *J* = 7.6 Hz, 2H), 2.40 (s, 3H), 2.36 (t, *J* = 7.6 Hz, 2H), 2.26 (q, *J* = 7.3 Hz, 2H), 1.59 (s, 3H); **^{13}C NMR** (101 MHz, CD_2Cl_2): δ 167.1, 154.8, 145.7, 136.7, 135.6, 133.1, 130.5, 127.1, 126.5, 122.7, 112.7, 111.9, 34.6, 27.7, 27.5, 24.1, 21.8, 15.8; **IR** (cm^{-1}) 2958, 2855, 1866, 1828, 1606, 1552, 1447, 1417, 1254, 1171, 1148, 981; **HRMS** (ESI+, *m/z*) $[M+MeOH+Na]^+$ calcd. for $C_{21}H_{26}N_2O_6SNa$: 457.1404, found: 457.1110.

(*E*)-3-{6-(Benzo[*b*]thiophen-2-yl)-3-methylhex-3-en-1-yl}-1,4,2-dioxazol-5-one (3.5g)

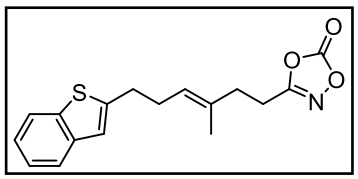

White solid (64%); **m. p.** 39 – 41 °C; **^{1}H NMR** (400 MHz, CD_2Cl_2): δ 7.76 (d, *J* = 8.4 Hz, 1H), 7.67 (d, *J* = 7.5 Hz, 1H), 7.33 – 7.22 (m, 2H), 7.01 (d, *J* = 0.9 Hz, 1H), 5.35 – 5.29 (t, 1H), 2.94 (t, *J* = 7.0 Hz, 2H), 2.74 (t, *J* = 7.6 Hz, 2H), 2.50 – 2.36 (m, 4H), 1.65 (s, 3H); **^{13}C NMR** (101 MHz, CD_2Cl_2): δ 167.1, 146.4, 140.7, 139.9, 133.6, 126.3, 124.6, 124.0, 123.3, 122.6, 121.3, 34.7, 31.2, 29.9, 24.2, 16.0; **IR** (cm^{-1}) 2952, 2851, 1866, 1832, 1604, 1547, 1429, 1363, 1293, 1235, 1192, 1075, 1019, 937; **HRMS** (ESI+, *m/z*) $[M+MeOH+Na]^+$ calcd. for $C_{18}H_{21}NO_4SNa$: 370.1083, found: 370.1079.

(*E*)-3-{6-(5-[{(*tert*-Butyldimethylsilyl)oxy}methyl]furan-2-yl)-3-methylhex-3-en-1-yl}-1,4,2-dioxazol-5-one (3.5a)

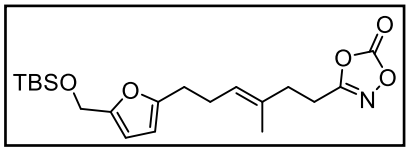

White solid (58%, melts at room temperature); **^{1}H NMR** (400 MHz, $CDCl_3$): δ 6.10 (d, *J* = 3.1 Hz, 1H), 5.88 (d, *J* = 3.0 Hz, 1H), 5.27 – 5.21 (m, 1H), 4.58 (s, 2H), 2.71 (t, *J* = 7.6 Hz, 2H), 2.62 (t, *J* = 7.4 Hz, 2H), 2.35 (m, *J* = 14.8, 7.5 Hz, 4H), 1.62 (s, 3H), 0.90 (s, 9H), 0.08 (s, 6H); **^{13}C NMR** (101 MHz, $CDCl_3$): δ 166.4, 155.2, 154.3, 152.8, 132.4, 126.3, 108.1, 105.85, 58.3, 34.3, 28.1, 26.6, 26.1, 23.8, 18.6, 15.7, -5.0; **IR** (cm^{-1}) 2945, 2851, 1864, 1829, 1621, 1455, 1391, 1370, 1299, 1252, 1068, 1038, 839; **HRMS** (ESI+, *m/z*) $[M+MeOH+Na]^+$ calcd. for $C_{21}H_{35}NO_6SiNa$: 448.2126, found: 448.2120.

(*E*)-3-{6-(Benzo[*b*]thiophen-3-yl)-3-methylhex-3-en-1-yl}-1,4,2-dioxazol-5-one (3.5h)

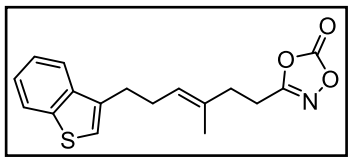

White solid (71%); **m. p.** 41 – 43 °C; **^{1}H NMR** (400 MHz, CD_2Cl_2): δ 7.88 – 7.85 (m, 1H), 7.78 – 7.74 (m, 1H), 7.41 – 7.32 (m, 2H), 7.10 (s, 1H), 5.39 – 5.31 (m, 1H), 2.90 – 2.85 (m, 2H), 2.71 (t, *J* = 7.6 Hz, 2H), 2.46 (q, *J* = 7.3 Hz, 2H), 2.38 (t, *J* = 7.6 Hz, 2H), 1.60 (s, 3H); **^{13}C NMR** (101 MHz, CD_2Cl_2) δ 167.2, 154.8, 140.9, 139.6, 136.9, 133.1, 126.9, 124.7, 124.4, 123.4, 122.2, 121.8, 34.7, 28.8, 28.1, 24.2, 15.9; **IR** (cm^{-1}) 2949, 2847, 1642, 1607, 1546, 1430, 1361, 1294, 1238, 1193, 1077, 1021, 937; **HRMS** (ESI+, *m/z*) $[M+MeOH+Na]^+$ calcd. for $C_{18}H_{21}NO_4SNa$: 370.1083, found: 370.1087.

(*E*)-3-{3-Methyl-6-(thiophen-3-yl)hex-3-en-1-yl}-1,4,2-dioxazol-5-one (3.5c)

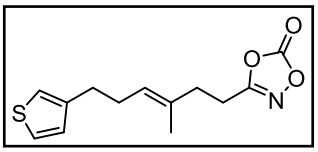

Colorless oil (61%); **^{1}H NMR** (400 MHz, $CDCl_3$): δ 7.24 (dd, *J* = 4.7, 3.2 Hz, 1H), 6.93 – 6.91 (m, 2H), 5.26 (t, *J* = 7.1 Hz, 1H), 2.72 (t, *J* = 8.0 Hz, 2H), 2.66 (t, *J* = 8.4 Hz, 2H), 2.41 – 2.29 (m, 4H), 1.61 (s, 3H); **^{13}C NMR** (101 MHz, $CDCl_3$): δ 166.3, 154.1, 142.1, 131.9, 128.2, 126.7, 125.3, 120.2, 34.2, 30.0, 28.9, 23.6, 15.6; **IR** (cm^{-1}) 2951, 2847, 1871, 1832, 1627, 1434, 1351, 1294, 1242, 1201, 1154, 838; **HRMS** (ESI+, *m/z*) $[M+MeOH+Na]^+$ calcd. for $C_{13}H_{16}NO_3SNa$: 320.0927, found: 320.0930.

(*E*)-3-{3-Methyl-6-(thiophen-2-yl)hex-3-en-1-yl}-1,4,2-dioxazol-5-one (3.5b)

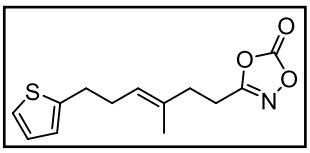

Colorless oil (65%); **^{1}H NMR** (400 MHz, $CDCl_3$): δ 7.12 (dd, *J* = 5.1, 1.2 Hz, 1H), 6.91 (dd, *J* = 5.1, 3.4 Hz, 1H), 6.78 – 6.75 (m, 1H), 5.28 (tq, *J* = 7.2, 1.5 Hz, 1H), 2.86 (t, *J* = 7.5 Hz, 2H), 2.73 (t, *J* = 7.5 Hz, 2H), 2.43 – 2.33 (m, 4H), 1.62 (s, 3H); **^{13}C NMR** (101 MHz, $CDCl_3$): δ 166.4, 154.3, 144.7, 132.7, 126.8, 126.3, 124.4, 123.3, 34.3, 30.2, 29.9, 23.8, 15.8; **IR** (cm^{-1}) 2951, 2850, 1870, 1832, 1628, 1432, 1351, 1293, 1241, 1198, 1154, 838; **HRMS** (ESI+, *m/z*) $[M+MeOH+Na]^+$ calcd. for $C_{13}H_{16}NO_3SNa$: 320.0927, found: 320.0932.

(*E*)-3-{7-(3,5-Dimethoxyphenyl)-3-methylhept-3-en-1-yl}-1,4,2-dioxazol-5-one (3.16)

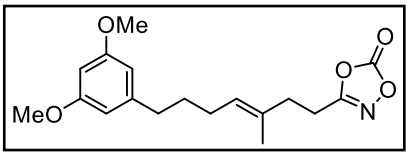

Colorless oil (98%); **^{1}H NMR** (400 MHz, $CDCl_3$): δ 6.33 (d, *J* = 2.2 Hz, 2H), 6.30 (t, *J* = 2.3 Hz, 1H), 5.24 (tq, *J* = 7.2, 1.3 Hz, 1H), 3.78 (s, 6H), 2.74 (t, *J* = 7.5 Hz, 2H), 2.53 (t, *J* = 7.5 Hz, 2H), 2.39 (t, *J* = 7.5 Hz, 2H), 2.03 (q, *J* = 7.4 Hz, 2H), 1.71 – 1.60 (m, 5H); **^{13}C NMR** (101 MHz, $CDCl_3$): δ 166.5, 160.9, 154.3, 144.9, 131.6, 127.5, 106.6, 97.9, 55.4, 35.9, 34.5, 31.0, 27.6, 23.8, 15.8; **IR** (cm^{-1}) 2934, 2836, 1865, 1831, 1633, 1598, 1458, 1421, 1349, 1307, 1217, 1161, 1072, 979, 935, 829; **HRMS** (ESI+, *m/z*) $[M+MeOH+Na]^+$ calcd. for $C_{19}H_{27}NO_6Na$: 388.1731, found: 388.1735.

(*E*)-3-{7-(3,5-Dimethoxyphenyl)-4-methylhept-4-en-2-yl}-1,4,2-dioxazol-5-one (*rac*-3.11)

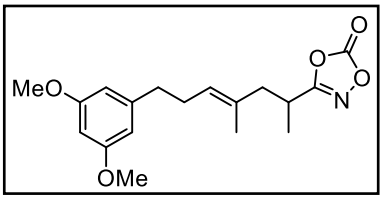

Colorless oil (50%, purified by chromatography); **^{1}H NMR** (400 MHz, $CDCl_3$): δ 6.33 (d, *J* = 2.25 Hz, 2H), 6.30 (m, *J* = 2.25 Hz, 1H), 5.26 (t, *J* = 6.63 Hz, 1H), 3.78 (s, 6H), 2.97 (h, *J* = 7.13 Hz, 1H), 2.57 (m, *J* = 7.44, 2.13 Hz, 2H), 2.40 (m, *J* = 13.57, 7.57 Hz, 1H), 2.31 (q, *J* = 7.50 Hz, 2H), 2.19 (m, *J* = 13.57, 7.82 Hz, 1H), 1.59 (s, 3H), 1.24 (d, *J* = 7.00 Hz, 3H); **^{13}C NMR** (101 MHz,$CDCl_3$): δ 169.6, 160.9, 154.4, 144.3, 131.0, 128.4, 107.6, 97.9, 55.9, 43.1, 36.1, 29.9, 29.7, 16.0, 15.7; **IR** (cm^{-1}) 2942, 2825, 1860, 1824, 1628, 1587, 1452, 1425, 1341, 1317, 1202, 1151, 1067, 954, 922, 830; **HRMS** (ESI+, *m/z*) $[M+MeOH+Na]^+$ calcd. for $C_{19}H_{27}NO_6Na$: 338.1731, found: 338.1726.

(*E*)-3-(3-Methyl-6-phenylhex-3-en-1-yl)-1,4,2-dioxazol-5-one (3.1a)

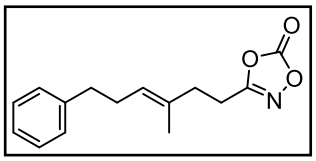

Colorless liquid (87%); **^{1}H NMR** (600 MHz, $CDCl_3$): δ 7.28 (t, *J* = 7.5 Hz, 2H), 7.19 (t, *J* = 7.4 Hz, 1H), 7.16 (d, *J* = 7.1 Hz, 2H), 5.29 – 5.25 (m, 1H), 2.71 (t, *J* = 7.6 Hz, 2H), 2.64 (t, *J* = 7.7 Hz, 2H), 2.37 (t, *J* = 7.6 Hz, 2H), 2.32 (q, *J* = 7.5 Hz, 2H), 1.58 (s, 3H); **^{13}C NMR** (151 MHz, $CDCl_3$): δ 166.4, 154.3, 141.9, 132.1, 128.5, 128.4, 126.8, 126.0, 35.8, 34.4, 29.9, 23.8, 15.7; **IR** (cm^{-1}) 2920, 1867, 1828, 1637, 1495, 1430, 1363, 1148, 984, 762, 752, 701; **HRMS** (EI, *m/z*) $[M]^+$ calcd. for $C_{15}H_{17}NO_3$: 259.1208, found: 259.1207.

(*Z*)-3-(3-Methyl-6-phenylhex-3-en-1-yl)-1,4,2-dioxazol-5-one (3.3c)

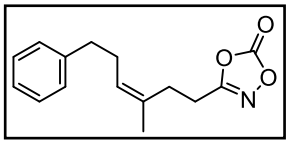

Colorless liquid (94%); **^{1}H NMR** (600 MHz, $CDCl_3$): δ 7.30 – 7.26 (m, 2H), 7.21 – 7.14 (m, 3H), 5.32 (t, *J* = 7.3 Hz, 1H), 2.68 – 2.61 (m, 2H), 2.48 – 2.43 (m, 2H), 2.35 – 2.28 (m, 4H), 1.70 (s, 3H); **^{13}C NMR** (151 MHz, $CDCl_3$): δ 166.4, 154.2, 141.8, 131.8, 128.7, 128.5, 127.7, 126.1, 36.1, 30.0, 26.8, 23.3, 22.8; **IR** (cm^{-1}) 2967, 1860, 1831, 1495, 1455, 1353, 1294, 1225, 1157, 1085, 991, 771; **HRMS** (EI, *m/z*) $[M]^+$ calcd. for $C_{15}H_{17}NO_3$: 259.1208, found: 259.1206.

(*E*)-3-{3-Methyl-6-(*p*-tolyl)hex-3-en-1-yl}-1,4,2-dioxazol-5-one (3.1d)

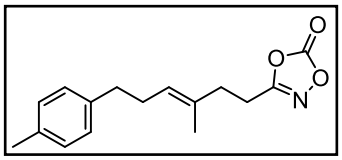

Colorless liquid (95%); **^{1}H NMR** (600 MHz, $CDCl_3$): δ 7.09 (d, *J* = 7.9 Hz, 2H), 7.05 (d, *J* = 7.9 Hz, 2H), 5.26 (t, *J* = 7.1 Hz, 1H), 2.71 (t, *J* = 7.6 Hz, 2H), 2.59 (t, *J* = 7.7 Hz, 2H), 2.37 (t, *J* = 7.6 Hz, 2H), 2.33 – 2.27 (m, 5H), 1.59 (s, 3H); **^{13}C NMR** (151 MHz, $CDCl_3$): δ 166.5, 154.3, 138.8, 135.5, 131.9, 129.1, 128.4, 126.9, 35.4, 34.3, 30.0, 23.8, 21.1, 15.7; **IR** (cm^{-1}) 2921, 1867, 1828, 1636, 1514, 1148, 984, 808, 763; **HRMS** (EI, *m/z*) $[M]^+$ calcd. for $C_{16}H_{19}NO_3$: 273.1365, found: 273.1367.

(*Z*)-3-{3-Methyl-6-(*p*-tolyl)hex-3-en-1-yl}-1,4,2-dioxazol-5-one (3.3d)

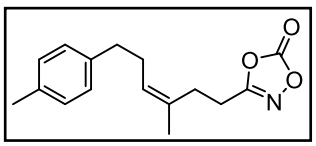

White solid (96%); **m. p.** 32 – 34 °C; **^{1}H NMR** (600 MHz, $CDCl_3$): δ 7.09 (d, *J* = 7.8 Hz, 2H), 7.05 (d, *J* = 7.9 Hz, 2H), 5.32 (t, *J* = 8.0 Hz, 1H), 2.60 (t, *J* = 7.5 Hz, 2H), 2.46 (t, *J* = 7.9 Hz, 2H), 2.35 – 2.31 (m, 5H), 2.28 (q, *J* = 7.5 Hz, 2H), 1.70 (s, 3H); **^{13}C NMR** (151 MHz, $CDCl_3$): δ 166.5, 154.2, 138.7, 135.6, 131.7, 129.2, 128.6, 127.8, 35.6, 30.2, 26.7, 23.3, 22.8, 21.1; **IR** (cm^{-1}) 2970, 2929, 2918, 1862, 1829, 1633, 1514, 1419, 1401, 1368, 1223, 1152, 985, 946, 830, 787, 771, 753, 550; **HRMS** (EI, *m/z*) $[M]^+$ calcd. for $C_{16}H_{19}NO_3$: 273.1365, found: 273.1367.

(*E*)-3-{3-Methyl-6-(naphthalen-1-yl)hex-3-en-1-yl}-1,4,2-dioxazol-5-one (3.1e)

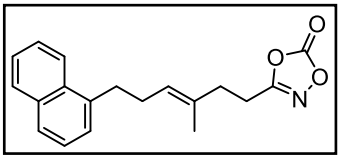

Colorless liquid (88%); **^{1}H NMR** (600 MHz, $CDCl_3$): δ 8.04 (d, *J* = 8.3 Hz, 1H), 7.86 (d, *J* = 8.0 Hz, 1H), 7.72 (d, *J* = 8.2 Hz, 1H), 7.54 – 7.50 (m, 1H), 7.50 – 7.46 (m, 1H), 7.43 – 7.37 (m, 1H), 7.29 (d, J = 6.9 Hz, 1H), 5.36 (t, *J* = 7.2 Hz, 1H), 3.10 (t, *J* = 7.8 Hz, 2H), 2.68 (t, *J* = 7.6 Hz, 2H), 2.47 (q, *J* = 7.3 Hz, 2H), 2.37 (t, *J* = 7.6 Hz, 2H), 1.53 (s, 3H); **^{13}C NMR** (151 MHz, $CDCl_3$): δ 166.5, 154.3, 137.9, 134.0, 132.3, 132.0, 129.0, 126.9, 126.8, 126.1, 125.9, 125.7, 125.6, 123.8, 34.3, 32.9, 29.2, 23.8, 15.7; **IR** (cm^{-1}) 2930, 1866, 1828, 1634, 1149, 984, 780; **HRMS** (EI, *m/z*) $[M]^+$ calcd. for $C_{19}H_{19}NO_3$: 309.1365, found: 309.1368.

3-{(3*E*,7*E*)-3,7-Dimethyl-10-phenyldeca-3,7-dien-1-yl}-1,4,2-dioxazol-5-one (3.1h)

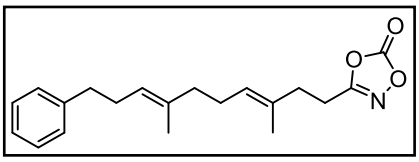

Colorless liquid (99%); **^{1}H NMR** (600 MHz, $CDCl_3$): δ 7.28 (t, *J* = 7.5 Hz, 2H), 7.21 – 7.16 (m, 3H), 5.21 – 5.15 (m, 2H), 2.72 (t, *J* = 7.6 Hz, 2H), 2.64 (t, *J* = 8.1, 7.4 Hz, 2H), 2.37 (t, *J* = 7.6 Hz, 2H), 2.31 (q, *J* = 7.5 Hz, 2H), 2.08 (q, *J* = 7.3 Hz, 2H), 1.98 (t, *J* = 7.6 Hz, 2H), 1.64 (s, 3H), 1.55 (s, 3H); **^{13}C NMR** (151 MHz, $CDCl_3$): δ 166.5, 154.3, 142.5, 135.4, 131.2, 128.6, 128.4, 127.5, 125.8, 124.1, 39.4, 36.2, 34.4, 30.0, 26.6, 23.9, 16.1, 15.8; **IR** (cm^{-1}) 2917, 1867, 1636, 1452, 1147, 983, 763, 700; **HRMS** (EI, *m/z*) $[M]^+$ calcd. for $C_{20}H_{25}NO_3$: 327.1834, found: 327.1833.

3.4.10. Preparation of iridium catalysts

Iridium complexes **Ir1** [27], **Ir2** [28], **Ir3** [28], **Ir4** [27], **Ir5** [28], **Ir7** [27] and **Ir8** [29] were prepared by literature procedure.

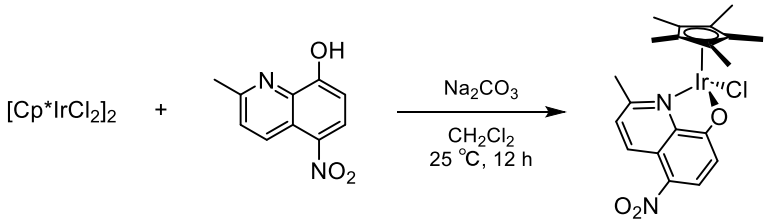

To a screw capped vial with a spinvane triangular-shaped Teflon stir bar were added $[Cp^*IrCl_2]_2$ (0.25 mmol), ligand (0.50 mmol), sodium carbonate (2.0 mmol), and CH_2Cl_2 (10 mL) under atmospheric condition. The reaction mixture was stirred for 12 h at 25 ℃, and then filtered through a pad of celite with CH_2Cl_2. The solvent was removed under reduced pressure and the residue was purified by column chromatography (SiO_2, CH_2Cl_2/MeOH 30:1 to 20:1) to afford the desired **Ir6**.

Iridium complex Ir6

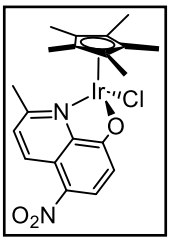

Red orange solid (87%); **m. p.** 315–320 °C (decomp.); **^{1}H NMR** (600 MHz, $CDCl_3$): δ 9.32 (d, *J* = 9.0 Hz, 1H), 8.52 (d, *J* = 9.2 Hz, 1H), 7.60 (d, *J* = 9.0 Hz, 1H), 6.84 (d, *J* = 9.2 Hz, 1H), 3.14 (s, 3H), 1.65 (s, 15H); **^{13}C NMR** (151 MHz, $CDCl_3$): δ 176.9, 158.5, 144.5, 136.0, 131.2, 130.0, 126.7, 124.9, 114.4, 85.8, 28.9, 9.4; **IR** (cm^{-1}) 1549, 1462, 1416, 1277, 1152, 857, 829, 743, 661, 455; **HRMS** (EI, *m/z*) $[M]^+$ calcd. for $C_{20}H_{22}ClIrN_2O_3$: 566.0948, found: 566.0952.

Procedures for the Ir-Catalyzed Biomimetic Cascade Cyclizations

3.4.11. Cyclization of (*E*)-olefinic dioxazolones

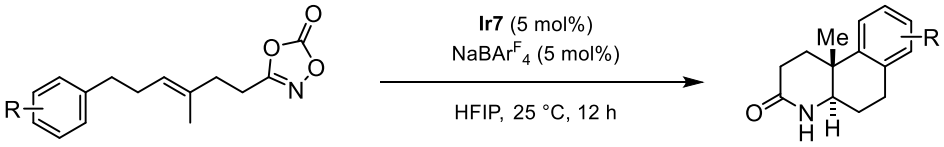

To an oven-dried screwed vial equipped with a spinvane triangular-shaped Teflon stirbar were added **Ir7** (5.0 mol%), sodium tetrakis{3,5-bis(trifluoromethyl)phenyl} borate (5.0 mol%), and 1,1,1,3,3,3-hexafluoro-2-propanol (0.5 mL). To the vial was added 1,4,2-dioxazol-5-one (0.1 mmol) and then sealed. The reaction mixture was vigorously stirred under ambient air atmosphere at 25 ℃. After completion, solvent was removed under reduced pressure, and desired product was obtained by silica chromatography (eluent for purification *n*-hexane/EtOAc/MeOH = 5:5:1).

(4a*R*,10b*R***)-10b-Methyl-1,4,4a,5,6,10b-hexahydrobenzo[*f*]quinolin-3(2*H*)-one (3.2a)**

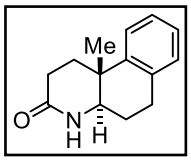

Pale yellow solid (72%); **m. p.** 166 – 170 °C; **^{1}H NMR** (600 MHz, $CDCl_3$): δ 7.30 – 7.27 (m, 1H), 7.22 – 7.14 (m, 2H), 7.11 (d, *J* = 7.1 Hz, 1H), 5.78 (s, 1H), 3.57 (dd, *J* = 12.8, 3.5 Hz, 1H), 3.07 – 2.94 (m, 2H), 2.68 – 2.52 (m, 2H), 2.43 (ddd, *J* = 13.1, 6.4, 2.5 Hz, 1H), 1.95 (tdd, *J* = 12.7, 10.7, 8.0 Hz, 1H), 1.89 – 1.76 (m, 2H), 1.18 (s, 3H); **^{13}C NMR** (151 MHz, $CDCl_3$) :δ 172.7, 143.5, 134.3, 129.5, 126.6, 126.3, 124.9, 56.9, 36.5, 32.6, 29.0, 27.8, 24.4, 21.0; **IR** (cm^{-1}) 3180, 3058, 2930, 1653, 1485, 1402, 1374, 1306, 824, 783, 762, 742, 573, 551, 526; **HRMS** (EI, *m/z*) $[M]^+$ calcd. for $C_{14}H_{17}NO$: 215.1310, found: 215.1311.

(4a*R*,10b*R***)-8,10-Dimethoxy-10b-methyl-1,4,4a,5,6,10b-hexahydrobenzo[*f*]quinolin-3(2*H*)-one (3.2b)**

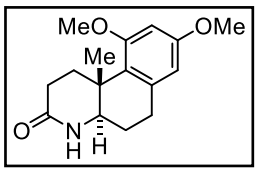

White solid (91%); **m. p.** 204 – 208 °C; **^{1}H NMR** (400 MHz, $CDCl_3$): δ 6.44 (brs, 1H), 6.31 (d, *J* = 2.3 Hz, 1H), 6.22 (d, *J* = 2.2 Hz, 1H), 3.78 (s, 3H), 3.76 (s, 3H), 3.51 (dd, *J* = 12.7, 2.6 Hz, 1H), 3.11 (ddd, *J* = 13.6, 7.5, 2.8 Hz, 1H), 2.99 (ddd, *J* = 18.6, 12.3, 6.8 Hz, 1H), 2.83 (dd, *J* = 17.2, 5.4 Hz, 1H), 2.60 – 2.41 (m, 2H), 1.86 (qd, *J* = 12.6, 5.9 Hz, 1H), 1.76 – 1.60 (m, 2H), 1.22 (s, 3H); **^{13}C NMR** (101 MHz, $CDCl_3$): δ 173.6, 160.1, 158.8, 137.4, 124.3, 104.9, 97.7, 58.9, 55.3, 55.2, 37.3, 31.8, 30.1, 29.5, 24.3, 16.7; **IR** (cm^{-1}) 3190, 3067, 3004, 2937, 2832, 1662, 1606, 1572, 1461, 1401, 1371, 1338, 1308, 1237, 1192, 1155, 1088, 1032, 943, 864; **HRMS** (ESI+, *m/z*) $[M+H]^+$ calcd. for $C_{16}H_{22}NO_3$: 276.1594, found: 276.1590.

(4a*R,10b*R**)-9-Methoxy-10b-methyl-1,4,4a,5,6,10b-hexahydrobenzo[*f*]quinolin-3(2*H*)-one (3.2c)**

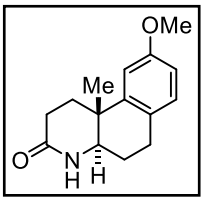

White solid (59%); **m. p.** 229 – 233 °C; **^{1}H NMR** (400 MHz, $CDCl_3$): δ 7.02 (d, *J* = 8.4 Hz, 1H), 6.89 (s, 1H), 6.81 (d, *J* = 2.6 Hz, 1H), 6.73 (dd, *J* = 8.4, 2.6 Hz, 1H), 3.78 (s, 3H), 3.54 (dd, *J* = 12.2, 4.0 Hz, 1H), 2.94 – 2.87 (m, 2H), 2.62 – 2.53 (m, 2H), 2.35 (ddd, *J* = 13.2, 6.1, 3.2 Hz, 1H), 1.99 – 1.79 (m, 3H), 1.17 (s, 3H); **^{13}C NMR** (101 MHz, $CDCl_3$) δ 172.7, 158.1, 144.7, 130.3, 126.3, 112.0, 110.7, 57.0, 55.4, 36.6, 32.6, 28.9, 27.0, 24.5, 20.9; **IR** (cm^{-1}) 3175, 3056, 2933, 2840, 1658, 1613, 1476, 1397, 1364, 1170, 1036, 827; **HRMS** (ESI+, *m/z*) $[M+Na]^+$ calcd. for $C_{15}H_{19}NO_2Na$: 268.1308, found: 268.1303.

(4a*R,10b*R**)-9,10b-Dimethyl-1,4,4a,5,6,10b-hexahydrobenzo[*f*]quinolin-3(2*H*)-one (3.2d)**

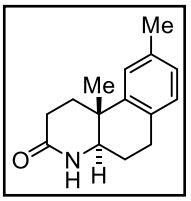

Pale yellow solid (81%); **m. p.** 220 – 224 °C; **^{1}H NMR** (600 MHz, $CDCl_3$): δ 7.09 (s, 1H), 7.03 – 6.96 (m, 2H), 5.85 (s, 1H), 3.55 (dd, *J* = 12.8, 3.5 Hz, 1H), 3.01 – 2.91 (m, 2H), 2.64 – 2.54 (m, 2H), 2.42 (ddd, *J* = 13.1, 6.4, 2.6 Hz, 1H), 2.32 (s, 3H), 1.93 (tdd, *J* = 12.7, 10.6, 8.3 Hz, 1H), 1.87 – 1.73 (m, 2H), 1.17 (s, 3H); **^{13}C NMR** (151 MHz, $CDCl_3$) δ 172.7, 143.3, 135.7, 131.1, 129.4, 127.4, 125.4, 57.0, 36.4, 32.6, 29.0, 27.4, 24.5, 21.3, 21.0; **IR** (cm^{-1}) 3164, 3040, 2941, 2915, 1675, 1501, 1407, 1309, 831, 810; **HRMS** (EI, *m/z*) $[M]^+$ calcd. for $C_{15}H_{19}NO$: 229.1467, found: 229.1464.

(4a*R,12a*R**)-4a-Methyl-3,4,4a,11,12,12a-hexahydronaphtho[2,1-*f*]quinolin-2(1*H*)-one (3.2e)**

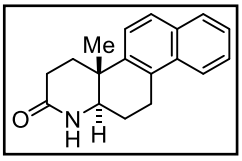

White solid (88%); **m. p.** 276 – 280 °C; **^{1}H NMR** (600 MHz, DMSO-d_6): δ 7.98 (d, *J* = 8.4 Hz, 1H), 7.85 (d, *J* = 7.9 Hz, 1H), 7.75 (d, *J* = 8.7 Hz, 1H), 7.66 (s, 1H), 7.58 – 7.51 (m, 2H), 7.48 (t, *J* = 7.3 Hz, 1H), 3.53 (d, *J* = 12.9 Hz, 1H), 3.31 – 3.24 (m, 1H), 3.14 (ddd, *J* = 18.3, 11.2, 8.1 Hz, 1H), 2.48 – 2.33 (m, 3H), 2.11 – 2.03 (m, 1H), 1.81 (tdd, *J* = 12.3, 7.2, 6.7 Hz, 1H), 1.71 (dd, *J* = 11.0 Hz, 1H), 1.14 (s, 3H); **^{13}C NMR** (151 MHz, DMSO- d_6) δ 170.5, 140.8, 131.7, 131.5, 129.1, 126.4, 126.1, 125.2, 123.5, 123.3, 55.8, 36.2, 32.4, 28.8, 24.6, 22.9, 20.2; **IR** (cm^{-1}) 2920, 1665, 1404, 1366, 1326, 815, 759, 511; **HRMS** (EI, *m/z*) $[M]^+$ calcd. for $C_{18}H_{19}NO$: 265.1467, found: 265.1469.

(4a*R,10b*R**)-7-Bromo-8,10-dimethoxy-10b-methyl-1,4,4a,5,6,10b-hexahydrobenzo[*f*]quinolin-3(2*H*)-one (3.2f)**

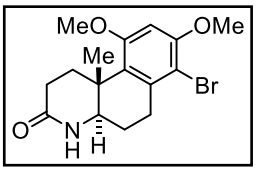

White solid (57%); **m. p.** 266 – 270 °C; **^{1}H NMR** (400 MHz, $CDCl_3$) δ 6.42 (s, 1H), 5.85 (s, 1H), 3.89 (s, 3H), 3.85 (s, 3H), 3.47 (dd, *J* = 12.6, 3.0 Hz, 1H), 3.08 – 3.15 (m, 1H), 3.02 (dd, *J* = 18.1, 4.6 Hz, 1H), 2.73 – 2.84 (m, 2H), 2.48 – 2.53 (m, 1H), 1.72 – 1.89 (m, 2H), 1.62 (s, 1H), 1.24 (s, 3H); **^{13}C NMR** (101 MHz, $CDCl_3$) δ 177.4, 158.8, 155.0, 136.8, 125.9, 105.9, 95.5, 58.4, 56.5, 55.5, 37.7, 31.8, 31.6, 29.7, 24.3, 16.5; **IR** (cm^{-1}) 3194, 3065, 2997, 2932, 2828, 1658, 1610, 1568, 1457, 1398, 1365, 1327, 1298, 1227, 1187, 1147, 1081, 1028, 932, 861, 560; **HRMS** (ESI+, *m/z*) $[M+H]^+$ calcd. for $C_{16}H_{21}NO_3Br$: 354.0699, found: 354.0694.

(4a*R*,10b*R***)-8-Methoxy-10b-methyl-1,4,4a,5,6,10b-hexahydrobenzo[*f*]quinolin-3(*2H*)-one (3.2g*p*)**

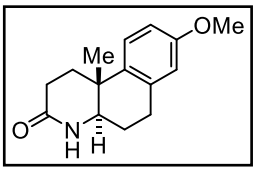

Isolated as a major isomer from the reaction of **3.1g**; White solid (50%, eluent: *n*-hexane/acetone 2:1); **m. p.** 224 – 228 °C; **^{1}H NMR** (400 MHz, $CDCl_3$): δ 7.18 (d, *J* = 8.7 Hz, 1H), 6.84 (s, 1H), 6.74 (dd, *J* = 8.6, 2.6 Hz, 1H), 6.63 (d, *J* = 2.4 Hz, 1H), 3.77 (s, 3H), 3.52 (dd, *J* = 12.4, 3.9 Hz, 1H), 3.05 – 2.88 (m, 2H), 2.57 (dd, *J* = 11.1, 5.2 Hz, 2H), 2.42 – 2.32 (m, 1H), 2.00 – 1.75 (m, 3H), 1.14 (s, 3H); **^{13}C NMR** (101 MHz, $CDCl_3$) δ 172.8, 158.1, 135.9, 135.7, 126.0, 113.9, 112.5, 57.1, 55.3, 35.9, 32.8, 29.0, 28.0, 24.4, 21.1; **IR** (cm^{-1}) 3175, 3052, 2937, 2832, 1654, 1613, 1498, 1364, 1252, 1151, 1043, 890, 838; **HRMS:** (ESI+, *m/z*) $[M+H]^+$ calcd. for $C_{15}H_{20}NO_2$: 246.1489, found: 246.1484.

(4a*R*,10b*R***)-10-Methoxy-10b-methyl-1,4,4a,5,6,10b-hexahydrobenzo[*f*]quinolin-3(*2H*)-one (3.2g*o*)**

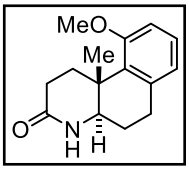

Isolated as a minor isomer from the reaction of **3.1g**; White solid (38%, eluent: *n*-hexane/acetone 2:1); **m. p.** 213 – 217 °C; **^{1}H NMR** (400 MHz, $CDCl_3$): δ 7.11 (t, *J* = 7.9 Hz, 1H), 6.79 (s, 1H), 6.71 (d, *J* = 7.9 Hz, 2H), 3.81 (s, 3H), 3.54 (dd, *J* = 12.6, 2.7 Hz, 1H), 3.16 (ddd, *J* = 13.6, 7.8, 2.8 Hz, 1H), 3.01 (ddd, *J* = 18.6, 12.3, 6.8 Hz, 1H), 2.87 (dd, *J* = 17.2, 5.4 Hz, 1H), 2.62 – 2.43 (m, 2H), 1.95 – 1.81 (m, 1H), 1.80 – 1.64 (m, 2H), 1.26 (s, 3H); **^{13}C NMR** (101 MHz, $CDCl_3$): δ 173.8, 159.0, 136.8, 131.6, 127.2, 122.2, 109.2, 58.7, 55.1, 37.8, 31.5, 29.7, 29.4, 24.1, 16.6; **IR** (cm^{-1}) 3198, 3075, 2937, 2881, 1658, 1572, 1453, 1401, 1371, 1304, 1248, 1203, 1073, 1021; **HRMS** (ESI+, *m/z*) $[M+H]^+$ calcd. for $C_{15}H_{20}NO_2$: 246.1489, found: 246.1484.

(4a*R*,4b*S***,10b*R***,12a*R***)-4a,10b-Dimethyl-3,4,4a,4b,5,6,10b,11,12,12a-decahydronaphtho[2,1-*f*]quinolin-2(1*H*)-one (3.2h)**

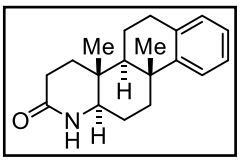

White solid (59%); **m. p.** 305 – 315 °C; **^{1}H NMR** (600 MHz, $CDCl_3$): δ 7.22 (d, *J* = 8.0 Hz, 1H), 7.14 (t, *J* = 7.4 Hz, 1H), 7.10 (t, *J* = 7.4 Hz, 1H), 7.05 (d, *J* = 7.8 Hz, 1H), 5.55 (s, 1H), 3.12 (dd, *J* = 12.4, 3.2 Hz, 1H), 3.03 – 2.96 (m, 1H), 2.93 – 2.85 (m, 1H), 2.54 – 2.43 (m, 2H), 2.42 – 2.37 (m, 1H), 2.01 (ddd, *J* = 12.6, 6.9, 3.1 Hz, 1H), 1.93 – 1.73 (m, 3H), 1.68 – 1.61 (m, 2H), 1.43 – 1.32 (m, 2H), 1.26 (s, 3H), 0.97 (s, 3H); **^{13}C NMR** (151 MHz, $CDCl_3$) δ 172.7, 149.2, 134.9, 129.2, 126.1, 125.8, 124.3, 60.9, 49.7, 38.3, 37.2, 36.9, 35.0, 30.1, 28.7, 25.9, 25.0, 18.5, 12.3; **IR** (cm^{-1}) 2933, 1667, 1487, 1403, 1360, 770, 725; **HRMS** (EI, *m/z*) $[M]^+$ calcd. for $C_{19}H_{25}NO$: 283.1936, found: 283.1934.

(4a*R,4b*S**,10b*R**,12a*R**)-8,10-Dimethoxy-4a,10b-dimethyl-3,4,4a,4b,5,6,10b,11,12,12a-decahydronaphtho[2,1-*f*]quinolin-2(1*H*)-one (3.2i)**

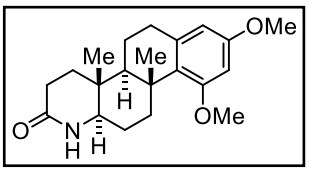

White solid (68%, eluent: toluene/acetone 2:1); **m. p.** 245 – 249 °C; **^{1}H NMR** (400 MHz, $CDCl_3$) δ 6.28 (d, *J* = 2.5 Hz, 1H), 6.20 (d, *J* = 2.6 Hz, 1H), 5.71 (s, 1H), 3.78 – 3.73 (m, 6H), 3.20 (dt, *J* = 13.8, 3.4 Hz, 1H), 3.09 (dd, *J* = 12.4, 3.8 Hz, 1H), 2.86 (dd, *J* = 8.9, 4.0 Hz, 2H), 2.51 – 2.44 (m, 2H), 2.05 – 1.95 (m, 1H), 1.80 – 1.73 (m, 1H), 1.70 (dd, *J* = 12.9, 3.1 Hz, 1H), 1.67 – 1.60 (m, 1H), 1.53 (dq, *J* = 13.0, 3.6 Hz, 1H), 1.41 – 1.33 (m, 2H), 1.32 – 1.27 (m, 4H), 0.93 (s, 3H); **^{13}C NMR** (101 MHz, $CDCl_3$): δ 172.7, 159.5, 158.2, 138.4, 129.2, 105.0, 97.8, 60.7, 55.3, 55.2, 52.7, 39.5, 37.2, 35.4, 35.3, 33.3, 28.6, 25.1, 21.1, 18.4, 12.8; **IR** (cm^{-1}) 3187, 3050, 2968, 2918, 2874, 2832, 1652, 1592, 1410, 1340, 1265, 1224, 1190, 1143, 1086, 1037, 936, 830; **HRMS** (ESI+, *m/z*) $[M+H]^+$ calcd. for $C_{21}H_{29}NO_3$: 344.2220, found: 344.2214.

(4a*R,7a*R**)-4a-Methyl-5-{(trimethylsilyl)carbonyl}octahydro-2*H*-cyclopenta[*b*]pyridin-2-one (3.8)**

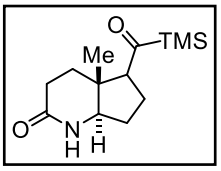

Synthesized with reaction of **3.7** *with* H_2O (5 equiv.), **Ir7** (10 mol%), *and* $NaBAr^F_4$ (10 mol%); White solid (55%, eluent: toluene/acetone 1:1); **m. p.** 115 – 117 °C; **^{1}H NMR** (400 MHz, $CDCl_3$): δ 5.99 (s, 1H), 3.45 (dd, *J* = 12.3, 5.1 Hz, 1H), 2.52 – 2.43 (m, 2H), 2.42 – 2.36 (m, 2H), 2.00 – 1.93 (m, 2H), 1.92 – 1.90 (m, 1H), 1.88 – 1.72 (m, 1H), 1.68 – 1.63 (m, 1H), 1.08 (s, 3H), 0.17 (s, 9H); **^{13}C NMR** (101 MHz, $CDCl_3$): δ 211.8, 171.8, 59.4, 54.5, 39.1, 38.2, 35.7, 27.9, 26.8, 15.3, 1.2; **IR** (cm^{-1}) 2950, 2848, 1662, 1642, 1469, 1406, 1363, 1249, 1218, 1135, 1027, 842; **HRMS** (ESI+, *m/z*) $[M+H]^+$ calcd. for $C_{13}H_{23}NO_2Si$: 254.1571, found: 254.1567.

(2*R*,4a*S*,10b*S*)-8,10-Dimethoxy-2,10b-dimethyl-1,4,4a,5,6,10b-hexahydrobenzo[*f*]quinolin-3(2*H*)-one (3.12)

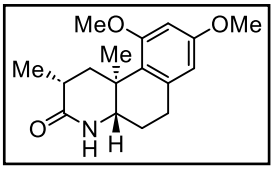

White solid (74%); **m. p.** 191 – 195 °C; **^{1}H NMR** (400 MHz, $CDCl_3$): δ 6.32 (d, *J* = 2.4 Hz, 1H), 6.21 (d, *J* = 2.3 Hz, 1H), 5.78 (s, 1H), 3.79 (s, 3H), 3.77 (s, 3H), 3.58 – 3.49 (m, 1H), 3.07 – 2.91 (m, 1H), 2.88 – 2.78 (m, 1H), 2.54 – 2.40 (m, 1H), 2.38 – 2.22 (m, 1H), 2.08 (dd, *J* = 14.2, 8.1 Hz, 1H), 1.93 – 1.79 (m, 2H), 1.21 (d, *J* = 6.8 Hz, 3H), 1.13 (s, 3H); **^{13}C NMR** (101 MHz, $CDCl_3$) δ 177.2, 159.7, 158.8, 136.5, 125.5, 104.6, 97.7, 56.4, 55.3, 55.2, 43.6, 39.1, 34.3, 30.1, 23.3, 20.8, 16.7; **IR** (cm^{-1}) 3205, 3082, 2963, 2934, 2871, 2838, 1670, 1604, 1582, 1461, 1420, 1338, 1310, 1285, 1270, 1194, 1157, 1075, 1047; **HRMS** (ESI+, *m/z*) $[M+H]^+$ calcd. for $C_{17}H_{24}NO_3$: 290.1751, found: 290.1749; **Specific Rotation** $[\alpha]_D^{25}$ −151.2 (c = 1.0, CH_2Cl_2); **HPLC Analysis:** Dicel CHIRALPAK IC-3, 25 °C, *n*-heptane:^{i}PrOH = 70:30, 1.0 mL/min, 212 nm, t_{R1} (minor) = 14.84 min, t_{R2} (major) = 16.927 min, 99.3:0.7 er.

(2*S,4a*R**,10b*R**)-8,10-Dimethoxy-2,10b-dimethyl-1,4,4a,5,6,10b-hexahydrobenzo[*f*]quinolin-3(2*H*)-one (*rac*-3.12)**

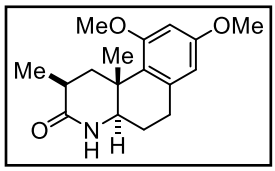

White solid (69%); **^{1}H NMR** (400 MHz, $CDCl_3$): δ 6.33 (d, *J* = 2.53 Hz, 1H), 6.20 (d, *J* = 2.52 Hz, 1H), 6.07 (s, 1H), 3.78 (d, *J* = 7.13 Hz, 6H), 3.56 – 3.49 (m, 1H), 3.04 – 2.93 (m, 1H), 2.87 – 2.79 (m, 1H), 2.51 – 2.42 (m, 1H), 2.34 – 2.26 (m, 1H), 2.08 (dd, *J* = 14.19, 8.06 Hz, 1H), 1.86 – 1.74 (m, 2H), 1.21 – 1.19 (m, 3H), 1.11 (s, 3H); **^{13}C NMR** (101 MHz, $CDCl_3$): δ 178.0, 159.5, 158.8, 136.2, 124.9, 104.5, 97.6, 56.4, 55.2, 55.1, 43.3, 38.9, 29.9, 25.4, 23.1, 20.7, 16.5; **IR** (cm^{-1}) 3203, 3080, 2960, 2933, 2870, 2836, 1672, 1605, 1582, 1463, 1421, 1342, 1312, 1284, 1270, 1195, 1160, 1071, 1042; **HRMS** (ESI+, *m/z*) $[M+H]^+$ calcd. for $C_{17}H_{24}NO_3$: 290.1751, found: 290.1749.

5-(6,8-Dimethoxy-1,2,3,4-tetrahydronaphthalen-1-yl)-5-methylpyrrolidin-2-one (3.17)

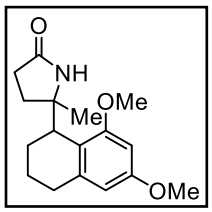

Colorless oil (72%, eluent: toluene/acetone 1:1); **^{1}H NMR** (400 MHz, $CDCl_3$): δ 6.31 (d, *J* = 2.5 Hz, 1H), 6.27 (d, *J* = 2.4 Hz, 1H), 6.09 (s, 1H), 3.80 (s, 3H), 3.77 (s, 3H), 3.38 (dd, *J* = 7.5, 4.4 Hz, 1H), 2.68 (t, *J* = 6.3 Hz, 2H), 2.29 – 2.18 (m, 1H), 1.98 – 1.79 (m, 4H), 1.78 – 1.67 (m, 2H), 1.53 – 1.41 (m, 1H), 1.37 (s, 3H); **^{13}C NMR** (101 MHz, $CDCl_3$) δ 176.4, 158.9, 158.5, 141.7, 117.5, 105.6, 96.7, 64.9, 55.6, 55.3, 38.5, 30.6, 30.2, 30.1, 27.6, 25.1, 21.3; **IR** (cm^{-1}) 3183, 3062, 2971, 2916, 2878, 2827, 1663, 1597, 1395, 1342, 1272, 1218, 1201, 1142, 1079, 1039, 941, 830; **HRMS** (ESI+, *m/z*) $[M+H]^+$ calcd. for $C_{17}H_{24}NO_3$: 290.1751, found: 290.1755.

3.4.12. Cyclization of (*Z*)-olefinic dioxazolones

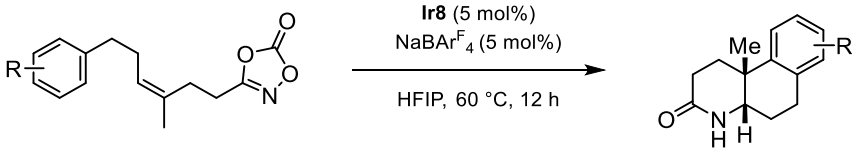

To an oven-dried screwed vial equipped with a spinvane triangular-shaped Teflon stirbar were added **Ir8** (5.0 mol%), sodium tetrakis{3,5-bis(trifluoromethyl)phenyl} borate (5.0 mol%), and 1,1,1,3,3,3-hexafluoro-2-propanol (0.5 mL). To the vial was added 1,4,2-dioxazol-5-one (0.1 mmol) and then sealed. The reaction mixture was vigorously stirred under ambient air atmosphere at 60 ℃. After completion, solvent was removed under reduced pressure, and desired product was obtained by silica chromatography (eluent for purification *n*-hexane/EtOAc/MeOH = 5:5:1).

(4a*S*,10b*R***)-8,10-Dimethoxy-10b-methyl-1,4,4a,5,6,10b-hexahydrobenzo[*f*]quinolin-3(2*H*)-one (3.4a)**

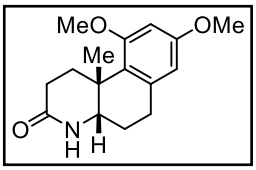

White solid (58%); **m. p.** 178 – 180 °C; **^{1}H NMR** (400 MHz, $CDCl_3$): δ 6.34 (brs, 1H), 6.31 (d, *J* = 2.4 Hz, 1H), 6.21 (d, *J* = 2.3 Hz, 1H), 3.78 (s, 3H), 3.76 (s, 3H), 3.48 (d, *J* = 4.4 Hz, 1H), 2.94 (ddd, *J* = 17.1, 11.4, 5.5 Hz, 1H), 2.84 (dt, *J* = 13.3, 4.6 Hz, 1H), 2.60 (dt, *J* = 17.0, 4.8 Hz, 1H), 2.21 (dt, *J* = 17.6, 4.5 Hz, 1H), 2.08 – 1.90 (m, 2H), 1.83 – 1.69 (m, 2H), 1.38 (s, 3H); **^{13}C NMR** (101 MHz, $CDCl_3$): δ 173.7, 160.1, 158.6, 138.8, 120.2, 105.1, 97.9, 59.8, 55.3, 55.2, 35.9, 31.1, 29.2, 26.0, 25.9, 25.2; **IR** (cm^{-1}) 3183, 3056, 2966, 2914, 2884, 2836, 1654, 1599, 1405, 1345, 1267, 1226, 1192, 1144, 1084, 1039, 943, 831; **HRMS** (ESI+, *m/z*) $[M+H]^+$ calcd. for $C_{16}H_{22}NO_3$: 276.1594, found: 276.1586.

(4a*S*,10b*R***)-9-Methoxy-10b-methyl-1,4,4a,5,6,10b-hexahydrobenzo[*f*]quinolin-3(2*H*)-one (3.4b)**

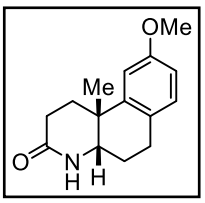

White solid (50%); **m. p.** 184 – 188 °C; **^{1}H NMR** (400 MHz, $CDCl_3$): δ 6.99 (d, *J* = 8.4 Hz, 1H), 6.79 (d, *J* = 2.4 Hz, 1H), 6.71 (dd, *J* = 8.4, 2.6 Hz, 1H), 6.57 (brs, 1H), 3.78 (s, 3H), 3.55 (d, *J* = 3.8 Hz, 1H), 2.82 (dd, *J* = 11.3, 5.6 Hz, 1H), 2.61 (dt, *J* = 16.8, 4.5 Hz, 1H), 2.32 – 2.20 (m, 2H), 2.12 – 2.00 (m, 2H), 1.95 – 1.85 (m, 1H), 1.84 – 1.75 (m, 1H), 1.34 (s, 3H); **^{13}C NMR** (101 MHz, $CDCl_3$) δ 173.0, 158.5, 141.1, 130.3, 127.8, 111.9, 111.8, 57.4, 55.4, 36.0, 33.6, 30.3, 28.6, 25.6, 23.9; **IR** (cm^{-1}) 3168, 3048, 2933, 1666, 1610, 1483, 1401, 1289, 1241, 1043, 864; **HRMS:** (ESI+, *m/z*) $[M+H]^+$ calcd. for $C_{15}H_{20}NO_2$: 246.1489, found: 246.1480.

(4a*S,10b*R**)-10b-Methyl-1,4,4a,5,6,10b-hexahydrobenzo[*f*]quinolin-3(2*H*)-one (3.4c)**

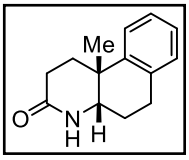

Pale yellow solid (36%); **m. p.** 172 – 176 °C; **^{1}H NMR** (600 MHz, CD_2Cl_2): δ 7.29 (d, *J* = 7.8 Hz, 1H), 7.19 (t, *J* = 7.5 Hz, 1H), 7.14 – 7.10 (m, 1H), 7.08 (d, *J* = 7.5 Hz, 1H), 5.84 (s, 1H), 3.58 (d, *J* = 3.5 Hz, 1H), 2.93 (ddd, *J* = 17.1, 11.5, 5.8 Hz, 1H), 2.69 (ddd, *J* = 17.0, 5.4, 3.8 Hz, 1H), 2.34 – 2.27 (m, 1H), 2.23 – 2.16 (m, 1H), 2.10 (dddd, *J* = 13.9, 11.5, 5.7, 2.4 Hz, 1H), 2.00 – 1.86 (m, 2H), 1.83 – 1.74 (m, 1H), 1.34 (s, 3H); **^{13}C NMR** (151 MHz, CD_2Cl_2): δ 172.7, 140.5, 136.3, 129.8, 127.2, 126.7, 126.6, 58.0, 36.2, 33.9, 30.5, 29.1, 25.8, 25.1; **IR** (cm^{-1}) 3162, 3061, 2917, 1672, 1488, 1445, 1410, 1346, 1304, 1225, 862, 760, 735; **HRMS** (EI, *m/z*) $[M]^+$ calcd. for $C_{14}H_{17}NO$: 215.1310, found: 215.1308.

(4a*S,10b*R**)-9,10b-Dimethyl-1,4,4a,5,6,10b-hexahydrobenzo[*f*]quinolin-3(2*H*)-one (3.4d)**

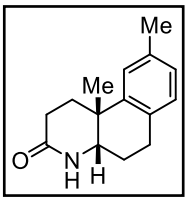

Pale yellow solid (38%); **m. p.** 201 – 205 °C; **^{1}H NMR** (600 MHz, $CDCl_3$): δ 7.06 (s, 1H), 6.99 – 6.90 (m, 2H), 5.92 (s, 1H), 3.57 (d, *J* = 4.1 Hz, 1H), 2.89 (ddd, *J* = 16.9, 11.3, 5.6 Hz, 1H), 2.65 (dt, *J* = 16.5, 4.4 Hz, 1H), 2.31 (s, 4H), 2.26 (dt, *J* = 17.8, 4.5 Hz, 1H), 2.12 – 2.02 (m, 2H), 1.90 (ddd, *J* = 13.6, 11.6, 5.1 Hz, 1H), 1.82 – 1.75 (m, 1H), 1.35 (s, 3H); **^{13}C NMR** (151 MHz, $CDCl_3$): δ 173.2, 139.7, 136.1, 132.5, 129.3, 127.2, 126.6, 57.6, 35.6, 33.4, 30.2, 28.6, 25.5, 24.4, 21.4; **IR** (cm^{-1}) 2960, 2917, 1671, 1616, 1489, 1445, 1410, 1323, 865, 809, 461; **HRMS** (EI, *m/z*) $[M]^+$ calcd. for $C_{15}H_{19}NO$: 229.1467, found: 229.1468.

(4a*S,10b*R**)-8-Methoxy-10b-methyl-1,4,4a,5,6,10b-hexahydrobenzo[*f*]quinolin-3(2*H*)-one (3.4e*p*)**

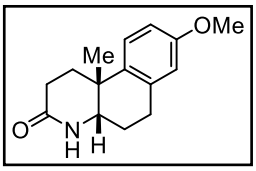

Isolated as a major isomer from the reaction of **3.3e**; White solid (40%, eluent: *n*-hexane/acetone 2:1); **m. p.** 184 – 188 °C; **^{1}H NMR** (400 MHz, $CDCl_3$): δ 7.17 (d, *J* = 8.7 Hz, 1H), 6.77 (dd, *J* = 8.7, 2.8 Hz, 1H), 6.59 (d, *J* = 2.8 Hz, 1H), 6.37 (brs, 1H), 3.77 (s, 3H), 3.56 (d, *J* = 3.4 Hz, 1H), 2.92 (ddd, *J* = 17.1, 11.4, 5.7 Hz, 1H), 2.65 (ddd, *J* = 17.1, 5.7, 3.5 Hz, 1H), 2.31 – 2.20 (m, 2H), 2.14 – 1.98 (m, 2H), 1.93 – 1.76 (m, 2H), 1.33 (s, 3H); **^{13}C NMR** (101 MHz, $CDCl_3$): δ 173.0, 157.8, 136.9, 131.8, 127.3, 113.6, 113.5, 57.6, 55.3, 35.2, 33.5, 30.4, 28.6, 25.5, 25.1; **IR** (cm^{-1}) 3168, 3063, 2929, 1669, 1610, 1405, 1349, 1304, 1267, 1230, 1162, 1028, 827; **HRMS** (ESI+, *m/z*) $[M+H]^+$ calcd. for $C_{15}H_{20}NO_2$: 246.1489, found: 246.1486.

(4a*S,10b*R**)-10-Methoxy-10b-methyl-1,4,4a,5,6,10b-hexahydrobenzo[*f*]quinolin-3(2*H*)-one (3.4e*o*)**

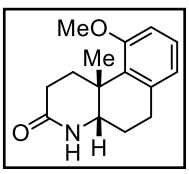

Isolated as a minor isomer from the reaction of **3.3e**; White solid (34%, eluent: *n*-hexane/acetone 2:1); **m. p.** 176 – 180 °C; **^{1}H NMR** (400 MHz, $CDCl_3$): δ 7.09 (t, *J* = 7.9 Hz, 1H), 6.72 – 6.67 (m, 2H), 6.60 (brs, 1H), 3.80 (s, 3H), 3.50 (d, *J* = 4.0 Hz, 1H), 3.00 – 2.86 (m, 2H), 2.68 – 2.59 (m, 1H), 2.23 (dt, *J* = 17.6, 4.5 Hz, 1H), 2.08 – 1.91 (m, 2H), 1.87 – 1.72 (m, 2H), 1.42 (s, 3H); **^{13}C NMR** (101 MHz, $CDCl_3$): δ 173.7, 159.0, 138.1, 127.7, 127.0, 122.3, 109.2, 59.8, 55.2, 36.3, 30.9, 29.2, 25.7, 25.5, 25.1; **IR** (cm^{-1}) 3186, 3060, 2937, 1654, 1572, 1449, 1401, 1349, 1304, 1248, 1080, 838; **HRMS:** (ESI+, *m/z*) $[M+H]^+$ calcd. for $C_{15}H_{20}NO_2$: 246.1489, found: 246.1481.

3.4.13. Cyclization of heterocyclic dioxazolones

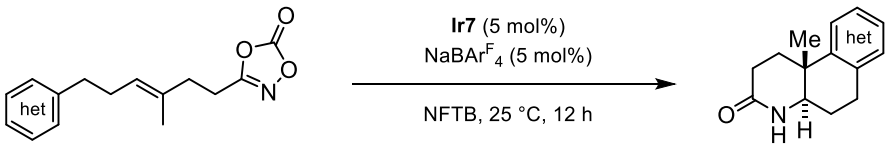

To an oven-dried screwed vial equipped with a spinvane triangular-shaped Teflon stir bar were added **Ir7** (5.0 mol%), sodium tetrakis{3,5-bis(trifluoromethyl)phenyl} borate (5.0 mol%), and nonafluoro-*tert*-butyl alcohol (0.5 mL). To the vial was added 1,4,2-dioxazol-5-one (0.1 mmol) and then sealed. The reaction mixture was vigorously stirred under ambient air atmosphere at 25 ℃. After completion, solvent was removed under reduced pressure, and desired product was obtained by silica chromatography (eluent for purification toluene/acetone 1:1).

(5a*R,9a*R**)-2-[{(tert-Butyldimethylsilyl)oxy}methyl]-9a-methyl-4,5a,6,8,9,9a-hexahydrofuro[3,2-*f*]quinolin-7(5*H*)-one (3.6a)**

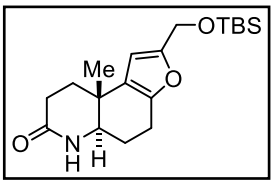

White solid (62%); **m. p.** 187 – 191 °C; **^{1}H NMR** (400 MHz, $CDCl_3$): δ 6.28 (s, 1H), 6.08 (s, 1H), 4.56 (s, 2H), 3.44 (dd, *J* = 12.4, 3.3 Hz, 1H), 2.76 – 2.70 (m, 2H), 2.55 – 2.49 (m, 2H), 2.07 – 1.99 (m, 1H), 1.98 – 1.90 (m, 1H), 1.87 – 1.80 (m, 1H), 1.77 – 1.69 (m, 1H), 1.11 (s, 3H), 0.90 (s, 9H), 0.08 (s, 6H); **^{13}C NMR** (101 MHz, $CDCl_3$) δ 172.9, 153.6, 147.7, 125.6, 105.1, 58.5, 57.6, 33.5, 32.6, 28.8, 26.1, 24.4, 22.1, 19.7, 18.6, -5.0; **IR** (cm^{-1}) 3180, 3069, 2930, 2856, 1663, 1620, 1472, 1392, 1377, 1303, 1254, 1075, 1044, 841; **HRMS** (ESI+, *m/z*) $[M+H]^+$ calcd. for $C_{19}H_{31}NO_3Si$: 350.2146, found: 350.2136.

(5a*R,9a*R**)-9a-Methyl-4,5a,6,8,9,9a-hexahydrothieno[3,2-*f*]quinolin-7(5*H*)-one (3.6b)**

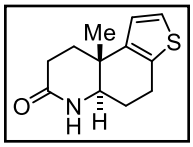

White solid (18%); **m. p.** 201 – 205 °C; **^{1}H NMR** (400 MHz, CD_2Cl_2) δ 7.10 (d, *J* = 5.2 Hz, 1H), 6.86 (d, *J* = 5.2 Hz, 1H), 6.47 (s, 1H), 3.53 (dd, *J* = 12.6, 3.4 Hz, 1H), 3.02 – 2.82 (m, 2H), 2.60 – 2.42 (m, 2H), 2.19 (ddd, *J* = 13.2, 6.7, 2.8 Hz, 1H), 2.03 – 1.91 (m, 1H), 1.88 – 1.75 (m, 2H), 1.13 (s, 3H); **^{13}C NMR** (101 MHz, CD_2Cl_2) δ 172.7, 143.6, 134.5, 124.6, 124.0, 57.7, 36.4, 33.6, 29.5, 25.3, 24.2, 20.2; **IR** (cm^{-1}) 3189, 3058, 2941, 2865, 1658, 1468, 1398, 1376, 1362, 1311, 1267, 1138, 1031, 830; **HRMS** (ESI+, *m/z*) $[M+H]^+$ calcd. for $C_{12}H_{15}NOS$: 222.0947, found: 222.0944.

(5a*R,9a*S**)-9a-Methyl-4,5a,6,8,9,9a-hexahydrothieno[2,3-*f*]quinolin-7(5*H*)-one (3.6c)**

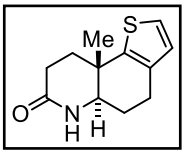

White solid (81%); **m. p.** 197 – 201 °C; **^{1}H NMR** (400 MHz, $CDCl_3$): δ 7.26 (s, 1H), 7.11 (d, *J* = 5.0 Hz, 1H), 6.73 (d, *J* = 5.1 Hz, 1H), 3.59 (dd, *J* = 12.1, 3.9 Hz, 1H), 2.87 – 2.69 (m, 2H), 2.59 – 2.53 (m, 2H), 2.17 – 2.10 (m, 1H), 1.98 – 1.88 (m, 3H), 1.25 (s, 3H); **^{13}C NMR** (101 MHz, $CDCl_3$): δ 175.1, 145.3, 133.9, 129.4, 124.9, 59.8, 36.5, 35.0, 29.3, 24.4, 24.2, 21.4; **IR** (cm^{-1}) 3190, 3060, 2938, 2870, 1663, 1470, 1399, 1376, 1362, 1309, 1271, 1138, 1038, 827; **HRMS** (ESI+, *m/z*) $[M+H]^+$ calcd. for $C_{12}H_{15}NOS$: 222.0947, found: 222.0945.

(5a*R,9a*R**)-9a-Methyl-3-tosyl-3,4,5,5a,6,8,9,9a-octahydro-7*H*-pyrrolo[3,2-*f*]quinolin-7-one (3.6d)**

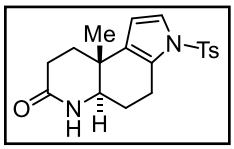

White solid (93%); **m. p.** 259 – 263 °C; **^{1}H NMR** (400 MHz, CD_2Cl_2): δ 7.68 – 7.62 (m, 2H), 7.33 (d, *J* = 7.9 Hz, 2H), 7.19 (d, *J* = 3.4 Hz, 1H), 6.17 (d, *J* = 3.4 Hz, 1H), 5.71 (s, 1H), 3.33 (dd, *J* = 12.4, 3.4 Hz, 1H), 2.94 (dd, *J* = 17.4, 6.4 Hz, 1H), 2.74 – 2.62 (m, 1H), 2.50 – 2.37 (m, 5H), 2.05 (dddd, *J* = 19.6, 13.1, 6.6, 2.9 Hz, 1H), 1.90 – 1.78 (m, 1H), 1.77 – 1.63 (m, 2H), 1.05 (s, 3H); **^{13}C NMR** (101 MHz, CD_2Cl_2): δ 172.4, 145.8, 136.6, 131.6, 130.6, 127.3, 127.0, 122.2, 108.9, 57.5, 34.2, 33.1, 29.3, 24.8, 22.5, 21.9, 20.1; **IR** (cm^{-1}) 3199, 3057, 2957, 2847, 1666, 1592, 1549, 1455, 1418, 1258, 1168, 1140, 962; **HRMS** (ESI+, *m/z*) $[M+H]^+$ calcd. for $C_{19}H_{22}N_2O_3S$: 359.1424, found: 359.1419.

(4a*R,11c*R**)-7,11c-Dimethyl-1,2,4,4a,5,6,7,11c-octahydro-3*H*-pyrido[2,3-*c*]carbazol-3-one (3.6e)**

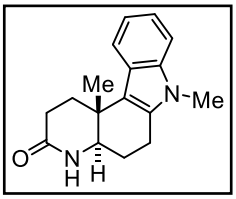

White solid (93%); **m. p.** 186 – 190 °C; **^{1}H NMR** (400 MHz, CD_2Cl_2): δ 7.60 (d, *J* = 8.0 Hz, 1H), 7.27 (d, *J* = 8.1 Hz, 1H), 7.13 (ddd, *J* = 8.2, 7.1, 1.2 Hz, 1H), 7.03 (ddd, *J* = 8.1, 7.0, 1.1 Hz, 1H), 6.49 (s, 1H), 3.65 – 3.57 (m, 4H), 2.92 – 2.83 (m, 2H), 2.76 (ddd, *J* = 13.1, 7.6, 2.2 Hz, 1H), 2.66 – 2.48 (m, 2H), 2.09 – 1.84 (m, 3H), 1.29 (s, 3H); **^{13}C NMR** (101 MHz, CD_2Cl_2): δ 173.2, 137.9, 134.1, 125.8, 120.9, 119.7, 119.2, 116.4, 109.4, 58.8, 35.6, 33.6, 29.6, 24.6, 21.8, 19.3; **IR** (cm^{-1}) 3180, 3060, 2944, 2855, 1657, 1540, 1470, 1416, 1402, 1375, 1306, 1223, 793; **HRMS** (ESI+, *m/z*) $[M+H]^+$ calcd. for $C_{17}H_{20}N_2O$: 269.1648, found: 269.1642.

(4a*R,11c*R**)-11c-Methyl-1,4,4a,5,6,11c-hexahydrobenzofuro[3,2-*f*]quinolin-3(2*H*)-one (3.6f)**

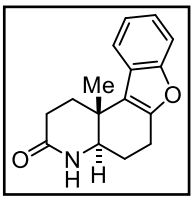

White solid (67%); **m. p.** 230 – 234 °C; **^{1}H NMR** (400 MHz, $CDCl_3$): δ 7.53 (d, *J* = 7.0 Hz, 1H), 7.42 (d, *J* = 7.4 Hz, 1H), 7.21 (pd, *J* = 7.3, 1.4 Hz, 2H), 6.59 (s, 1H), 3.63 (dd, *J* = 12.3, 3.3 Hz, 1H), 2.94 – 2.87 (m, 2H), 2.67 – 2.57 (m, 3H), 2.11 – 1.91 (m, 3H), 1.30 (s, 3H); **^{13}C NMR** (101 MHz, $CDCl_3$): δ 173.1, 155.2, 151.6, 126.8, 123.4, 122.5, 119.6, 119.5, 111.4, 57.8, 34.7, 32.1, 29.4 – 28.3, 24.1, 22.4, 18.6; **IR** (cm^{-1}) 3200, 3077, 2937, 2860, 1659, 1590, 1451, 1400, 1366, 1316, 1226, 1205, 1048, 921; **HRMS** (ESI+, *m/z*) $[M+H]^+$ calcd. for $C_{16}H_{17}NO_2$: 256.1332, found: 256.1328.

(4a*R,11c*R**)-6a-{(1,1,1,3,3,3-Hexafluoropropan-2-yl)oxy}-11c-methyl-1,4,4a,5,6,6a,11b,11c-octahydrobenzofuro[3,2-*f*]quinolin-3(2*H*)-one (3.6f-HFIP)**

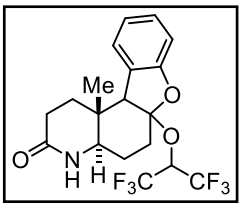

Synthesized with reaction of **3.5f** *with* HFIP *as solvent instead of* NFTB; White solid (21%); **^{1}H NMR** (400 MHz, CD_2Cl_2): δ 7.30 – 7.20 (m, 2H), 7.03 (t, *J* = 7.5 Hz, 1H), 6.91 (d, *J* = 8.1 Hz, 1H), 5.94 (s, 1H), 4.73 (hept, *J* = 6.1 Hz, 1H), 3.40 (dd, *J* = 11.1, 4.3 Hz, 1H), 3.03 (s, 1H), 2.51 (dt, *J* = 14.4, 3.7 Hz, 1H), 2.38 (dd, *J* = 11.5, 7.3 Hz, 1H), 2.31 – 2.17 (m, 1H), 2.19 – 2.00 (m, 2H), 1.88 – 1.69 (m, 1H), 1.72 – 1.60 (m, 2H), 0.35 (s, 3H); **^{13}C NMR** (101 MHz, CD_2Cl_2): δ 171.8, 157.7, 129.3, 129.0, 125.6, 123.1, 120.2, 113.2, 111.6, 68.8 (p, *J* = 33.1 Hz), 57.8, 57.7, 36.9, 34.6, 30.7 (q, *J* = 2.5 Hz), 28.5, 24.9, 12.7; **IR** (cm^{-1}) 3207, 3060, 2940, 2859, 1661, 1588, 1449, 1398, 1354, 1304, 1226, 1198, 1112, 921; **HRMS** (ESI+, *m/z*) $[M+H]^+$ calcd. for $C_{19}H_{20}F_6NO_3$: 424,1342, found: 424,1338.

(4a*R,11c*R**)-11c-Methyl-1,4,4a,5,6,11c-hexahydrobenzo[4,5]thieno[3,2-*f*]quinolin-3(2*H*)-one (3.6g)**

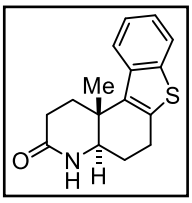

White solid (27%); **m. p.** 274 – 278 °C; **^{1}H NMR** (400 MHz, DMSO-d_6): δ 7.95 (d, *J* = 8.0 Hz, 1H), 7.86 (d, *J* = 7.5 Hz, 1H), 7.73 (s, 1H), 7.34 – 7.24 (m, 2H), 3.58 (dd, *J* = 12.4, 2.8 Hz, 1H), 2.97 – 2.90 (m, 2H), 2.83 – 2.76 (m, 1H), 2.43 – 2.37 (m, 2H), 1.98 – 1.91 (m, 1H), 1.84 – 1.72 (m, 2H), 1.23 (s, 3H); **^{13}C NMR** (101 MHz, DMSO-d_6): δ 171.1, 138.8, 137.8, 136.1, 135.8, 123.9, 123.4, 122.9, 122.7, 57.3, 37.3, 31.5, 28.9, 24.8, 23.2, 17.5; **IR** (cm^{-1}) 3209, 3079, 2957, 2848, 1659, 1604, 1533, 1460, 1436, 1401, 1362, 1305, 1238, 1120, 1020; **HRMS** (ESI+, *m/z*) $[M+H]^+$ calcd. for $C_{16}H_{17}NOS$: 272.1104, found: 272.1101.

(4a*R,11b*S**)-11b-Methyl-1,4,4a,5,6,11b-hexahydrobenzo[4,5]thieno[2,3-*f*]quinolin-3(2*H*)-one (3.6h)**

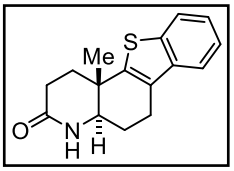

White solid (68%); **m. p.** 266 – 270 °C; **^{1}H NMR** (400 MHz, DMSO-d_6): δ 7.90 (d, *J* = 7.5 Hz, 1H), 7.77 (s, 1H), 7.61 (d, *J* = 7.3 Hz, 1H), 7.39 – 7.29 (m, 2H), 3.59 (dd, *J* = 12.8, 3.0 Hz, 1H), 2.91 (dd, *J* = 17.1, 5.9 Hz, 1H), 2.79 – 2.69 (m, 1H), 2.42 – 2.36 (m, 2H), 2.06 – 1.97 (m, 2H), 1.97 – 1.75 (m, 2H), 1.20 (s, 3H); **^{13}C NMR** (101 MHz, DMSO-d_6) δ 170.5, 144.7, 138.8, 137.8, 127.6, 124.2, 124.1, 122.7, 121.2, 56.9, 36.0, 34.1, 28.8, 22.8, 22.0, 20.3; **IR** (cm^{-1}) 3209, 3081, 2956, 2848, 1660, 1607, 1533, 1462, 1438, 1399, 1362, 1303, 1238, 1119, 1022; **HRMS** (ESI+, *m/z*) $[M+H]^+$ calcd. for $C_{16}H_{17}NOS$: 272.1104, found: 272.1101.

3.4.14. Procedures for further derivatization

3.4.14.1. Synthesis of 3.13

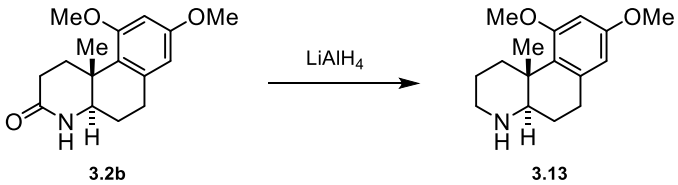

3.2b **3.13**

This procedure was adapted from a literature procedure [30].

A flame-dried vial was charged with **3.2b** (0.11 mmol, 1.0 equiv.) and then dissolved in THF (0.2 M). The mixture was cooled down to 0 °C, and after that, a solution of lithium aluminum hydride (1.0 M, 2.0 equiv.). The reaction was stirred at 50 °C for 12 h. Upon completion, the reaction was cooled to room temperature, diluted with EtOAc, and quenched with water. The two phases were separated, and the aqueous phase was extracted with EtOAc. The combined organic phases were dried over $MgSO_4$, filtered, and then the solvent was removed under reduced pressure. The crude product was purified by column chromatography (SiO_2, *n*-hexane/EtOAc/MeOH 2:2:1) to obtain (4a*R**,10b*R**)-8,10-dimethoxy-10b-methyl-1,2,3,4,4a,5,6,10b-octahydrobenzo[*f*]quinoline **3.13** (19 mg, 67%) as a white solid.

(4a*R,10b*R**)-8,10-Dimethoxy-10b-methyl-1,2,3,4,4a,5,6,10b-octahydrobenzo[*f*]quinoline (3.13)**

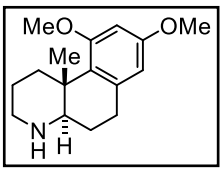

White solid (67%); **m. p.** 255 – 259 °C; **^{1}H NMR** (400 MHz, $CDCl_3$): δ 6.30 (d, *J* = 2.5 Hz, 1H), 6.19 (d, *J* = 2.5 Hz, 1H), 4.93 (s, 1H), 3.77 (s, 3H), 3.76 (s, 3H), 3.49 (dd, *J* = 12.4, 4.7 Hz, 1H), 3.18 (dt, *J* = 13.8, 3.6 Hz, 1H), 3.09 – 2.97 (m, 2H), 2.95 – 2.78 (m, 2H), 2.29 – 2.20 (m, 1H), 2.12 (dt, *J* = 14.2, 4.3 Hz, 1H), 2.08 – 1.97 (m, 1H), 1.78 – 1.68 (m, 1H), 1.48 (s, 3H), 1.36 (td, *J* = 13.7, 4.0 Hz, 1H); **^{13}C NMR** (101 MHz, $CDCl_3$): δ 159.9, 158.9, 136.9, 124.4, 104.9, 98.0, 63.2, 55.3, 55.2, 45.6, 37.4, 33.6, 30.4, 22.9, 19.9, 17.8; **IR** (cm^{-1}) 3357, 2937, 2845, 1605, 1580, 1381, 1269, 1194, 1154, 1029, 841; **HRMS** (ESI+, *m/z*) $[M+H]^+$ calcd. for $C_{16}H_{24}NO_2$: 262.1802, found: 262.1800.

3.4.14.2. Synthesis of 3.14

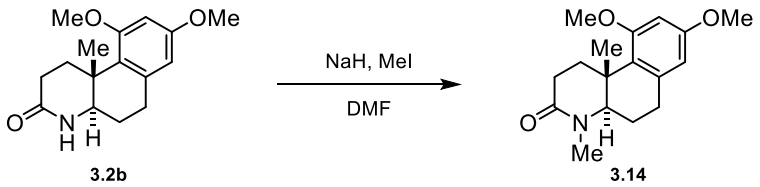

This procedure was adapted from a literature procedure [31].

A flame-dried flask under an argon atmosphere was charged with sodium hydride (0.36 mmol 2.0 equiv., 60 % dispersion in mineral oil). The solid was washed three times with dry *n*-hexane (2 mL). Afterwards, the solid was suspended in dry DMF (0.2 M), and the mixture was cooled down to 0 °C. Next, compound **3.2b** (0.18 mmol, 1.0 equiv.) and iodomethane (0.36 mmol, 2.0 equiv.) were added sequentially. The reaction was stirred at room temperature for 12 h. Upon completion, the reaction was quenched with a saturated solution of NH_4Cl, diluted with water, and extracted with *n*-hexane. The organic phases were washed with brine and dry over $MgSO_4$. The solid was filtered, and the solvent was removed under reduced pressure to obtain (4a*R**,10b*R**)-8,10-dimethoxy-4,10b-dimethyl-1,4,4a,5,6,10b-hexahydrobenzo[*f*]quinolin-3(2*H*)-one **3.14** (38 mg, 72%) as a light-yellow oil.

(4a*R,10b*R**)-8,10-Dimethoxy-4,10b-dimethyl-1,4,4a,5,6,10b-hexahydrobenzo[*f*]quinolin-3(2*H*)-one (3.14)**

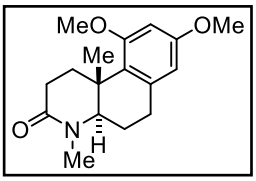

Light-yellow oil (72%); **^{1}H NMR** (400 MHz, $CDCl_3$): δ 6.32 (d, *J* = 2.5 Hz, 1H), 6.21 (d, *J* = 2.4 Hz, 1H), 3.78 (s, 3H), 3.76 (s, 3H), 3.57 (dd, *J* = 13.0, 2.8 Hz, 1H), 3.01 (s, 3H), 2.99 – 2.84 (m, 2H), 2.69 (ddd, *J* = 14.0, 8.1, 6.5 Hz, 1H), 2.57 – 2.36 (m, 2H), 2.16 (ddt, *J* = 12.1, 5.3, 2.6 Hz, 1H), 1.88 (td, *J* = 12.6, 6.5 Hz, 1H), 1.84 – 1.74 (m, 1H), 1.15 (s, 3H); **^{13}C NMR** (101 MHz, $CDCl_3$): δ 172.6, 159.7, 158.8, 136.4, 125.3, 104.3, 97.8, 62.2, 55.3, 55.1, 39.0, 32.6, 31.0, 30.2, 28.8, 22.0, 19.0; **IR** (cm^{-1}) 2940, 2839, 1645, 1606, 1584, 1461, 1397, 1240, 1192, 1156, 1030, 829; **HRMS** (ESI+, *m/z*) $[M+H]^+$ calcd. for $C_{17}H_{24}NO_3$: 290.1751, found: 290.1755.

3.4.14.3. Synthesis of 3.15

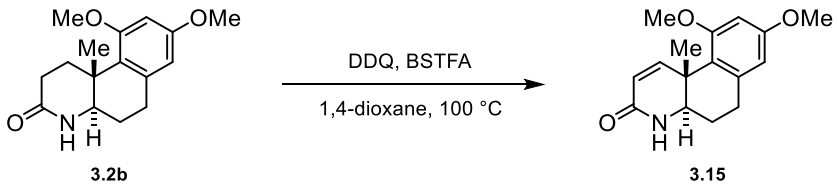

3.2b **3.15**

This procedure was adapted from a literature procedure [32].

A flame-dried pressure vessel was charged with the cyclized compound **3.2b** (1.0 equiv.), 2,3-dichloro-5,6-dicyano-1,4-benzoquinone (1.5 equiv.), and *N*,*O*-bis(trimethylsilyl)trifluoroacetamide (4.0 equiv.). The mixture was dissolved in 1,4-dioxane (0.05 M) at room temperature. The pressure vessel was then sealed and heated up to 100 °C. The reaction was stirred for 12 h. After that, the mixture was cooled to room temperature, diluted with EtOAc, and quenched with a saturated solution of $NaHCO_3$. The two phases were separated and the aqueous phase was extracted with EtOAc. The combined organic phases were dried over $MgSO_4$, filtered, and then the solvent was removed under reduced pressure. The crude product was purified by column chromatography (SiO_2, toluene/acetone 1:1) (4a*R**,10b*R**)-8,10-dimethoxy-10b-methyl-4a,5,6,10b-tetrahydrobenzo[*f*]quinolin-3(4*H*)-one **3.15** (27 mg, 55%) as a pale orange solid.

(4a*R,10b*R**)-8,10-Dimethoxy-10b-methyl-4a,5,6,10b-tetrahydrobenzo[*f*]quinolin-3(4*H*)-one (3.15)**

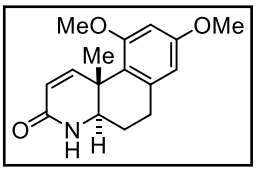

Pale orange solid (55%); **m. p**. 175 – 179 °C; **^{1}H NMR** (400 MHz, $CDCl_3$): δ 7.87 (d, *J* = 10.1 Hz, 1H), 6.43 (s, 1H), 6.34 (d, *J* = 2.5 Hz, 1H), 6.25 (d, *J* = 2.4 Hz, 1H), 5.82 (dd, *J* = 10.1, 2.4 Hz, 1H), 3.84 (s, 3H), 3.80 – 3.74 (m, 4H), 3.07 – 2.97 (m, 1H), 2.85 (dd, *J* = 17.1, 5.4 Hz, 1H), 2.04 – 1.92 (m, 1H), 1.84 – 1.78 (m, 1H), 1.33 (s, 3H); **^{13}C NMR** (101 MHz, $CDCl_3$): δ 167.7, 159.3, 159.2, 153.4, 137.6, 122.5, 120.6, 105.4, 97.6, 57.7, 55.4, 55.2, 40.1, 29.9, 23.3, 19.3; **IR** (cm^{-1}) 3204, 2933, 2851, 1674, 1598, 1582, 1462, 1421, 1375, 1199, 1154, 1046, 820; **HRMS** (ESI+, *m/z*) $[M+H]^+$ calcd. for $C_{16}H_{20}NO_3$: 274.1438, found: 274.1434.

3.4.14.4. Synthesis of 3.2f

Preparation of brominated arenes

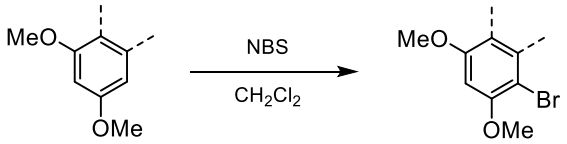

A flamed-dried vial under an argon atmosphere was charged with starting substrate (1.0 equiv.) and dissolved in anhydrous CH_2Cl_2 at 0 °C (0.2 M). Afterward, *N*-bromosuccinimide (1.0 equiv.) was added portion wise. The reaction was stirred for 18 h at room temperature, and then it was quenched with a saturated solution of $NaHCO_3$ and water. The two phases were separated, and the aqueous phase was extracted with CH_2Cl_2. The combined organic phases were dried over $MgSO_4$, filtered, and then the solvent was removed under reduced pressure to obtain the desired product.

(*E*)-3-{6-(2-Bromo-3,5-dimethoxyphenyl)-3-methylhex-3-en-1-yl}-1,4,2-dioxazol-5-one (3.1f)

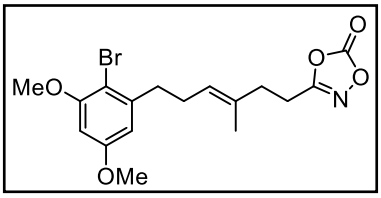

*Starting from compound **3.1b***. Colorless oil (quantitative yield); **^{1}H NMR** 400 MHz, $CDCl_3$): δ 6.38 (d, *J* = 2.8 Hz, 1H), 6.36 (d, *J* = 2.8 Hz, 1H), 5.30 (m, 1H), 3.86 (s, 3H), 3.79 (s, 3H), 2.73 (m, 4H), 2.35 (m, 4H), 1.61 (s, 3H); **^{13}C NMR** (101 MHz, $CDCl_3$) δ 166.5, 159.6, 156.8, 154.3, 143.2, 132.5, 126.2, 107.1, 104.8, 97.5, 56.4, 55.6, 36.6, 34.3, 28.4, 23.7, 15.8; **IR** (cm^{-1}) 2937, 2839, 1868, 1830, 1634, 1596, 1460, 1429, 1349, 1314, 1205, 1151, 1066, 983, 929, 833, 574; **HRMS** (ESI+, m/z) $[M+MeOH+Na]^+$ calcd. for $C_{18}H_{24}O_6NaBr$: 452.0679, found: 452.0683.

(4a*R,10b*R**)-7-Bromo-8,10-dimethoxy-10b-methyl-1,4,4a,5,6,10b-hexahydrobenzo[*f*]quinolin-3(2*H*)-one (2f)**

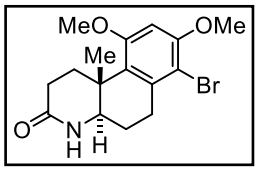

White solid (quantitative yield from **3.2b**);

The NMR data corresponds to the data of compound 3.**2f**.

One-pot reaction for 3.2f synthesis

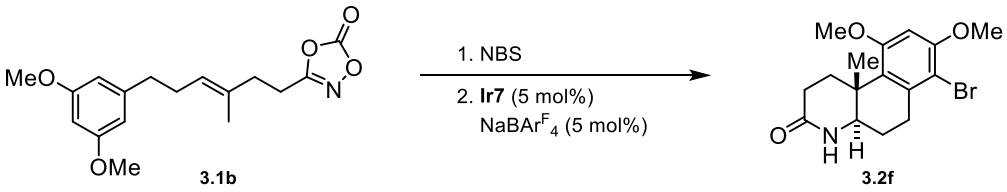

A flame-dried vial under an argon atmosphere was charged with dioxazolone **3.1b** (0.16 mmol, 1.0 equiv.) and then dissolved in 1,1,1,3,3,3-hexafluoro-2-propanol (0.2 M). The mixture was cooled down to 0 °C, and sequentially *N*-bromosuccinimide (0.16 mmol, 1.0 equiv.) was added, and then stirred for 30 h at room temperature. After that, **Ir7** catalyst (7.8 µmol, 5 mol%) and $NaBAr^F_4$ (7.8 µmol, 5 mol%) were added, and the solution was stirred for 14 h. Upon completion, the reaction was quenched with saturated solution $NaHCO_3$ and water. The two phases were separated and the aqueous phase was extracted with CH_2Cl_2. The combined organic phases were dried over $MgSO_4$, filtered, and then the solvent was removed under reduced pressure. The crude product was purified by column chromatography (SiO_2, toluene/acetone 1:1) to obtain the desired product **2f** (37 mg, 67%) as a white solid.

The NMR data of the product correspond to the data of the compound **3.2f.**

3.4.15. Crystallographic details

SC-XRD of 3.2a (CCDC 2282780)

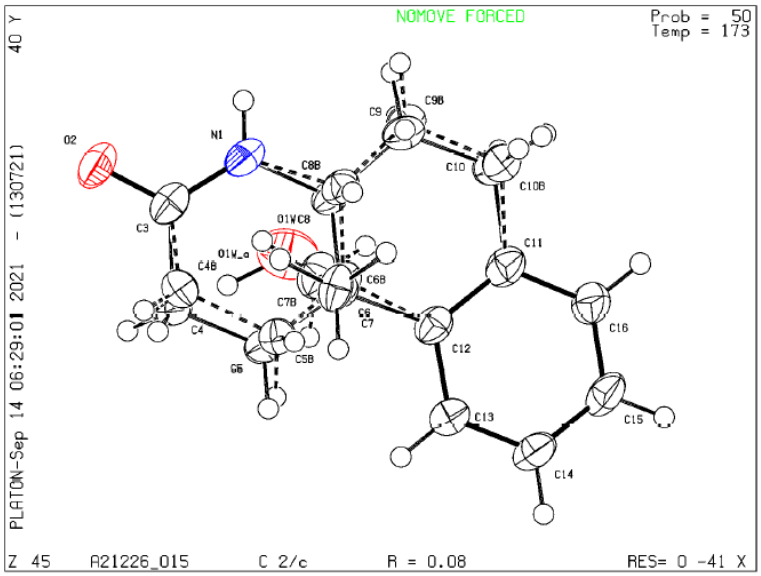

Crystal data and structure refinement for **3.2a**.

Empirical formula	$C_{14}\ H_{17.77}\ N\ O_{1.39}$ [$C_{14}\ H_{17}\ N\ O$, $(H_2\ O)_{0.386}$]
Formula weight	222.24
Temperature	173(2) K
Wavelength	0.71073 Å
Crystal system	Monoclinic
Space group	*C*2/*c*
Unit cell dimensions	a = 25.935(2) Å α = 90°
	b = 6.8017(5) Å β = 92.278(4)°
	c = 13.5117(9) Å γ = 90°
Volume	2381.6(3) $Å^3$
Z	8
Density (calculated)	1.240 Mg/m^3
Absorption coefficient	0.080 mm^{-1}
F(000)	959
Crystal size	0.268 x 0.187 x 0.031 mm^3
Theta range for data collection	3.018 to 27.531°.
Index ranges	–33<=h<=33, –8<=k<=8, –17<=l<=17
Reflections collected	20710
Independent reflections	2727 [R(int) = 0.0926]
Completeness to theta = 25.242°	99.1 %
Absorption correction	Semi-empirical from equivalents
Max. and min. transmission	0.7456 and 0.5645
Refinement method	Full-matrix least-squares on F^2
Data / restraints / parameters	2727 / 278 / 222
Goodness-of-fit on F^2	1.131
Final R indices [I>2sigma(I)]	R1 = 0.0775, wR2 = 0.1709
R indices (all data)	R1 = 0.1028, wR2 = 0.1839
Largest diff. peak and hole	0.240 and –0.336 $e·Å^{-3}$

SC-XRD of 3.2b (CCDC 2282653)

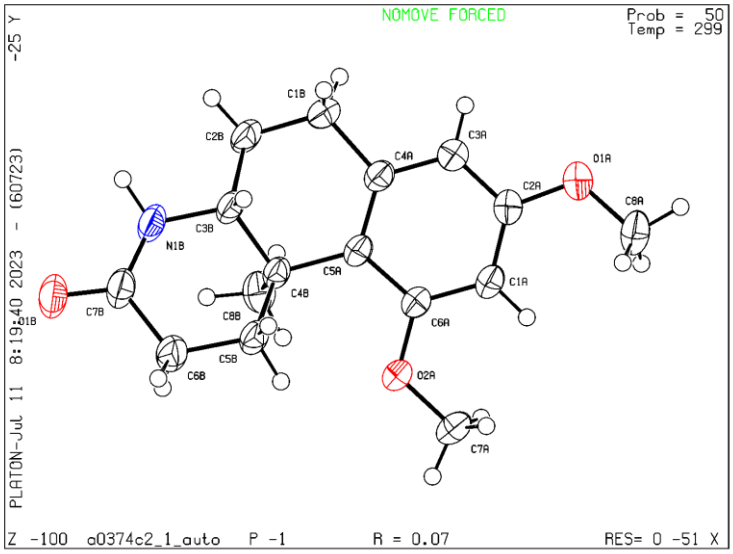

Crystal data and structure refinement for **3.2b**.

Empirical formula	$C_{16}H_{21}NO_3$
Formula weight	275.34
Temperature	298.6(2) K
Wavelength	0.71073 Å
Crystal system	Triclinic
Space group	$P\bar{1}$
Unit cell dimensions	a = 7.4443 (6) Å α = 115.403 (7)°
	b = 10.1200 (9) Å β = 108.297 (7)°
	c = 11.0699 (7) Å γ = 93.756 (7)°
Volume	695.49 (10) $Å^3$
Z	2
Density (calculated)	1.315 Mg/m^3
Absorption coefficient	0.090 mm^{-1}
F(000)	296
Crystal size	0.2 × 0.15 × 0.05 mm^3
Theta range for data collection	2.2 to 32.8 °.
Index ranges	–11<=h<=11, –14<=k<=14, –16<=l<=16
Reflections collected	11639
Independent reflections	4619 [R(int) = 0.0589]
Completeness to theta = 25.242°	99.9 %
Absorption correction	Multi-scan
Max. and min. transmission	0.681 and 1.000
Refinement method	Full-matrix least-squares on F^2
Data / restraints / parameters	4619/ 0 /188
Goodness-of-fit on F^2	1.035
Final R indices [I>2sigma(I)]	R1 = 0.0676, wR2 = 0.1907
R indices (all data)	R1 = 0.1037, wR2 = 0.22050
Largest diff. peak and hole	0.73 and –0.24 $e·Å^{-3}$

SC-XRD of 3.2*gp* (CCDC 2282654)

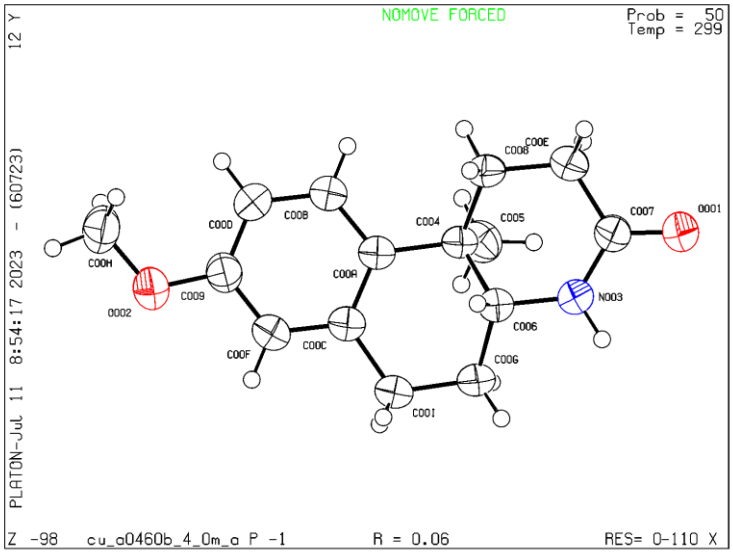

Crystal data and structure refinement for **3.2*gp***.

Empirical formula	$C_{15}H_{19}NO_2$	
Formula weight	245.31	
Temperature	299(2) K	
Wavelength	1.54178 Å	
Crystal system	Triclinic	
Space group	$P\bar{1}$	
Unit cell dimensions	a = 7.6419(11) Å	α = 73.201(7)°
	b = 9.1867(13) Å	β = 71.168(6)°
	c = 10.6756(14) Å	γ = 66.604(6)°
Volume 639.77(16) $Å^3$		
Z	2	
Density (calculated)	1.273 Mg/m^3	
Absorption coefficient	0.670 mm^{-1}	
F(000)	264	
Crystal size	0.1 × 0.06 × 0.03 mm^3	
Theta range for data collection	4.5 to 79.5°	
Index ranges	–9<=h<=9, –11<=k<=11, –14<=l<=14	
Reflections collected	16573	
Independent reflections	2740 [R(int) = 0.0594]	
Completeness to theta = 25.242°	99.7 %	
Absorption correction	Multi-scan	
Max. and min. transmission	0.555 and 0.754	
Refinement method	Full-matrix least-squares on F^2	
Data / restraints / parameters	2740/ 0 /171	
Goodness-of-fit on F^2	1.098	
Final R indices [I>2sigma(I)]	R1 = 0.0611, wR2 = 0.1874	
R indices (all data)	R1 = 0.0680, wR2 = 0.1969	
Largest diff. peak and hole	0.28 and –0.24 $e·Å^{-3}$	

SC-XRD of 3.2h (CCDC 2282779)

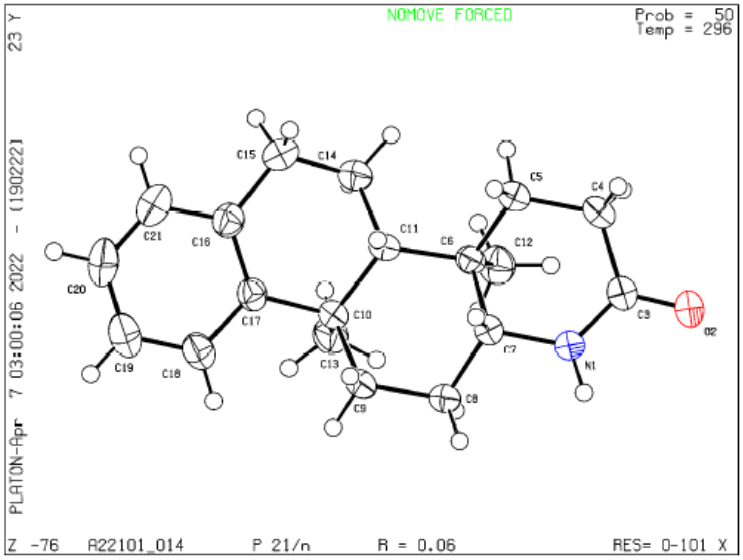

Crystal data and structure refinement for **3.2h**.

Empirical formula	$C_{19}H_{25}NO$
Formula weight	283.40
Temperature	296(2) K
Wavelength	0.71073 Å
Crystal system	Monoclinic
Space group	*P*2/*n*
Unit cell dimensions	a = 7.1428(6) Å α = 90°
	b = 18.1121(14) Å β = 99.125(2)°
	c = 11.9449(9) Å γ = 90°
Volume	1525.8(2) Å^3
Z	4
Density (calculated)	1.234 Mg/m^3
Absorption coefficient	0.075 mm^{-1}
F(000)	616
Crystal size	0.112 x 0.087 x 0.042 mm^3
Theta range for data collection	2.836 to 27.553°.
Index ranges	–9<=h<=8, –23<=k<=23, –15<=l<=15
Reflections collected	19573
Independent reflections	3476 [R(int) = 0.0702]
Completeness to theta = 25.242°	99.1 %
Absorption correction	Semi-empirical from equivalents
Max. and min. transmission	0.7456 and 0.7079
Refinement method	Full-matrix least-squares on F^2
Data / restraints / parameters	3476 / 0 / 201
Goodness-of-fit on F^2	1.030
Final R indices [I>2sigma(I)]	R1 = 0.0614, wR2 = 0.1264
R indices (all data)	R1 = 0.1059, wR2 = 0.1430
Largest diff. peak and hole	0.228 and –0.188 e·Å^{-3}

SC-XRD of 3.4c (CCDC 2282781)

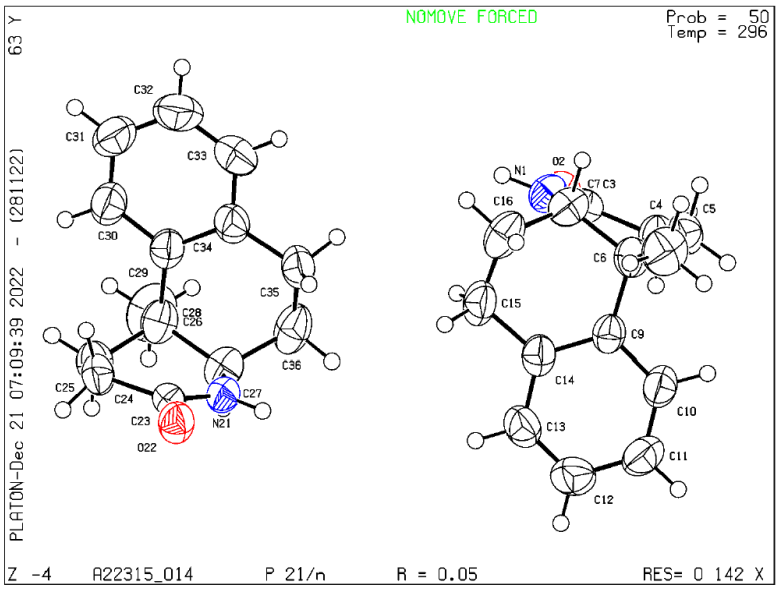

Crystal data and structure refinement for **3.4c**.

Empirical formula	C_{14} H_{17} N O	
Formula weight	215.28	
Temperature	296(2) K	
Wavelength	0.71073 Å	
Crystal system	Monoclinic	
Space group	$P2_1/n$	
Unit cell dimensions	a = 11.3300(6) Å	α = 90°
	b = 13.5785(7) Å	β = 104.8175(18)°
	c = 15.9250(9) Å	γ = 90°
Volume	2368.5(2) $Å^3$	
Z	8	
Density (calculated)	1.207 Mg/m^3	
Absorption coefficient	0.076 mm^{-1}	
F(000)	928	
Crystal size	0.231 x 0.205 x 0.125 mm^3	
Theta range for data collection	2.490 to 27.035°.	
Index ranges	–14<=h<=14, –17<=k<=17, –20<=l<=19	
Reflections collected	37363	
Independent reflections	5176 [R(int) = 0.0694]	
Completeness to theta = 25.242°	99.8 %	
Absorption correction	Semi-empirical from equivalents	
Max. and min. transmission	0.7455 and 0.6207	
Refinement method	Full-matrix least-squares on F^2	
Data / restraints / parameters	5176 / 0 / 303	
Goodness-of-fit on F^2	1.028	
Final R indices [I>2sigma(I)]	R1 = 0.0470, wR2 = 0.1170	
R indices (all data)	R1 = 0.0736, wR2 = 0.1327	
Largest diff. peak and hole	0.184 and –0.137 $e·Å^{-3}$	

SC-XRD of 3.4e*p* (CCDC 2283921)

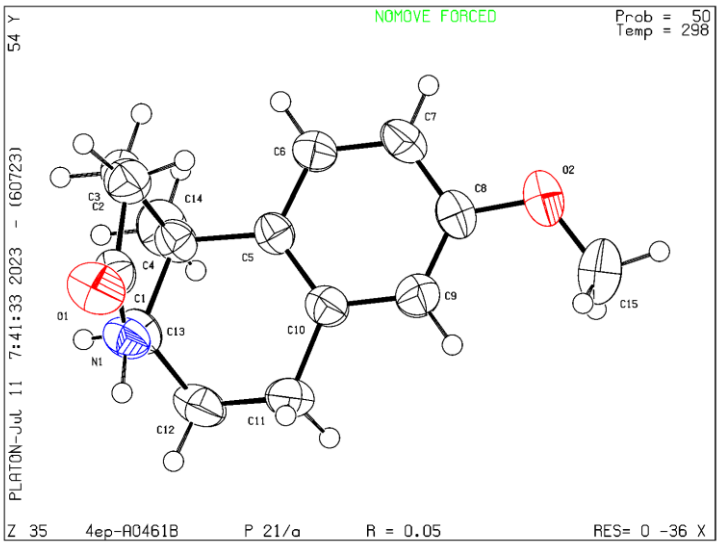

Crystal data and structure refinement for **3.4e*p***.

Empirical formula	C_{15} H_{19} N O_2
Formula weight	245.31
Temperature	298(2) K
Wavelength	0.7107 Å
Crystal system	Monoclinic
Space group	$P2_1/a$
Unit cell dimensions	a = 11.578(5) Å α = 90°
	b = 7.536(2) Å β = 103.72(3)°
	c = 15.355(6) Å γ = 90°
Volume	1301.5(8) $Å^3$
Z	4
Density (calculated)	1.252 Mg/m^3
Absorption coefficient	0.083 mm^{-1}
F(000)	528
Crystal size	0.58 x 0.36 x 0.29 mm^3
Theta range for data collection	1.365 to 25.068°.
Index ranges	–13<=h<=13, –8<=k<=8, 0<=l<=18
Reflections collected	4554
Independent reflections	2302 [R(int) = 0.0346]
Completeness to theta = 25.068°	100.0 %
Absorption correction	none
Max. and min. transmission	n.d.
Refinement method	Full-matrix least-squares on F^2
Data / restraints / parameters	2302 / 1 / 166
Goodness-of-fit on F^2	1.070
Final R indices [I>2sigma(I)]	R1 = 0.0506, wR2 = 0.1182
R indices (all data)	R1 = 0.0691, wR2 = 0.1306
Largest diff. peak and hole	0.199 and –0.119 $e·Å^{-3}$

SC-XRD of 3.4*eo* (CCDC 2283922)

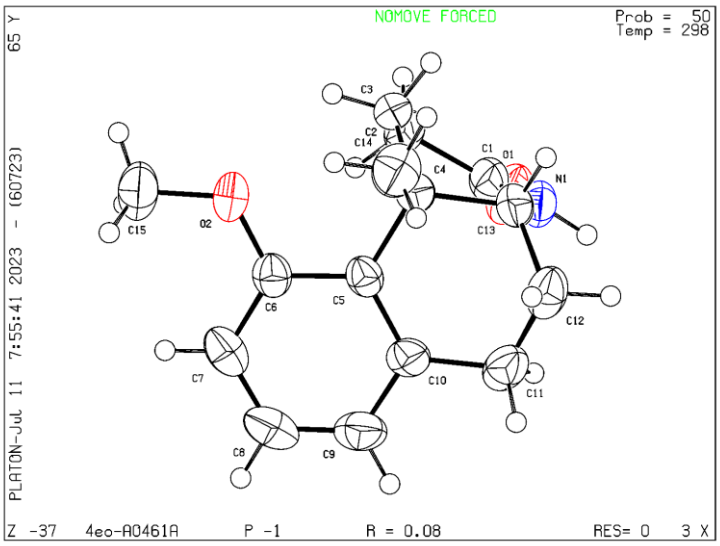

Crystal data and structure refinement for **3.4*eo***.

Empirical formula	C_{15} H_{19} N O_2
Formula weight	245.31
Temperature	298(2) K
Wavelength	0.7107 Å
Crystal system	Triclinic
Space group	*P*-1
Unit cell dimensions	a = 6.561(3) Å α = 96.45(2)°
	b = 7.669(5) Å β = 94.04(2)°
	c = 13.961(3) Å γ = 113.00(5)°
Volume	637.5(6) $Å^3$
Z	2
Density (calculated)	1.278 Mg/m^3
Absorption coefficient	0.084 mm^{-1}
F(000)	264
Crystal size	0.60 x 0.43 x 0.22 mm^3
Theta range for data collection	1.479 to 24.997°.
Index ranges	–7<=h<=7, –9<=k<=9, -4<=l<=16
Reflections collected	2256
Independent reflections	2256 [R(int) = n.d.]
Completeness to theta = 24.997°	100.0 %
Absorption correction	none
Max. and min. transmission	n.d.
Refinement method	Full-matrix least-squares on F^2
Data / restraints / parameters	2256 / 1 / 167
Goodness-of-fit on F^2	1.097
Final R indices [I>2sigma(I)]	R1 = 0.0815, wR2 = 0.2327
R indices (all data)	R1 = 0.1269, wR2 = 0.2767
Largest diff. peak and hole	0.220 and –0.311 $e·Å^{-3}$

SC-XRD of 3.6f (CCDC 2283923)

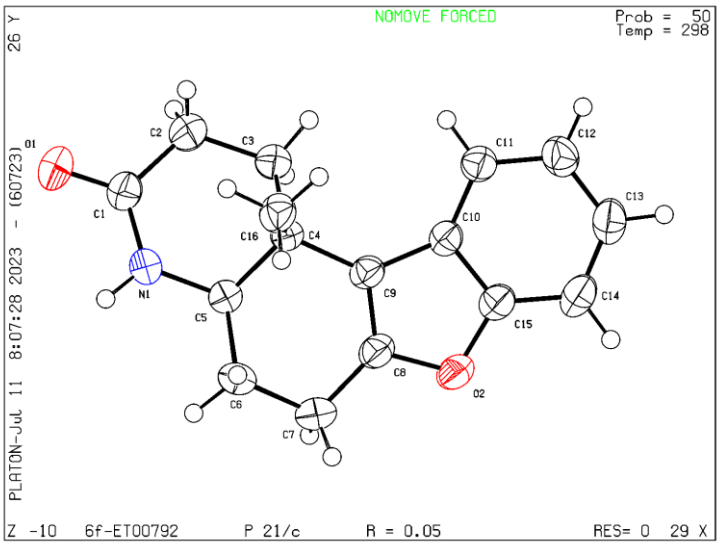

Crystal data and structure refinement for **3.6f**.

Empirical formula	C_{16} H_{17} N O_2
Formula weight	255.31
Temperature	298(2) K
Wavelength	0.7107 Å
Crystal system	Monoclinic
Space group	$P2_1/c$
Unit cell dimensions	a = 14.7947(13) Å α = 90°
	b = 7.9210(6) Å β = 100.789(9)°
	c = 11.1650(10) Å γ = 90°
Volume	1285.29(19) $Å^3$
Z	4
Density (calculated)	1.319 Mg/m^3
Absorption coefficient	0.087 mm^{-1}
F(000)	544
Crystal size	0.23 x 0.13 x 0.06 mm^3
Theta range for data collection	2.803 to 30.062°.
Index ranges	–20<=h<=20, –11<=k<=11, -15<=l<=14
Reflections collected	16651
Independent reflections	3771 [R(int) = 0.0332]
Completeness to theta = 30.062°	100.0 %
Absorption correction	Semi-empirical from equivalents
Max. and min. transmission	0.821 and 0.995
Refinement method	Full-matrix least-squares on F^2
Data / restraints / parameters	3771 / 1 / 176
Goodness-of-fit on F^2	1.038
Final R indices [I>2sigma(I)]	R1 = 0.0489, wR2 = 0.1163
R indices (all data)	R1 = 0.0877, wR2 = 0.1325
Largest diff. peak and hole	0.222 and –0.176 $e·Å^{-3}$

3.5. References

1 a) N. Birudukota, M. M. Mudgal, V. Shanbhag: Discovery and development of azasteroids as anticancer agents. *Steroids* **2019**, *152*, 108505. DOI: 10.1016/j.steroids.2019.108505

b) S. Thareja: Steroidal 5α-Reductase Inhibitors: A Comparative 3D-QSAR Study Review. *Chem. Rev.* **2015**, *115*, 8, 2883–2894. DOI: 10.1021/cr5005953

c) T. Y. Hiyama, M. Yoshida, M. Matsumoto, R. Suzuki, T. Matsuda, E. Watanabe, M. Noda: Endothelin-3 Expression in the Subfornical Organ Enhances the Sensitivity of Na_x, the Brain Sodium-Level Sensor, to Suppress Salt Intake. DOI: 10.1016/j.cmet.2013.02.018

d) S. V. Stulov, A. Y. Misharin: Synthesis of steroids with nitrogen-containing substituents in ring D (Review). Chem. Heterocycl. Comp. **2013**, *48*, 1431–1472. DOI: 10.1007/s10593-013-1158-8

e) M. Ibrahim-Ouali, L. Rocheblave: Recent advances in azasteroids chemistry. *Steroids* **2008**, *73*, 375–407. DOI: 10.1016/j.steroids.2007.12.013

f) M. Ibrahim-Ouali: Total synthesis of steroids and heterosteroids from BISTRO. *Steroids* **2015**, *98*, 9–28. DOI: 10.1016/j.steroids.2015.02.014

2 N. Banka, M. J. K. Bunagan, J. Shapiro: Pattern Hair Loss in Men: Diagnosis and Medical Treatment. *Dermatologic Clinics* **2013**, *31*, 1, 129–140. DOI: 10.1016/j.det.2012.08.003

3 S. Y. Hong, D. Kim, S. Chang: Catalytic access to carbocation intermediates via nitrenoid transfer leading to allylic lactams. *Nat. Catal.* **2021**, *4*, 79–88. DOI: 10.1038/s41929-020-00558-x

4 S. Kim, D. Kim, S. Y. Hong, S. Chang: Tuning Orbital Symmetry of Iridium Nitrenoid Enables Catalytic Diastereo- and Enantioselective Alkene Difunctionalizations. *J. Am. Chem. Soc.* **2021**, *143*, 3993−4004. DOI: 10.1021/jacs.1c00652

5 G. Stork, A. W. Burgstahler: The Stereochemistry of Polyene Cyclization. *J. Am. Chem. Soc.* **1955**, *77*, 19, 5068–5077. DOI: 10.1021/ja01624a038

6 A. Eschenmoser, L. Ruzicka, O. Jeger, D. Arigoni: Zur Kenntnis der Triterpene. 190. Mitteilung. Eine stereochemische Interpretation der biogenetischen Isoprenregel bei den Triterpenen. *Helv. Chim. Acta* **1955**, *38*, 1890−1904. DOI: 10.1002/hlca.19550380728

7 R. L. Snowden, J. C. Eichenberger, S. M. Linder, P. Sonnay, C. Vial, and K. H. Schulte-Elte: Internal nucleophilic termination in biomimetic acid mediated polyene cyclizations: stereochemical and mechanistic implications. Synthesis of (.+-.)-Ambrox and its diastereoisomers. *J. Org. Chem.* **1992**, *57*, 3, 955–960. DOI: 10.1021/jo00029a031

8 S. A. Snyder, D. S. Treitler, A. P. Brucks: Simple Reagents for Direct Halonium-Induced Polyene Cyclizations. *J. Am. Chem. Soc.* **2010**, *132*, 40, 14303–14314. DOI: 10.1021/ja106813s

9 S. J. Plamondon, J. M. Warnica, D. Kaldre, J. L. Gleason: Hydrazide-Catalyzed Polyene Cyclization: Asymmetric Organocatalytic Synthesis of cis-Decalins. *Angew. Chem., Int. Ed.* **2020**, *59*, 253−258. DOI: 10.1002/anie.201911952

10 O. García-Pedreroa, F. Rodríguez: Cationic cyclization reactions with alkyne terminating groups: a useful tool in biomimetic synthesis. *Chem. Commun.* **2022**, *58*, 1089−1099. DOI: 10.1039/D1CC05826F

11 D. A. Evans, M. D. Ennis, D. J. Mathre: Asymmetric alkylation reactions of chiral imide enolates. A practical approach to the enantioselective synthesis of .alpha.-substituted carboxylic acid derivatives. *J. Am. Chem. Soc.* **1982**, *104*, 6, 1737–1739. DOI: 10.1021/ja00370a050

12 M. Huang, T. Yang, J. D. Paretsky, J. F. Berry, J. M. Schomaker: Inverting Steric Effects: Using "Attractive" Noncovalent Interactions To Direct Silver-Catalyzed Nitrene Transfer. *J. Am. Chem. Soc.* **2017**, *139*, 48, 17376–17386. DOI: 10.1021/jacs.7b07619

13 H. Jung, M. Schrader, D. Kim, M.-H. Baik, Y. Park, S. Chang: Harnessing Secondary Coordination Sphere Interactions That Enable the Selective Amidation of Benzylic C–H Bonds. *J. Am. Chem. Soc.* **2019**, *141*, 38, 15356–15366. DOI: 10.1021/jacs.9b07795

14 K. Surendra, E. J. Corey: Rapid and Enantioselective Synthetic Approaches to Germanicol and Other Pentacyclic Triterpenes. *J. Am. Chem. Soc.* **2008**, *130*, 27, 8865–8869. DOI: 10.1021/ja802730a

15 S. A. Syder, E. J. Corey: Concise Total Syntheses of Palominol, Dolabellatrienone, β-Araneosene, and Isoedunol via an Enantioselective Diels−Alder Macrobicyclization. *J. Am. Chem. Soc.* **2006**, *128*, 3, 740–742. DOI: 10.1021/ja0576379

16 K. Surendra, W. Qiu, E. J. Corey: A Powerful New Construction of Complex Chiral Polycycles by an Indium(III)-Catalyzed Cationic Cascade. *J. Am. Chem. Soc.* **2011**, *133*, 25, 9724–9726. DOI: 10.1021/ja204142n

17 B. Li, Y.-J. Zhao, Y.-C. Lai, T.-P. Loh: Asymmetric Syntheses of 8-Oxabicyclo[3,2,1]octanes: A Cationic Cascade Cyclization. *Angew. Chem., Int. Ed.* **2012**, *51*, 8041–8045. DOI: 10.1002/anie.201202699

18 J. Yao, C.-L. Li, X. Fan, Z. Wang, Z.-X. Yu, J. Zhao: Ynamide Protonation-Initiated Cis-Selective Polyene Cyclization and Reaction Mechanism. *CCS Chem.* **2022**, *4*, 2991–3001. DOI: 10.31635/ccschem.021.202101331

19 S. J. Harwood, M. D. Palkowitz, C. N. Gannett, P. Perez, Z. Yao, L. Sun, H. D. Abruña, S. L. Anderson, P. S. Baran: Modular terpene synthesis enabled by mild electrochemical couplings. *Science* **2022**, *375*,745–752. DOI: 10.1126/science.abn1395

20 J. Rojas-Martín, M. Veguillas, M. Ribagorda, C. Carreño: Synthesis of Indole Substituted Twistenediones from a 2-Quinonyl Boronic Acid. *Org. Lett.* **2013**, *15*, 22, 5686–5689. DOI: 10.1021/ol402689b

21 S. Movahhed, J. Westphal, M. Dindaroğlu, A. Falk, H.-G. Schmalz: Low-Pressure Cobalt-Catalyzed Enantioselective Hydrovinylation of Vinylarenes. *Chem. Eur. J*. **2016**, *22*, 7381–7384. DOI: 10.1002/chem.201601283

22 L. Zhang, Z. Huang: Synthesis of 1,1,1-Tris(boronates) from Vinylarenes by Co-Catalyzed Dehydrogenative Borylations–Hydroboration. *J. Am. Chem. Soc.* **2015**, *137*, 50, 15600–15603. DOI: 10.1021/jacs.5b11366

23 S. Niyomchon, A. Oppedisano, P. Aillard, N. Maulide: A three-membered ring approach to carbonyl olefination. *Nat Commun.* **2017**, *8*, 1091. DOI: 10.1038/s41467-017-01036-y

24 S. Musa, A. Ghosh, L. Vaccaro, L. Ackermann, D. Gelman: Efficient E-Selective Transfer Semihydrogenation of Alkynes by Means of Ligand-Metal Cooperating Ruthenium Catalyst. *Adv. Synth. Catal.* **2015**, *357*, 2351–2357. DOI: 10.1002/adsc.201500372

25 P. Winter, W. Hiller, M. Christmann: Access to Skipped Polyene Macrolides through Ring-Closing Metathesis: Total Synthesis of the RNA Polymerase Inhibitor Ripostatin B. *Angew. Chem. Int. Ed.* **2012**, *51*, 3396–3400. DOI: 10.1002/anie.201108692

26 K. Michigami, T. Mita, Y. Sato: Cobalt-Catalyzed Allylic C(sp^3)–H Carboxylation with CO_2. *J. Am. Chem. Soc.* **2017**, *139*, 17, 6094–6097. DOI: 10.1021/jacs.7b02775

27 M. Lee, H. Jung, D. Kim, J.-W. Park, S. Chang: Modular Tuning of Electrophilic Reactivity of Iridium Nitrenoids for the Intermolecular Selective α-Amidation of β-Keto Esters. *J. Am. Chem. Soc.* **2020**, *142*, 28, 11999–12004. DOI: 10.1021/jacs.0c04344

28 Y. Hwang, H. Jung, E. Lee, D. Kim, S. Chang: Quantitative Analysis on Two-Point Ligand Modulation of Iridium Catalysts for Chemodivergent C–H Amidation. *J. Am. Chem. Soc.* **2020**, *142*, 19, 8880–8889. DOI: 10.1021/jacs.0c02079

29 B. Pakyapan, S. B. Kavukcu, Z. S. Sahin, H. Türkmen: Synthesis and catalytic applications of Ru and Ir complexes containing N,O-chelating ligand. *J. Organomet. Chem*. **2020**, *925*, 121486. DOI: 10.1016/j.jorganchem.2020.121486

30 B. Wanner, I. Kreituss, O. Gutierrez, M. C. Kozlowski, J. W. Bode: Catalytic Kinetic Resolution of Disubstituted Piperidines by Enantioselective Acylation: Synthetic Utility and Mechanistic Insights. *J. Am. Chem. Soc.* **2015**, *137*, 35, 11491–11497. DOI: 10.1021/jacs.5b07201

31 T. Nanjo, E. C. de Lucca Jr., M. C. White: Remote, Late-Stage Oxidation of Aliphatic C–H Bonds in Amide-Containing Molecules. *J. Am. Chem. Soc.* **2017**, *139*, 41, 14586–14591. DOI: 10.1021/jacs.7b07665

32 C. Zhu, Z. Liu, G. Chen, K. Zhang, H. Ding: Total Synthesis of Indole Alkaloid Alsmaphorazine D. *Angew. Chem. Int. Ed.* **2015**, *54*, 879–882. DOI: 10.1002/anie.201409827

Chapter 4: Electrochemically generated oxocarbenium species as initiators for polyene cyclizations

4.1. Introduction

As discussed in Chapter 2, electrochemical generation of reactive species is opening new modes of reactivity, compared to classical methods or even photochemical transformations. When this is combined with short-lived species, certain transformations can be achieved that might not be available in other reaction modes. Generally, a lot of electrochemical transformations happen in the presence of all reaction partners present in the reaction mixture at the time of electrochemical step, which can cause undesired reactivity with reduction or oxidation of substrates that are not meant to be electrochemically altered. Sometimes this problem can be solved by divided cell setup in contrast to undivided one. Considering this limitation, cation pool (Scheme 4.1) offers a great method of generation of reactive species and their accumulation until the electrochemical step is finished, and substrates are introduced to the reaction mixture in further step, without being exposed to electric potential generated by electrodes. Cations generated with this method are short-lived and their stabilization can be achieved 1) with neighboring atoms or groups to the atom which is bearing a positive charge; 2) with suitable counter anions provided by supporting electrolyte; and 3) with low temperatures.

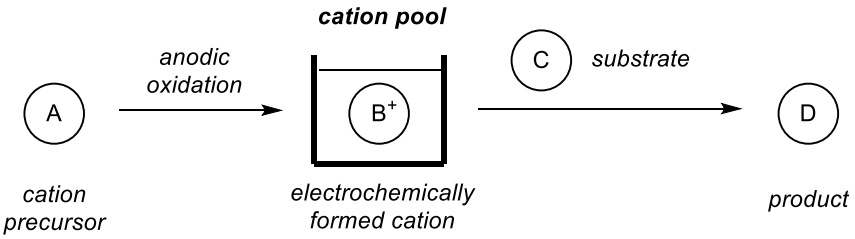

***Scheme 4.1**: Cation pool method.*

Since the discovery of the cation pool method, there has been an increasing interest in this methodology and several advances have been achieved in its diversification and applicability to different transformations as shown in Chapter 2. Generation of alkoxycarbenium ions, which inspired our experimental work, will be presented in this introduction.

Electroauxiliaries (electroauxiliary groups) are very frequently used in cation pool strategy since they lower the oxidation potential of cation precursors. Silyl groups are frequently used as electroauxiliaries, but rarely in the case of α-silyl ethers participating in direct cation pool generation. Yoshida and coworkers [1,2] have reported generation of alkoxycarbenium ions from α-silyl ethers, which were further reacted with 1-(trimethylsilyl)cyclohex-2-en (Scheme 4.2). The yield of corresponding allylated product was increased when reaction occurred in presence of ether additives, suggesting that reactive species is stabilized in form of oxonium species. Intramolecular stabilization of oxocarbenium species by alkyl ether moiety proved to be operational and reaction with silyl-containing nucleophiles resulted in good to excellent yields of the corresponding products (Figure 4.1).

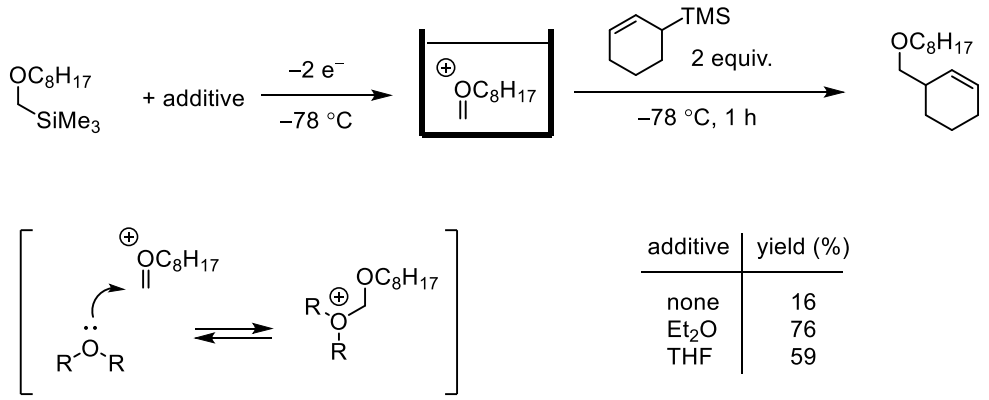

additive	yield (%)
none	16
Et_2O	76
THF	59

***Scheme 4.2**: Reactivity of α-silyl ethers in cation pool strategy.*

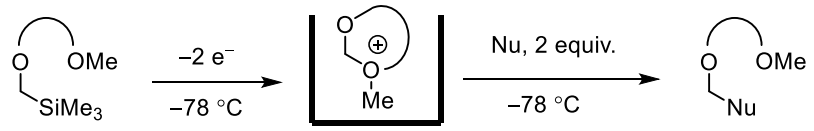

substrate	nucleophile	product	reaction time (min)	yield (%)
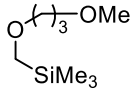	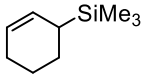	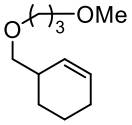	15 60 120	39 77 93
	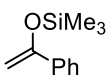	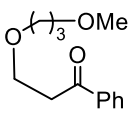	15	60

***Figure 4.1**: Reactivity of α-silyl ethers with intramolecular stabilization.*

Thioacetals appear more frequently as alkoxycarbenium ion precursors, possessing arylthio group as electroauxiliary. The mechanism of generation (Scheme 4.3) is believed to proceed through one electron oxidation which forms radical cation that undergoes C–S bond cleavage, forming alkoxycarbenium ion and arylthio radical, which forms disulfide upon homodimerization [3]. This strategy has been employed in several examples [3–5]. When several thioacetals were examined in reactions with trimethylallylsilane (Figure 4.2), corresponding allylated products were obtained in good to excellent yields even with different substituents on the phenyl ring of the arylthio portion [3]. However, thioacetal with a phenyl substituent in the α-position to the central carbon atom showed only moderate product yield. Examples of intramolecular nucleophile trapping [2–4] (Scheme 4.4) have also been shown, where fluorine atom from supporting electrolyte was incorporated into the final product. In the same transformation, additionally to thioacetals, cation precursors having different electroauxiliaries ($SiMe_3$, $SnBu_3$) were used.

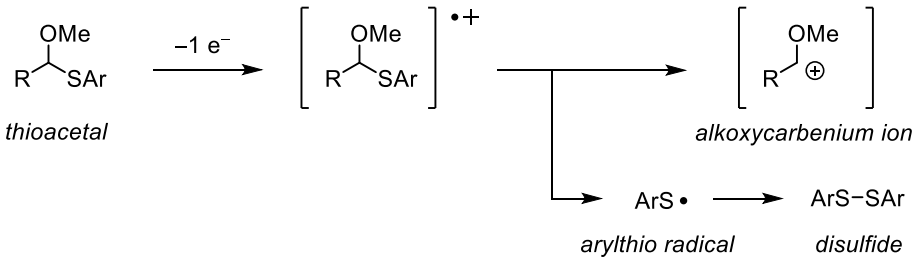

***Scheme 4.3**: Proposed mechanism of alkoxycarbenium ion formation from thioacetal.*

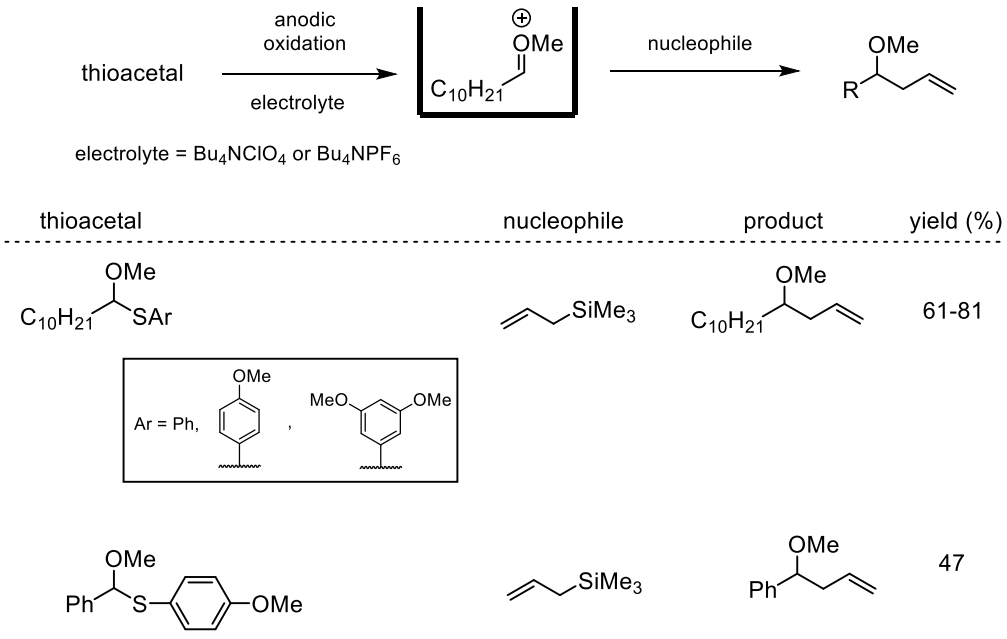

***Figure 4.2**: Reactivity of thioacetals in cation pool method.*

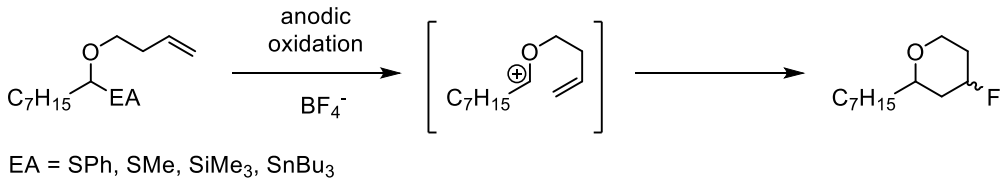

***Scheme 4.4**: Reactivity of electroauxiliary-bearing alkoxycarbenium ion precursors with intramolecular nucleophylic site.*

To avoid possible side reactivity of arylthio radicals, an indirect generation of alkoxycarbenium ions was introduced [5,6]. Disulfides are subjected to electrochemical oxidation and formally form sulfenium ions which are stabilized by remaining disulfides (Scheme 4.5). They further react with thioacetals, but exact mechanism of this process has not been clarified yet; however, ionic mechanism is believed to be more plausible in contrast to single electron mechanism (Scheme 4.6). When this methodology was used in reaction with various carbon nucleophiles, a scope of products has been prepared in good to excellent yields (Scheme 4.7). Thioacetal, bearing linear alkyl side chain, was tested with several nucleophilic partners that gave corresponding yields – linear (89%) and cyclic (91%) silanes, silyl enol ether (79%), silyl ketene acetal (67%) and vinyl acetate (63%). When various thioacetals were screened, thioacetals with halogen substituent (Cl or F) on the phenyl ring at para position preformed slightly better (82–83%) than with methyl substituent (72%). Benzaldehyde derived thioacetal gave excellent yield (91%). Cyclohexyl group decreased a yield to 68%. 5- or 6-membered cyclic thioacetals performed well with cyclic allyl silanes, resulting in 85–86% reaction yield.

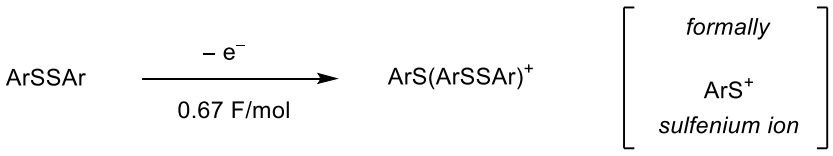

***Scheme 4.5**: Electrochemical generation of stabilized sulfenium ion pool.*

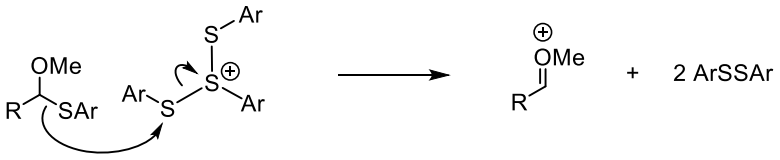

***Scheme 4.6**: Indirect cation pool strategy - generation of alkoxycarbenium species by electrochemically generated (ArSSAr)ArS^+ species – proposed ionic mechanism.*

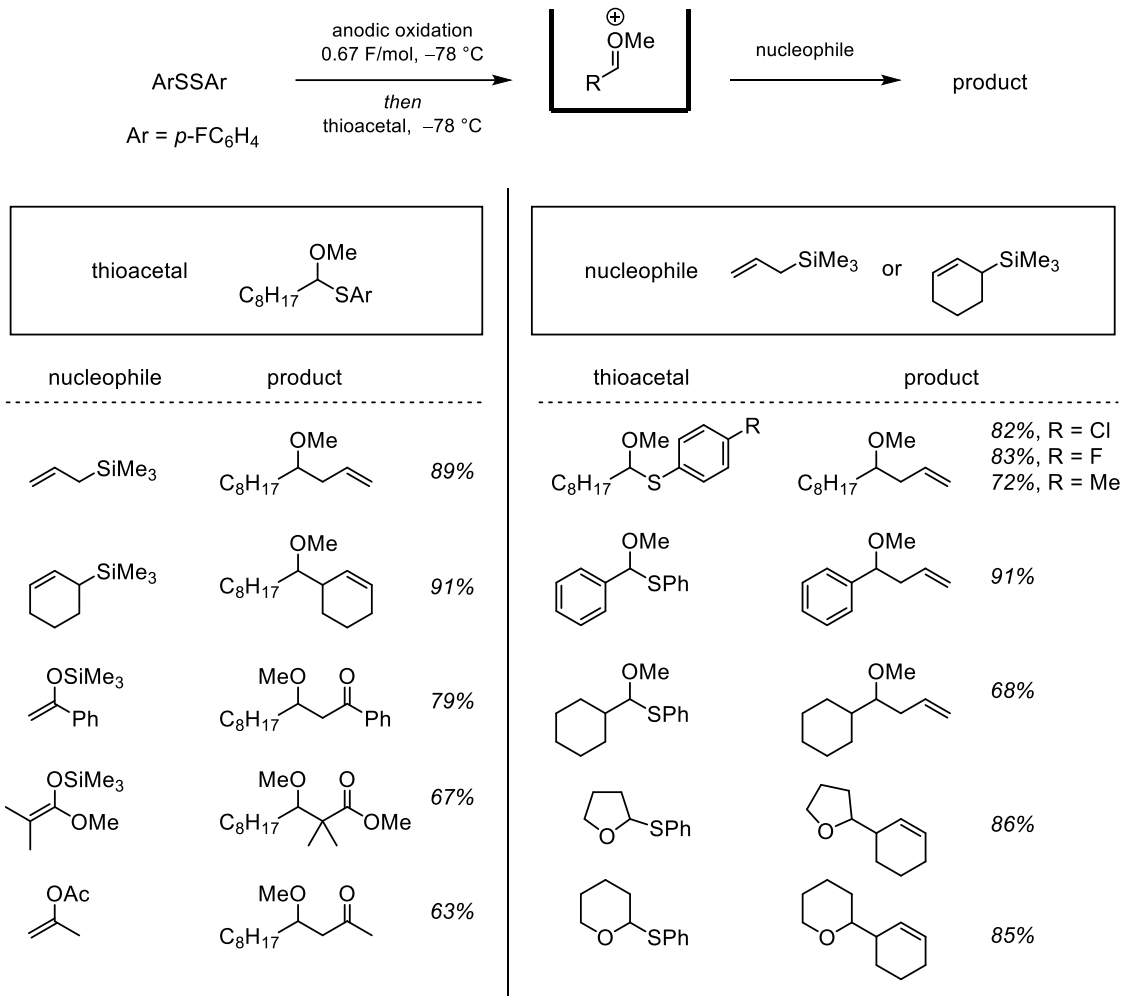

***Scheme 4.7**: Indirect generation of alkoxycarbenium cation pools using with different cation precursors and further reaction with various nucleophiles.*

Incorporation of flow electrochemical setup, shown in further development, enabled direct flash (rapid) generation of alkoxycarbenium ions using several thioacetals (cyclic and acyclic) as cation precursors (Scheme 4.8) [7]. Rapid generation of these short-lived species offered shorter time between their generation and their further reaction with corresponding nucleophile, and consequentially gave an option for a higher working temperature at generation and reaction step. When thioacetals were reacted with silyl enol ethers in flow setting, it was shown that products were formed in good to excellent yields even at higher reaction temperature.

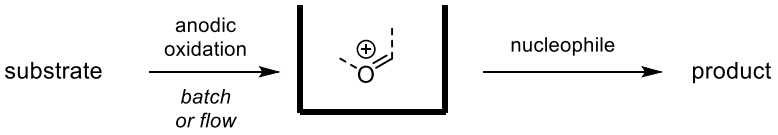

substrate	nucleophile	product	temperature (°C)	yield (%) batch	yield (%) flow
Ar = *p*-FC_6H_4					
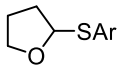		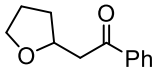	0	2	82
			–75	17	87
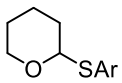	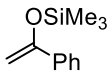	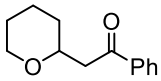	–50	4	59
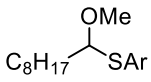		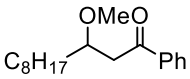	0	4	69

***Scheme 4.8**: Comparison of reactivity of thioacetals in direct cation pool and direct cation flow setup.*

Similarly, indirect cation flow setup [8] was achieved with anodic flash oxidation of disulfides. Formed sulfonium ions were in the next step mixed with thioacetals (Scheme 4.9). Resulting alkoxycarbenium ions were in the second mixing point introduced to silyl enol ether. Combinations of residence times and temperatures were screened, reaching up to 93% product yield with optimal conditions.

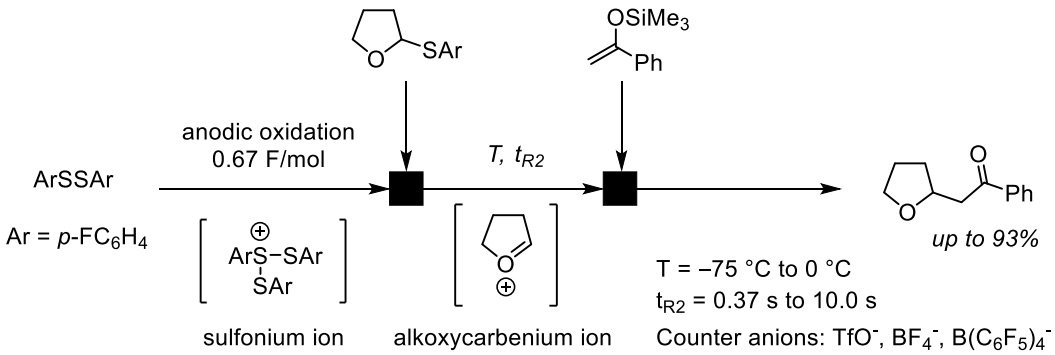

***Scheme 4.9**: Indirect cation flow setup for generation of alkoxycarbenium intermediates and in flow reaction with nucleophile.*

Alkoxycarbenium ions, formed by several methods, have been shown to react with various nucleophiles. With this background, we were expecting polyenes to be good nucleophilic partners and that polyene cyclization cascade could be promoted.

4.2. Results and discussion

We have started exploring the feasibility of transformations where polyenes would take part in cascade cyclization reactions with electrochemically generated alkoxycarbenium species as cyclization initiators. Since there are a lot of parameters that can be modified in electrochemical reactions, we decided to begin with cation pool reactions before moving further to operationally more complex flow electrochemical reactions.

4.2.1. Cation pool reactions with two polyene substrates

As a model substrate for our cation pool strategy, we have first turned to substrate **4.3** which features allyl silane structural motif. Plain trimethylallylsilane has been previously used in similar transformations [3–5] and gave good results in reactions with stabilized carbocations. We have first explored the indirect alkoxycarbenium generation (Table 4.1). Anodic oxidation of 1.5 equivalents of disulfide **4.1** with 0.67 F/mol (based on disulfide) formed 1.0 equivalent of intermediate sulfenium species, which upon addition of 1.0 equivalent of thioacetal **4.2** formed the reactive alkoxycarbenium species. We have theoretically accumulated 1.0 equivalent of the stabilized carbocation and then used the diene **4.3** in excess (1.5 equivalents).

Table 4.1**: Indirect cation pool - optimization of reaction conditions with substrate **4.3

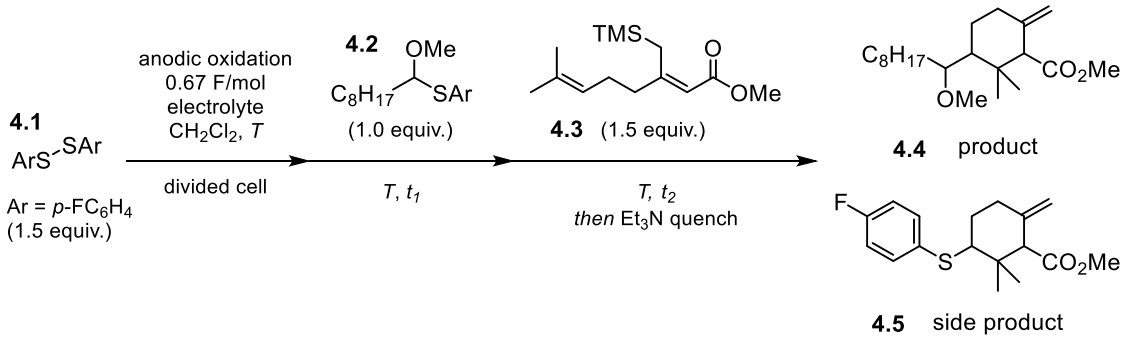

Entry	Electrolyte	T (°C)	t_1 (min)	t_2 (min)	Product 4.4 yield	Side product 4.5 yield
1	Bu_4NBF_4 (0.1 M)	−78	10	60	34%	14%
2	Bu_4NBF_4 (0.1 M)	−50	10	60	28%	31%
3	$Bu_4NB(C_6F_5)_4$ (0.1 M)	−78	10	60	15%	35%
4	$Bu_4NB(C_6F_5)_4$ (0.1 M)	−50	10	60	8%	37%
5	Bu_4NOTf (0.1 M)	−78	10	60	4%	Not observed
6	Bu_4NOTf (0.1 M)	−50	10	60	8%	Not observed

Yields determined by ^1H NMR with trichloroethene as internal standard.

After screening several combinations of different electrolytes and reaction temperatures we have observed that reactions with Bu_4NBF_4 (Table 4.1, entries 1–2) gave rather low but promising results in terms of target product yields (around 30%). However, we have observed formation of the undesired side product **4.5,** which was more prominent at a higher reaction temperature. When $Bu_4NB(C_6F_5)_4$ was used as electrolyte (entries 3–4), the target product **4.4** was formed in much lower yields and with an increased relative amount of the side product. Lower temperature had beneficial effect on the yield of the target product regardless of the electrolyte used, and we believe this is due to lower stability of carbocationic species at higher temperatures. At reactions where Bu_4NOTf was used as electrolyte (entries 5–6) the desired product was observed only in traces.

We tried to solve the issue of the undesired side product formation with the direct cation pool strategy where α-silyl ether **4.6**, as a cation precursor, undergoes direct anodic oxidation (Table 4.2). Based on previous findings, we kept the reaction temperature at −78 °C. With initial reaction conditions we reached 30% product yield (entry 1), which was not significantly changed when we increased the electrolyte concentration (entry 2). In these conditions, the yield has decreased when higher excess of the diene was used, regardless of the electrolyte concentration (entries 3–4).

Table 4.2**: Direct cation pool - optimization of reaction conditions with substrate **4.3

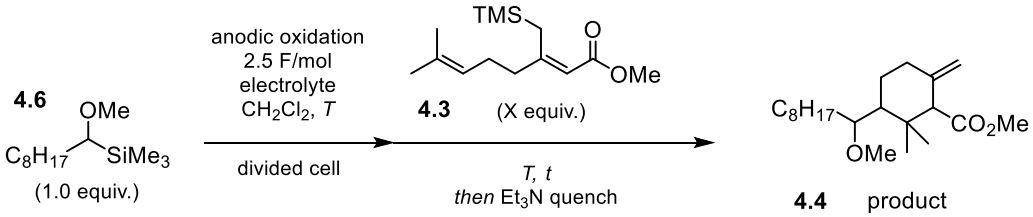

Entry	Electrolyte	X (diene equiv.)	T (°C)	t (min)	Product yield
1	Bu_4NBF_4 (0.1 M)	1.5	−78	60	30%
2	Bu_4NBF_4 (0.3 M)	1.5	−78	60	32%
3	Bu_4NBF_4 (0.1 M)	3.0	−78	60	20%
4	Bu_4NBF_4 (0.3 M)	3.0	−78	60	16%

Yields determined by ^1H NMR with trichloroethene as internal standard.

We further tested direct cation pool method with thioacetal **4.2** as cation precursor (Table 4.3). With unchanged reaction temperature (−78 °C) and excess of the diene (1.5 equivalents) we observed that reaction with 0.1 M Bu_4NBF_4 as electrolyte yielded 27% of the target product and 5% of the side product (entry 1). With increased electrolyte concentration to 0.3 M (entry 2) yields have slightly increased and reached 35% for target product and 16% for side product. These results have given us good grounds to use direct cation formation also in flow experiments.

Table 4.3**: Direct cation pool - optimization of reaction conditions with substrate **4.3

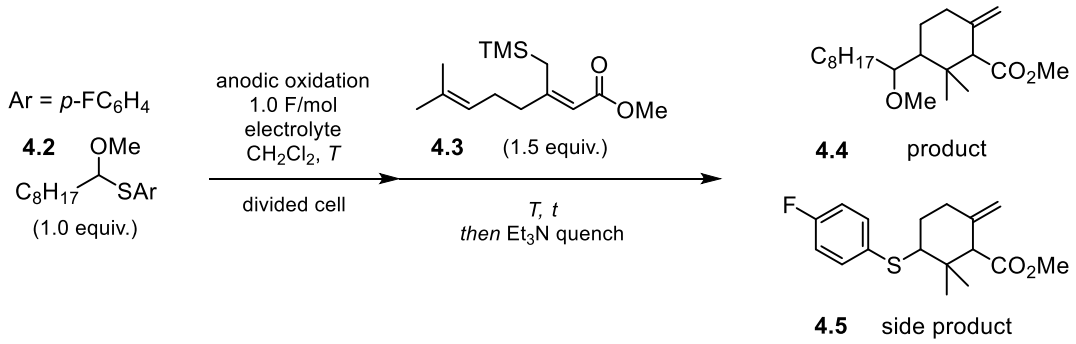

Entry	Electrolyte	T (°C)	t (min)	Product 4.4 yield	Side product 4.5 yield
1	Bu_4NBF_4 (0.1 M)	−78	60	27%	5%
2	Bu_4NBF_4 (0.3 M)	−78	60	35%	16%

Yields determined by ^{1}H NMR with trichloroethene as internal standard.

However, before we moved to flow setup, we tested another diene substrate, **4.7a**, in cation pool conditions as it was expected for this cyclization cascade to be more challenging. With the indirect pool (Table 4.4), we have first tested initial reaction conditions with 0.1 M Bu_4NBF_4, 1.5 equivalents of diene and reaction temperature of −78 °C (entry 1) which gave the tricyclic product **4.8a** in 54% yield. With increased electrolyte concentration (0.3 M) we have observed slightly decreased yield of 45% (entry 2). The higher excess of the diene has not increased the yield and gave a more complex reaction outcome (entry 3). With shorter reaction time allowed for cyclization (10 min instead of 60 min) we observed lower yield of 33% (entry 4) compared to initial conditions.

Table 4.4**: Indirect pool method - optimization of reaction conditions with substrate **4.7a

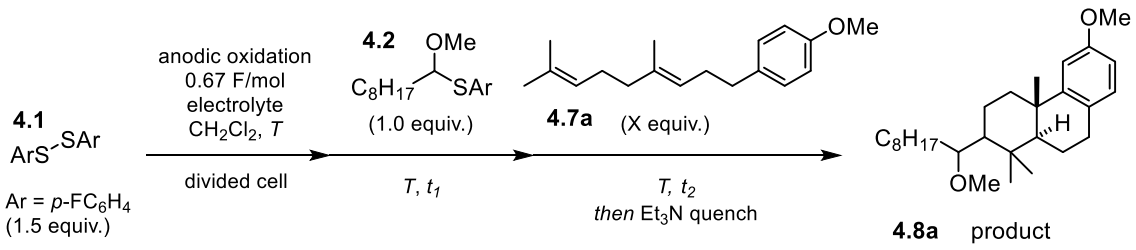

Entry	Electrolyte	X (diene equiv.)	T (°C)	t_1 (min)	t_2 (min)	Product yield
1	Bu_4NBF_4 (0.1 M)	1.5	−78	15	60	54%
2	Bu_4NBF_4 (0.3 M)	1.5	−78	15	60	45%
3	Bu_4NBF_4 (0.1 M)	3.0	−78	15	60	55%
4	Bu_4NBF_4 (0.3 M)	1.5	−78	15	10	33%

Yields determined by ^{1}H NMR with trichloroethene as internal standard.

When the diene **4.7a** was subjected to direct pool conditions (0.1 M Bu_4NBF_4, 1.5 equivalents of diene, reaction temperature −78 °C) with α-silyl ether **4.6** as cation precursor, the tricyclic product **4.8a** was formed in 55% yield (Table 4.5, entry 1). Increasing reaction temperature at the cyclization step (entries 2–3) has decreased the product yield. This is believed to be a consequence of lower stability of short-lived carbocationic species at increased temperatures. When we have increased the electrolyte concentration and the excess of the diene (entry 4), the product yield dropped to 34%. To have a better control over the source of limiting reagent we decided to form cationic species in 2.0 equivalents, and use the diene as a limiting reagent (entry 5). In this case the tricyclic product **4.8a** was obtained in 50% yield, which was comparable to the yield obtained with initial conditions. Changing the electrolyte to 0.1 M $Bu_4NB(C_6F_5)_4$ with excess of diene at two reaction temperatures (entries 6–7) yielded the desired product only in traces.

Table 4.5**: Direct cation pool - optimization of reaction conditions with substrate **4.7a

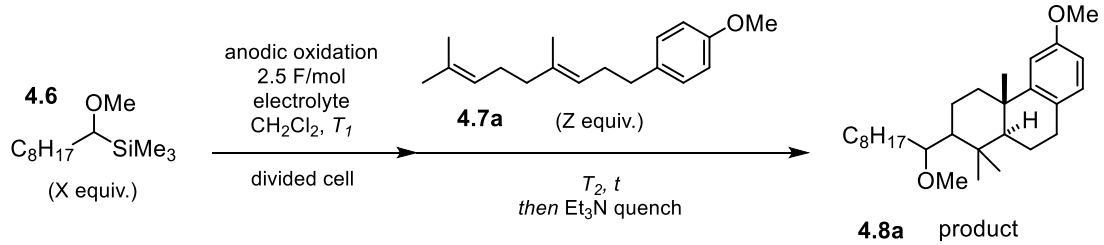

Entry	Electrolyte	X (cation precursor equiv.)	Z (diene equiv.)	T_1 (°C)	T_2 (°C)	t (min)	Product yield
1	Bu_4NBF_4 (0.1 M)	1.0	1.5	−78	−78	60	55%
2	Bu_4NBF_4 (0.1 M)	1.0	1.5	−78	−70	60	50%
3	Bu_4NBF_4 (0.1 M)	1.0	1.5	−78	−65	60	45%
4	Bu_4NBF_4 (0.3 M)	1.0	3.0	−78	−78	60	34%
5	Bu_4NBF_4 (0.3 M)	2.0	1.0	−78	−78	60	50%
6	$Bu_4NB(C_6F_5)_4$ (0.1 M)	1.0	1.5	−78	−78	60	traces
7	$Bu_4NB(C_6F_5)_4$ (0.1 M)	1.0	1.5	−60	−60	60	traces

Yields determined by ^1H NMR with trichloroethene as internal standard.

4.2.2. Cation flow reactions – towards the optimization of multiple parameters

As our main goal was to achieve cyclization cascade and form polycyclic compounds, we have first turned to extensive optimization of cation flow conditions with the diene **4.7a**. Reaction time achieved by our flow setup usually spans from few seconds to one or two minutes, but rarely longer. Because we anticipated for this cyclization cascade to be rather challenging, we first tested the feasibility of this transformation in flow. To simplify the reaction setup, which is relatively complex (anhydrous conditions, electrochemical cell cooled to −78 °C, coordination of several syringe pumps, one or two mixing points), we initially opted out to quench the reaction mixture externally, with the addition of Et_3N after collection of the reaction mixture, with its exposure to atmospheric conditions for a short period of time. We have set our initial flow reaction conditions (flow rate, F/mol, electrolyte concentration and some other parameters - see experimental part for details) based on previous cation flow research [7]. We decided to start with stoichiometric ratio 1:1 of alkoxycarbenium species and the diene. We observed that reaction with quenching reagent Et_3N already present in the collecting flask at the time of collection, formed the target tricyclic product **4.8a** in 36% yield (Table 4.6, entry 1). When Et_3N was introduced just after collection (2 min), the yield was surprisingly increased and reached 58% (entry 2). With extended waiting time after collection and before addition of Et_3N (10 min or 60 min, entries 3–4) (reaction mixtures were kept at 0 °C), yields reached 42% and 34%, respectively. We concluded that sufficient amount of time is needed for the reaction to proceed, however, extended reaction times at elevated temperature probably made reactive intermediates to decompose. With higher temperature of cation formation and further reactions (−50 °C) we observed yields between 36% and 38%, regardless of the addition time (2 or 10 min) of Et_3N after collection of reaction mixture (entries 5–6).

In the next step we tested the influence of the flow rate – which also influences the cation generation time – to the reaction outcome (Table 4.7). We increased the amount of the diene to 1.5 equivalents based on alkoxycarbenium species. The initial time of cation generation was 4.8 s (entry 1), and was increased to 9.6 s (entry 2) and 24.0 s (entry 3). Obtained yields of the target tricyclic product **4.8a** were 46%, 43% and 30%, respectively. With these results in hand we concluded that extremely long generation times of cationic species (above 10 s) might be significantly decreasing the yield, which might also be a limitation of the flow setup – connection between the cell and further micromixing reactor is partially and briefly exposed to elevated temperature, which at lower flow rates (and higher generation times) causes faster decomposition of reactive intermediates. Compared to previous results, excess of diene was not beneficial to the reaction yield.

***Table 4.6**: Flow experiment with external quenching - screening of quenching conditions*

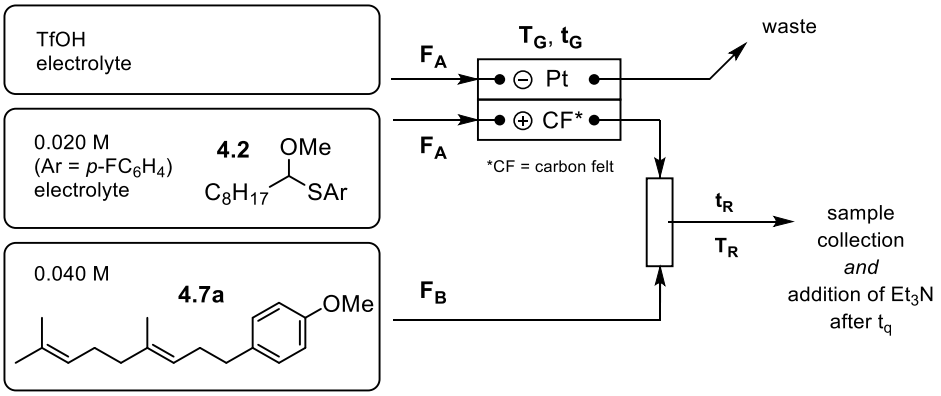

Entry	Electrolyte	F_A, F_B (mL/min)	$T_G = T_R$ (°C)	t_G (s)	t_R (s)	t_q (min)	Product 4.8a yield
1	Bu_4NBF_4 (0.3 M)	5.0, 2.5	−78	4.8	26.4	0	36%
2	Bu_4NBF_4 (0.3 M)	5.0, 2.5	−78	4.8	26.4	2	58%
3	Bu_4NBF_4 (0.3 M)	5.0, 2.5	−78	4.8	26.4	10	42%
4	Bu_4NBF_4 (0.3 M)	5.0, 2.5	−78	4.8	26.4	60	34%
5	Bu_4NBF_4 (0.3 M)	5.0, 2.5	−50	4.8	26.4	2	36%
6	Bu_4NBF_4 (0.3 M)	5.0, 2.5	−50	4.8	26.4	10	38%

Yields determined by ^{1}H NMR with trichloroethene as internal standard.

***Table 4.7**: Flow experiment with external quenching - screening of influence of flow rate*

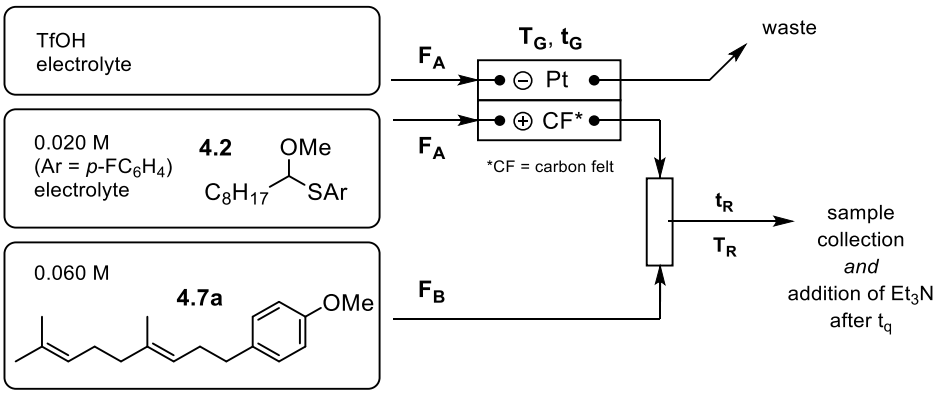

Entry	Electrolyte	F_A (mL/min)	F_B (mL/min)	$T_G = T_R$ (°C)	t_G (s)	t_R (s)	t_q (min)	Product 4.8a yield
1	Bu_4NBF_4 (0.3 M)	5.0	2.5	−78	4.8	26.4	2	46%
2	Bu_4NBF_4 (0.3 M)	2.5	1.25	−78	9.6	52.8	4	43%
3	Bu_4NBF_4 (0.3 M)	1.0	0.5	−78	24.0	131.9	8	30%

Yields determined by ^{1}H NMR with trichloroethene as internal standard.

Encouraged by results, we moved to the flow setup with internal introduction of Et_3N as a reaction quencher. We repeated the examination of the flow rate influence, this time with increased residence time and with stoichiometric ratio of 1:1.1 of alkoxycarbenium species and the diene, respectively. Results have shown that lower flow rate slightly increases the reaction yield (Table 4.8, entries 1–2). Previous experiments suggested that generation time does not have a big influence if it is in a range below 10 s, and we speculated that longer residence time (comparing 100.5 s, entry 2, versus 50.3 s, entry 1) might be slightly more beneficial for cyclization cascade to proceed to a higher extent (comparing product yields of 41% and 37%, respectively).

***Table 4.8**: Flow setup with internal quenching - flow rate screening*

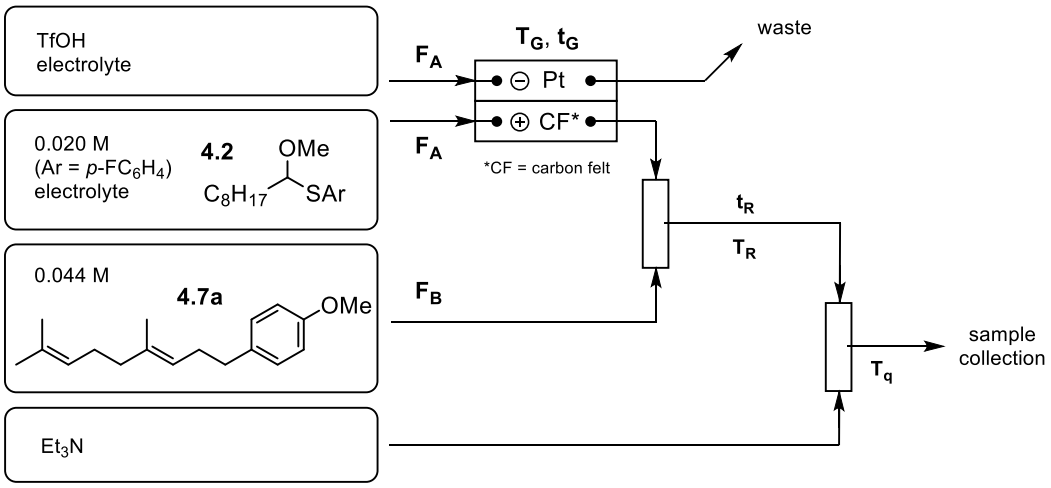

Entry	Electrolyte	F_A, F_B (mL/min)	$T_G = T_R = T_q$ (°C)	t_G (s)	t_R (s)	Product 4.8a yield
1	Bu_4NBF_4 (0.3 M)	5.0, 2.5	−78	4.8	50.3	37%
2	Bu_4NBF_4 (0.3 M)	2.5, 1.25	−78	9.6	100.5	41%

Yields determined by ^1H NMR with trichloroethene as internal standard.

When we examined the amount of electric charge transferred during anodic oxidation of thioacetal **4.2**, we observed that its higher excess (above the theoretical 1.0 F/mol) is not having a practical significance to the reaction yield which was in a range of 39–43% (Table 4.9, entries 1–4).

***Table 4.9**: Influence of F/mol amount (based on thioacetal)*

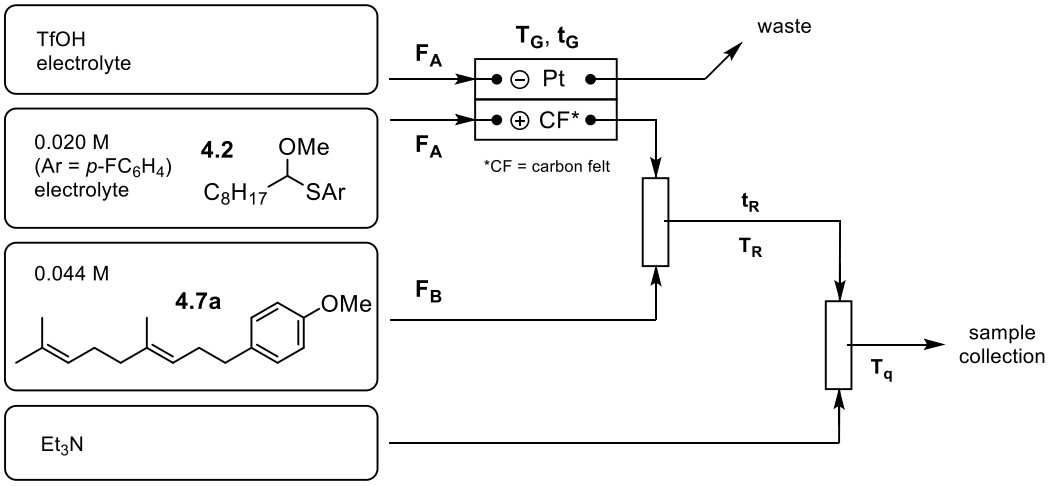

Entry	Electrolyte	F/mol (based on 4.2)	F_A, F_B (mL/min)	$T_G = T_R$ (°C)	t_G (s)	t_R (s)	Product 4.8a yield
1	Bu_4NBF_4 (0.3 M)	1.10	2.5, 1.25	−78	9.6	100.5	41%
2	Bu_4NBF_4 (0.3 M)	1.25	2.5, 1.25	−78	9.6	100.5	39%
3	Bu_4NBF_4 (0.3 M)	1.50	2.5, 1.25	−78	9.6	100.5	43%
4	Bu_4NBF_4 (0.3 M)	2.00	2.5, 1.25	−78	9.6	100.5	43%

Yields determined by ^{1}H NMR with trichloroethene as internal standard.

However, we were interested in changing the reaction conditions in such a way that the diene would be limiting reagent. Therefore, we were exposing the diene to different stoichiometric ratios of generated alkoxycarbenium species, namely, 1.0, 1.3, 1.5 and 2.0 equivalents (Table 4.10, entries 1–4, respectively). We observed that the reaction with 1:1 ratio reached 42% yield of the product **4.8a.** When the excess of alkoxycarbenium species was used, 1.5 equivalents of cationic species generated the highest (56%) yield of the tricyclic product **4.8a** (entry 3). The latter conditions were chosen to be used for further flow optimizations.

***Table 4.10**: Influence of excess of alkoxycarbenium species*

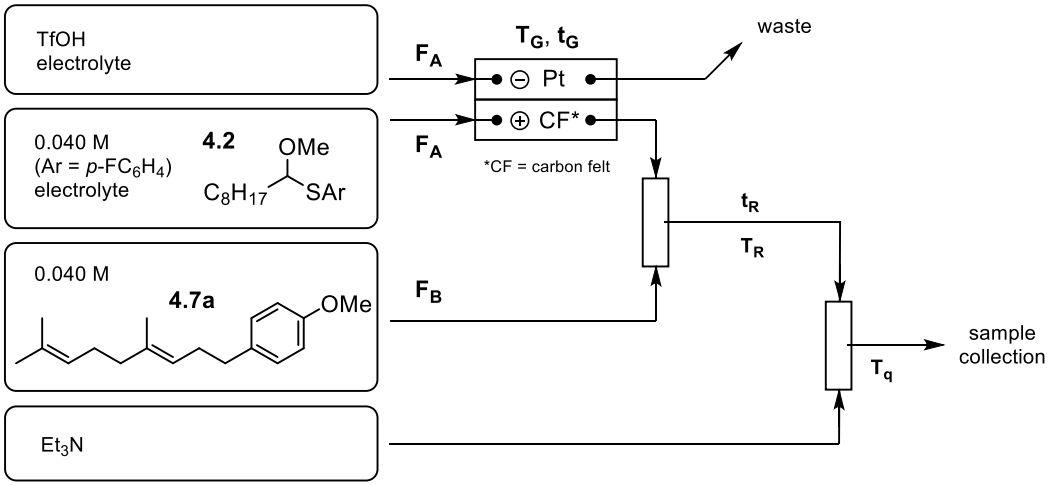

Entry	Electrolyte	Alkoxycarbenium (based on 4.7a)	F_A, F_B (mL/min)	$T_G = T_R$ (°C)	t_G (s)	t_R (s)	Product 4.8a yield
1	Bu_4NBF_4 (0.3 M)	1.0 equiv.	2.5, 1.25	−78	9.6	100.5	42%
2	Bu_4NBF_4 (0.3 M)	1.3 equiv.	2.5, 1.25	−78	9.6	100.5	52%
3	Bu_4NBF_4 (0.3 M)	1.5 equiv.	2.5, 1.25	−78	9.6	100.5	56%
4	Bu_4NBF_4 (0.3 M)	2.0 equiv.	2.5, 1.25	−78	9.6	100.5	53%

Yields determined by ^{1}H NMR with trichloroethene as internal standard.

With evaluation of the total reaction concentration (Table 4.11) we had in mind intramolecular cyclization cascade that benefits from lower reaction concentrations. On the other hand, the concentrations of the species must be sufficient to interact in the reaction mixture. And nonetheless, concentration might also influence the efficiency of the electrooxidation step. Therefore, we decided to decrease the total reaction concentration (of the cation precursor **4.2** and diene **4.7a**) to half (entry 1) and to increase it to double value (entry 3) compared to initial reaction concentration (entry 2). The concentration of the electrolyte has remained the same in all the experiments. We observed that both changes decreased the product yield of 56% achieved at initial conditions, and that higher reaction concentration decreased the yield more significantly. The effect of the concentration on the outcome is complex as it influences electrolysis efficiency, mixing of different species and their interaction, and possible intramolecular processes.

***Table 4.11**: Flow setting - influence of reaction concentration*

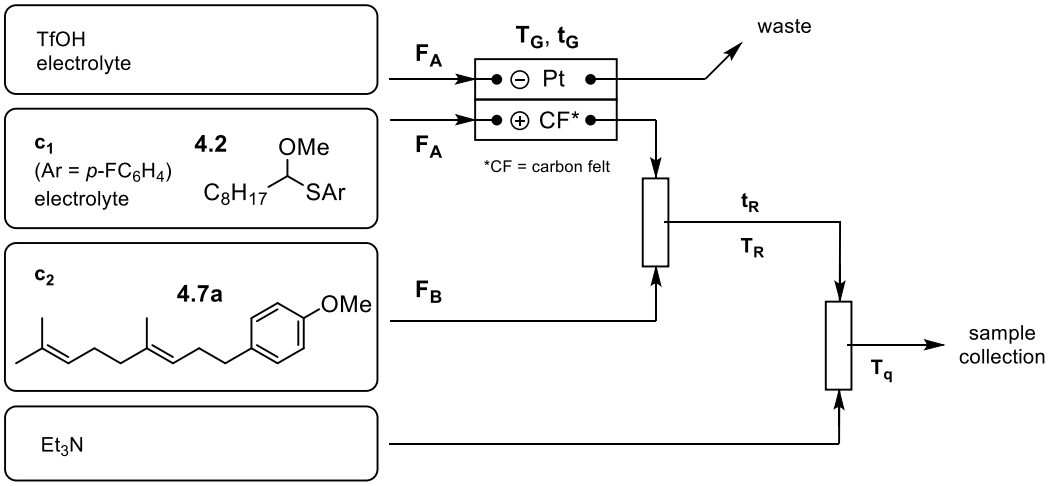

Entry	Electrolyte	$c_1 = c_2$ (M)	F_A, F_B (mL/min)	$T_G = T_R$ (°C)	t_G (s)	t_R (s)	Product 4.8a yield
1	Bu_4NBF_4 (0.3 M)	0.020	2.5, 1.25	−78	9.6	100.5	51%
2	Bu_4NBF_4 (0.3 M)	0.040	2.5, 1.25	−78	9.6	100.5	56%
3	Bu_4NBF_4 (0.3 M)	0.060	2.5, 1.25	−78	9.6	100.5	47%

Yields determined by ^{1}H NMR with trichloroethene as internal standard.

Since the cyclization cascade might be a stepwise process, we wanted to investigate if changing the reaction temperature, after the diene is mixed with cationic species, has any beneficial influence on the reaction outcome. We introduced a step temperature change in flow system and we were changing the point at the flow timeline where the temperature change occurred. In this way, after the initial mixing, the reaction mixture was exposed to two different temperatures (−78 °C and 0 °C) for different amounts of time but with the same total reaction time – the total residence time was slightly increased (to 106.8 s) (Table 4.12). With longer residence time and constant temperature of −78 °C, we achieved 58% yield of the tricyclic product **4.8a** (entry 1) – the highest yield reached in the flow setting. The first of applied modifications was to only quench the reaction mixture with Et_3N at higher temperature (entry 2) which has not changed the reaction yield. When the reaction mixture had a residence time of 56.6 s (t_{R1}) at −78 °C and 50.3 s (t_{R2}) at 0 °C the yield of the product (**4.8a**) slightly decreased to 54% (entry 3). With very short residence time at −78 °C (t_{R1} = 6.3 s) and long residence time at 0 °C (t_{R2} = 100.5 s) the yield of the product **4.8a** decreased significantly and reached 38% (entry 4). We concluded that higher reaction temperature is not providing better reaction outcome for this substrate.

***Table 4.12**: Flow setup - screening of reaction temperature conditions*

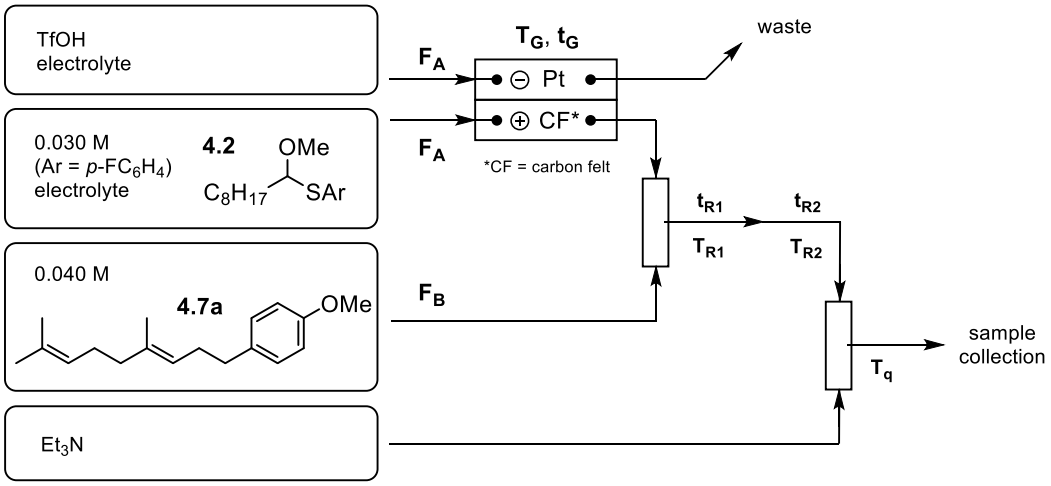

Entry	Electrolyte	t_G (s)	F_A, F_B (mL/min)	$T_G = T_{R1}$ (°C)	t_{R1} (s)	T_{R2} (°C)	t_{R2} (s)	T_q (°C)	Product 4.8a yield
1	Bu_4NBF_4 (0.3 M)	9.6	2.5, 1.25	−78	106.8	-	-	−78	58%
2	Bu_4NBF_4 (0.3 M)	9.6	2.5, 1.25	−78	106.8	-	-	0	58%
3	Bu_4NBF_4 (0.3 M)	9.6	2.5, 1.25	−78	56.6	0	50.3	0	54%
4	Bu_4NBF_4 (0.3 M)	9.6	2.5, 1.25	−78	6.3	0	100.5	0	38%

Yields determined by ^{1}H NMR with trichloroethene as internal standard.

Encouraged by the results achieved with electro-flow setup, we decided to explore the scope of this cyclization cascade with other substrates, using the best reaction conditions (Figure 4.3). The more electron rich substrate **4.7b**, bearing two methoxy substituents on the phenyl ring, gave a poor yield (21%) of the tricyclic product **4.8b**. The diene **4.7c**, with 3-methoxyphenyl group, gave a mixture of constitutional isomers **4.8c*o*** (30%) and **4.8c*p*** (14%) in combined yield of 44%. We were delighted to observe that the substrate **4.7d,** with plain phenyl group, gave the tricyclic product **4.8d** in 45% yield. When we subjected the substrate **4.9**, which has incorporated an oxygen linker between the phenyl group and the alkyl chain, we observed the unexpected fluorine-incorporated partially cyclized product **4.10** in 45% as the major product.

It is needed to mention that all the reaction mixtures of the cation pool and cation flow setup were rather complex which made evaluation of the mixtures difficult. We were able to isolate and identify the major products that were formed; however, some of the products might have been formed in much smaller quantities (compared to major products) and extremely difficult to isolate, therefore, they were not identified. The structural elucidation with different NMR techniques of all tricyclic products was not completely successful. We confirmed the identity of the frameworks of the products; however, it was not possible to determine the relative stereochemistry of the stereocenters due to a long alkyl chain (eight carbon atoms) that made signals in the ^{1}H NMR spectrum to heavily overlap. This resulted in unsuccessful solving of the

relative stereochemistry with NOESY experiments. Therefore, we proposed the relative stereochemistry of the groups (Me and H) at ring fusion as *trans*, which has strong support in literature when starting substrates are *E*-polyenes (see discussion in Chapter 1). Despite the difficulties with determination of stereochemistry of the products, we have observed, isolated, and identified single diastereoisomers as major products in all cyclization reactions.

***Figure 4.3**: Expanding substrate scope with flow setup*

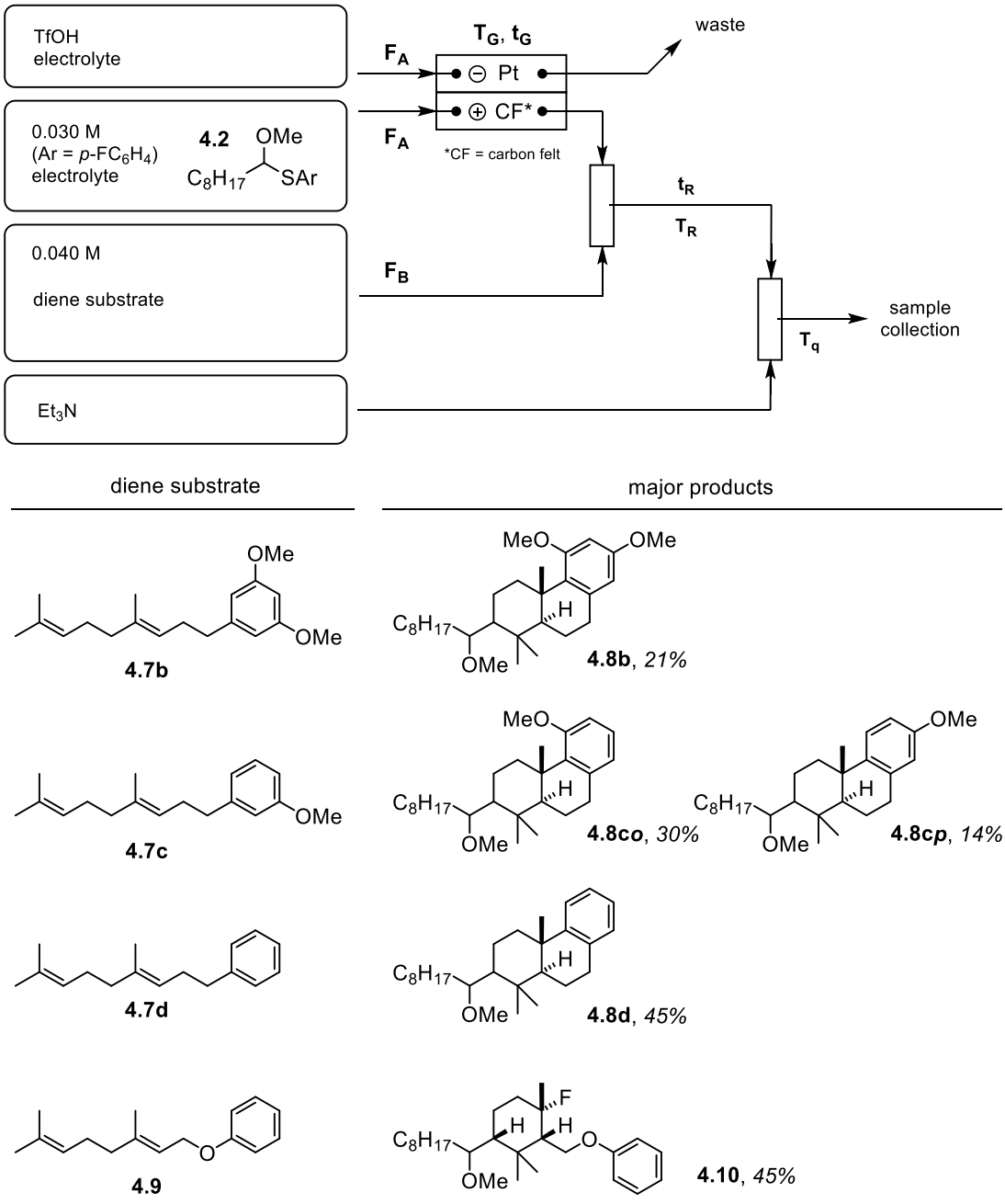

Electrolyte	t_G (s)	F_A, F_B (mL/min)	$T_G = T_R$ (°C)	T_q (°C)
Bu_4NBF_4 (0.3 M)	9.6	2.5, 1.25	−78	−78

Yields determined by ^{1}H NMR with trichloroethene as internal standard.

To complete the scope with the diene substrate **4.3**, we have done a brief screening of flow conditions with external an internal quenching. Reaction conditions, including flow rate, electrolyte and F/mol, were based on previous findings. We opted out for 1:1.5 stoichiometric ratio of alkoxycarbenium to diene **4.3**. With the first set of experiments, we were testing how quenching time (addition of Et_3N) influences the reaction outcome when quenching is external. We have observed that quenching at the time when reaction solution is being collected, formed the target cyclic product **4.4** in 32% yield with side product **4.5** in 6% (Table 4.13, entry 1). When Et_3N was introduced just after collection (4 min), after 10 min or after 60 min (entries 2–4, respectively), the yields of product **4.4** were in the range of 35–38% and the side product was formed in 11–13%. However, when the electrolyte concentration was decreased, the yields have been reduced by half (entry 5, compared to entry 3).

Table 4.13**: Flow experiment with external quenching - screening of quenching conditions, substrate **4.3

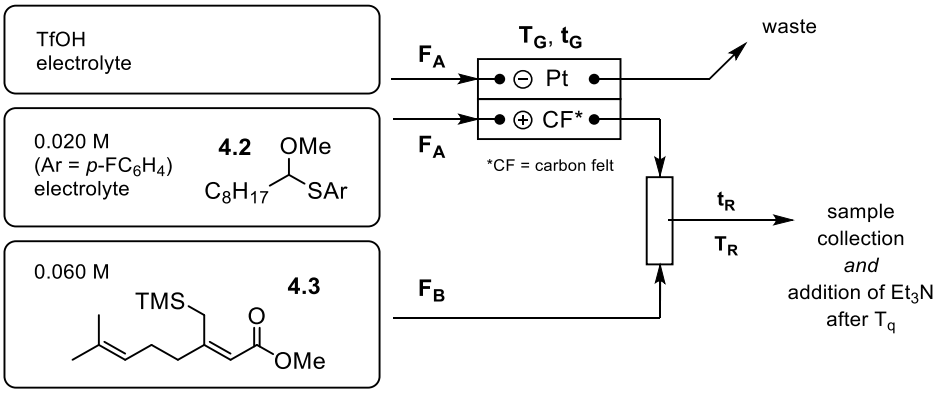

Entry	Electrolyte	F_A, F_B (mL/min)	T_R (°C)	t_G (s)	t_R (s)	t_q (min)	Product 4.4 yield	Side product 4.5 yield
1	Bu_4NBF_4 (0.3 M)	2.5, 1.25	−78	9.6	52.8	0	32%	6%
2	Bu_4NBF_4 (0.3 M)	2.5, 1.25	−78	9.6	52.8	4	36%	13%
3	Bu_4NBF_4 (0.3 M)	2.5, 1.25	−78	9.6	52.8	10	38%	13%
4	Bu_4NBF_4 (0.3 M)	2.5, 1.25	−78	9.6	52.8	60	35%	11%
5	Bu_4NBF_4 (0.1 M)	2.5, 1.25	−78	9.6	52.8	10	18%	5%

Yields determined by ^1H NMR with trichloroethene as internal standard.

In the flow setting with internal quenching, we decided to screen the stoichiometric ratios of alkoxycarbenium species and diene **4.3**. We have observed that regardless of given stoichiometry between species (Table 4.14), the reaction outcome was similar in terms of product **4.4** yield (37–38%) when the alkoxycarbenium species was a limiting reagent. However, when the limiting reagent was diene 4.3 (entry 3), the yield of the product **4.4** increased to 50% together with 10% of side product **4.5**.

Table 4.14**: Flow setup – screening of stoichiometry ratios - substrate **4.3

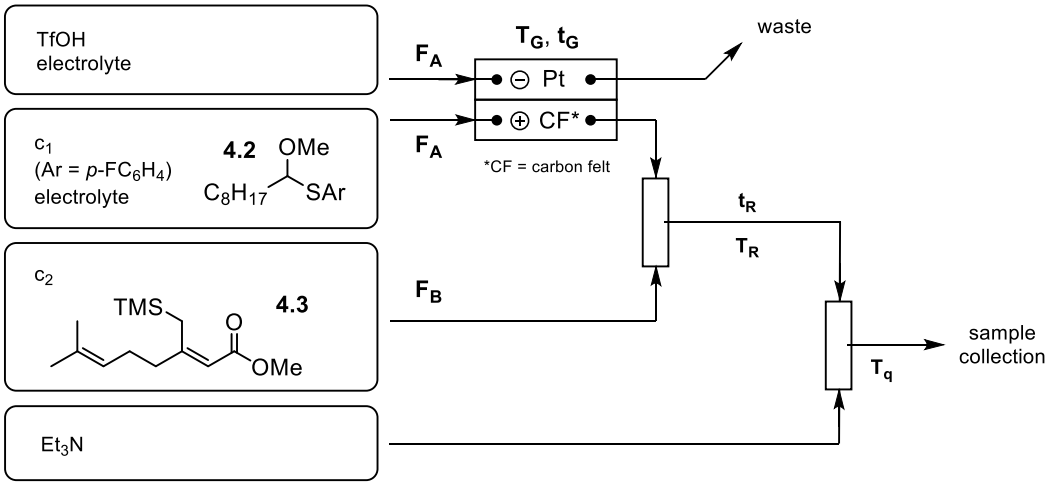

Entry	Electrolyte	n(alkoxycarbenium)/ n(diene 4.3)	F_A, F_B (mL/min)	T_R (°C)	t_G (s)	T_q (°C)	t_R (s)	Product 4.4 yield	Side product 4.5 yield
1	Bu_4NBF_4 (0.3 M)	1.0 / 1.5	2.5, 1.25	−78	9.6	−78	106.8	37%	5%
2	Bu_4NBF_4 (0.3 M)	1.0 / 1.0	2.5, 1.25	−78	9.6	−78	106.8	38%	9%
3	Bu_4NBF_4 (0.3 M)	1.5 / 1.0	2.5, 1.25	−78	9.6	−78	106.8	50%	10%

Yields determined by ^{1}H NMR with trichloroethene as internal standard.

Lastly, we investigated a step temperature change after the initial mixing. The reaction mixture was exposed to two different temperatures (−78 °C and 0 °C) for different amounts of time, with the same total reaction time – the total residence time was 106.8 s (Table 4.15). With longer residence time and constant temperature of −78 °C, we achieved 50% yield of product **4.4** (entry 1). When a higher temperature was introduced to the reaction mixture only at the quenching step, the reaction yield slightly increased (entry 2). If the reaction mixture was exposed to −78 °C for 56.6 s (t_{R1}) and to 0 °C for 50.3 s (t_{R2}), the yield of the product **4.4** reached maximum value of 54% together with 16% of a side product **4.5** (entry 3). With very short residence time (t_{R1} = 6.3 s) at −78 °C and long residence time (t_{R2} = 100.5 s) at 0 °C, the yield of the product **4.4** decreased significantly and reached 20% (entry 4). We concluded that for substrate **4.3** higher reaction temperature might be beneficial to some extent.

Table 4.15**: Flow setup - screening of reaction temperature - substrate **4.3

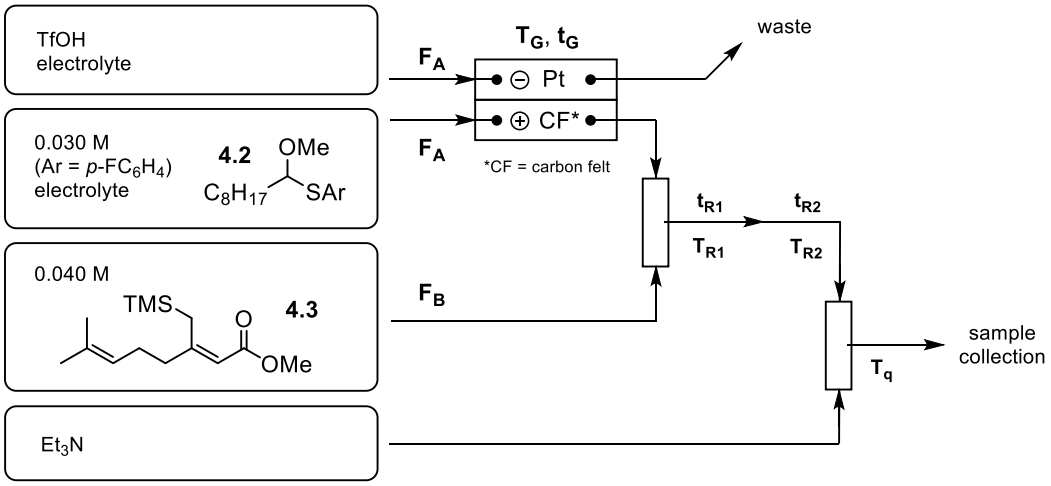

Entry	Electrolyte	F_A, F_B (mL/min)	t_G (s)	$T_G = T_{R1}$ (°C)	t_{R1} (s)	T_{R2} (°C)	t_{R1} (s)	T_q (°C)	Product 4.4 yield	Side product 4.5 yield
1	Bu_4NBF_4 (0.3 M)	2.5, 1.25	9.6	−78	106.8	-	-	−78	50%	10%
2	Bu_4NBF_4 (0.3 M)	2.5, 1.25	9.6	−78	106.8	-	-	0	52%	14%
3	Bu_4NBF_4 (0.3 M)	2.5, 1.25	9.6	−78	56.6	0	50.3	0	54%	16%
4	Bu_4NBF_4 (0.3 M)	2.5, 1.25	9.6	−78	6.3	0	100.5	0	20%	13%

Yields determined by ^{1}H NMR with trichloroethene as internal standard.

4.3. Conclusions

In this chapter we have shown that electrochemically generated short-lived alkoxycarbenium species (stabilized carbocations) are able to participate in cyclization (cascade) reactions of (poly)olefins with allylsilane or aryl termini. We have used two strategies of electrochemical production of cationic species. With cation pool method we electrochemically generated reactive species in direct or indirect way and accumulated them until the electrochemical step was finished, and only then further diene substrates have been introduced. In contrast, with cation flow method, reactive species were continuously and rapidly formed in flow and were further reacted with diene substrates.

We have chosen diene with allylsilane moiety as initial substrate for condition screening. With the indirect cation pool method, we observed that reaction temperature of −78 °C is needed for the best survival of reactive species and that Bu_4NBF_4 is superior electrolyte for these transformations compared to $Bu_4NB(C_6F_5)_4$ and Bu_4NOTf. With direct cation pool we have observed that higher excess of the diene is decreasing the product yields and that higher electrolyte concentration in some cases helps to increase the product yields. Moreover, we were pleased to see that diene can also be used as a limiting reagent. When we moved to extensive optimization of cation flow method, we came to several general conclusions: 1) low temperature (−78 °C) being necessary at cation generation step and at the cyclization step; 2) appropriate flow rate ensures good formation of short-lived carbocationic species and their survival, and influences the residence time which has to be long enough for cyclization cascade to proceed to the final product.

In conclusion, after screening of reaction parameters for cation pool and cation flow setups, we have proved that with cation flow method we could prepare several (poly)cyclic products in sufficient to good yields, considering how challenging this transformation might be. Despite a variety of side products formed in low quantities, we isolated major products. Nonetheless, we have observed that cation flow offers a rapid and continuous cation formation (scalability), offers better control over mixing of reactants which minimizes side reactivity and increases the reproducibility of the process.

4.4. Experimental section

4.4.1. General experimental

Dry tetrahydrofuran, diethyl ether, dichloromethane and hexane were purchased from Kanto Chemical Co., Inc. or Fujifilm Wako Pure Chemicals and used without further purification. Other solvents were purchased from commercial sources, unless otherwise stated. All solution preparations and reactions were carried out in a flame-dried glassware under argon atmosphere using anhydrous solvents, unless otherwise noted.

Flash chromatography was carried out on a silica gel (Kanto Chem. Co., Silica Gel N, spherical, neutral, 40–100 μm). TLC analyses were performed on Merck pre-coated silica gel F254 plates (thickness 0.25 mm). Visualization of spots was done by UV light (254 nm) or with anisaldehyde visualization stain (3.7 mL *p*-anisaldehyde, 135 mL absolute ethanol, 5 mL conc. sulfuric acid, 1.5 mL glacial acetic acid).

Stainless steel T-shaped micromixers (inner diameters of 500 μm or 1000 μm) were manufactured by Sanko Seiki Co., Inc (SUS304). Stainless steel microtube reactors (inner diameter of 1000 μm) (SUS316) were purchased from GL Sciences. The micromixers and microtube reactors were connected with stainless steel fittings (GL Sciences, 1/16 OUW). PTFE tubes (inner diameter of 1000 μm) was purchased from ISIS Co., Ltd. The syringe pumps (Harvard Model PHD ULTRA) equipped with gastight syringes (purchased from SGE) were used for introduction of the solutions into the microreactor systems via stainless steel fittings (GL Sciences, 1/16 OUW).

The divided electrochemical flow reactor consists of stainless-steel chambers and PTFE plates, (manufactured at DFC Co., Ltd). Carbon felt for anode (GF-20-P7) was purchased from Nippon Carbon Co., Ltd. and dried at 110 °C for 24 h before use. Pt plate for cathode was purchased from Nilaco Co., Ltd. and its surface was roughened to increase the surface area. Glass filter (Whatman, GF/A) and PTFE membrane (Millipore, pore size is 0.2 μm) for filtration were purchased from commercial suppliers and cut before use. Peltier cooling system was purchased from DFC Co., Ltd.

A Kikusui PMC350-0.2A was used as a direct current power supply for the electrolysis. The flow microreactor system was immersed in a cold cry ice and acetone bath to control the temperature. Solutions were continuously introduced to the flow microreactor system using syringe pumps (Harvard PHD2000), equipped with gastight syringes purchased from SGE. All reactions were carried out under an atmosphere of argon.

GPC separations were performed on Japan Analytical Industry Co., Ltd LC-9201, with recycling mode.

NMR spectra were recorded on JEOL JNM-ECZ400S spectrometer: ^{1}H spectra at 400 MHz, using Me_4Si as an internal standard; ^{13}C at 100 MHz, using $CHCl_3$ in $CDCl_3$ as a standard; ^{19}F at 376 MHz, using NaOTf (−78.8 ppm) in CD_2Cl_2 as an external standard. NMR yields were calculated by ^{1}H NMR analyses with 10 s relaxation delay (d1) using trichloroethene as an internal standard.

High-resolution mass spectra (HRMS) were measured by Instrumental Analysis Service at Hokkaido University.

4.4.2. Cation pool reactions and optimization of parameters

Cation pool reactions were conducted in glass H-type divided electrochemical cell with effective compartment (half-cell) size of 10 mL. Prior to experiment execution, electrochemical cell was assembled with Pt cathode and carbon felt anode, sealed, and dried with heat source under high vacuum. After it was cooled down to room temperature, the system was refilled with argon and solution of electrolyte (10 mL) was added to each of the cell compartments. Appropriate amounts of cation precursors have been added to anodic compartment and TfOH has been added to cathodic compartment. Reactions have been performed with 0.16 mmol of corresponding dienes. Both compartments were submerged to acetone/dry ice cooling bath to achieve and maintain appropriate reaction temperature. Constant current electrolysis has been started and finished, after the amount of time has passed needed to achieve the desired current applied to the system, followed by addition of substrate (or substrates) in stated order. After the final reaction time, reaction was quenched by addition of Et_3N (0.2 mL) to each of the cell compartments, kept stirring at final reaction temperature for 15 min and then warmed to room temperature. Obtained anodic solution was transferred to a flask and solvent was removed under reduced pressure. The remaining mixture was passed through a short silica pad with 1:1 mixture of *n*-hexane and ethyl acetate to remove the electrolyte. After evaporation of the solvents, NMR samples were prepared using trichloroethene as internal standard. Isolation of the analytically pure products has been executed in two steps. First with flash chromatography (*n*-hexane and ethyl acetate elution mixture) and in the second step with recycling GPC (gel permeation chromatography) with chloroform as a solvent.

4.4.2.1. Indirect cation pool - optimization of reaction conditions with substrate 4.3

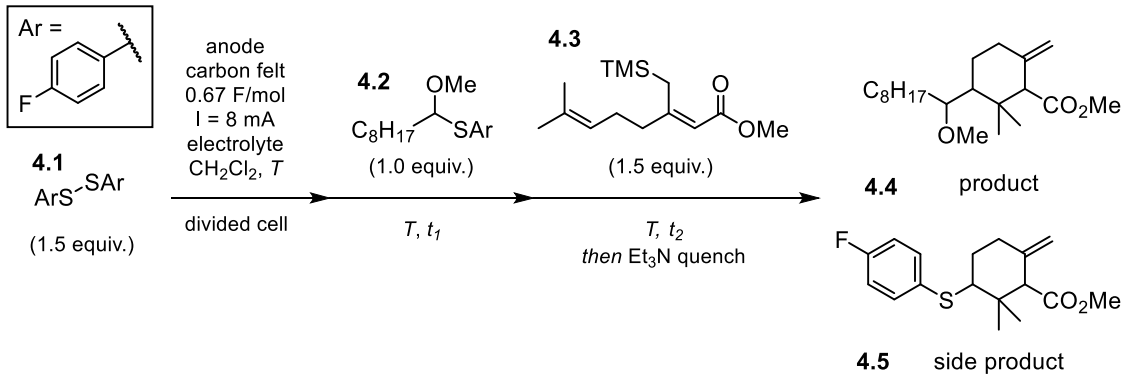

entry	Electrolyte	T (°C)	t_1 (min)	t_2 (min)	Product yield	Side product yield
1	Bu_4NBF_4 (0.1 M)	−78	10	60	34%	14%
2	Bu_4NBF_4 (0.1 M)	−50	10	60	28%	31%
3	$Bu_4NB(C_6F_5)_4$ (0.1 M)	−78	10	60	15%	35%
4	$Bu_4NB(C_6F_5)_4$ (0.1 M)	−50	10	60	8%	37%
5	Bu_4NOTf (0.1 M)	−78	10	60	4%	Not observed
6	Bu_4NOTf (0.1 M)	−50	10	60	8%	Not observed

Yields are based on ^1H NMR with trichloroethene as internal standard.

4.4.2.2. Direct cation pool - optimization of reaction conditions with substrate 4.3

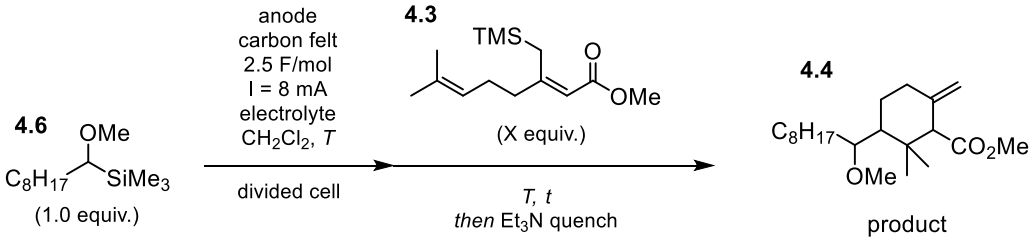

entry	Electrolyte	X (diene equiv.)	T (°C)	t (min)	Product yield
1	Bu_4NBF_4 (0.1 M)	1.5	−78	60	30%
2	Bu_4NBF_4 (0.3 M)	1.5	−78	60	32%
3	$Bu_4N\ BF_4$ (0.1 M)	3.0	−78	60	20%
4	$Bu_4N\ BF_4$ (0.3 M)	3.0	−78	60	16%

Yields are based on ^1H NMR with trichloroethene as internal standard.

4.4.2.3. Direct cation pool - optimization of reaction conditions with substrate 4.3

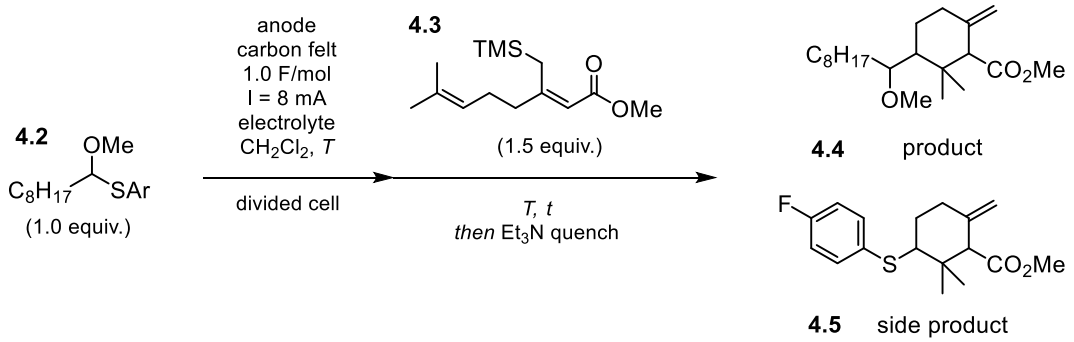

entry	Electrolyte	T (°C)	t (min)	Product yield	Side product yield
1	Bu_4NBF_4 (0.1 M)	−78 °C	60	27%	5%
2	Bu_4NBF_4 (0.3 M)	−78 °C	60	35%	16%

Yields are based on ^{1}H NMR with trichloroethene as internal standard.

4.4.2.4. Indirect cation pool - optimization of reaction conditions with substrate 4.7a

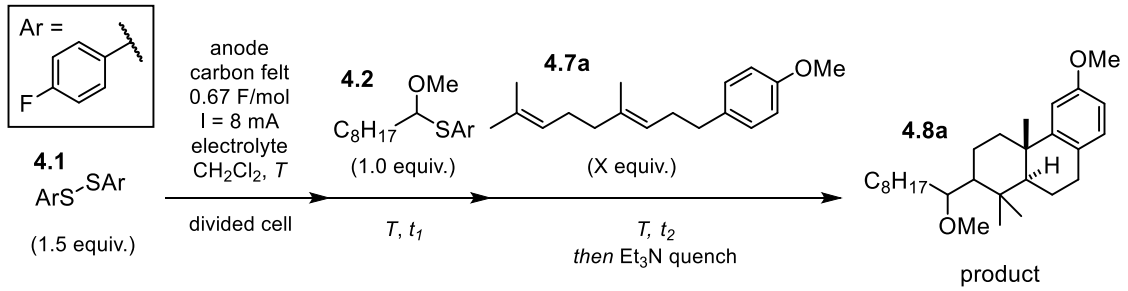

entry	Electrolyte	X (diene equiv.)	T (°C)	t_1 (min)	t_2 (min)	Product yield
1	Bu_4NBF_4 (0.1 M)	1.5	−78	15	60	54%
2	Bu_4NBF_4 (0.3 M)	1.5	−78	15	60	45%
3	Bu_4NBF_4 (0.1 M)	3.0	−78	15	60	55%
4	Bu_4NBF_4 (0.3 M)	1.5	−78	15	10	33%

Yields are based on ^{1}H NMR with trichloroethene as internal standard.

4.4.2.5. Direct cation pool - optimization of reaction conditions with substrate 4.7a

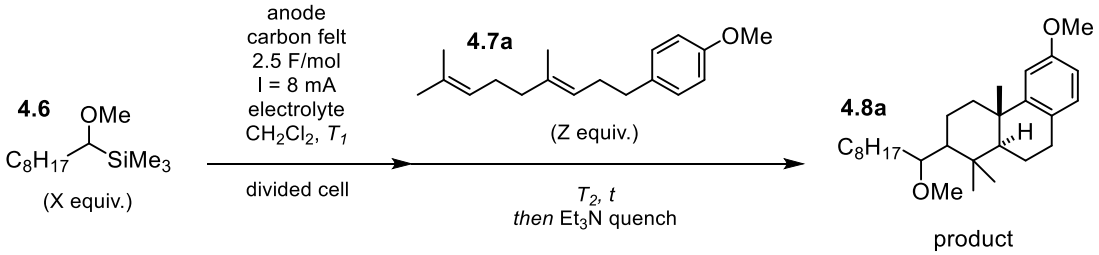

Entry	Electrolyte	X (silyl ether equiv.)	Z (diene equiv.)	T_1 (°C)	T_2 (°C)	t (min)	Product yield
1	Bu_4NBF_4 (0.1 M)	1.0	1.5	−78	−78	60	55%
2	Bu_4NBF_4 (0.1 M)	1.0	1.5	−78	−78	60	50%
3	Bu_4NBF_4 (0.1 M)	1.0	1.5	−78	−70	60	45%
4	Bu_4NBF_4 (0.3 M)	1.0	3.0	−78	−65	60	34%
5	Bu_4NBF_4 (0.3 M)	2.0	1.0	−78	−78	60	50%
6	$Bu_4NB(C_6F_5)_4$ (0.1 M)	1.0	1.5	−78	−78	60	traces
7	$Bu_4NB(C_6F_5)_4$ (0.1 M)	1.0	1.5	−60	−60	60	traces

Yields are based on ^1H NMR with trichloroethene as internal standard.

4.4.3. Cation flow reactions and optimizations of parameters

Cation flow solutions of reactants were prepared in flame-dried flasks under argon with anhydrous solvents. Syringes were filled with corresponding solutions and their introduction to reaction system in constant flow mode was achieved by syringe pumps. Electrochemical cell was cooled with Peltier cooling system and further flow reactors were submerged in dry ice/acetone bath with appropriate temperature. Before the collection of the reaction mixtures, systems have been equilibrated. Obtained solutions were transferred to flasks and solvents were evaporated at reduced pressure. The remaining mixtures were passed through a short silica pad with 1:1 mixture of *n*-hexane and ethyl acetate to remove the electrolyte. After evaporation of the solvents, NMR samples were prepared using trichloroethene as internal standard. Isolation of the analytically pure products has been executed in two steps. First with flash chromatography (*n*-hexane and ethyl acetate elution mixture) and in the second step with recycling GPC (gel permeation chromatography) with chloroform as a solvent.

4.4.3.1. Flow experiment with external quenching - screening of quenching conditions

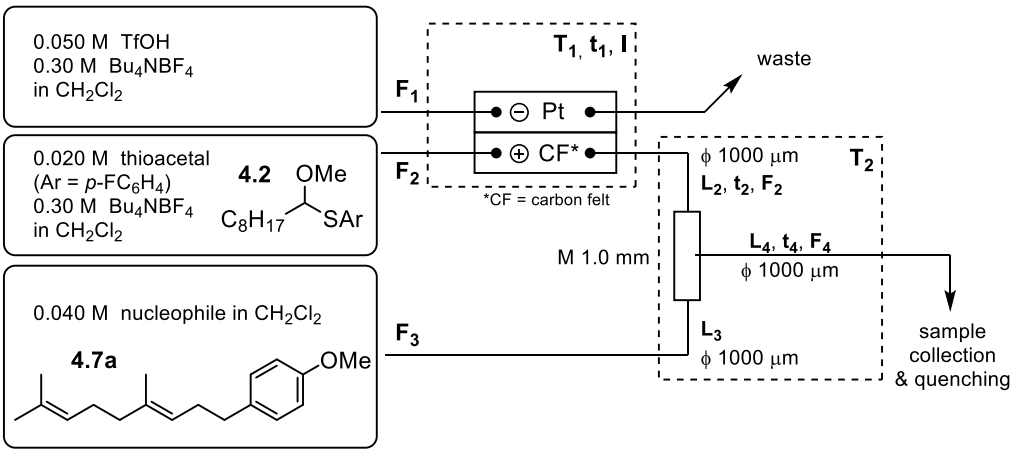

alkoxycarbenium / nucleophile = 1:1

T_1 = –78 °C	F_1 = 5.0 mL/min	t_1 = 4.8 s	.
T_2 = –78 °C	F_2 = 5.0 mL/min	t_2 = 20.7 s	L_2 = 220 cm
	F_3 = 2.5 mL/min	.	L_3 = 200 cm
I = 200 mA	F_4 = 7.5 mL/min	t_4 = 26.4 s	L_4 = 420 cm
(1.25 F/mol)			

Equilibration time 2.5 min, collection time 2.0 min

T_1 = –50 °C	F_1 = 5.0 mL/min	t_1 = 4.8 s	.
T_2 = –50 °C	F_2 = 5.0 mL/min	t_2 = 20.7 s	L_2 = 220 cm
	F_3 = 2.5 mL/min	.	L_3 = 200 cm
I = 200 mA	F_4 = 7.5 mL/min	t_4 = 26.4 s	L_4 = 420 cm
(1.25 F/mol)			

Equilibration time 2.5 min, collection time 2.0 min

Entry	Electrolyte	F_1=F_2 (mL/min)	F_3 (mL/min)	T_1 = T_2 (°C)	t_1 (s)	t_4 (s)	t_q (min)	Product 4.8a yield
1	Bu_4NBF_4 (0.3 M)	5.0	2.5	−78	4.8	26.4	0	36%
2	Bu_4NBF_4 (0.3 M)	5.0	2.5	−78	4.8	26.4	2	58%
3	Bu_4NBF_4 (0.3 M)	5.0	2.5	−78	4.8	26.4	10	42%
4	Bu_4NBF_4 (0.3 M)	5.0	2.5	−78	4.8	26.4	60	34%
5	Bu_4NBF_4 (0.3 M)	5.0	2.5	−50	4.8	26.4	2	36%
6	Bu_4NBF_4 (0.3 M)	5.0	2.5	−50	4.8	26.4	10	38%

Yields are based on ^{1}H NMR with trichloroethene as internal standard.

4.4.3.2. Flow experiment with external quenching - screening of influence of flow rate

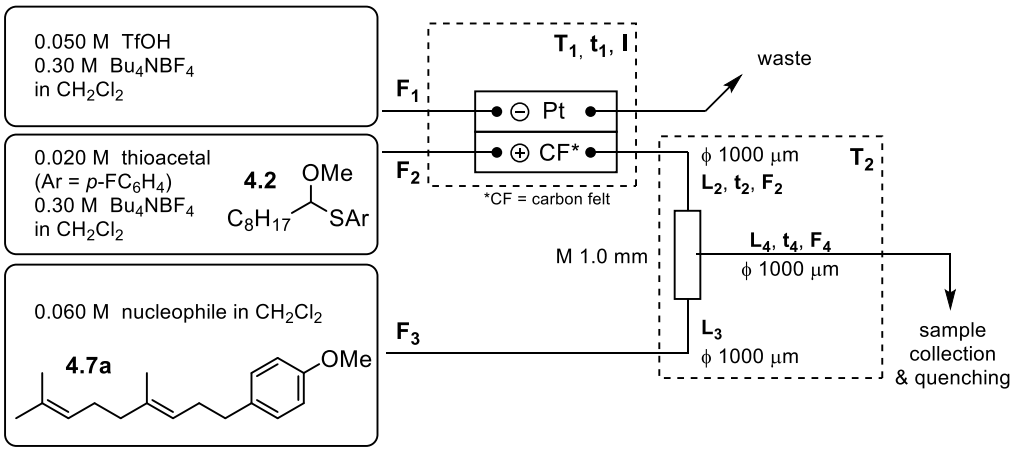

alkoxycarbenium / nucleophile = 1:1.5

T_1 = –78 °C T_2 = –78 °C I = 200 mA (1.25 F/mol) (U = ~12V)	F_1 = 5.0 mL/min F_2 = 5.0 mL/min F_3 = 2.5 mL/min F_4 = 7.5 mL/min	t_1 = 4.8 s t_2 = 20.7 s . t_4 = 26.4 s	. L_2 = 220 cm L_3 = 200 cm L_4 = 420 cm
Equilibration time 2.5 min, collection time 2.0 min			
T_1 = –78 °C T_2 = –78 °C I = 100 mA (1.25 F/mol) (U = ~8V)	F_1 = 2.5 mL/min F_2 = 2.5 mL/min F_3 = 1.25 mL/min F_4 = 3.75 mL/min	t_1 = 9.6 s t_2 = 41.5 s . t_4 = 52.8 s	. L_2 = 220 cm L_3 = 200 cm L_4 = 420 cm
Equilibration time 5.0 min, collection time 4.0 min			
T_1 = –78 °C T_2 = –78 °C I = 40 mA (1.25 F/mol) (U = ~6V)	F_1 = 1.0 mL/min F_2 = 1.0 mL/min F_3 = 0.5 mL/min F_4 = 1.5 mL/min	t_1 = 24.0 s t_2 = 103.7 s . t_4 = 131.9 s	. L_2 = 220 cm L_3 = 200 cm L_4 = 420 cm
Equilibration time 10.0 min, collection time 8.0 min			

Entry	Electrolyte	F_1=F_2 (mL/min)	F_3 (mL/min)	T_1 = T_2 (°C)	t_1 (s)	t_4 (s)	t_q (min)	Product 4.8a yield
1	Bu_4NBF_4 (0.3 M)	5.0	2.5	−78	4.8	26.4	2	46%
2	Bu_4NBF_4 (0.3 M)	2.5	1.25	−78	9.6	52.8	4	43%
3	Bu_4NBF_4 (0.3 M)	1.0	0.5	−78	24.0	131.9	8	30%

Yields are based on ^{1}H NMR with trichloroethene as internal standard.

4.4.3.3. Flow setup with internal quenching - flow rate screening - substrate 4.7a

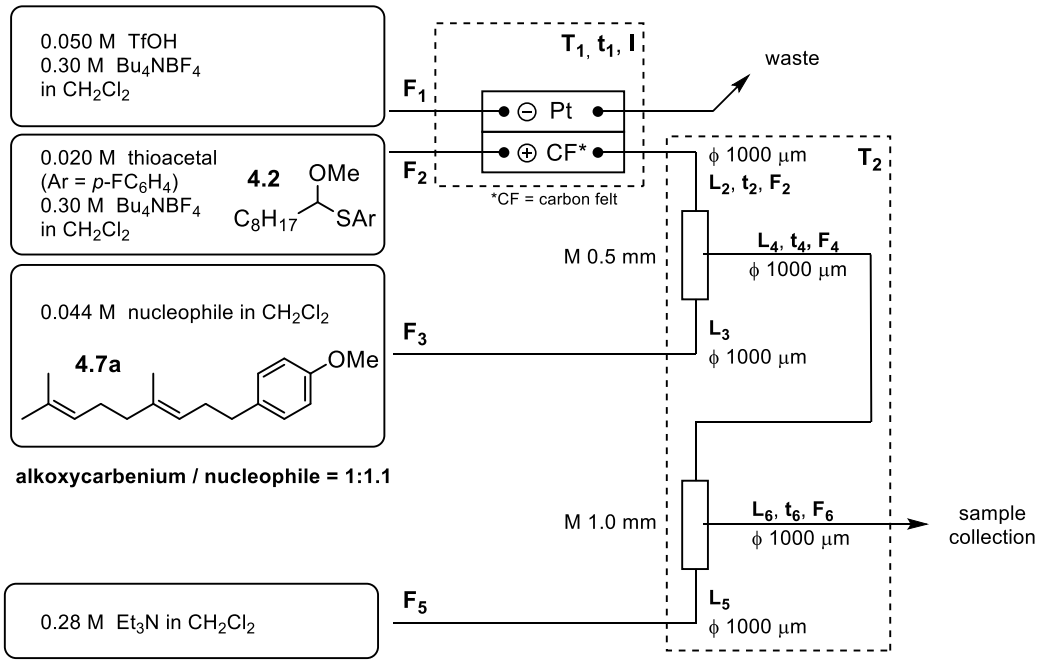

T_1 = –78 °C	F_1 = 5.0 mL/min	t_1 = 4.8 s	.	
T_2 = –78 °C	F_2 = 5.0 mL/min	t_2 = 20.7 s	L_2 = 220 cm	
	F_3 = 2.5 mL/min	.	L_3 = 200 cm	
I = 200 mA	F_4 = 7.5 mL/min	t_4 = 50.3 s	L_4 = 800 cm	
(1.25 F/mol)	F_5 = 2.5 mL/min	.	L_5 = 200 cm	
(U = ~12V)	F_6 = 10.0 mL/min	t_6 = 0.9 s	L_6 = 20 cm	

Equilibration time 2.5 min, collection time 2.0 min

T_1 = –78 °C	F_1 = 2.5 mL/min	t_1 = 9.6 s	.	
T_2 = –78 °C	F_2 = 2.5 mL/min	t_2 = 41.5 s	L_2 = 220 cm	
	F_3 = 1.25 mL/min	.	L_3 = 200 cm	
I = 100 mA	F_4 = 3.75 mL/min	t_4 = 100.5 s	L_4 = 800 cm	
(1.25 F/mol)	F_5 = 1.25 mL/min	.	L_5 = 200 cm	
(U = ~11V)	F_6 = 5.0 mL/min	t_6 = 1.9 s	L_6 = 20 cm	

Equilibration time 5.0 min, collection time 4.0 min

Entry	Electrolyte	F_1=F_2 (mL/min)	F_3 (mL/min)	T_1 = T_2 = T_q (°C)	t_1 (s)	t_4 (s)	Product 4.8a yield
1	Bu_4NBF_4 (0.3 M)	5.0	2.5	−78	4.8	50.3	37%
2	Bu_4NBF_4 (0.3 M)	2.5	1.25	−78	9.6	100.5	41%

Yields are based on ^{1}H NMR with trichloroethene as internal standard.

4.4.3.4. Influence of F/mol (based on thioacetal 4.2) - screening

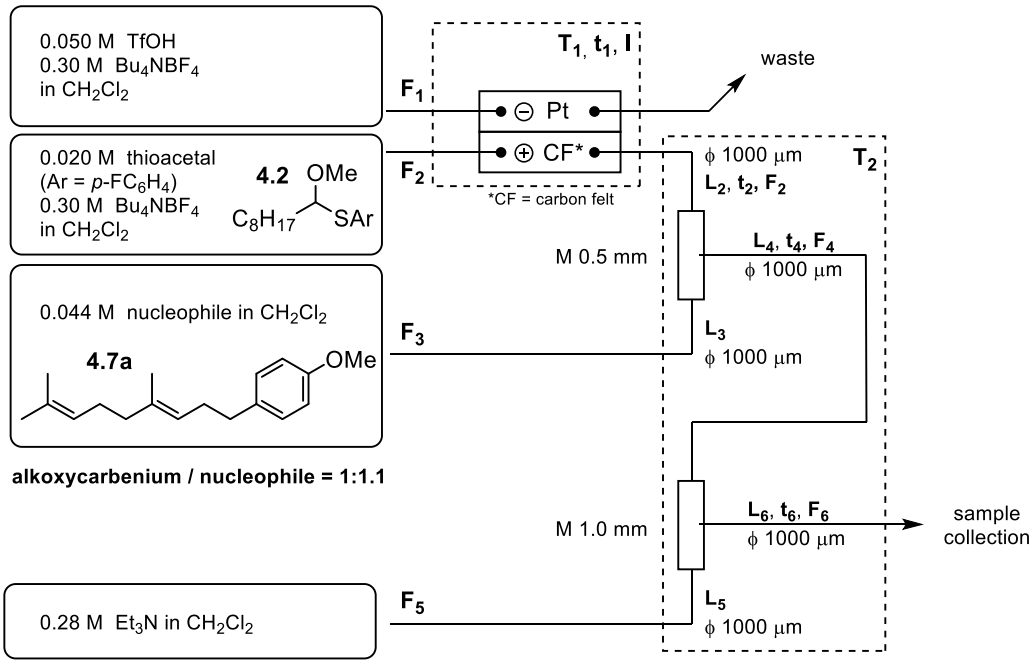

T_1 = –78 °C	F_1 = 2.5 mL/min	t_1 = 9.6 s	.	L_2 = 220 cm
T_2 = –78 °C	F_2 = 2.5 mL/min	t_2 = 41.5 s	.	L_3 = 200 cm
	F_3 = 1.25 mL/min	.	t_4 = 100.5 s	L_4 = 800 cm
	F_4 = 3.75 mL/min	t_4 = 100.5 s	.	L_5 = 200 cm
	F_5 = 1.25 mL/min	.	t_6 = 1.9 s	L_6 = 20 cm
	F_6 = 5.0 mL/min	t_6 = 1.9 s		

Equilibration time 5.0 min, collection time 4.0 min

Variation between experiments:
F/mol based on thioacetal

1) 1.10 F/mol, I = 88 mA (U = 8 V)
2) 1.25 F/mol, I = 100 mA (U = 9 V)
3) 1.50 F/mol, I = 120 mA (U = 11 V)
4) 2.00 F/mol, I = 160 mA (U = 13 V)

Entry	Electrolyte	F/mol (based on 4.2)	F_1=F_2, F_3 (mL/min)	T_1 = T_2 (°C)	t_1 (s)	t_4 (s)	Product 4.8a yield
1	Bu_4NBF_4 (0.3 M)	1.10	2.5, 1.25	−78	9.6	100.5	41%
2	Bu_4NBF_4 (0.3 M)	1.25	2.5, 1.25	−78	9.6	100.5	39%
3	Bu_4NBF_4 (0.3 M)	1.50	2.5, 1.25	−78	9.6	100.5	43%
4	Bu_4NBF_4 (0.3 M)	2.00	2.5, 1.25	−78	9.6	100.5	43%

Yields are based on ^{1}H NMR with trichloroethene as internal standard.

4.4.3.5. Influence of excess of alkoxycarbenium species

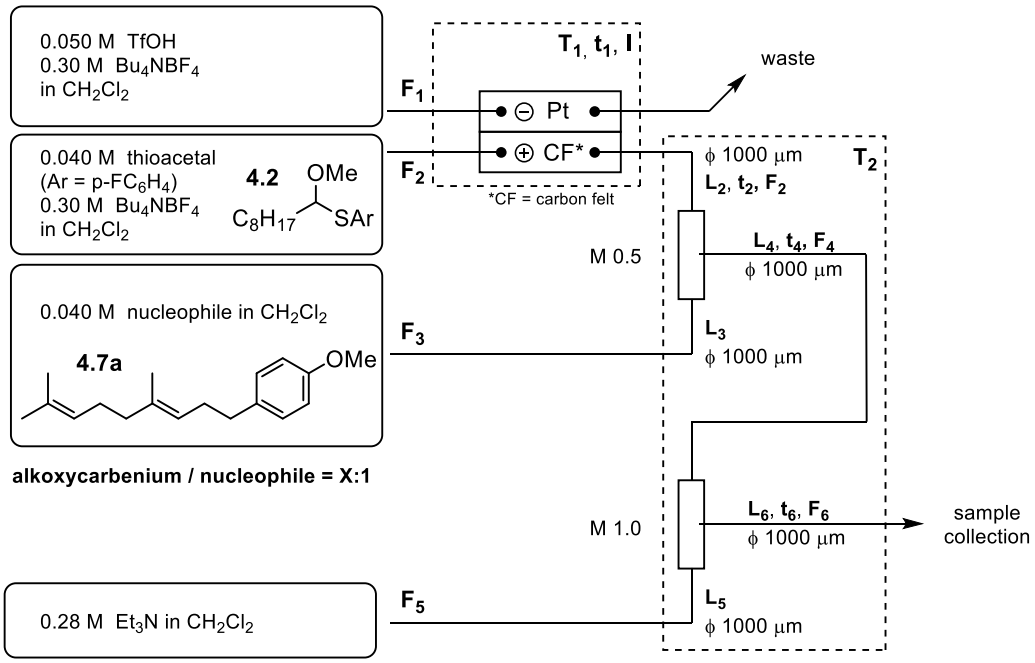

T_1 = –78 °C	F_1 = 2.5 mL/min	t_1 = 9.6 s	.	
T_2 = –78 °C	F_2 = 2.5 mL/min	t_2 = 41.5 s	L_2 = 220 cm	
	F_3 = 1.25 mL/min	.	L_3 = 200 cm	
	F_4 = 3.75 mL/min	t_4 = 100.5 s	L_4 = 800 cm	
	F_5 = 1.25 mL/min	.	L_5 = 200 cm	
	F_6 = 5.0 mL/min	t_6 = 1.9 s	L_6 = 20 cm	

Equilibration time 5.0 min, collection time 4.0 min

Variation between experiments:
amount of alkoxycarbenium species generated

1) 0.50 F/mol, I = 80 mA, **X = 1.0**
2) 0.65 F/mol, I = 104 mA, **X = 1.3**
3) 0.75 F/mol, I = 120 mA, **X = 1.5**
4) 1.00 F/mol, I = 160 mA, **X = 2.0**

Entry	Electrolyte	alkoxycarbenium (based on 4.7a)	F_1=F_2, F_3 (mL/min)	T_1 = T_2 (°C)	t_1 (s)	t_4 (s)	Product 4.8a yield
1	Bu_4NBF_4 (0.3 M)	1.0 equiv.	2.5, 1.25	−78	9.6	100.5	42%
2	Bu_4NBF_4 (0.3 M)	1.3 equiv.	2.5, 1.25	−78	9.6	100.5	52%
3	Bu_4NBF_4 (0.3 M)	1.5 equiv.	2.5, 1.25	−78	9.6	100.5	56%
4	Bu_4NBF_4 (0.3 M)	2.0 equiv.	2.5, 1.25	−78	9.6	100.5	53%

Yields are based on ^{1}H NMR with trichloroethene as internal standard.

4.4.3.6. Flow setting - influence of reaction concentration

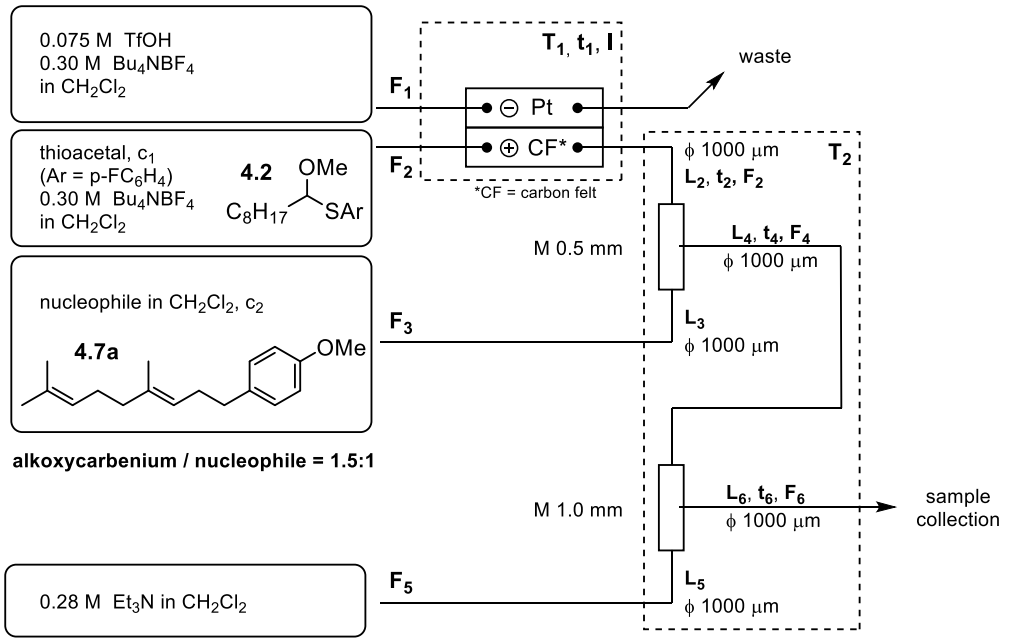

Variation between experiments: concentrations of thioacetal and nucleophile (while keeping the same flow rate).

0.020 M thioacetal
0.020 M nucleophile
quench: Et_3N (14 equiv.)

0.75 F/mol based on thioacetal
I = 60 mA, (U = 7.2 V)

T_1 = –78 °C
T_2 = –78 °C

F_1 = 2.5 mL/min
F_2 = 2.5 mL/min
F_3 = 1.25 mL/min
F_4 = 3.75 mL/min
F_5 = 1.25 mL/min
F_6 = 5.0 mL/min

t_1 = 9.6 s
t_2 = 41.5 s
t_4 = 100.5 s
t_6 = 1.9 s

L_2 = 220 cm
L_3 = 200 cm
L_4 = 800 cm
L_5 = 200 cm
L_6 = 20 cm

Equilibration time 6.0 min, collection time 8.0 min

0.040 M thioacetal
0.040 M nucleophile
quench: Et_3N (7.0 equiv.)

0.75 F/mol based on thioacetal
I = 120 mA, (U = 10.1 V)

T_1 = –78 °C
T_2 = –78 °C

F_1 = 2.5 mL/min
F_2 = 2.5 mL/min
F_3 = 1.25 mL/min
F_4 = 3.75 mL/min
F_5 = 1.25 mL/min
F_6 = 5.0 mL/min

t_1 = 9.6 s
t_2 = 41.5 s
t_4 = 100.5 s
t_6 = 1.9 s

L_2 = 220 cm
L_3 = 200 cm
L_4 = 800 cm
L_5 = 200 cm
L_6 = 20 cm

Equilibration time 5.0 min, collection time 4.0 min

0.080 M thioacetal
0.080 M nucleophile
quench: Et_3N (3.5 equiv.)

0.75 F/mol based on thioacetal
I = 240 mA, (U = 14.6 V)

T_1 = –78 °C
T_2 = –78 °C

F_1 = 2.5 mL/min
F_2 = 2.5 mL/min
F_3 = 1.25 mL/min
F_4 = 3.75 mL/min
F_5 = 1.25 mL/min
F_6 = 5.0 mL/min

t_1 = 9.6 s
t_2 = 41.5 s
t_4 = 100.5 s
t_6 = 1.9 s

L_2 = 220 cm
L_3 = 200 cm
L_4 = 800 cm
L_5 = 200 cm
L_6 = 20 cm

Equilibration time 5.0 min, collection time 4.0 min

Entry	Electrolyte	$c_1 = c_2$ (M)	F_1=F_2, F_3 (mL/min)	$T_1 = T_2$ (°C)	t_1 (s)	t_4 (s)	Product 4.8a yield
1	Bu_4NBF_4 (0.3 M)	0.020	2.5, 1.25	−78	9.6	100.5	51%
2	Bu_4NBF_4 (0.3 M)	0.040	2.5, 1.25	−78	9.6	100.5	56%
3	Bu_4NBF_4 (0.3 M)	0.060	2.5, 1.25	−78	9.6	100.5	47%

Yields are based on ^{1}H NMR with trichloroethene as internal standard.

4.4.3.7. Flow setup - screening of reaction temperature conditions

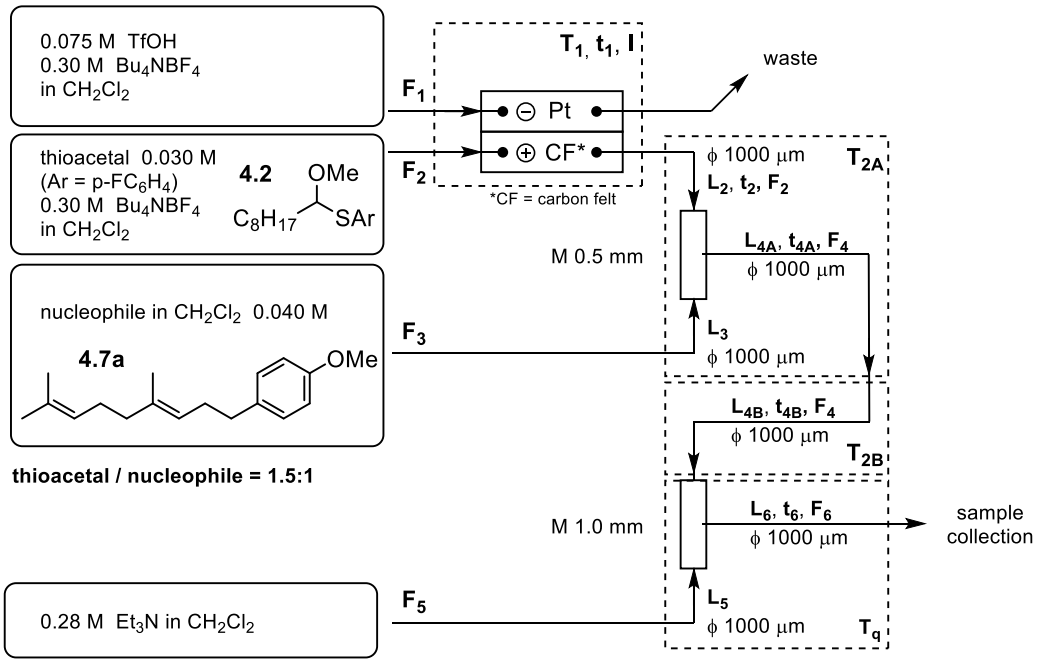

Variation between experiments: reaction temperature (step change)

0.030 M thioacetal	T_1 = –78 °C	F_1 = 2.5 mL/min	t_1 = 9.6 s	.
0.040 M nucleophile	T_2 = changing	F_2 = 2.5 mL/min	t_2 = 41.5 s	L_2 = 220 cm
quench: Et_3N (~5 equiv.)	T_q = changing	F_3 = 1.25 mL/min	.	L_3 = 200 cm
		F_4 = 3.75 mL/min	t_4 = changing	L_4 = changing
1.0 F/mol based on thioacetal		F_5 = 1.25 mL/min	.	L_5 = 200 cm
I = 120 mA, (U = ~ 10.4 V)		F_6 = 5.0 mL/min	t_6 = 1.9 s	L_6 = 20 cm

Equilibration time 5.0 min, collection time 4.0 min

1) T_{2A} = –78 °C	2) T_{2A} = –78 °C	3) T_{2A} = –78 °C	4) T_{2A} = –78 °C
L_{4A} = 850 cm	L_{4A} = 850 cm	L_{4A} = 450 cm	L_{4A} = 50 cm
t_{4A} = 106.8 s	t_{4A} = 106.8 s	t_{4A} = 56.6 s	t_{4A} = 6.3 s
T_{2B} = /	T_{2B} = /	T_{2B} = 0 °C	T_{2B} = 0 °C
L_{4B} = /	L_{4B} = /	L_{4B} = 400 cm	L_{4B} = 800 cm
t_{4B} = /	t_{4B} = /	t_{4B} = 50.3 s	t_{4B} = 100.5 s
T_q = –78 °C	T_q = 0 °C	T_q = 0 °C	T_q = 0 °C

Entry	Electrolyte	t_1 (s)	F_1=F_2, F_3 (mL/min)	T_1 = T_{2A} (°C)	t_{4A} (s)	T_{2B} (°C)	t_{4B} (s)	T_q (°C)	Product 4.8a yield
1	Bu_4NBF_4 (0.3 M)	9.6	2.5, 1.25	−78	106.8	-	-	−78	58%
2	Bu_4NBF_4 (0.3 M)	9.6	2.5, 1.25	−78	106.8	-	-	0	58%
3	Bu_4NBF_4 (0.3 M)	9.6	2.5, 1.25	−78	56.6	0	50.3	0	54%
4	Bu_4NBF_4 (0.3 M)	9.6	2.5, 1.25	−78	6.3	0	100.5	0	38%

Yields are based on ^{1}H NMR with trichloroethene as internal standard.

4.4.3.8. Expanding substrate scope with flow setup

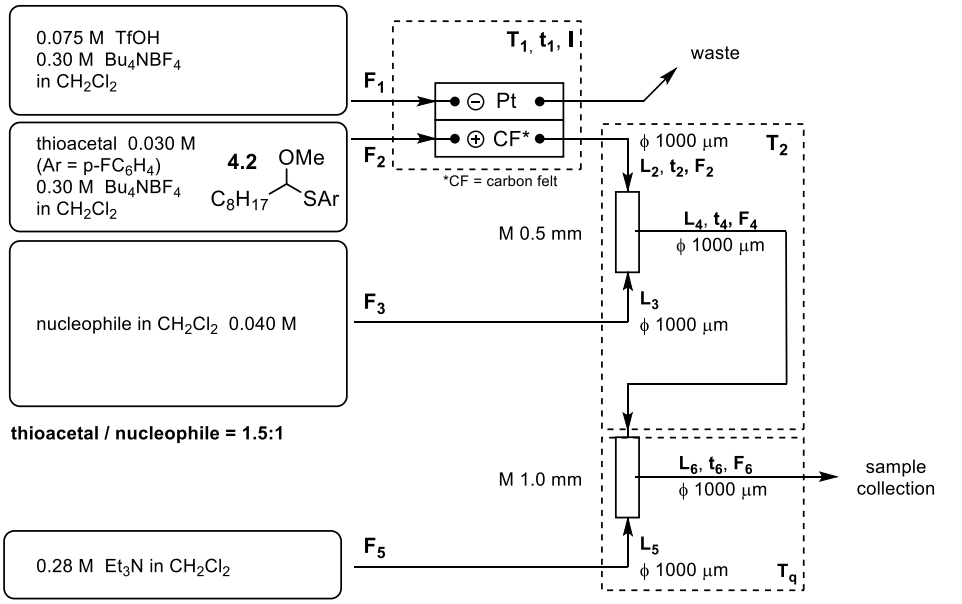

0.030 M thioacetal	T_1 = –78 °C	F_1 = 2.5 mL/min	t_1 = 9.6 s	.
0.040 M nucleophile	T_2 = –78 °C	F_2 = 2.5 mL/min	t_2 = 41.5 s	L_2 = 220 cm
quench: Et_3N (~5 equiv.)	T_q = –78 °C	F_3 = 1.25 mL/min	.	L_3 = 200 cm
		F_4 = 3.75 mL/min	t_4 = 106.8 s	L_4 = 850 cm
1.0 F/mol based on thioacetal		F_5 = 1.25 mL/min	.	L_5 = 200 cm
I = 120 mA, (U = ~ 10.0-12.0 V)		F_6 = 5.0 mL/min	t_6 = 1.9 s	L_6 = 20 cm

Equilibration time 5.0 min, collection time 4.0 min

diene substrate	major products
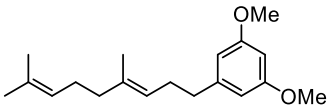 **4.7b**	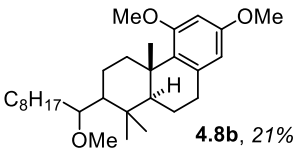 **4.8b**, *21%*
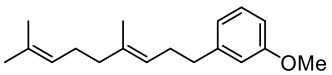 **4.7c**	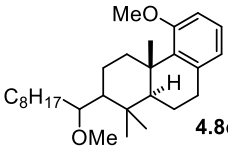 **4.8co**, *30%* 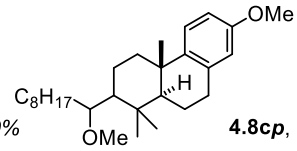 **4.8cp**, *14%*
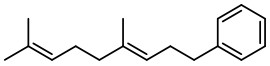 **4.7d**	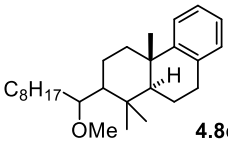 **4.8d**, *45%*
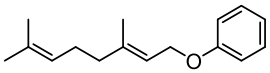 **4.9**	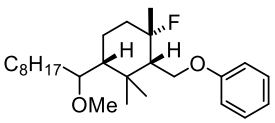 **4.10**, *45%*

Electrolyte	t_1 (s)	F_1=F_2, F_3 (mL/min)	T_1 = T_2 (°C)	T_q (°C)
Bu_4NBF_4 (0.3 M)	9.6	2.5, 1.25	−78	−78

4.4.3.9. Flow experiment with external quenching - screening of quenching conditions, substrate 4.3

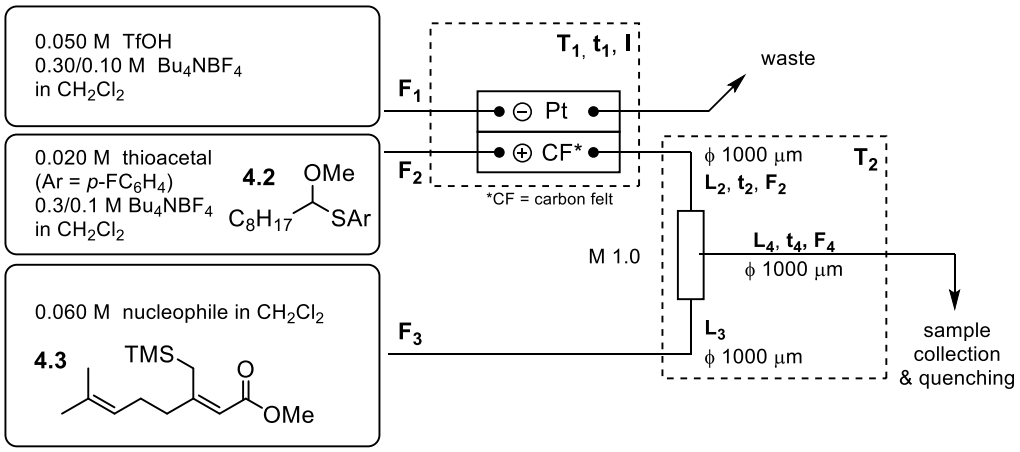

alkoxycarbenium / nucleophile = 1:1.5

T_1 = –78 °C	F_1 = 2.5 mL/min	t_1 = 9.6 s	.
T_2 = –78 °C	F_2 = 2.5 mL/min	t_2 = 41.5 s	L_2 = 220 cm
	F_3 = 1.25 mL/min	.	L_3 = 200 cm
I = 80 mA	F_4 = 3.75 mL/min	t_4 = 52.8 s	L_4 = 420 cm
(1.0 F/mol)			

Equilibration time 5.0 min, collection time 4.0 min

Entry	Electrolyte	F_1=F_2, F_3 (mL/min)	T_2 (°C)	t_1 (s)	t_4 (s)	t_q (min)	Product 4.4 yield	Side product 4.5 yield
1	Bu_4NBF_4 (0.3 M)	2.5, 1.25	−78	9.6	52.8	0	32%	6%
2	Bu_4NBF_4 (0.3 M)	2.5, 1.25	−78	9.6	52.8	4	36%	13%
3	Bu_4NBF_4 (0.3 M)	2.5, 1.25	−78	9.6	52.8	10	38%	13%
4	Bu_4NBF_4 (0.3 M)	2.5, 1.25	−78	9.6	52.8	60	35%	11%
5	Bu_4NBF_4 (0.1 M)	2.5, 1.25	−78	9.6	52.8	10	18%	5%

Yields are based on ^{1}H NMR with trichloroethene as internal standard.

4.4.3.10. Flow setup – screening of stoichiometry ratios - substrate 4.3

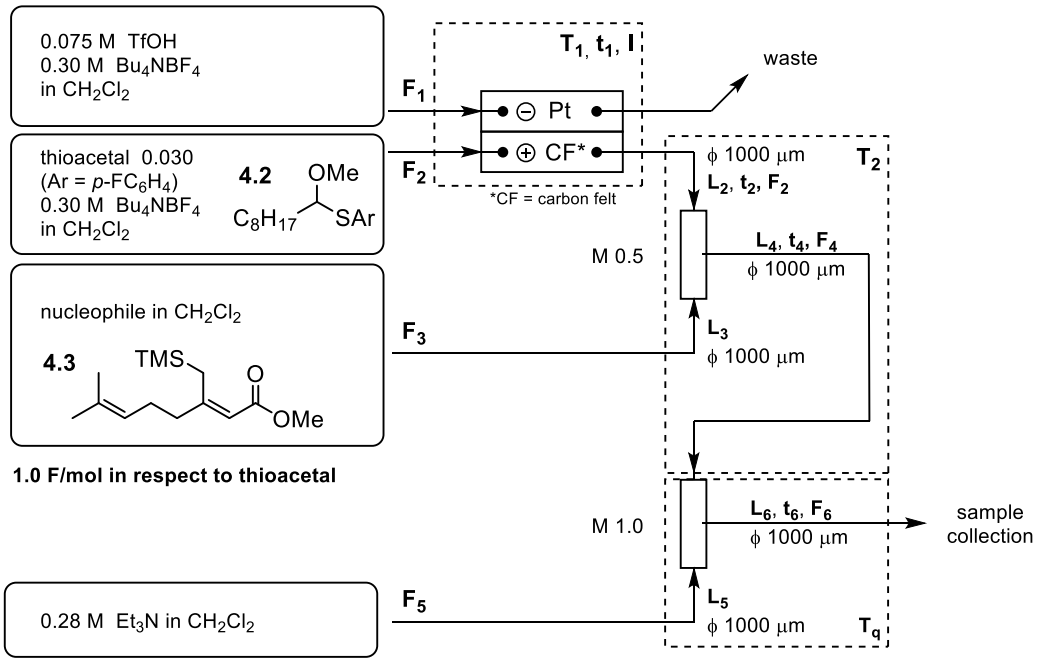

Variation between experiments: stoichiometry

0.030/0.020 M thioacetal
0.040/0.060 M nucleophile
quench: Et_3N (~5-7 equiv.)

1.0 F/mol based on thioacetal
I = 80/120 mA, (U = ~8.5/9.8 V)

T_1 = –78 °C
T_2 = changing

F_1 = 2.5 mL/min
F_2 = 2.5 mL/min
F_3 = 1.25 mL/min
F_4 = 3.75 mL/min
F_5 = 1.25 mL/min
F_6 = 5.0 mL/min

t_1 = 9.6 s
t_2 = 41.5 s
t_4 = 106.8 s
t_6 = 1.9 s

L_2 = 220 cm
L_3 = 200 cm
L_4 = 850 cm
L_5 = 200 cm
L_6 = 20 cm

Equilibration time 5.0 min, collection time 4.0 min

1) 1.0:1.5 cation/diene, 80 mA, 0.020 M thioacetal, 0.060 M diene, $T_2 = T_q$ = –78 °C
2) 1.0:1.0 cation/diene, 80 mA, 0.020 M thioacetal, 0.040 M diene, $T_2 = T_q$ = –78 °C
3) 1.5:1.0 cation/diene, 120 mA, 0.030 M thioacetal, 0.040 M diene, $T_2 = T_q$ = –78 °C

Entry	Electrolyte	n(alkoxycarbenium) / n(diene 4.3)	F_1=F_2, F_3 (mL/min)	$T_2 = T_q$ (°C)	t_1, t_4 (s)	Product 4.4 yield	Side product 4.5 yield
1	Bu_4NBF_4 (0.3 M)	1.0 / 1.5	2.5, 1.25	−78	9.6, 106.8	37%	5%
2	Bu_4NBF_4 (0.3 M)	2.0 / 1.0	2.5, 1.25	−78	9.6, 106.8	38%	9%
3	Bu_4NBF_4 (0.3 M)	1.5 / 1.0	2.5, 1.25	−78	9.6, 106.8	50%	10%

Yields are based on ^{1}H NMR with trichloroethene as internal standard.

4.4.3.11. Flow setup - screening of reaction temperature - substrate 4.3

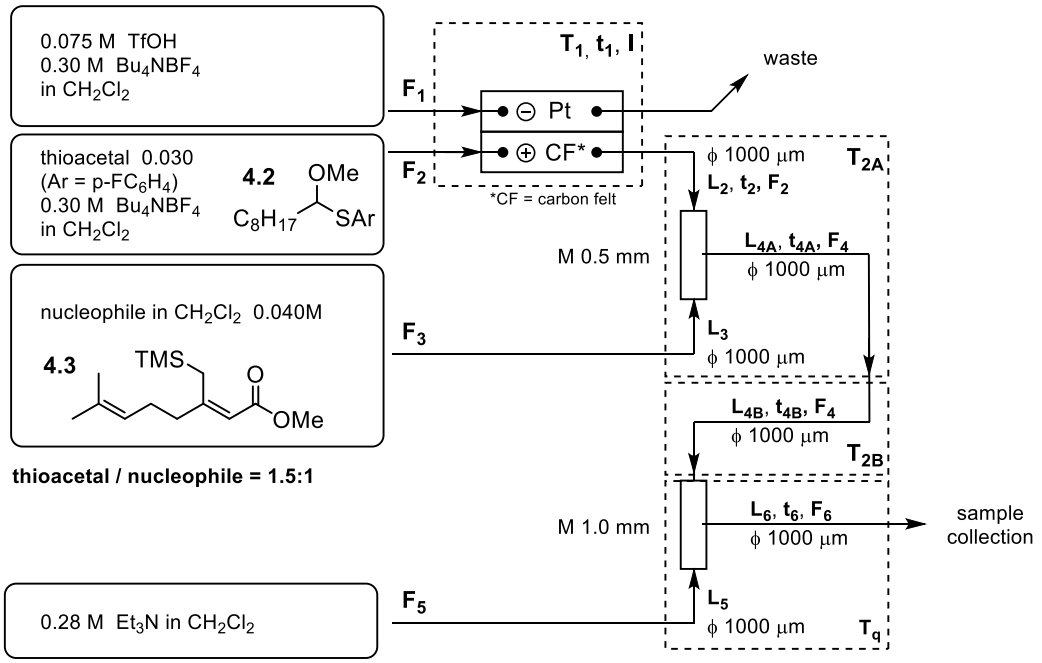

Variation between experiments: reaction temperature step change)

0.030 M thioacetal 0.040 M nucleophile quench: Et_3N (~5 equiv.) 1.0 F/mol based on thioacetal I = 120 mA, (U = ~ 9.9 V)	T_1 = –78 °C T_2 = changing T_q = changing	F_1 = 2.5 mL/min F_2 = 2.5 mL/min F_3 = 1.25 mL/min F_4 = 3.75 mL/min F_5 = 1.25 mL/min F_6 = 5.0 mL/min	t_1 = 9.6 s t_2 = 41.5 s . t_4 = changing . t_6 = 1.9 s	. L_2 = 220 cm L_3 = 200 cm L_4 = changing L_5 = 200 cm L_6 = 20 cm

Equilibration time 5.0 min, collection time 4.0 min

1) T_{2A} = –78 °C	2) T_{2A} = –78 °C	3) T_{2A} = –78 °C	4) T_{2A} = –78 °C
L_{4A} = 850 cm	L_{4A} = 850 cm	L_{4A} = 450 cm	L_{4A} = 50 cm
t_{4A} = 106.8 s	t_{4A} = 106.8 s	t_{4A} = 56.6 s	t_{4A} = 6.3 s
T_{2B} = /	T_{2B} = /	T_{2B} = 0 °C	T_{2B} = 0 °C
L_{4B} = /	L_{4B} = /	L_{4B} = 400 cm	L_{4B} = 800 cm
t_{4B} = /	t_{4B} = /	t_{4B} = 50.3 s	t_{4B} = 100.5 s
T_q = –78 °C	T_q = 0 °C	T_q = 0 °C	T_q = 0 °C

Entry	Electrolyte	F_1=F_2, F_3 (mL/min)	t_1 (s)	T_1 = T_{2A} (°C)	t_{2A} (s)	T_{2B} (°C)	t_{4A} (s)	T_q (°C)	Product 4 yield	Side product 5 yield
1	Bu_4NBF_4 (0.3 M)	2.5, 1.25	9.6	−78	106.8	-	-	−78	50%	10%
2	Bu_4NBF_4 (0.3 M)	2.5, 1.25	9.6	−78	106.8	-	-	0	52%	14%
3	Bu_4NBF_4 (0.3 M)	2.5, 1.25	9.6	−78	56.6	0	50.3	0	54%	16%
4	Bu_4NBF_4 (0.3 M)	2.5, 1.25	9.6	−78	6.3	0	100.5	0	20%	13%

Yields are based on ^{1}H NMR with trichloroethene as internal standard.

4.4.4. Characterization of cyclization products

methyl (1*R,3*S**)-3-(1-methoxynonyl)-2,2-dimethyl-6-methylenecyclohexane-1-carboxylate (4.4)**

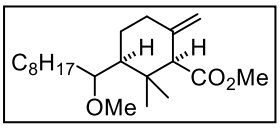

Colorless oil; **^{1}H NMR** (400 MHz, $CDCl_3$): δ 4.87 – 4.82 (m, 1H), 4.67 – 4.63 (m, 1H), 3.67 (s, 3H), 3.28 – 3.21 (m, 4H), 2.88 (s, 1H), 2.40 (dt, *J* = 13.0, 3.5 Hz, 1H), 2.07 – 1.94 (m, 1H), 1.68 – 1.52 (m, 3H), 1.42 – 1.17 (m, 14H), 1.04 (s, 3H), 0.99 (s, 3H), 0.91 – 0.86 (m, 3H); **^{13}C NMR** (101 MHz, $CDCl_3$): δ 172.41, 144.00, 108.50, 79.74, 61.21, 56.93, 51.16, 51.14, 38.84, 36.15, 32.60, 32.01, 29.97, 29.76, 29.42, 27.49, 26.46, 22.80, 22.57, 16.11, 14.25; **R_f** (9:1 hexane/EtOAc) = 0.59; **R_f** (1:1 hexane/toluene) = 0.16; **HRMS** (ESI+, m/z) $[M+Na]^+$ calcd. for $C_{21}H_{38}O_3Na$: 361.2713, found: 361.2703.

methyl (1*R,3*S**)-3-((4-fluorophenyl)thio)-2,2-dimethyl-6-methylenecyclohexane-1-carboxylate (4.5)**

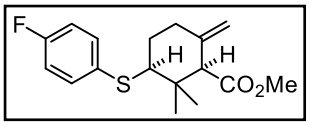

Colorless oil; **^{1}H NMR** (400 MHz, $CDCl_3$): δ 7.46 – 7.38 (m, 2H), 7.04 – 6.94 (m, 2H), 4.90 – 4.87 (m, 1H), 4.73 – 4.70 (m, 1H), 3.69 (s, 3H), 2.94 (s, 1H), 2.83 (dd, *J* = 12.3, 4.0 Hz, 1H), 2.38 (ddd, *J* = 12.9, 4.5, 2.2 Hz, 1H), 2.09 – 1.90 (m, 2H), 1.76 (qd, *J* = 13.4, 12.9, 4.5 Hz, 1H), 1.24 (s, 3H), 1.12 (s, 3H); **^{13}C NMR** (101 MHz, $CDCl_3$): δ 171.71, 162.39 (d, *J* = 247.3 Hz), 142.34, 135.13 (d, *J* = 8.1 Hz), 131.21 (d, *J* = 3.3 Hz), 116.19 (d, *J* = 21.7 Hz), 109.95, 61.46, 60.49, 51.44, 40.36, 35.96, 31.72, 28.02, 16.11; **^{19}F NMR** (376 MHz, $CDCl_3$): δ −114.31 – −114.43 (m); **R_f** (9:1 hexane/EtOAc) = 0.52; **R_f** (1:1 hexane/toluene) = 0.33. **HRMS** (ESI+, m/z) $[M+Na]^+$ calcd. for $C_{17}H_{21}O_2FNaS$: 331.1139, found: 331.1130.

(4a*S,10a*S**)-6-methoxy-2-(1-methoxynonyl)-1,1,4a-trimethyl-1,2,3,4,4a,9,10,10a-octahydrophenanthrene (4.8a)**

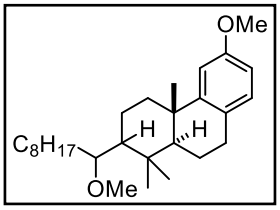

Colorless oil; **^{1}H NMR** (400 MHz, $CDCl_3$): δ 6.96 (d, *J* = 8.3 Hz, 1H), 6.82 (d, *J* = 2.6 Hz, 1H), 6.66 (dd, *J* = 8.3, 2.6 Hz, 1H), 3.77 (s, 3H), 3.30 (s, 3H), 3.25 (dd, *J* = 9.1, 3.8 Hz, 1H), 2.90 (dd, *J* = 16.7, 5.3 Hz, 1H), 2.83 – 2.71 (m, 1H), 2.33 (dt, *J* = 12.6, 3.2 Hz, 1H), 1.93 – 1.84 (m, 1H), 1.84 – 1.78 (m, 1H), 1.77 – 1.67 (m, 1H), 1.67 – 1.56 (m, 2H), 1.48 – 1.37 (m, 2H), 1.36 – 1.15 (m, 16H), 1.10 (dd, *J* = 12.6, 3.1 Hz, 1H), 0.97 (s, 3H), 0.91 – 0.85 (m, 6H); **^{13}C NMR** (101 MHz, $CDCl_3$) δ 157.79, 151.44, 129.77, 127.52, 111.12, 110.21, 80.60, 56.69, 55.39, 52.09, 51.01, 39.24, 38.31, 36.92, 32.19, 32.01, 30.30, 30.01, 29.99, 29.75, 29.41, 26.58, 24.88, 22.80, 19.70, 18.31, 17.96, 14.25; **R_f** (9:1 hexane/EtOAc) = 0.52; **R_f** (1:1 hexane/toluene) = 0.20; **HRMS** (ESI+, m/z) $[M+Na]^+$ calcd. for $C_{28}H_{46}O_2Na$: 437.3390, found: 437.3382.

(4a*S,10a*S**)-5-methoxy-2-(1-methoxynonyl)-1,1,4a-trimethyl-1,2,3,4,4a,9,10,10a-octahydrophenanthrene (4.8c*o*)**

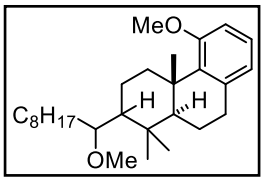

Colorless oil; **^{1}H NMR** (400 MHz, $CDCl_3$): δ 7.04 (t, *J* = 7.8 Hz, 1H), 6.67 (d, *J* = 8.3 Hz, 2H), 3.78 (s, 3H), 3.29 (s, 3H), 3.26 – 3.17 (m, 2H), 2.89 – 2.82 (m, 2H), 1.88 – 1.72 (m, 2H), 1.64 – 1.36 (m, 4H), 1.35 – 1.13 (m, 17H), 1.10 (dd, *J* = 12.7, 3.4 Hz, 1H), 0.97 (s, 3H), 0.91 – 0.85 (m, 6H); **^{13}C NMR** (101 MHz, $CDCl_3$): δ 158.92, 138.35, 137.64, 126.04, 122.29, 109.30, 80.74, 56.74, 55.19, 55.09, 50.89, 40.01, 37.33, 36.64, 33.52, 32.25, 32.02, 30.47, 30.02, 29.76, 29.42, 26.61, 22.80, 19.60, 19.49, 18.45, 18.28, 14.26; **R_f** (9:1 hexane/EtOAc) = 0.62; **R_f** (1:1 hexane/toluene) = 0.43; **HRMS** (ESI+, m/z) $[M+Na]^+$ calcd. for $C_{28}H_{46}O_2Na$: 437.3390, found: 437.3388.

(4a*S,10a*S**)-7-methoxy-2-(1-methoxynonyl)-1,1,4a-trimethyl-1,2,3,4,4a,9,10,10a-octahydrophenanthrene (4.8c*p*)**

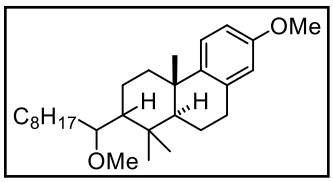

Colorless oil; **^{1}H NMR** (400 MHz, $CDCl_3$): δ 7.18 (d, *J* = 8.8 Hz, 1H), 6.70 (dd, *J* = 8.7, 2.8 Hz, 1H), 6.57 (d, *J* = 2.7 Hz, 1H), 3.76 (s, 3H), 3.29 (s, 3H), 3.25 (dd, *J* = 8.9, 4.2 Hz, 1H), 2.97 – 2.77 (m, 2H), 2.34 (dt, *J* = 12.6, 3.3 Hz, 1H), 1.93 – 1.85 (m, 1H), 1.85 – 1.56 (m, 4H), 1.48 – 1.20 (m, 15H), 1.18 (s, 3H), 1.10 (dd, *J* = 12.6, 3.2 Hz, 1H), 0.97 (s, 3H), 0.90 – 0.86 (m, 6H); **^{13}C NMR** (101 MHz, $CDCl_3$): δ 157.11, 142.75, 136.61, 125.82, 113.20, 112.00, 80.63, 56.70, 55.25, 52.37, 51.07, 39.42, 37.56, 36.84, 32.21, 32.01, 31.40, 30.00, 30.00, 29.74, 29.41, 26.58, 25.04, 22.80, 19.60, 18.32, 17.90, 14.25; **R_f** (9:1 hexane/EtOAc) = 0.54; **R_f** (1:1 hexane/toluene) = 0.29; **HRMS** (ESI+, m/z) $[M+Na]^+$ calcd. for $C_{28}H_{46}O_2Na$: 437.3390, found: 437.3378.

(4a*S,10a*S**)-5,7-dimethoxy-2-(1-methoxynonyl)-1,1,4a-trimethyl-1,2,3,4,4a,9,10,10a-octahydrophenanthrene (4.8b)**

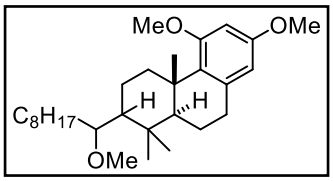

Colorless oil; **^{1}H NMR** (400 MHz, $CDCl_3$): δ 6.28 (d, *J* = 2.6 Hz, 1H), 6.19 (d, *J* = 2.5 Hz, 1H), 3.76 (s, 3H), 3.75 (s, 3H), 3.28 (s, 3H), 3.23 (dd, *J* = 8.7, 3.7 Hz, 1H), 3.15 (dt, *J* = 13.0, 3.5 Hz, 1H), 2.85 – 2.80 (m, 2H), 1.85 – 1.70 (m, 2H), 1.64 – 1.35 (m, 4H), 1.35 – 1.06 (m, 18H), 0.97 (s, 3H), 0.91 – 0.84 (m, 6H); **^{13}C NMR** (101 MHz, $CDCl_3$): δ 159.89, 157.88, 138.90, 130.47, 104.85, 97.70, 80.75, 56.74, 55.28, 55.22, 55.17, 50.93, 39.47, 37.27, 36.95, 34.01, 32.25, 32.01, 30.48, 30.02, 29.75, 29.42, 26.60, 22.80, 19.76, 19.53, 18.40, 18.29, 14.25; **R_f** (9:1 hexane/EtOAc) = 0.49; **R_f** (1:1 hexane/toluene) = 0.20; **HRMS** (ESI+, m/z) $[M+H]^+$ calcd. for $C_{29}H_{49}O_3$: 445.3676, found: 445.3665.

(4a*S,10a*S**)-2-(1-methoxynonyl)-1,1,4a-trimethyl-1,2,3,4,4a,9,10,10a-octahydrophenanthrene (4.8d)**

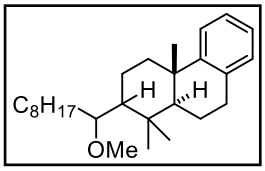

Colorless oil; **^{1}H NMR** (400 MHz, $CDCl_3$): δ 7.29 – 7.26 (m, 1H), 7.15 – 7.01 (m, 3H), 3.30 (s, 3H), 3.26 (dd, *J* = 9.2, 3.9 Hz, 1H), 2.96 (dd, *J* = 16.4, 5.8 Hz, 1H), 2.85 (ddd, *J* = 17.4, 11.7, 7.1 Hz, 1H), 2.38 (dt, *J* = 12.6, 3.3 Hz, 1H), 1.95 – 1.87 (m, 1H), 1.87 – 1.67 (m, 2H), 1.66 – 1.57 (m, 2H), 1.48 – 1.37 (m, 2H), 1.36 – 1.18 (m, 16H), 1.11 (dd, *J* = 12.6, 3.2 Hz, 1H), 0.98 (s, 3H), 0.91 – 0.85 (m, 6H); **^{13}C NMR** (101 MHz, $CDCl_3$): δ 150.18, 135.29, 129.01, 125.76, 125.29, 124.74, 80.62, 56.70, 52.10, 51.07, 39.21, 38.12, 36.92, 32.22, 32.01, 31.13, 30.00, 30.00, 29.75, 29.41, 26.58, 24.98, 22.80, 19.58, 18.32, 17.95, 14.25; **R_f** (9:1 hexane/EtOAc) = 0.68; **R_f** (1:1 hexane/toluene) = 0.61; **HRMS** (ESI+, m/z) $[M+Na]^+$ calcd. for $C_{27}H_{44}ONa$: 407.3284, found: 407.3280.

(((1*S,3*R**,6*S**)-6-fluoro-3-(1-methoxynonyl)-2,2,6-trimethylcyclohexyl)methoxy)benzene (4.10)**

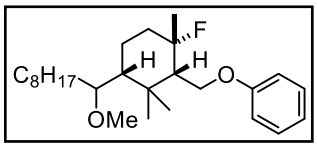

Proposed relative stereochemistry; colorless oil; **^{1}H NMR** (400 MHz, $CDCl_3$): δ 7.33 – 7.27 (m, 2H), 6.98 – 6.91 (m, 3H), 4.21 (dd, *J* = 9.9, 6.2 Hz, 1H), 4.09 – 4.03 (m, 1H), 3.30 – 3.23 (m, 4H), 2.09 – 1.96 (m, 1H), 1.91 – 1.77 (m, 1H), 1.66 – 1.14 (m, 21H), 1.06 (s, 3H), 0.92 (d, *J* = 2.1 Hz, 3H), 0.89 (t, *J* = 7.0 Hz, 3H). *Separately observed at 1.36 ppm* (d, *J* = 21.2 Hz, 3H); **^{13}C NMR** (101 MHz, $CDCl_3$): δ 158.85, 129.57, 120.79, 114.79, 96.31 (d, *J* = 172.5 Hz), 80.06, 65.71 (d, *J* = 2.4 Hz), 56.77, 54.57 (d, *J* = 19.4 Hz), 51.11, 38.69 (d, *J* = 22.5 Hz), 37.11, 32.55, 32.02, 30.00, 29.77, 29.42, 28.57, 27.15 (d, *J* = 25.4 Hz), 26.52, 22.81, 17.88 (d, *J* = 6.6 Hz), 17.20, 14.26; **^{19}F NMR** (376 MHz, $CDCl_3$): δ −157.93 (m); **R_f** (9:1 hexane/EtOAc) = 0.75**;** **R_f** (1:1 hexane/toluene) = 0.36; **HRMS** (ESI+, m/z) [M+H]+ calcd. for $C_{26}H_{43}O_2F$: 429.3139, found: 429.3130.

4.4.5. Synthesis of polyene substrates

(*E*)-(4,8-dimethylnona-3,7-dien-1-yl)benzene (4.7d)

Modified version of reported procedure [9] was used for synthesis.

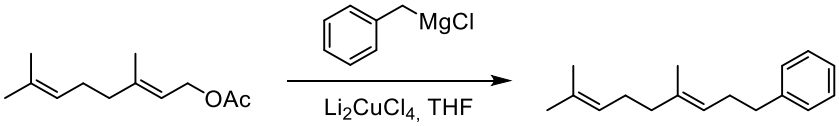

To the solution of geranyl acetate (6.43 mL, 30.0 mmol, 1.0 equiv.) in anhydrous THF (250 mL) at 0 °C was added Li_2CuCl_4 (9.90 mL, 0.1 M in THF, 0.99 mmol, 3.3 mol %). After 10 min, benzylmagnesium chloride (30.0 mL, 2.0 M in THF, 60.0 mmol, 2 equiv.) was added dropwise. The reaction mixture was stirred for 4 h at 0 °C and then quenched with aq. NH_4Cl (sat., 100 mL) and 50 mL of water was added. Layers were separated and aqueous phase was extracted with Et_2O (3 × 75 mL). Combined organic phases were dried over $MgSO_4$, filtered, and concentrated under reduced pressure. The crude product was purified by column chromatography (SiO_2, *n*-hexane) to give the corresponding product (4.32 g, 63% yield) as a colorless oil.

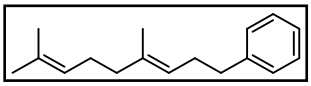

^{1}H NMR (400 MHz, $CDCl_3$): δ 7.30 – 7.23 (m, 2H), 7.22 – 7.13 (m, 3H), 5.22 – 5.15 (m, 1H), 5.12 – 5.05 (m, 1H), 2.68 – 2.60 (m, 2H), 2.30 (q, *J* = 7.5 Hz, 2H), 2.11 – 2.01 (m, 2H), 2.01 – 1.94 (m, 2H), 1.68 (s, 3H), 1.60 (s, 3H), 1.55 (s, 3H); **^{13}C NMR** (101 MHz, $CDCl_3$): δ 142.55, 135.90, 131.48, 128.62, 128.34, 125.79, 124.48, 123.73, 39.85, 36.28, 30.11, 26.83, 25.85, 17.83, 16.09. *Data consistent with those reported in literature* [9].

(*E*)-1-(4,8-dimethylnona-3,7-dien-1-yl)-4-methoxybenzene (4.7a)

Modified version of reported procedure [10] was used for synthesis.

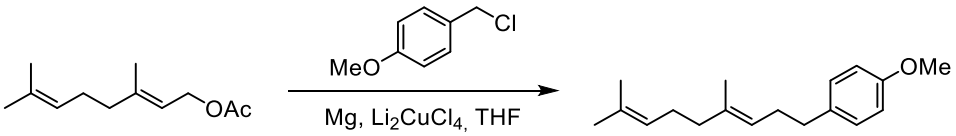

A flame-dried flask was charged with magnesium turnings (5.94 g, 244 mmol, 8.0 equiv.) and anh. THF (150 mL) and cooled to 0 °C. To initiate the reaction, 1,2-dibromoethane (3 drops) was added after some of the initial 1-(chloromethyl)-4-methoxybenzene (8.28 mL, 61.1 mmol, 2 equiv.) had already been added and then followed by dropwise addition of the rest of the halide. The reaction mixture was stirred at constant temperature for 1.5 h and then immediately used in next step.

Separately, to the solution of geranyl acetate (6.55 mL, 30.6 mmol, 1.0 equiv.) in anhydrous THF (50 mL) at 0 °C was added Li_2CuCl_4 (10.1 mL, 0.1 M in THF, 1.01 mmol, 3.3 mol %). After 10 min, freshly prepared Grignard solution (see above) was added dropwise. The reaction mixture was stirred for 4 h at 0 °C and then quenched with aq. NH_4Cl (sat., 100 mL) and 50 mL of water was added. Layers were separated and aqueous phase was extracted with Et_2O (3 × 75 mL).

Combined organic phases were dried over $MgSO_4$, filtered, and concentrated under reduced pressure. The crude product was purified by column chromatography (SiO_2, *n*-hexane/EtOAc 99:1 → 97:3). The by-product, 1-methoxy-4-methylbenzene, was removed by drying the sample (50 °C, 0.1 mmHg) for 5 h to give the corresponding product (6.62 g, 84% yield) as a colorless oil.

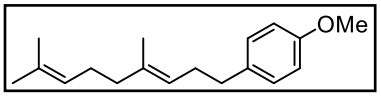

^{1}H NMR (400 MHz, $CDCl_3$): δ 7.15 – 7.09 (m, 2H), 6.86 – 6.80 (m, 2H), 5.22 – 5.15 (m, 1H), 5.13 – 5.07 (m, 1H), 3.80 (s, 3H), 2.62 – 2.56 (m, 2H), 2.28 (q, *J* = 7.5 Hz, 2H), 2.12 – 2.03 (m, 2H), 2.02 – 1.96 (m, 2H), 1.70 (s, 3H), 1.61 (s, 3H), 1.56 (s, 3H); **^{13}C NMR** (101 MHz, $CDCl_3$): δ 157.80, 135.81, 134.69, 131.47, 129.48, 124.50, 123.81, 113.75, 55.37, 39.85, 35.34, 30.33, 26.84, 25.84, 17.83, 16.11. *Data consistent with those reported in literature* [10].

(*E*)-1-(4,8-dimethylnona-3,7-dien-1-yl)-3-methoxybenzene (4.7c)

A procedure similar as for synthesis of (*E*)-1-(4,8-dimethylnona-3,7-dien-1-yl)-4-methoxybenzene was used.

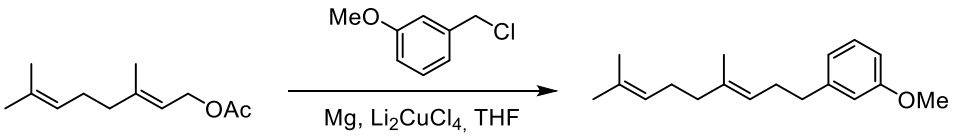

A flame-dried flask was charged with magnesium turnings (5.83 g, 240 mmol, 8.0 equiv.) and anh. THF (200 mL) and cooled to 0 °C. To initiate the reaction, 1,2-dibromoethane (3 drops) was added after some of the initial 1-(chloromethyl)-3-methoxybenzene (8.10 mL, 60.0 mmol, 2 equiv.) had already been added and then followed by dropwise addition of the rest of the halide. The reaction mixture was stirred at constant temperature for 2 h and then immediately used in next step.

Separately, to the solution of geranyl acetate (6.43 mL, 30.0 mmol, 1.0 equiv.) in anhydrous THF (50 mL) at 0 °C was added Li_2CuCl_4 (9.90 mL, 0.1 M in THF, 0.99 mmol, 3.3 mol %). After 10 min, freshly prepared Grignard solution (see above) was added dropwise. The reaction mixture was stirred for 3 h at 0 °C and then quenched with aq. NH_4Cl (sat., 100 mL) and 50 mL of water was added. Layers were separated and aqueous phase was extracted with Et_2O (3 × 75 mL). Combined organic phases were dried over $MgSO_4$, filtered, and concentrated under reduced pressure. The crude product was purified by column chromatography (SiO_2, *n*-hexane/EtOAc 99:1 → 98:2). The by-product, 1-methoxy-3-methylbenzene, was removed by drying the sample (65 °C, 0.1 mmHg) for 10 h to give the corresponding product (5.49 g, 71% yield) as a colorless oil.

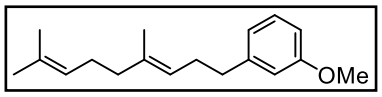

^{1}H NMR (400 MHz, $CDCl_3$): δ 7.23 – 7.17 (m, 1H), 6.82 – 6.78 (m, 1H), 6.77 – 6.71 (m, 2H), 5.23 – 5.16 (m, 1H), 5.13 – 5.07 (m, 1H), 3.81 (s, 3H), 2.68 – 2.56 (m, 2H), 2.31 (q, *J* = 7.4 Hz, 2H), 2.12 – 2.03 (m, 2H), 2.03 – 1.96 (m, 2H), 1.69 (s, 3H), 1.61 (s, 3H), 1.58 (s, 3H); **^{13}C NMR** (101 MHz, $CDCl_3$): δ 159.68, 144.24, 135.92, 131.50, 129.29, 124.46, 123.70, 121.06, 114.36, 111.06, 55.25, 39.84, 36.32, 29.98, 26.85, 25.83, 17.82, 16.13. *Data consistent with those reported in literature* [11].

(*E*)-1-(4,8-dimethylnona-3,7-dien-1-yl)-3,5-dimethoxybenzene (4.7b)

A procedure similar as for synthesis of (*E*)-1-(4,8-dimethylnona-3,7-dien-1-yl)-4-methoxybenzene was used.

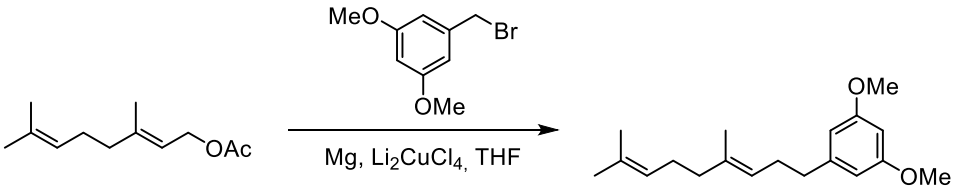

A flame-dried flask was charged with magnesium turnings (5.94 g, 244 mmol, 8.0 equiv.) and anh. THF (100 mL) and cooled to 0 °C. To initiate the reaction, 1,2-dibromoethane (3 drops) was added after some of the initial solution of 1-(bromomethyl)-3,5-dimethoxybenzene (14.1 g, 61.1 mmol, 2 equiv.) in 50 mL anh. THF had already been added, and then followed by dropwise addition of the rest of the halide. The reaction mixture was stirred at constant temperature for 2 h and then immediately used in next step.

Separately, to the solution of geranyl acetate (6.55 mL, 30.6 mmol, 1.0 equiv.) in anhydrous THF (50 mL) at 0 °C was added Li_2CuCl_4 (10.1 mL, 0.1 M in THF, 1.01 mmol, 3.3 mol %). After 10 min, freshly prepared Grignard solution (see above) was added dropwise. The reaction mixture was stirred for 4 h at 0 °C and then quenched with aq. NH_4Cl (sat., 100 mL) and 50 mL of water was added. Layers were separated and aqueous phase was extracted with Et_2O (3 × 75 mL). Combined organic phases were dried over $MgSO_4$, filtered, and concentrated under reduced pressure. The crude product was first triturated with hexane and filtered to remove precipitated by-products, and then purified by column chromatography (SiO_2, *n*-hexane/EtOAc 98:2 → 96:4). The remaining by-product, 1,3-dimethoxy-5-methylbenzene, was removed by drying the sample (110 °C, 0.1 mmHg) for 2 h to give the corresponding product (5.68 g, 64% yield) as a colorless oil.

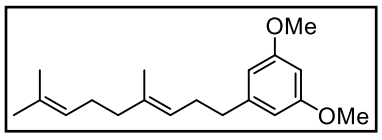

^{1}H NMR (400 MHz, $CDCl_3$): δ 6.37 (d, *J* = 2.3 Hz, 2H), 6.31 (t, *J* = 2.3 Hz, 1H), 5.22 – 5.16 (m, 1H), 5.13 – 5.06 (m, 1H), 3.78 (s, 6H), 2.61 – 2.56 (m, 2H), 2.34 – 2.26 (m, 2H), 2.11 – 2.03 (m, 2H), 2.02 – 1.95 (m, 2H), 1.69 (s, 3H), 1.61 (s, 3H), 1.59 (s, 3H); **^{13}C NMR** (101 MHz, $CDCl_3$): δ 160.80, 145.02, 135.93, 131.51, 124.45, 123.68, 106.64, 97.79, 55.36, 39.84, 36.58, 29.87, 26.87, 25.82, 17.82, 16.16. *Data consistent with those reported in literature* [12].

methyl (*Z*)-3-((diethoxyphosphoryl)oxy)-7-methylocta-2,6-dienoate

A modified literature procedure [13] was used for synthesis.

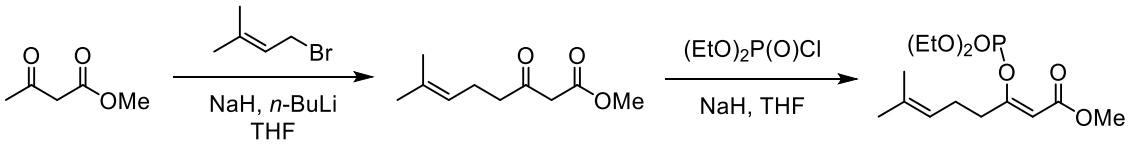

To the suspension of NaH (55% dispersion in paraffin oil, 2.09 g, 48.0 mmol, 1.2 equiv.) in anh. THF (150 mL) at 0 °C was added methyl acetoacetate (4.32 mL, 40.0 mmol, 1.0 equiv.) dropwise. The reaction mixture was stirred for 15 min and then *n*-butyl lithium (26.3 mL, 1.6 M in *n*-hexane, 42.0 mmol, 1.05 equiv.) was added dropwise. After 10 min, 1-bromo-3-methylbut-2-ene (4.85 mL, 42.0 mmol, 1.05 equiv.) was added and the reaction mixture was stirred for 2 h at 0 °C. Reaction was quenched by addition of aq. NH_4Cl (sat., 100 mL), followed by addition of Et_2O (100 mL). Layers were separated and aqueous phase was extracted with Et_2O (3 × 100 mL). Combined organic phases were washed with brine (50 mL), dried over $MgSO_4$, filtered, and concentrated under reduced pressure. The crude product, methyl 7-methyl-3-oxooct-6-enoate, was used in the next step without purification.

Crude methyl 7-methyl-3-oxooct-6-enoate (7.37 g, 40.0 mmol, 1.0 equiv.) was dissolved in anh. THF (50 mL) and added dropwise to a suspension of NaH (55% dispersion in paraffin oil, 2.09 g, 48.0 mmol, 1.2 equiv.) in anh. THF (100 mL) at 0 °C. After 10 min, diethyl chlorophosphate (6.08 mL, 42.0 mmol, 1.05 mmol) was added dropwise and the reaction mixture was stirred for 2 h at 0 °C. HCl (1 M, 75 mL) was carefully added, layers were separated, and aqueous phase was extracted with Et_2O (3x 100 mL). Combined organic phases were washed first with aq. $NaHCO_3$ (sat., 2x 50 mL) and then with brine (50 mL). Washed organic phase was dried over $MgSO_4$, filtered, and concentrated under reduced pressure. The crude product was purified by column chromatography (SiO_2, *n*-hexane/EtOAc 6:1 → 4:1 → 3:1 → 2:1.) to give the corresponding product (8.80 g, 69% yield over 2 steps) as a pale-yellow oil.

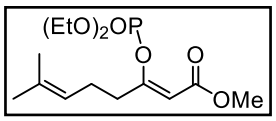

^{1}H NMR (400 MHz, $CDCl_3$): δ 5.29 (s, 1H), 5.04 – 4.96 (m, 1H), 4.24 – 4.14 (m, 4H), 3.62 (s, 3H), 2.38 (t, *J* = 7.6 Hz, 2H), 2.19 (q, *J* = 7.4 Hz, 2H), 1.61 (s, 3H), 1.54 (s, 3H), 1.33 – 1.26 (m, 6H); **^{13}C NMR** (101 MHz, $CDCl_3$): δ 164.20 (d, *J* = 1.6 Hz), 161.61 (d, *J* = 7.1 Hz), 133.34, 121.86, 104.86 (d, *J* = 7.7 Hz), 64.72 (d, *J* = 6.3 Hz), 51.06, 35.19, 25.60, 24.92, 17.68, 16.03 (d, *J* = 7.2 Hz). *Data consistent with those reported in literature* [13].

methyl (*Z*)-7-methyl-3-((trimethylsilyl)methyl)octa-2,6-dienoate (4.3)

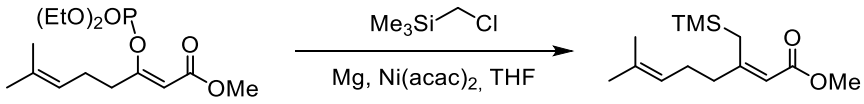

A flame-dried flask was charged with magnesium turnings (2.40 g, 98.9 mmol, 3.6 equiv.) and anh. THF (100 mL) followed by dropwise addition of (chloromethyl)trimethylsilane (6.90 mL, 49.5 mmol, 1.8 equiv.). When reaction mixture started to warm up, it was cooled to 0 °C and stirred at the same temperature for 2 h.

In a separate flame-dried flask, methyl (*Z*)-3-((diethoxyphosphoryl)oxy)-7-methylocta-2,6-dienoate (8.80 g, 27.5 mmol, 1.0 equiv.) was dissolved in 50 mL THF and cooled to 0 °C. Then $Ni(acac)_2$ (494 mg, 1.92 mmol, 7 mol %) was added, followed by dropwise addition of previously prepared Grignard reagent. The reaction mixture was stirred for 2.5 h at 0 °C and then quenched with aq. HCl (1 M, 75 mL). Layers were separated, and aqueous phase was extracted with Et_2O (3 × 100 mL). Combined organic phases were washed first with aq. $NaHCO_3$ (sat., 50 mL) and then with brine (50 mL). Washed organic phase was dried over $MgSO_4$, filtered, and concentrated under reduced pressure. The crude product was purified by column chromatography (SiO_2, *n*-hexane/EtOAc 99:1 → 98:2) to give the corresponding product (5.50 g, 69% yield) as a very pale-yellow oil.

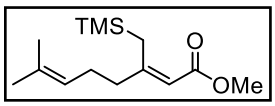

^{1}H NMR (400 MHz, $CDCl_3$): δ 5.54 (s, 1H), 5.11 – 5.05 (m, 1H), 3.65 (s, 3H), 2.41 (s, 2H), 2.19 – 2.11 (m, 2H), 2.10 – 2.03 (m, 2H), 1.68 (s, 3H), 1.59 (s, 3H), 0.04 (s, 9H); **^{13}C NMR** (101 MHz, $CDCl_3$): δ 167.90, 164.69, 132.67, 123.22, 111.06, 50.69, 40.78, 26.74, 26.29, 25.81, 17.83, −0.69. *Data consistent with those reported in literature* [13].

4.4.6. Synthesis of substrates used for electrochemical transformations

4-fluorophenyl)(1-methoxynonyl)sulfane (4.2)

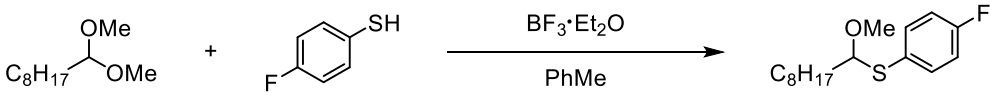

To a solution of 1,1-dimethoxynonane (11.1 mL, 50 mmol, 1.0 equiv.) in toluene (350 mL) under argon atmosphere was added 4-fluorothiophenol (5.5 mL, 51 mmol, 1.0 equiv.) and cooled to −78 °C. Then, boron trifluoride ethyl etherate was added (6.2 mL, 50 mmol, 1.0 equiv.) and reaction was stirred for 2 h. Reaction was quenched by addition of saturated aqueous $NaHCO_3$solution (300 mL). Layers were separated and aqueous phase was extracted with Et_2O (2 × 200 mL). Combined organic phases were washed with additional saturated aqueous $NaHCO_3$ solution (100 mL), dried over $MgSO_4$, filtered, and concentrated under reduced pressure. The crude product was purified by column chromatography (SiO_2, *n*-hexane/EtOAc 98:2) to give the corresponding product (10.2 g, 71% yield) as a colorless oil.

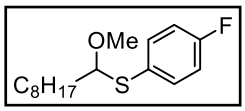

^{1}H NMR (400 MHz, $CDCl_3$): δ 7.49 – 7.40 (m, 2H), 7.04 – 6.93 (m, 2H), 4.52 (t, *J* = 6.6 Hz, 1H), 3.47 (s, 3H), 1.75 – 1.58 (m, 2H), 1.47 – 1.36 (m, 2H), 1.33 – 1.17 (m, 10H), 0.87 (t, *J* = 6.9 Hz, 3H); **^{13}C NMR** (101 MHz, $CDCl_3$): δ 162.81 (d, *J* = 247.8 Hz), 136.28 (d, *J* = 8.1 Hz), 127.98 (d, *J* = 3.3 Hz), 115.94 (d, *J* = 21.7 Hz), 91.16, 55.62, 35.65, 31.97, 29.58, 29.33, 29.26, 26.33, 22.79, 14.24; **^{19}F NMR** (376 MHz, $CDCl_3$): δ −113.89*. Data consistent with those reported in literature [5].*

bis(4-fluorophenyl) disulfide (4.1)

Compound was provided by Nagaki group, synthesized by reported literature procedure [14].

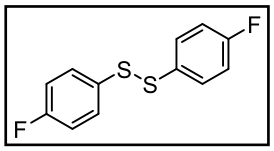

Yellow oil or white solid; **^{1}H NMR** (400 MHz, $CDCl_3$): δ 7.48 – 7.41 (m, 4H), 7.06 – 6.96 (m, 4H). *Data consistent with those reported in literature [15].*

(1-methoxynonyl)trimethylsilane (4.6)

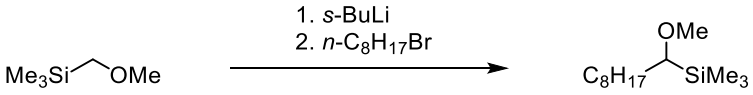

Synthetic procedure was adapted from literature [16].

To a flame-dried flask under argon atmosphere containing anh. THF (70 mL) was added (methoxymethyl)trimethylsilane (4.7 mL, 30 mmol, 1.0 equiv.) and solution was cooled to −78 °C. *s*-BuLi (1.2 M in cyclohexane, 25.0 mL, 30 mmol, 1.0 equiv.) was slowly added and reaction mixture was stirred for 1 h at −78 °C and additionally for 0.5 h at −23 °C. When reaction mixture was cooled again to −78 °C, *n*-octyl bromide (4.83 mL, 28 mmol, 0.93 equiv.) was added slowly and reaction mixture was stirred at the same temperature for 10 min. Reaction was then quenched by addition of saturated aqueous NH_4Cl solution. Layers were separated and aqueous phase was extracted with Et_2O (3 ×). Combined organic phases were washed with brine, dried over $MgSO_4$, filtered, and concentrated under reduced pressure. The crude product was purified by column chromatography (SiO_2, *n*-hexane/EtOAc 99:1 → 98:2) to give the corresponding product (1.15 g, 18% yield) as a colorless oil.

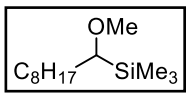

^{1}H NMR (400 MHz, $CDCl_3$): δ 3.35 (s, 3H), 2.78 (dd, *J* = 7.8, 5.0 Hz, 1H), 1.57 – 1.38 (m, 3H), 1.37 – 1.20 (m, 11H), 0.91 – 0.85 (m, 3H), 0.03 (s, 9H). **^{13}C NMR** (101 MHz, $CDCl_3$): δ 76.73, 60.21, 32.06, 31.34, 30.12, 29.78, 29.51, 27.41, 22.85, 14.30, −2.86. *Data consistent with those reported in literature [16].*

4.5. References

1 S. Suga, S. Suzuki, J. Yoshida: Intramolecular Participation in Alkoxycarbenium Ion Pools. *Org. Lett.* **2005**, *7*, 21, 4717−4720. DOI: 10.1021/ol051915r

2 J. Yoshida, Y. Ishichi, S. Isoe: Intramolecular carbon-carbon bond formation by the anodic oxidation of unsaturated .alpha.-stannyl heteroatom compounds. Synthesis of fluorine containing heterocyclic compounds. *J. Am. Chem. Soc.* **1992**, *114*, 19, 7594–7595. DOI: 10.1021/ja00045a060

3 J. Yoshida, M. Sugawara, M. Tatsumi, N. Kise: Electrooxidative Inter- and Intramolecular Carbon−Carbon Bond Formation Using Organothio Groups as Electroauxiliaries. *J. Org. Chem.* **1998**, *63*, 5950−5961. DOI: 10.1021/jo980601x

4 J. Yoshida, M. Sugawara, N. Kise: Organothio groups as electroauxiliaries: Electrooxidative inter- and intramolecular carbon-carbon bond formation. *Tetrahedron Letters* **1996**, *37*, 18, 3157−3160. DOI: 10.1016/0040-4039(96)00516-3

5 K. Matsumoto, K. Ueoka, S. Suzuki, S. Suga, J. Yoshida: Direct and indirect electrochemical generation of alkoxycarbenium ion pools from thioacetals. *Tetrahedron* **2009**, *65,* 10901–10907. DOI: 10.1016/j.tet.2009.09.020

6 S. Suga, K. Matsumoto, K. Ueoka, J. Yoshida: Indirect Cation Pool Method. Rapid Generation of Alkoxycarbenium Ion Pools from Thioacetals. *J. Am. Chem. Soc*. **2006**, *128*, 7710−7711. DOI: 10.1021/ja0625778

7 M. Takumi, H. Sakaue, A. Nagaki: Flash Electrochemical Approach to Carbocations. *Angew. Chem. Int. Ed.* **2022**, *61*, e202116177. DOI: 10.1002/anie.202116177

8 M. Takumi, H. Sakaue, D. Shibasaki, A. Nagaki: Rapid access to organic triflates based on flash generation of unstable sulfonium triflates in flow. *Chem. Commun*. **2022**, *58*, 8344−8347. DOI: 10.1039/D2CC02344J

9 K. Surendra, E. J. Corey: Highly Enantioselective Proton-Initiated Polycyclization of Polyenes. *J. Am. Chem. Soc.* **2012**, *134*, 11992−11994. DOI: 10.1021/ja305851h

10 Z. Tao, K. A. Robb, K. Zhao, S. E. Denmark: Enantioselective, Lewis Base-Catalyzed Sulfenocyclization of Polyenes. *J. Am. Chem. Soc.* **2018**, *140*, 3569−3573. DOI: 10.1021/jacs.8b01660

11 Y.-J. Zhao, S.-S. Chng, T.-P. Loh: Lewis Acid-Promoted Intermolecular Acetal-Initiated Cationic Polyene Cyclizations. *J. Am. Chem. Soc.* **2007**, *129*, 492−493. DOI: 10.1021/ja067660+

12 J. Li, S. G. Ballmer, E. P. Gillis, S. Fujii, M. J. Schmidt, A. M. E. Palazzolo, J. W. Lehmann, G. F. Morehouse, M. D. Burke: Synthesis of many different types of organic small molecules using one automated process. *Science* **2015**, *347*, 6227, 1221−1226. DOI: 10.1126/science.aaa5414

13 S. D. Schnell, A. Linden, K. Gademann: Synthesis of Two Key Fragments of the Complex Polyhalogenated Marine Meroterpenoid Azamerone. *Org. Lett.* **2019**, *21*, 1144−1147. DOI: 10.1021/acs.orglett.9b00090

14 R. Leino, J.-E. Lönnqvist: A very simple method for the preparation of symmetrical disulfides. *Tetrahedron Lett.* **2004**, *45*, 8489–8491. DOI: 10.1016/j.tetlet.2004.09.100

15 D. P. Becker, C. I. Villamil, T. E. Barta, L. J. Bedell, T. L. Boehm, G. A. DeCrescenzo, J. N. Freskos, D. P. Getman, S. Hockerman, R. Heintz, S. Carol Howard, M. H. Li, J. J. McDonald, C. P. Carron, C. L. Funckes-Shippy, P. P. Mehta, G. E. Munie, C. A. Swearingen: Synthesis and Structure-Activity Relationships of, β- and α-Piperidine Sulfone Hydroxamic Acid Matrix Metalloproteinase Inhibitors with Oral Antitumor Efficacy. *J. Med. Chem.* **2005**, *48*, 6713–6730. DOI: 10.1021/jm0500875

16 S. Suga, S. Suzuki, A. Yamamoto, J. Yoshida: Electrooxidative Generation and Accumulation of Alkoxycarbenium Ions and Their Reactions with Carbon Nucleophiles. *J. Am. Chem. Soc*. **2000**, *122*, 41, 10244–10245. DOI: 10.1021/ja002123p